Multimode and Multiband Microstrip Antennas

Alaa Ibrahim Abunjaileh

Submitted in accordance with the requirements for the degree of Doctor of Philosophy

The University of Leeds

School of Electronic and Electrical Engineering

November 2007

The candidate confirms that the work submitted is his own and that appropriate credit has been given where reference has been made to the work of others.

This copy has been supplied on the understanding that it is copyright material and that no quotation from the thesis may be published without proper acknowledgement

Abstract

This thesis describes original work on the broadband and multiband matching of microstrip patch antennas. Microstrip patch antennas suffer from many constraints on their performance. One major restriction is their narrow impedance bandwidth. An effective method to resolve this is adding more resonators to the antenna structure to achieve multi-resonance and hence wider bandwidth. Structures such as circular, square and triangular patch antennas may support two orthogonal resonant modes or polarisations. This allows excitation of an additional resonance beside the fundamental. With the correct coupling between the resonant modes, the impedance bandwidth can be significantly increased. The equivalent circuit of such structures is similar to those used in microwave filter design. Using techniques normally employed in filter synthesis, the equivalent circuits can be generated, and aid in finding the couplings and dimensions of the specified antenna requirement. The bandwidth of circular microstrip patch antennas is significantly increased by exciting two modes on a single circular microstrip antenna, and four modes using two stacked circular microstrip patches. In this work, the designs are also extended into multimode antennas achieving multi-frequency operation.

Acknowledgment

I would like to express my deep and sincere gratitude to Professor Ian Hunter and Dr. Andy Kemp for their much needed support and guidance.

I also would like to express my gratitude to all those who supported me to complete my research and this thesis. I would like to acknowledge Dr. Andy Guyette of Naval Research Lab, Washington DC, Steve Middleditch, Mohammed Zewani, Dr. David Denis, Emika Sandhiya and the rest of the IMP staff for their kind help and advice.

I am deeply indebted to my parents and family for their valuable help and support throughout my research and writing of this thesis.

I am deeply grateful to my lovely wife Nadia for her encouragement and kindness throughout this stressful period.

List of Figures

List of Abbreviations

PMC	Perfect Magnetic Conductor
PEC	Perfect Electric Conductor
$E_{\rho,\Phi \text{ or } z}$	Electric field in cylindrical coordinates
$H_{\rho,\Phi \text{ or } z}$	Magnetic field in cylindrical coordinates
ω	Angular frequency in rad/s
μ	Permeability
ε	Permittivity
J	Current density
d or h	Substrate thickness
r or a	Radius
a_e	Effective radius
χ'_{mn}	Zeros of the derivative of the Bessel function $J_m(x)$
R	Resistance
G	Conductance or Gain
V	Voltage
I	Current
J	Impedance inverter
c	Velocity of light
D	Directivity
f	Frequency
k	Wave number
Q	Quality factor
tanδ	Loss tangent
Z	Impedance
β or k_0	Propagation constant
λ	Wavelength

Chapter 1. Introduction

The microstrip patch antenna is simply a patch which radiates from one face. The patch size is a fraction of the wavelength, faced with a ground plane on the non-radiating side. A dielectric material of low relative permittivity is usually separating the two sides, and the radiation is a result of the fringing fields between the patch and the ground plane [1, 2]. Research in microstrip patch antenna started more than 50 years ago [3]. However, there is an increasing demand for integration of antennas in wireless sensor and communication systems. Microstrip patch antennas have many benefits over other types of antennas, the main advantages of microstrip antennas are [1, 2, 4, 5]:

- Low cost, light weight, low volume planar structure.
- Ease of fabrication and mass production.
- Size can be reduced for mobile devices.
- Allow linear and circular polarisation.
- Array configurations are possible.

Thus, patch antennas are probably the most likely option to be integrated in microwave systems. However, there are some serious limitations on the performance of microstrip patch antennas, among these are [1, 2, 4-6]:

- High quality factor, low efficiency and narrow bandwidth.
- Rapid change of the input impedance with respect to frequency.
- Most microstrip antennas radiate into on side only due to the ground plane.

- For high performance arrays, complex feed structures are required.
- Poor polarisation quality.
- Low power capability (around 100W).

The attractive properties of the microstrip antenna make it the most favourable option for numerous applications. Microstrip antennas have been used in [1, 7, 8]:

- Telemetry and communications antennas for missiles, due to the small and planar size of the antenna.
- Satellite links, mobile applications and WLAN due to the low power handling capability and possible miniaturisation.
- Satellite imaging and radar altimeters use small arrays of microstrip antennas.
- Global positioning systems (GPS) and global systems for mobile (GSM) use microstrip antennas as they are capable of multiband operation.

Although microstrip antennas were simply introduced as two metal sheets separated by a dielectric, with the ongoing developments and research, the structure is becoming more complex and complicated. Different materials, patch shapes, feeding techniques, multilayer and planar multipatch configurations have been investigated.

The constant demand of integrated antennas with wider bandwidth, where a number of antennas are fitted into a given volume requires more efficient bandwidth optimisation [9]. Designing for a multiradio environment is a key part of design in industrial laboratories, where "the antenna design is one of the most traditional radio frequency competences, but it is still a huge challenge" [10].

There are fundamental factors considered in the performance of antennas, these are efficiency, impedance matching and frequency bandwidth [11]. The easiest and most well known method of improving the bandwidth is by increasing the height of the substrate [4], however, this is not a desirable option as it leads to introducing power loss and surface waves.

The focus of this thesis is addressing the narrow impedance bandwidth limitation of microstrip antennas, which is known to be one of the major issues when dealing with such antennas. Techniques typically used in circuit theory and microwave filter synthesis are applied to the design of broadband microstrip antennas in this thesis.

1.1. Literature Review

Microstrip antenna engineering has a history of over 60 years [1], they were initially introduced back in the 1950's. However, serious attention to microstrip radiators was not given until the 1970's, where they started maturing considerably and many of their constraints were overcome. Yet it remains in the words of recent articles, "… a vibrant field which is bursting with activity, and is likely to remain so in the foreseeable future" [5]. In particular, there has been an increasing interest in circular microstrip patch antennas technologies.

In 1952, Englemann proposed the invention of the microstrip antenna [1], following this in 1953, the Deschamps and Sichak proposal was one of the first to introduce the concept of microstrip radiators [3, 12-16]. In a commemoration to their work, it was quoted that their paper "fostered the beginning of new discipline within the antenna community…" [3]. Two years later a patent was issued to Gutton and Baissinot in France [1, 12, 14, 15]. In 1960, Lewin shown interest in the radiation from stripline discontinuities, and towards the end of that decade, in unreported work, Kaloi studied rectangular and square structures [15]. In the sixties, Collings filed a patent for a strip radiator with multiple feed points [14, 17], Troughton and Watkins have also studied open circuited circular resonant structures in microstrip, and also considered the energy loss due to radiation [18, 19]. There was apparently no interest in making use of this nature of striplines or radiation from these resonant structures, and this is where the antenna concept went dormant until the early seventies.

In the seventies, the availability of good substrates with low loss tangent and attractive thermal and mechanical properties accelerated the development and fabrication [14]. Byron presented the concept of conducting half wave length wide and several wavelength long strip radiator built on a dielectric substrate, and fed by coaxial connections. Also mentioned is that Theo Cheston from National Research Labortory (NRL) has suggested that such an element is well-suited for phased array applications [14, 15]. Howell and Munson were the first to practically develop microstrip antennas in the seventies [3, 16, 20, 21]. Various microstrip geometries were developed by Weinschel in 1973 for use on rockets, and in the following year, Sanford presented microstrip elements in conformal phased array for aircraft

applications [15]. Extensive research and development followed shortly after, exploiting their numerous advantages, including reduction in size, weight and cost, besides the need for low-profile antennas on the emerging new generation of missiles. In 1975, microstrip patch antenna elements were further investigated by Garvin et al, Howell, Janes and Wilson [15, 20], studying missile based mounted microstrip antennas and new design techniques for antenna arrays. Mathematical analysis and modelling started to get attention that year to further understand the theory. Initial investigations applied the concept of transmission lines to simple rectangular patches, and a year later Carver presented a paper describing the radiation pattern of microstrip disc antennas [15, 20].

Microstrip antennas have been of huge interest to the military as well. In 1977, John Kerr, US Army Electronics Command presented a new technique of controlling the resonant frequency of microstrip antenna [3]. This was achieved by introducing a cut in the centre of the patch, removing metallization and making the patch electrically smaller. The full theory was presented by Mink three years later [22], as well as introducing the concept of ring antennas. In 1978, Kerr also introduced the concept of tunable antennas by adding reactance to the resonance, this was done by utilising a length of transmission line [3]. In the same paper, he employed the concept of removal of metallization to achieve the appropriate conditions for circular polarisation from patch antennas having single feed [3]. Following Kerr's discovery, Jones et al presented a technique for tuning the operating frequency of microstrip patch antennas using vias, or shorting posts adding inductive reactance that leads to raising the resonant frequency [3]. In the same year, Lo et al. introduced the first theoretical electromagnetic solution [3, 23], this is the Cavity model. In the same meeting, Montgomery introduced the full wave method [3], which also considers thicker dielectric and various shapes. Other similar work by Derneyard, Shen and Long, and Carver and Coffey were reported on advanced theoretical investigations [15].

October 1979 witnessed the earliest international workshop on Printed Circuit Antennas (and first most significant) which was held in the New Mexico State University, Las Cruces, New Mexico. Its proceedings were presented in a major IEEE Transactions special edition, alongside co-sponsorship by the US Army research office and NMSU's Physical Science Laboratory [15, 20]. The early 1980s were a focal point in publications, there was practical realism of microstrip antennas, two

books were published by Bahl, Bhartia & James and Hall & Wood, which remain in current use [12, 16]. Also substrates manufacturers started to offer wider ranges of products which could be used for microstrip antennas. Advantages of microstrip antennas, mainly ease of manufacture, low cost and profile, outweighed their performance disadvantages, i.e. narrow bandwidth. Therefore more interest was given for patch antennas to be used for applications operating at frequencies higher than 30 GHz such as aircraft to satellite communications. Studies on thick substrates and higher dielectric constants microstrip antennas were also reported [24]. Nonetheless, most of the research in the early eighties was aiming to improve the inherent issue of microstrip patch antenna, i.e. the narrow impedance bandwidth [8]. Edge and probe fed antennas were the first two methods known for feeding into microstrip antennas. Both excitation methods are inductive, dominating the frequency response at lower frequencies. However, for the patch to resonate, the inductive and capacitive components should cancel each other to achieve a zero reactance [16]. New feeding techniques, proximity and aperture coupled patch, were introduced to overcome this issue and achieve a wider bandwidth [8, 25]. Microstrip patch antenna arrays were widely studied and developed in the eighties, as well as circular and other types of polarisation [8, 26].

By the end of the eighties, there was a better understanding of microstrip patch antennas. In the nineties, microstrip patch antennas started invading the commercial systems market, satisfying the increasing need for mobile communication systems [2]. The availability of high speed processors and sophisticated simulation tools aided the fast developments in the field, and gave the opportunity for companies to develop their own version of microstrip antennas to meet their own demands. Extensive studies on Impedance bandwidth of microstrip antennas were reported, including excellent results of up to 67% [8], and investigations to improve the efficiency as well as further methods of integrating microstrip antennas into MMIC technology [27]. By the mid-nineties the development of handheld communications devices had increased the demand for smaller and lighter antennas, and hence, investigations were performed to reduce the size of microstrip antennas [8, 28]. At the start of the 21st century, microstrip antennas have been very popular for mobile systems, various methods of further improving the performance have been studied, such as Genetic Algorithm [29]. More interest and research are being pursued, trying to optimise the

design in terms of wider bandwidth, radiation efficiency, controlling polarisation properties and array architecture.

At present, microstrip antennas remain the topic of many publications and industrial development and indeed exciting a continuous development on electronic system design.

1.2. Review of Thesis

In chapter 2 microstrip patch antennas are reviewed. The basic characteristics of circular patches and aspects such as modelling techniques, fields, resonant frequency and quality factor are discussed. Various feeding techniques are also presented.

Chapter 3 presents a new original work of utilising the dual-mode property to increase the bandwidth of microstrip antennas. The input impedance of such a dual-mode antenna may be represented as a second-order ladder network of coupled resonators, where each resonator is coupled to a load resistor. A theoretical method for evaluating the coupling values in the network is presented, enabling the bandwidth of a dual-mode antenna to be maximised.

The dual-mode design approach is extended by stacking two dual-mode antennas, resulting in a quad resonance antenna. The equivalent circuit of the antenna is similar to that of microwave filters, thus filter design techniques maybe employed to synthesize the antenna and to obtain maximum return loss bandwidth. This is the first time an increase in the bandwidth is achieved on a relatively thin substrate antenna as a result of coupling four resonant modes using two stacked circular microstrip patches. Electromagnetic simulation and measured results demonstrate bandwidth improvement of over 4 times that of a single mode design

Chapter 4 presents a new technique of transforming the dualmode antenna into a dualband one. The transformation is performed with reference to techniques normally used in filter synthesis. The design has been developed reaching multi-port design and utilising an external matching circuit allowing the antenna to be matched at four distinct frequencies.

Chapter 5 presents some concluding remarks, along with ideas for future research.

Chapter 2. Review of Patch Antennas

In many applications varying from spacecraft and planes to hand held mobile phones, size and weight are constraints, consequently, microstrip patch antennas would present an ideal tool for transmission. Microstrip antennas are found in many applications in the military and civil sectors, as they are economical, small and light to design and construct.

A microstrip device is formed of two parallel conductors separated by a thin dielectric substrate (thickness $<< \lambda$), with the lower conductor acting as a ground plane and the upper conductor is a patch that is an appreciable function of the wavelength [1, 8, 30]. The upper patch can be a conductor of any shape. It is typically copper or gold, and regular common shapes are used to simplify analysis and design. Shapes such as circular, square, rectangular and triangular are most common, and the dielectric constant of the substrate used is commonly low (less than 10) to enhance radiation [1, 8, 12].

Radiation is broad beam broadside to the plane of the substrates, and mainly occurs from the fringing fields between the conductor edge and the ground plane [1, 12]. Microstrip patch antennas can be analysed using various reported methods, among these are the Cavity Method and the Transmission Line Method. Both of these alongside the most common feeding techniques will be discussed in this chapter. This type of antenna can be easily fabricated using photolithographic technique, which potentially implies easy and low cost fabrication, as well as allowing microstrip antennas to be fabricated easily in research laboratories.

Typically patch antennas are used for frequencies ranging from 1GHz to 100GHz [1, 21]. Microstrip antennas suffer many constraints and restrictions on their performance. Essentially, the inherent narrow bandwidth is a major issue for quick and high bulk transmission, besides the low efficiency, low power, high Q factor, poor polarisation purity and the spurious feed radiation all constrain the performance [1, 21].

2.1. Basic Characteristics

Consider a basic microstrip antenna structure shown in Figure 2.1 [5]:

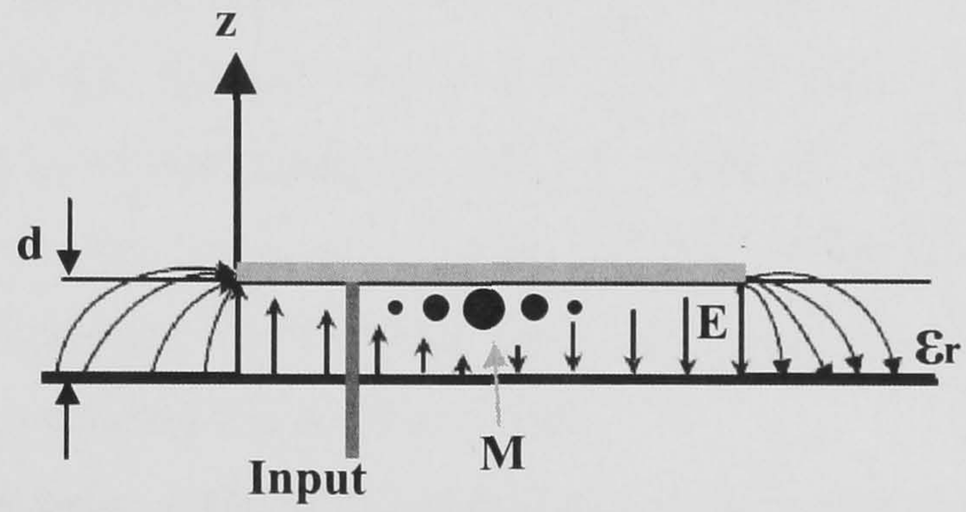

Figure 2.1 Cross-section view of microstrip patch antenna showing the electric and magnetic fields for the TM_{11} mode [31].

The microstrip patch antenna consists of a thin metallic strip with thickness much smaller than the operating wavelength, whilst the width or radius is a considerable fraction of the wavelength. The strip is separated from the ground plane by a substrate of thickness (d) smaller than 0.05λ. The probe feed drives the antenna with a voltage between the patch and the ground plane. This excites a current on the patch and hence a vertical electric field between the patch and the ground plane [5, 8]. Therefore, the electric field within the substrate has only a "z" component and the magnetic field only has "x" and "y" components, as shown in Figure 2.1 [4]. These assumptions are important in order to carry out the analysis which follows in this chapter. As the substrate height is very small, the fields do not vary along the "z" direction, and the component of the current normal to the edge approaches zero. This implies that the tangential component of the magnetic field at the edge is vanishingly small [4, 32], these assumptions are explained further later in this section.

The patch element resonates when its diameter is near $\lambda_g/2$, leading to relatively large current and field amplitudes, and the radiation mechanism occurs from the fringing fields between the edge of the microstrip and the ground plane.

The modes supported by a circular patch antenna can be found by treating the patch, the ground plane and the material between the two as a circular cavity. The supported modes -given that the substrate height is small ($h<<\lambda$)- are TM^Z where "z" is perpendicular to the patch.

The choice of the substrate used is important (dielectric constant, thickness and loss tangent). However, for one particular substrate, the circular patch has only one degree of freedom to control, clearly it is the radius and in turn, changing the radius affects the resonant frequency of the antenna [4]. There are various shapes of resonant patch elements (circular being the most common) [16], however, the principles of operation are essentially the same. The microstrip antennas considered in this thesis are of circular geometry. Circular patches offer advantages over other geometries for applications such as arrays, and can also be easily modified to produce a range of impedance values and radiation pattern.

Microstrip patch antennas enjoy many advantages when compared to other types of antennas, they are relatively small, low profile, low cost, light weight and can be integrated to other circuit or active devices which can possibly result in a single board solution, unlike wire, waveguide or horn antennas for example. This also allows this type of antenna to be easily mounted on objects such as computers or flying bodies, and can be easily employed for array design [8, 16].

The most common disadvantage of microstrip antennas is the inherent narrow impedance bandwidth, this is due to the thickness which is normally thin. Also the circular microstrip antennas can be addressed as a circular resonant cavity of high quality factor, and the antenna has a resonant style, where efficient resonance is achieved over a narrow bandwidth. The latter issue is studied in this thesis and analysed to address the improvement of the narrow impedance bandwidth. The easiest and most well known method of improving the bandwidth is by increasing the height of the substrate [4], this has the effect of increasing the radiation conductance. However, this is not a desirable option as it leads to introducing surface waves and power loss, but usually works well for bandwidths up to 4-6% [14].

Other disadvantages of microstrip patch antenna are low efficiency, low power and poor polarisation purity [1, 4, 8, 16].

2.2. Analysis methods

There are various methods reported for the analysis of a disk antenna, primarily used for calculations of the radiated fields and input impedance. Among these are the transmission line model; the most simplistic and least accurate, but gives a good understanding to the input impedance across the antenna [15, 20]. The cavity model; more complicated and can predict the fields within the antenna and the radiation pattern [4, 32]. The modal expansion model, the wire grid model [33] and the full wave method [4, 12]. However, in all cases the substrate thickness h, is assumed much less than the wavelength λ.

Radiation from a microstrip line can be reduced considerably if the substrate employed is thin, and has a higher relative dielectric constant. However, microstrip antennas are encouraged for a better radiation efficiency, therefore thick substrates with low dielectric constant are used (typically in the range 2-10). Radiation can be determined from the field distribution between the patch metallization and the ground plane. Early reported analysis techniques including Transmission line model which treats the antenna as a transmission line resonator, and the Cavity model which treats the antenna as a closed cavity with magnetic sidewalls will be discussed in this chapter [14].

2.2.1. Transmission Line Model

The transmission line model was used in the early stages of studying microstrip antennas to predict the performance and the patch size [3]. The transmission line model assumes the antenna as an open-circuited transmission line with light loading at the ends accounting for the fringing fields and radiation. The voltage and current can be approximated as [5]:

$$Voltage = V(x) = V_0 \cos(\pi x / L) \qquad 2.1$$

$$Current = I(x) = \frac{V_0}{Z_0} \sin(\pi x / L) \qquad 2.2$$

Where x is the distance from the edge to the centre, and L is the antenna's width or diameter. These equations explain the variation of the input impedance of the antenna,

depending on the location from the patch centre. For a feed point at the radiating edge (i.e. x = 0 or x = L), according to the equations above, the voltage is maximum and the current is minimum, this results in maximum value input impedance at the antenna edge. On the other hand, for a feed point at the centre, the voltage is zero and the current is maximum, hence the input impedance at the centre of the patch is zero as observed by Kerr [3]. Therefore, the input impedance can be controlled by adjusting the position of the feed point, typically, the input impedance at the edge of the patch ranges from 150Ω to 450Ω [1, 5, 12, 16].

It is rather difficult to predict the exact input impedance of microstrip antenna using this method, however, it gives a reasonable understanding. This is discussed in more detail later in this chapter.

2.2.2. The Cavity Model

The Cavity model was first introduced by Lo et al. in 1978 [3]. Although Howell has expressed the similarity between microstrip patch antennas and a cavity that has top and bottom electric walls and magnetic walls on the sides [21], however, it remained for Lo *et al* to develop and publish the electromagnetic theoretical solution of the Microstrip Antenna [3].

The cavity method treats the space between the patch and the ground plane as a "Resonant Electromagnetic Cavity", which leaks and hence radiates via its lateral surface, it yields good results for an approximation. This gives a good physical insight, more accurate than the transmission line model, however, it is more complex and difficult to model [34].

When a microstrip antenna is connected to a microwave source, the patch is energised and the charge distribution on the upper and lower surfaces of the patch as well as on the ground plane is shown in Figure 2.2 [4].

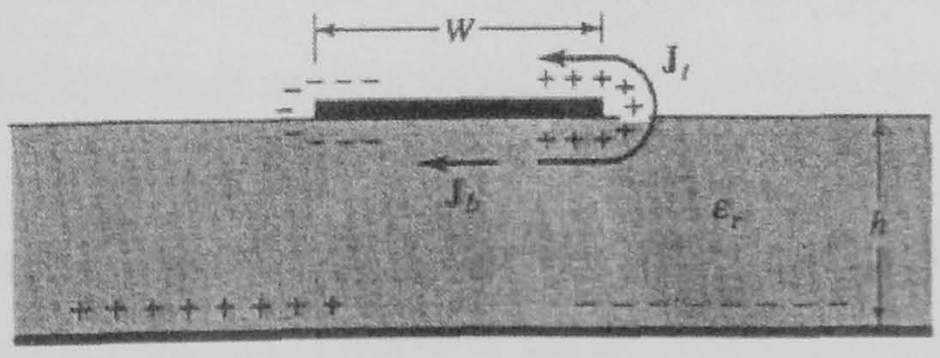

Figure 2.2 Charge distribution on microstrip patch antenna.

The distribution of the charges is controlled by two mechanisms; attractive and repulsive mechanisms. The attractive mechanism occurs between the opposite charges on the lower side of the patch and the ground plane which tends to maintain the charge concentration on the bottom of the patch, and the repulsive mechanism which is between alike charges on the lower surface of the patch which tends to repel some charges from the bottom of the patch around the edge to the top surface [4].

As a result of the movement of charges around the patch, current densities $\vec{J}_{bottom}$ and $\vec{J}_{top}$ at the sides of the patch are generated. For most microstrip antennas, the height-to-width ratio is very small, and therefore, the attractive mechanism dominates and most of the charge concentration and current flow remains underneath the patch. The small amount of current that flows around the edge of the patch to its top surface decreases as the height-to-width ratio decreases. The following analysis assumes that the current flow is almost zero, which in turn would not create any tangential magnetic field component to the edge of the patch. This assumption allows the side walls to be modelled as a perfect magnetic conducting surface which does not disturb the magnetic field and hence the electric field distribution beneath the patch. As a result it is a good approximation to the cavity model to treat the side walls as *Perfect Magnetic Conductors* [4]. This model produces a good normalised electric and magnetic field distribution of modes beneath the patch.

Since the height of the substrate is very small, the field variation across the height is considered constant, this also implies that the fringing fields along the edge of the patch are also small. The electric field is approximately normal to the surface of the patch, therefore only TM^Z field configurations will be assumed within the cavity between the patch and the ground plane. Hence, the top and bottom walls of the cavity are modelled as *Perfect Conducting Electric Walls* [4, 35].

The key points in the cavity model are [1, 4, 16]:

- The patch is assumed to be a perfectly conducting metallic surface.
- The patch is deposited on dielectric substrate of permittivity ε_r and thickness h, where the thickness is much smaller than the wavelength λ.
- The electric field E and magnetic field H are mainly localised on the cylinder height between the patch and the ground plane, where E only has the non-variant E_z component and H has only the transverse components H_x and H_y.

- The radiation is the result of leakage of E fields from the cylindrical cavity, via the cavity laterals.
- Cavity models treat the side walls as *Perfect Magnetic Conductors (PMC),* while the top and bottom walls of the cavity are *Perfect Electric Conductors (PEC).*

To study the cavity model in more detail, consider the microstrip antenna in Figure 2.3, expressed in the cylindrical coordinates:

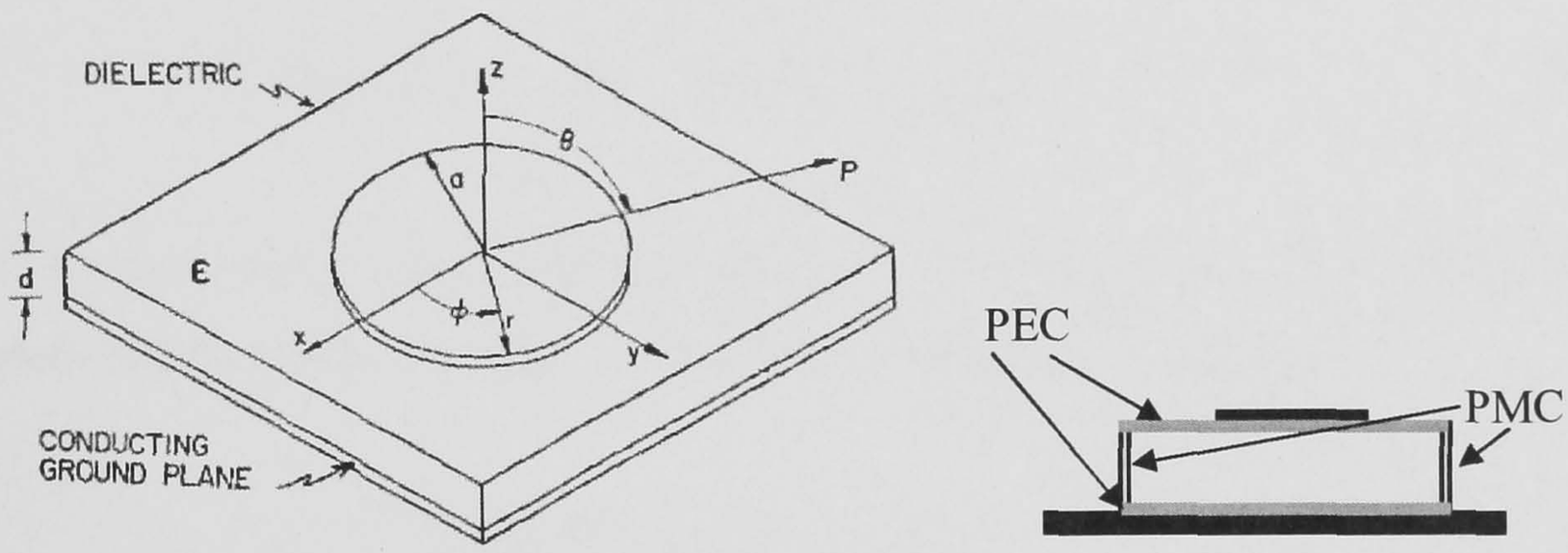

Figure 2.3 Circular microstrip patch antenna [36].

The cavity is composed of two PEC at the top and bottom representing the patch and the ground plane. A cylindrical PMC is considered around the circular periphery of the cavity. The fringing fields between the patch and the ground plane make the antenna look electrically longer than its physical dimensions. Therefore, the dielectric material of the substrate is assumed to be truncated beyond the area of the patch, this has an effect on the resonance frequency of the antenna [4]. The small height (d) of the substrate material only allows fields of TM^Z modes within the substrate with respect to the z-axis.

Fields inside the Cavity

The vector potential approach is used to find the fields within the cavity, and hence the radius of the antenna resonating at a particular frequency. The expressions for the Electric and Magnetic fields can be obtained by the superposition of the individual fields due to the Magnetic vector potentials A and the Electric vector potential F [32]. Since that TM^Z field configurations are considered, F is equal to zero. For TM^Z, the magnetic vector potential A must be solved, which satisfies the homogeneous wave equation, written in cylindrical coordinates i.e. [1, 4, 32];

$$\nabla^2 \mathbf{A} + \beta^2 \mathbf{A} = -\mu \mathbf{J} \qquad \text{where } \beta = \omega\sqrt{\mu\varepsilon} \tag{2.3}$$

Let $\mathbf{A} = \hat{a}_z A_z(\rho,\phi,z)$, and assuming there are no sources in the cavity region, the current density J reduces to zero, and therefore, equation (2.3) reduces to:

$$\nabla^2 A_z(\rho,\phi,z) + \beta^2 A_z(\rho,\phi,z) = 0 \tag{2.4}$$

the electric and magnetic fields are related to the vector potential A_Z by the equations below (using cylindrical coordinates) [4, 32]:

$$E_\rho = -j\frac{1}{\omega\mu\varepsilon}\frac{\partial^2 A_Z}{\partial\rho\partial z} \qquad H_\rho = \frac{1}{\mu}\frac{1}{\rho}\frac{\partial A_Z}{\partial\Phi} \tag{2.5}$$

$$E_\Phi = -j\frac{1}{\omega\mu\varepsilon}\frac{1}{\rho}\frac{\partial^2 A_Z}{\partial\Phi\partial z} \qquad H_\Phi = -\frac{1}{\mu}\frac{\partial A_Z}{\partial\rho} \tag{2.6}$$

$$E_Z = -j\frac{1}{\omega\mu\varepsilon}\left(\frac{\partial^2}{\partial z^2} + B^2\right)A_Z \qquad H_Z = 0 \tag{2.7}$$

If the boundary conditions discussed earlier are assumed:

- Side walls are PMC:

i.e. $$H_\Phi = (\rho = a, 0 \le \Phi \le 2\pi, 0 \le z \le h) = 0 \tag{2.8}$$

- Top and bottom walls are PEC:

$$\text{i.e. Top} \qquad E_\rho = (0 \le \rho \le a, 0 \le \Phi \le 2\pi, z = 0) = 0 \tag{2.9}$$

$$\text{Bottom} \qquad E_\rho = (0 \le \rho \le a, 0 \le \Phi \le 2\pi, z = h) = 0 \tag{2.10}$$

Equation 2.4 above can be solved using the separation of variables method with reference to equations 2.5-2.10, and as shown in [4, 32], the Magnetic Vector Potential may reduce to:

$$A_z(\rho, \Phi, z) = B_{mn} J_m(B_\rho \rho)\left[C_2 \cos(m\Phi) + D_2 \sin(m\Phi)\right]\left[C_3 \cos(B_z z) + D_3 \sin(B_z z)\right] \tag{2.11}$$

Where J_m is the Bessel function of the first kind of order m and

$$B_r{}^2 = B_z^2 + B_\rho^2 = \omega_r^2 \mu\varepsilon \tag{2.12}$$

From equation 2.5-2.7 above

$$H_\Phi = \frac{-1}{\mu}\frac{\partial Az}{\partial \rho} \tag{2.13}$$

$$\text{and} \qquad E_\rho = -j\frac{1}{\omega\mu\varepsilon}\frac{\partial^2 Az}{\partial\rho\partial z} \tag{2.14}$$

Hence applying (2.13) to (2.11) taking into account the boundary condition in (2.8):

$$H_\Phi = \frac{-1}{\mu} B_{mn} J'_m(B_\rho a) B_\rho \left[C_2 \cos(m\Phi) + D_2 \sin(m\Phi)\right]\left[C_3 \cos(B_z z) + D_3 \sin(B_z z)\right] = 0 \tag{2.15}$$

since the radial component of the surface current is assumed to reduce to zero at the edge of the cylindrical cavity, therefore;

$$J'_m(B'_\rho a) = 0 \text{ where } B'_\rho = \frac{\chi'_{mn}}{a} \tag{2.16}$$

for m = 0, 1, 2,… and χ'_{mn} is the zero of the derivative of the Bessel function J_m [36]. Applying (2.14) to (2.11) with reference to the boundary condition (2.9) [4, 32];

$$E_\rho = -j\frac{1}{\omega\mu\varepsilon}B_{mn}J'_m(B_\rho a)B_\rho\left[C_2\cos(m\Phi)+D_2\sin(m\Phi)\right]\left[B_zC_3(-\sin B_z z)+B_zD_3\cos(B_z z)\right]=0 \qquad 2.17$$

for z = 0

$$E_\rho = C_3(0)+D_3(1)=0 \qquad \text{therefore, } D_3=0 \qquad 2.18$$

applying (2.14) to (2.11) with reference to the boundary condition (2.10):

$$E_\rho = -j\frac{1}{\omega\mu\varepsilon}B_{mn}J'_m(B_\rho a)B_\rho\left[C_2\cos(m\Phi)+D_2\sin(m\Phi)\right]\left[B_zC_3(-\sin B_z z)+B_zD_3\cos(B_z z)\right]=0 \qquad 2.19$$

$D_3 = 0$ and $z = h$ from above, therefore

$$E_\rho = -B_zC_3(\sin B_z h)=0 \qquad \text{i.e. } E_\rho=(\sin B_z h)=0 \qquad 2.20$$

$$\text{where } B_z=\frac{\pi}{h}or\frac{p\pi}{h} \text{ and p = 0,1,2,3 … etc.} \qquad 2.21$$

Using (2.12), (2.16) and (2.21) above

$$B_r{}^2 = B_z^2+B_\rho^2=\left(\frac{\chi'_{mn}}{a}\right)^2+\left(\frac{p\pi}{h}\right)^2=\omega_r^2\mu\varepsilon \qquad 2.22$$

$$fr_{mnp}^{TMz}=\frac{c}{2\pi\sqrt{\mu\varepsilon}}\sqrt{\left(\frac{\chi'_{mn}}{a}\right)^2+\left(\frac{p\pi}{h}\right)^2} \qquad v_g=\frac{c}{\sqrt{\varepsilon_r}}=\frac{1}{\sqrt{\mu\varepsilon}} \qquad 2.23$$

$$fr_{mnp}^{TMz}=\frac{c}{2\pi\sqrt{\varepsilon_r}}\sqrt{\left(\frac{\chi'_{mn}}{a}\right)^2+\left(\frac{p\pi}{h}\right)^2} \qquad 2.24$$

And using (2.18), the magnetic vector potential A_z reduces to

$$Az(\rho,\Phi,z)=B_{mn}J_m(B_\rho\rho)C_3\cos(B_z z)\left[C_2\cos(m\Phi)+D_2\sin(m\Phi)\right] \qquad 2.25$$

To find the fields within the cavity, the vector potential approach can be further used, and the electric fields within the cylindrical region are given by [1, 4, 16, 31, 32, 36]:

$$E_z = E_o J_n(B\rho)\cos n\phi \qquad 2.26$$

$$H_\rho = -\frac{j}{\omega\mu\rho}\cdot E_0 \cdot J_n(B\rho)\sin n\phi \qquad 2.27$$

$$H_\phi = \frac{j}{\omega\mu}\cdot E_0 \cdot J'_n(B\rho)\cos n\phi \qquad 2.28$$

Where J_n is the Bessel function of the first kind and order n. Figure 2.4 [1] below shows the fields distribution inside the cavity for various $TM_{mn}{}^{Z}$ modes.

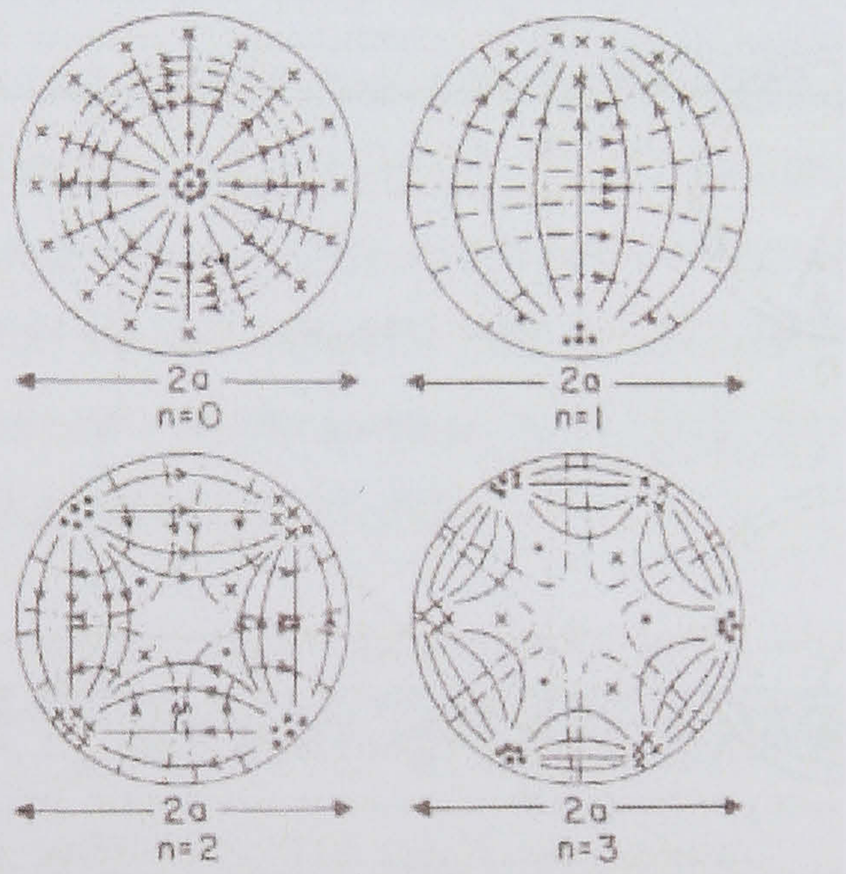

Figure 2.4 Fields distribution for various modes at resonance (m=1) assuming PMC at the sides and PEC at the top and bottom [1].

If the E and M fields in Figure 2.4 are replaced with each other, and the boundary conditions changed to PEC on the top and bottom, then those diagrams are the same as the fields pattern for TE_{mn} circular wave guides shown in Figure 2.5.

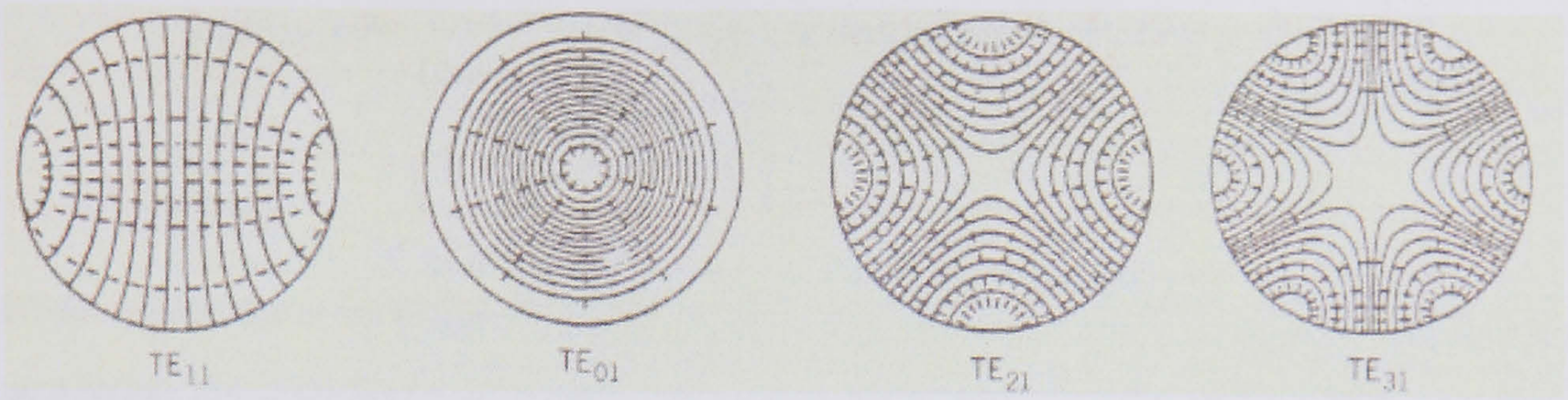

Figure 2.5 Circular waveguide Fields distribution for various modes at resonance [1].

Far Fields

The far fields of a circular microstrip antenna can be found using the potential functions [12], either by considering the E_z field across the aperture between the disk and the ground plane at $\rho = a$ (i.e. using vector electric potentials) or from currents in the disk conductor (i.e. using vector magnetic potential). The radiation in the upper half space is derived using the image theory [4, 12, 32]. The ground plane is replaced by an equivalent magnetic current, which results in doubling the equivalent magnetic current, and the vector electric potential can be calculated by integrating this equivalent magnetic current over the aperture. As a result, the far fields in standard spherical coordinates is given by [12, 31, 36]:

$$E_\theta = -j_n \cdot \frac{VaK_0}{2} \cdot \frac{e^{-jkor}}{r} \cos n\phi \cdot [J_{n+1}(K_0 a \sin\theta) - J_{n-1}(K_0 a \sin\theta)] \qquad 2.28$$

$$E_\phi = -j_n \cdot \frac{VaK_0}{2} \cdot \frac{e^{-jkor}}{r} (\cos\phi)(\sin n\phi) \cdot [J_{n+1}(K_0 a \sin\theta) - J_{n-1}(K_0 a \sin\theta)] \qquad 2.29$$

where a is the radius of the disc.

K_0 is wave number.

V is the edge voltage.

electric source currents can also be employed to derive expressions for the far fields [4]:

$$E_\theta = -j_n \cdot \frac{VaK_0}{2} \cdot \frac{e^{-jkor}}{r} \cos n\phi \cdot \frac{\sin(K_0 h \cos\theta)}{K_0 h \cdot \cos\theta} \cdot [J_{n+1}(K_0 a \sin\theta) - J_{n-1}(K_0 a \sin\theta)] \qquad 2.30$$

$$E_\phi = -j_n \cdot \frac{VaK_0}{2} \cdot \frac{e^{-jkor}}{r} (\cos\phi)(\sin n\phi) \cdot \frac{\sin(K_0 h \cos\theta)}{K_0 h \cdot \cos\theta} \cdot [J_{n+1}(K_0 a \sin\theta) - J_{n-1}(K_0 a \sin\theta)] \quad 2.31$$

Both expressions in (2.28-31) leading to the same field are different [12]. The field equations derived from the vector electric potential approach differ from the ones derived from the vector magnetic potential approach by a factor F,

$$\text{where F} = \frac{\sin(K_0 h \cos\theta)}{K_0 h \cdot \cos\theta} \quad 2.32$$

However, employing the assumption $h << \lambda$, or $K_0 h << 1$, F reduces to unity and therefore, the assumption $h << \lambda$ made the fields essentially independent of the manner of the derivation. The radiation pattern expression (2.28) and (2.29) were computed for the TM_{11} mode and shown in Figure 2.6 (Code can be found in Appendix A).

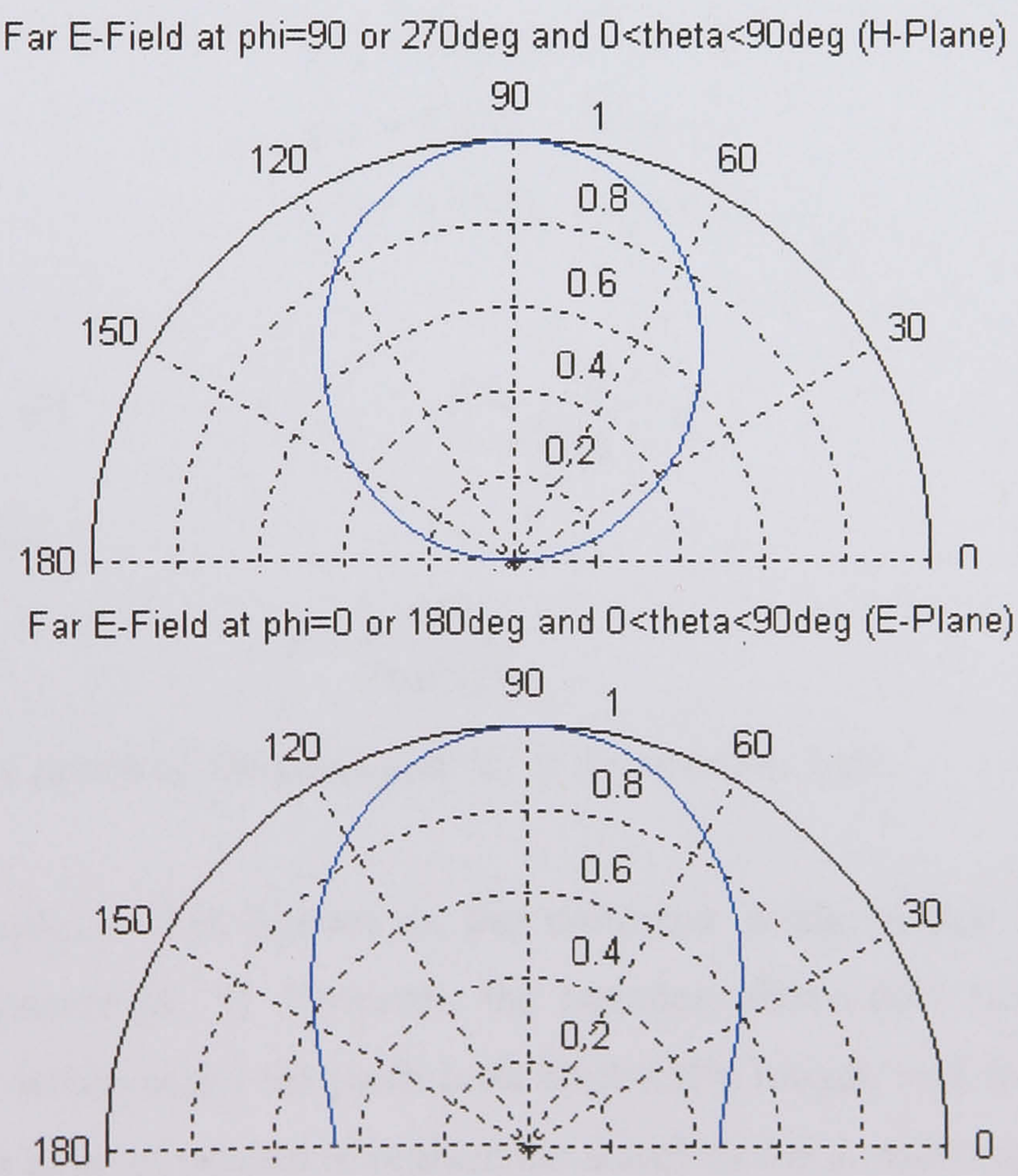

Figure 2.6 Antennas Radiation pattern for the TM11 mode, (a) E fields at Φ=0 and (b) E fields at Φ=90.

Resonant Frequency

The resonant frequency of the cavity, and accordingly the antenna are found using the analysis earlier. Considering that the substrate height is very small ($h < 0.05\ \lambda$) for most microstrip antennas, the fields along "z" are essentially constant. Therefore the resonant frequency for the TM_{mn0} modes can be derived from equation (2.24) as follows [1, 4, 16, 21, 36, 37]

$$\frac{\chi'_{mn}}{a} = \frac{2\pi f_r (\varepsilon_r)^{1/2}}{c} \qquad 2.33$$

Where χ'_{mn} in the equation above is the zeros of the derivative of the Bessel function $J_m(x)$ and they determine the order of the resonant frequency.

The first four values for χ'_{11} are:

$$\chi'_{11} = 1.8412 \quad \text{for } n = 1$$
$$\chi'_{21} = 3.0542 \quad \text{for } n = 2$$
$$\chi'_{01} = 3.832 \quad \text{for } n = 0$$
$$\chi'_{31} = 4.2012 \quad \text{for } n = 3$$

from (2.33)
$$f_r = \frac{c\chi'_{mn}}{2\pi a(\varepsilon_r)^{1/2}} \qquad 2.34$$

and for the $TM_{110,}$

$$f_r = \frac{1.8412 \cdot c}{2\pi a(\varepsilon_r)^{1/2}} \qquad 2.35$$

where "a" is the radius of the patch and "c" is the speed of light.

The TM_{110} mode is also known as the dominant mode, which has the lowest resonance frequency [4, 5]. However, the equation above does not count for the fringing fields, which make the patch look electrically longer, and therefore the term effective radius a_e is introduced to replace the actual radius a, where a_e equals to [1, 4, 12, 16, 31, 38-40]:

$$a_e = a\{1 + \frac{2h}{\pi a \varepsilon_r}[\ln\frac{\pi a}{2h} + 1.7726]^{1/2}\} \qquad 2.36$$

and the resonant frequency in (2.35) for the dominant mode TM_{110} becomes [4, 12, 31, 37, 41]:

$$f_{r(110)} = \frac{1.8412 \cdot c}{2\pi a_e (\varepsilon_r)^{1/2}} \qquad 2.37$$

This is known as the zero[th]-order resonant frequency of the antenna, thus the lowest order mode is the TM_{110}. Looking at the values of zeros of the derivative of the Bessel function, it is obvious that the next higher order modes are the TM_{210}, the TM_{010} and the TM_{310} modes [41].

Equation (2.37) was originally found by Wolff, other methods were also proposed by Howell, Derneryd and Kumprasert [37]. A comparison in terms of accuracy is shown in Figure 2.7 from a study that Kumprasert performed [37].

r (cm)	h (cm)	ε_r –	h/λ_d –	Measured (GHz)	Howell (GHz)	Wolff (GHz)	Derneryd (GHz)	Kumprasert (GHz)
3.493	0.1588	2.50	0.013	1.570	1.580	1.569	1.537	1.555
1.270	0.0794	2.59	0.018	4.070	4.290	4.267	4.159	4.175
3.493	0.3175	2.50	0.025	1.510	1.580	1.526	1.478	1.522
13.894	1.2700	2.70	0.026	0.378	0.387	0.362	0.350	0.370
4.950	0.2350	4.55	0.014	0.825	0.833	0.836	0.814	0.827
3.975	0.2350	4.55	0.017	1.030	1.037	1.042	1.009	1.027
2.990	0.2350	4.55	0.023	1.360	1.379	1.384	1.332	1.358
2.000	0.2350	4.55	0.034	2.003	2.061	2.067	1.965	2.009
1.040	0.2350	4.55	0.063	3.750	3.963	3.950	3.661	3.744
0.770	0.2350	4.55	0.083	4.945	5.353	5.308	4.848	4.938

Figure 2.7 Comparison of measured and calculated resonant frequencies of circular microstrip disk antenna [37].

In most cases, the calculated resonance frequency is found higher than the measured one, the error is typically less than ±2.5% [31, 41]. As shown above, Kumprasert achieved most accurate results so far, but Wolff also obtained fairly accurate results too. Various alternative methods of analysis have been also reported, among these are Wire Grid Model, Modal Analysis, Full wave analysis method and Greens functions Method [12].

2.3. Conductance, Directivity and Gain

The conductance due to the radiated power of circular microstrip patch antenna can be defined as [4, 12, 31]:

$$G_{rad} = 2P_{rad}/|V_0|^2 \qquad 2.38$$

Where P_{rad} is the radiated power. Conduction (ohmic) and dielectric losses should also be taken into account and this results in total conductance [4, 31]:

$$G_{tot} = G_{rad} + G_c + G_d \qquad 2.39$$

Where

$$G_{rad} = \varepsilon_{m0} \cdot \frac{(k_0 \cdot a)^2}{480} \cdot \int_0^{\pi/2} [B_M{}^2(k_0 \cdot a \cdot \sin\theta) + \cos^2\theta \cdot B_P{}^2(k_0 \cdot a \cdot \sin\theta)] \cdot \sin\theta \cdot d\theta \qquad 2.40$$

$$B_P(X) = J_{m-1}(X) + J_{m+1}(X)$$

$$B_M(X) = J_{m-1}(X) - J_{m+1}(X)$$

ε_{m0} → 2 for m = 0

→ 1 for all other values of m.

$$G_c = \frac{\varepsilon_{m0}\pi(\pi\mu_0 f_r)^{-3/2}}{4h^2\sqrt{\sigma}}\left[(ka_e)^2 - m^2\right] \qquad 2.41$$

$$G_d = \frac{\varepsilon_{m0}\tan\delta}{4\mu_0 h f_r}\left[(ka_e)^2 - m^2\right] \qquad 2.42$$

Equations (2.38-2.42) were computed in Matlab as shown in Figure 2.8 (code can be found in appendix A). A comparison of the radiation conductance for various TM_{mn} modes is also shown [31].

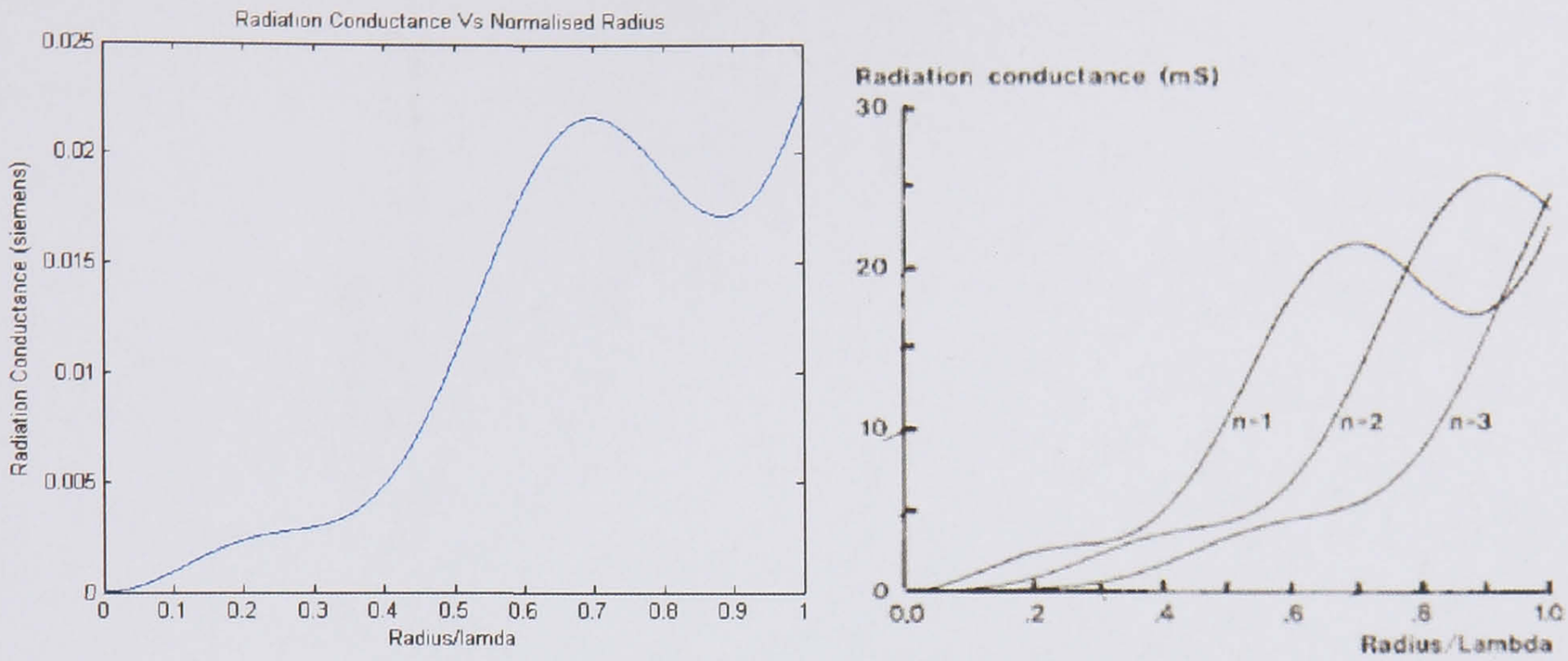

Figure 2.8 Left: Radiation conductance against the normalised radius at resonance of disk antenna excited in TM_{11} mode. Right: Comparison of the radiation conductance at various TM modes. [31]

The directivity of an antenna is "the ratio of the radiation intensity in a given direction from the antenna to the radiation intensity averaged over all directions" [4] and can be expressed as;

$$Do = P_{max}/P_{avg} \qquad 2.43$$

For microstrip antennas it can be expressed as [4, 31];

$$D_0 = (K_0\, a_e)/120G_{rad} \qquad 2.44$$

The directivity represents the maximum power density to the average radiated power density. Equation (2.44) was plotted using Matlab in Figure 2.9 (code can be found in appendix A). The directivity is plotted as a function of the radius and resonant frequency for various substrates of the disk in Figure 2.10 [31].

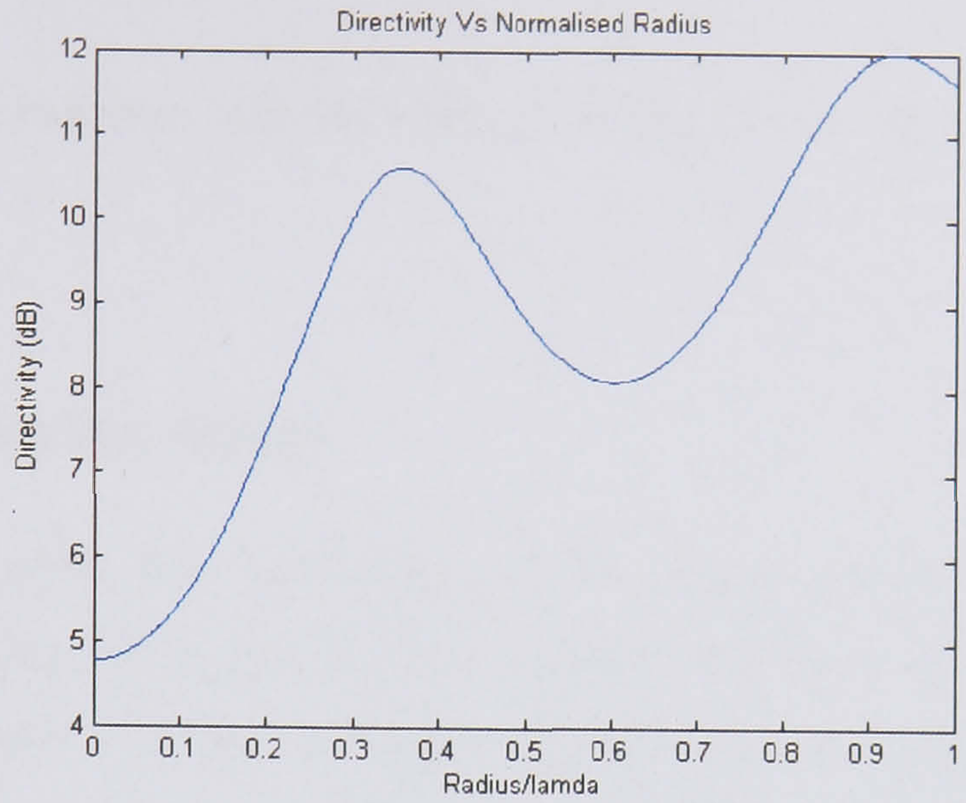

Figure 2.9 Directivity as a function of the radius of the disk [31]

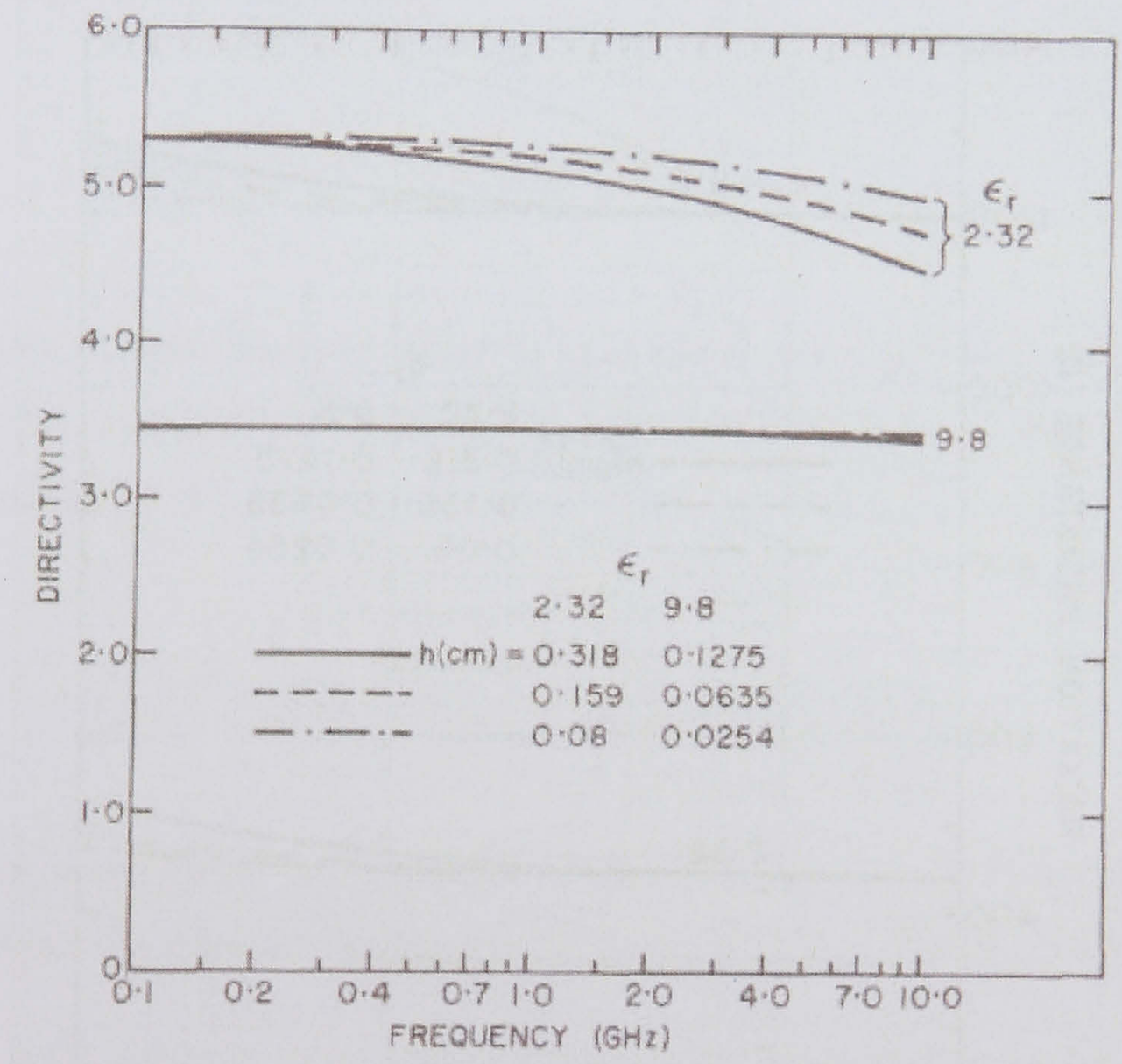

Figure 2.10 Directivity as a function of frequency for various substrates of the disk [31]

The gain of circular microstrip antennas G_n can be defined as the ratio of the radiation intensity in a given direction to the power fed to the antenna. This power includes all ohmic and the dielectric losses. The gain can be defined as:

$$G_n = 4\pi U/P_{in} \rightarrow \qquad G_n = e_r D_0 \qquad 2.45$$

Where "e_r" is the radiation efficiency shown in Figure 2.12 and defined in the next section.

2.4. Quality factor

The quality factor and bandwidth of the antenna besides beam width and efficiency are mainly the figures of merit of microstrip patch antennas. They are all interrelated and there is always a tradeoff between them in arriving at an optimum performance. The Q factor represents the antenna losses, these are radiation, conduction (ohmic), dielectric and surface wave losses. A simple expression for the quality factor was reported in [18]:

$$Q = \frac{b\mu_0\omega\delta\sigma}{2} = 0.707(\omega\mu_0\sigma)^{0.5} b \qquad 2.46$$

However, the expression above does not count for the fringing fields and the radiation from the disc. In general, considering the latter factors, the total quality factor Q can be expressed as [4, 15, 31]:

$$\frac{1}{Q_{total}} = \frac{1}{Q_{radiation}} + \frac{1}{Q_{conduction}} + \frac{1}{Q_{dielectric}} + \frac{1}{Q_{SurfaceWaves}} \qquad 2.47$$

The surface wave factor is very small (negligible) for very thin substrates (i.e. the assumption $h<<\lambda$), however the rest can be approximated in equations (2.48-50) [1, 4, 15, 31]:

$$Q_{conduction} = h\sqrt{\pi f\mu\sigma} \qquad 2.48$$

$$Q_{dielectric} = \frac{1}{\tan\delta} \qquad 2.49$$

$$Q_{radiation} = \frac{30\left[(ka)^2 - n^2\right]}{hf\mu_0 (k_0 a)^2 I_1} \qquad 2.50$$

$$\text{Where } I_1 = \int_0^{\pi/2}\left[J_n'^2(k_0 a\sin\theta) + \cos^2\theta J_n^2 \frac{(k_0 a\sin\theta)}{(k_0 a\sin\theta)^2}\right]\sin\theta d\theta$$

As shown in (2.50), $Q_{radiation}$ is inversely proportional to the height of the substrate, and for very thin substrates is usually the dominant factor. This also explains why the bandwidth of the antenna increases if the substrate height is increased.

Figure 2.11 shows the variation of the total quality factor Q against the resonant frequency for various substrate thicknesses and dielectric constants.

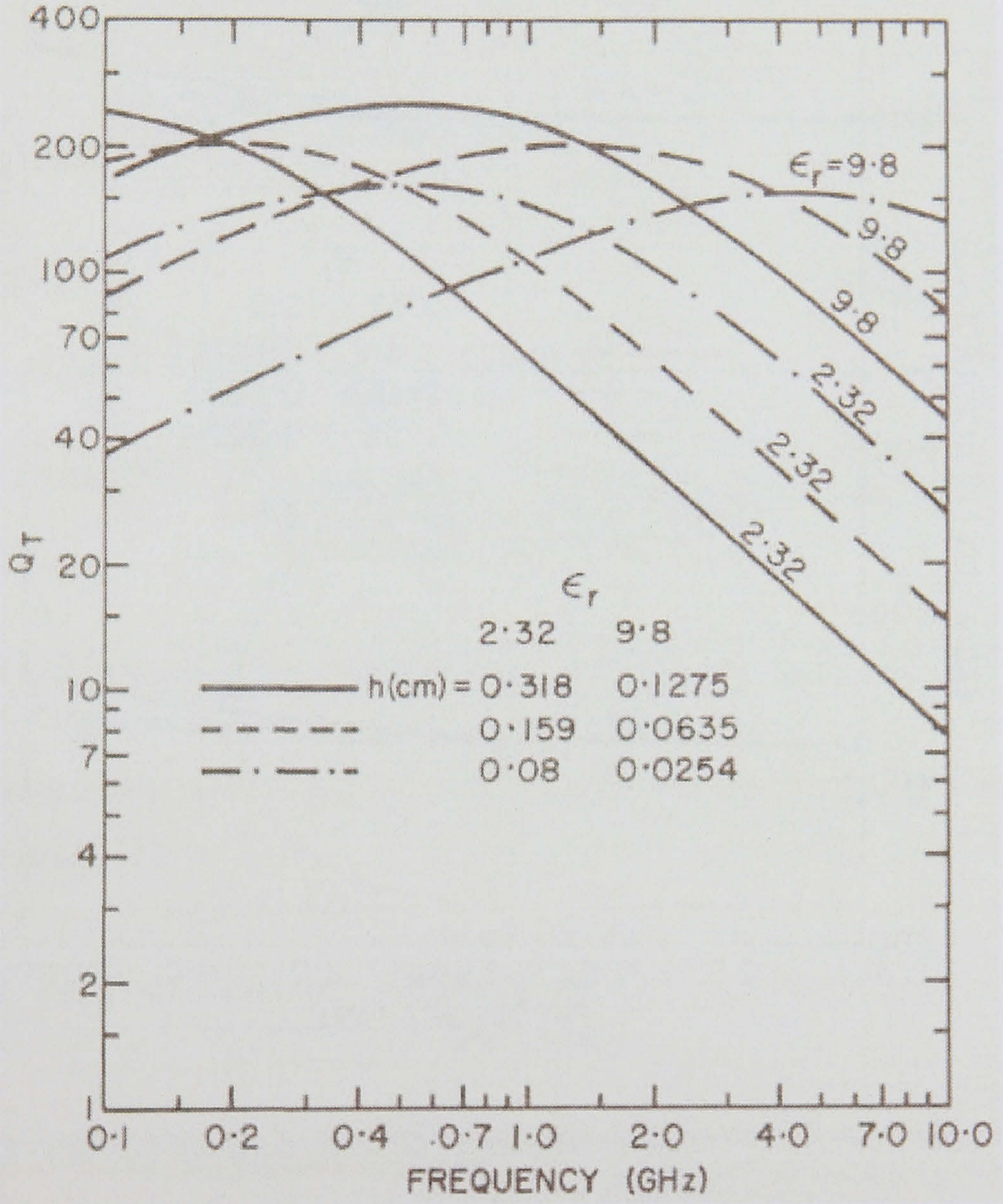

Figure 2.11 Total Quality Factor against frequency for antennas with various dielectric constants and thicknesses. [1, 12, 16]

As shown, increasing the thickness and reducing the dielectric constant reduce the value of the total quality factor. The fractional bandwidth of the antenna is inversely proportional to the total quality factor,

$$\text{i.e.} \quad \frac{\Delta f}{f_0} \propto \frac{1}{Q_t} \qquad \text{since} \qquad BW = \frac{VSWR - 1}{Q\sqrt{VSWR}} \qquad 2.51$$

The bandwidth is inversely proportional to the square root of the dielectric constant [4]. Figure 2.12 shows typical variations of the bandwidth as a function of the normalised height of the substrate [4, 5]. It is clearly shown that the bandwidth increases as the substrate height increases.

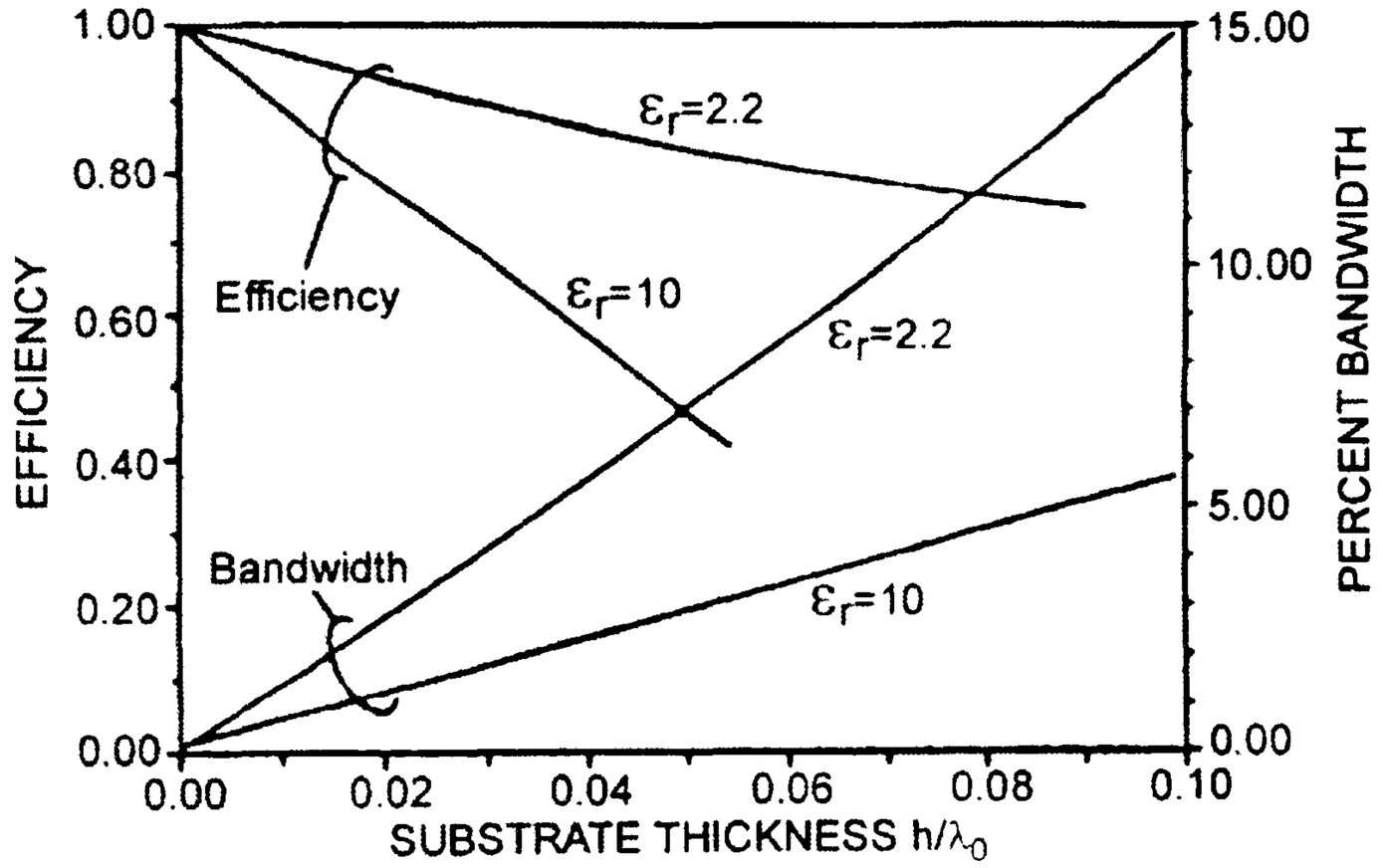

Figure 2.12. Efficiency and bandwidth in terms of substrate thickness and permittivity [4, 5].

The radiation efficiency, i.e. the radiated power over the input power, can also be expressed as [4, 15],

$$e_{cdsw} = \frac{1/Q_{rad}}{1/Q_{tot}} = \frac{Q_{tot}}{Q_{rad}} \qquad 2.52$$

Variations of this are also shown in Figure 2.12.

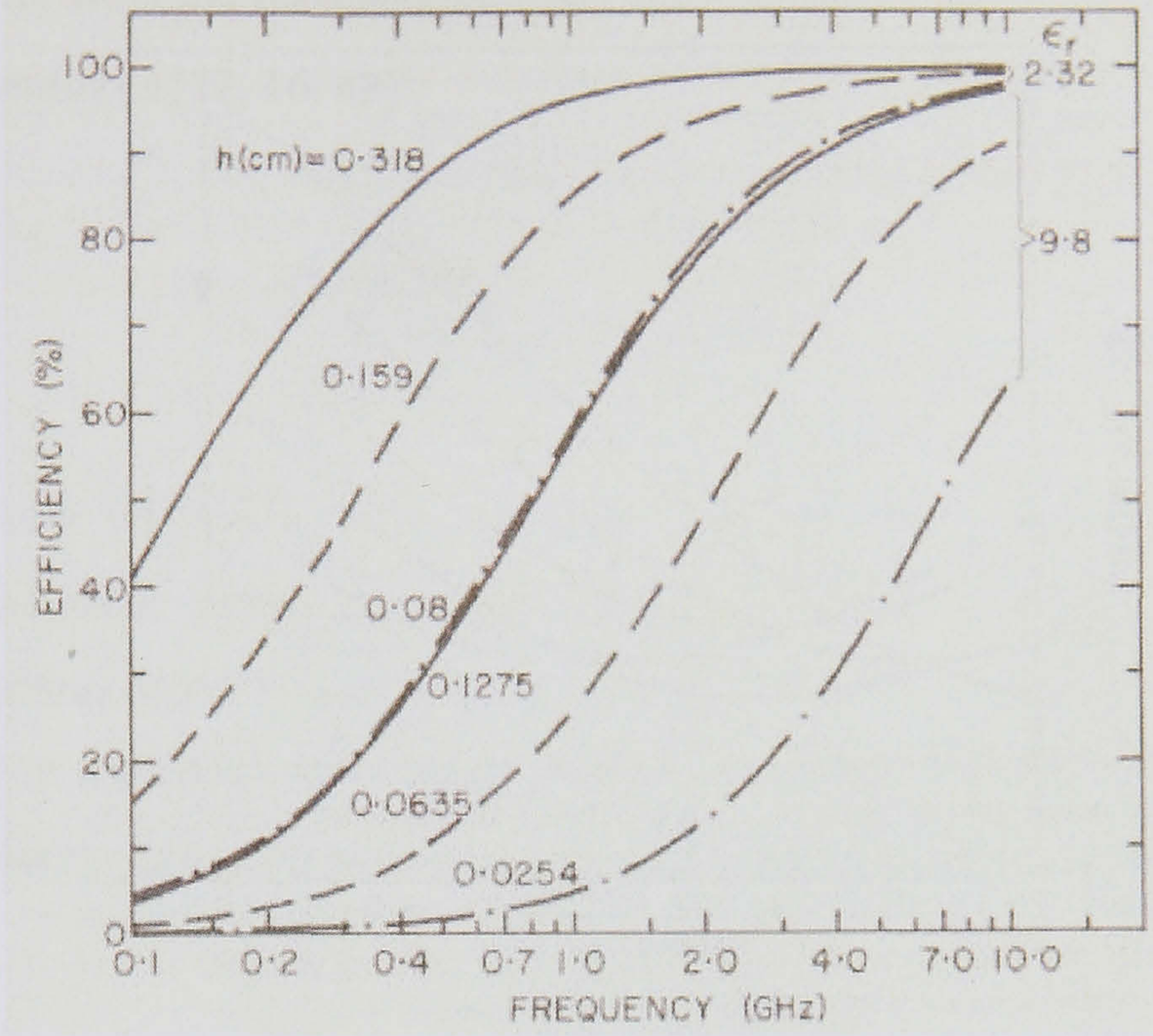

Figure 2.13 Antennas radiation efficiency against frequency for various dielectric constant and thickness [1, 12, 16].

Although the overall efficiency decreases as the substrate height increase, the radiation efficiency increases with thicker substrates as shown in Figure 2.13. This may result in wider bandwidth (as Figure 2.12 implies) but the trade-off here is the antenna efficiency. If lower efficiencies can be tolerated, thicker substrates may be used to achieve wider bandwidths.[14, 16]

2.5. Input impedance

The input impedance of a microstrip antenna at resonance is real. The resonant resistance can be presented using the total Power lost P_t [12]:

$$R = \frac{V^2}{2P_t} \text{ where V is the edge peak voltage} = hE_0 Jn(ka) \qquad 2.53$$

Furthermore, if R_0 is the resistance at resonance for the feed location $\rho_0 = a$ then R can be represented as [12, 16, 42]:

$$R = R_0 \cdot \frac{Jn^2(k\rho_0)}{Jn^2(ka)} = \frac{1}{G_T} \cdot \frac{Jn^2(k\rho_0)}{Jn^2(ka)} \qquad 2.54$$

Where ρ_0 is the radius, G is the total conductance which accounts for radiated, dielectric and ohmic conductance. Equation (2.54) is plotted in Figure 2.14a for a circular microstrip patch antenna built on Duroid 5880 and operating at 2GHz (code can be found in Appendix A). Figure 2.14b-c also shows the total conductance for various substrate heights and the variation of the input impedance as a function of the radius [31].

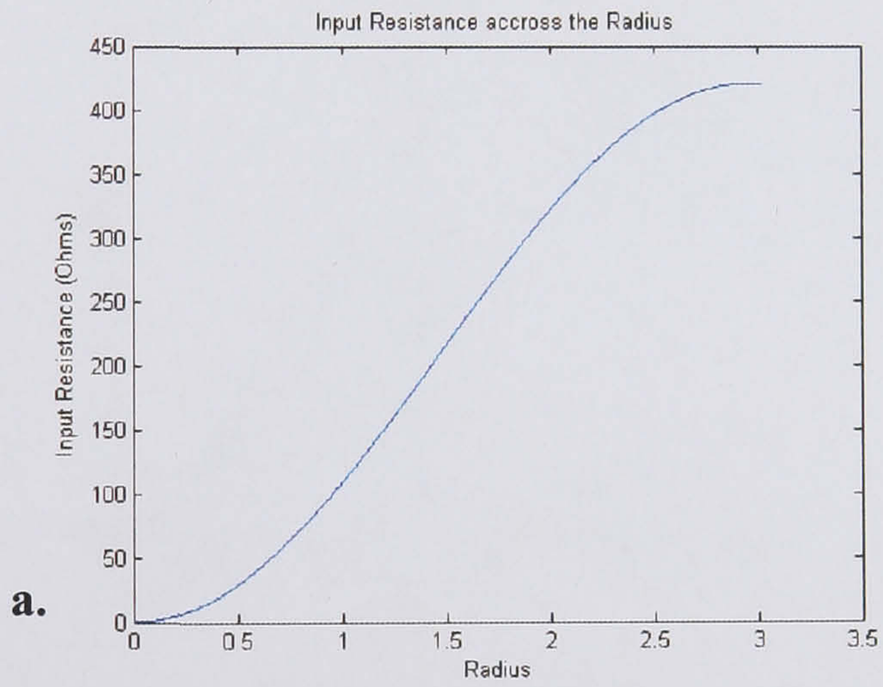

a.

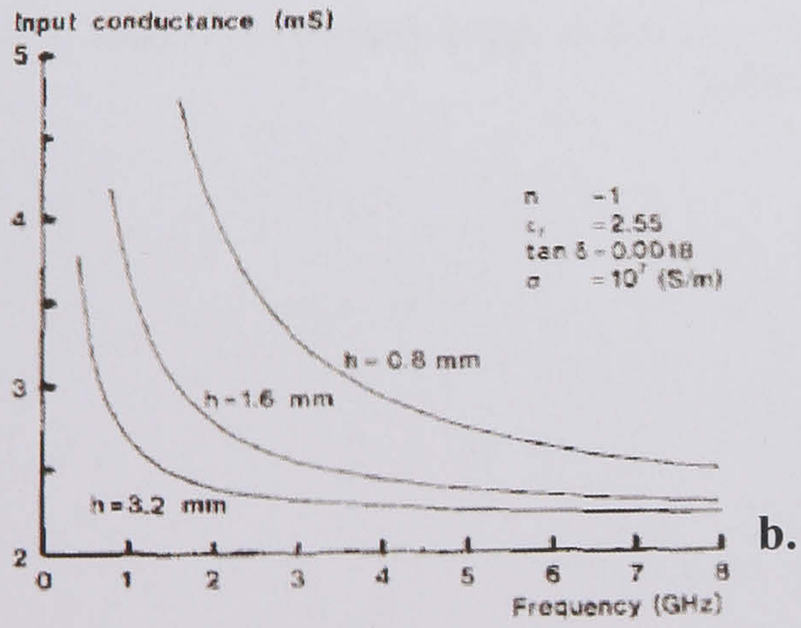

b.

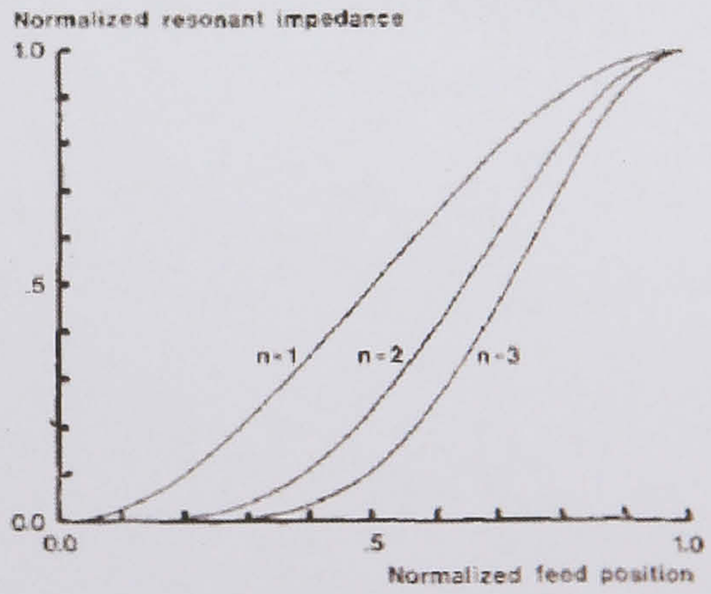

c.

Figure 2.14. A. the input conductance of circular patch antenna designed at 2GHz and excited in TM modes. B. Input conductance as a function of frequency for various substrates. C. Comparison of the circular patch antenna input impedance excited in TM_{1n} modes.

Figure 2.15 shows the input impedance of circular microstrip antenna as a function of the feed point along the disc radius for different substrate thicknesses.

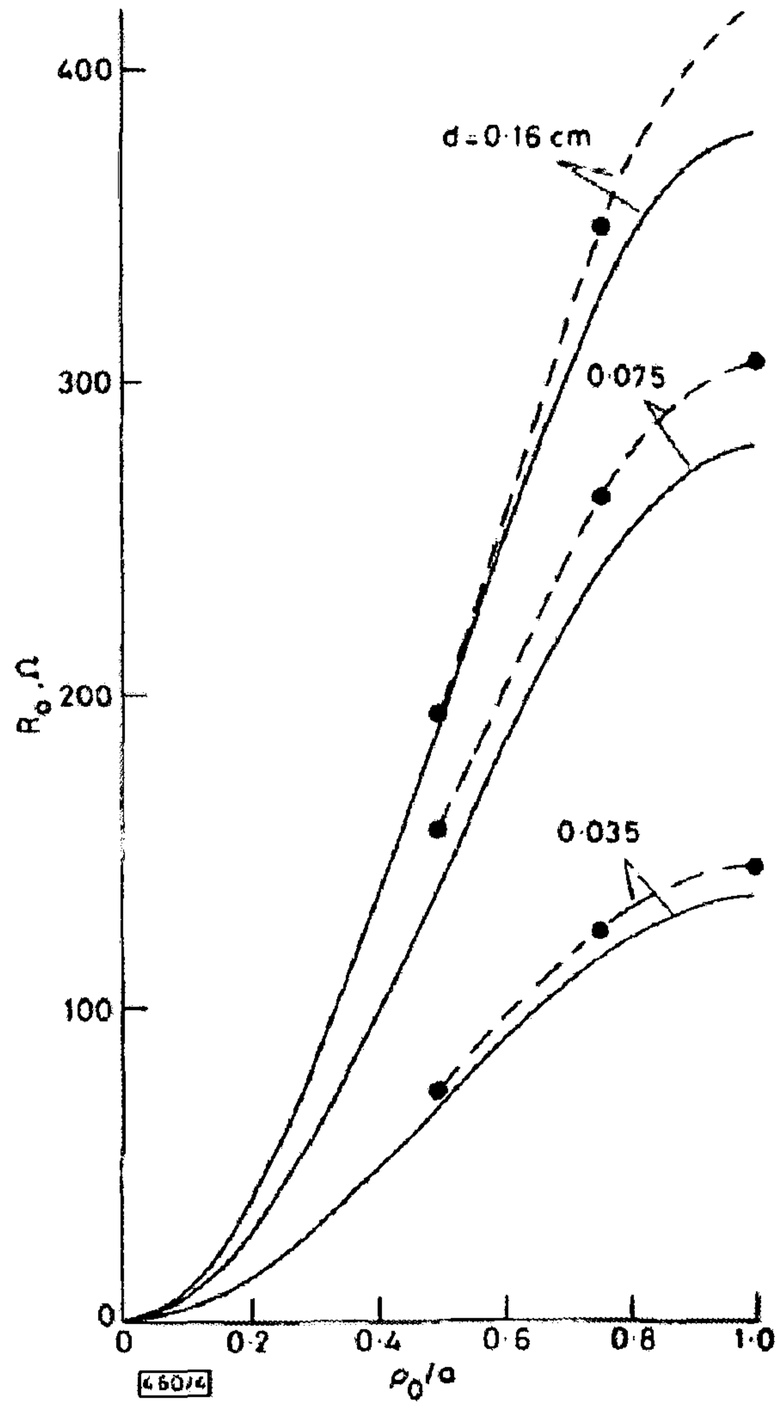

Figure 2.15 Antenna input resistance plotted against feed point position for various substrate thicknesses. [12, 43]

2.6. Feeding methods

Various feeding techniques have been developed, and the selection is governed by many factors and considerations. The most significant is an efficient power transfer between the feed and the radiating elements (i.e. The impedance matching between the two). Associated with this are impedance transformers, bends, stubs, junctions and transitions, which introduce discontinuities leading to spurious radiation. Besides this is the suitability of the feed for array applications. Below is a summeay of feeding techniques used for patch antennas.

2.6.1. Microstrip line feed

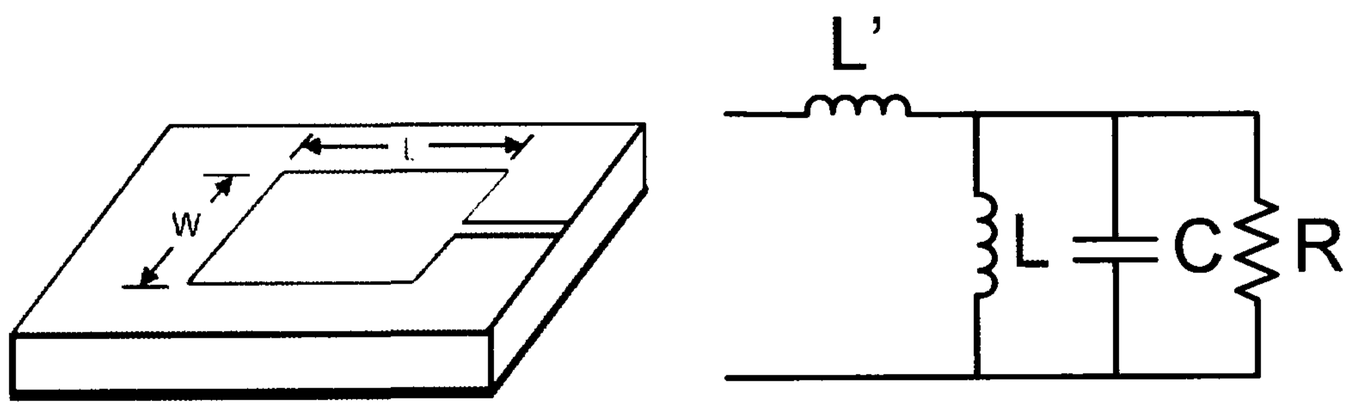

Figure 2.16. Microstrip line feed and the equivalent circuit.

Features [2, 4];

- First introduced in the 1970s.
- Easy to fabricate, and allows the total structure to remain planar.
- Simple to match by controlling the inset position.
- Simple to model.
- As thickness increases surface waves and spurious feed radiation increase.
- Narrow bandwidth.

2.6.2. Coaxial line feed

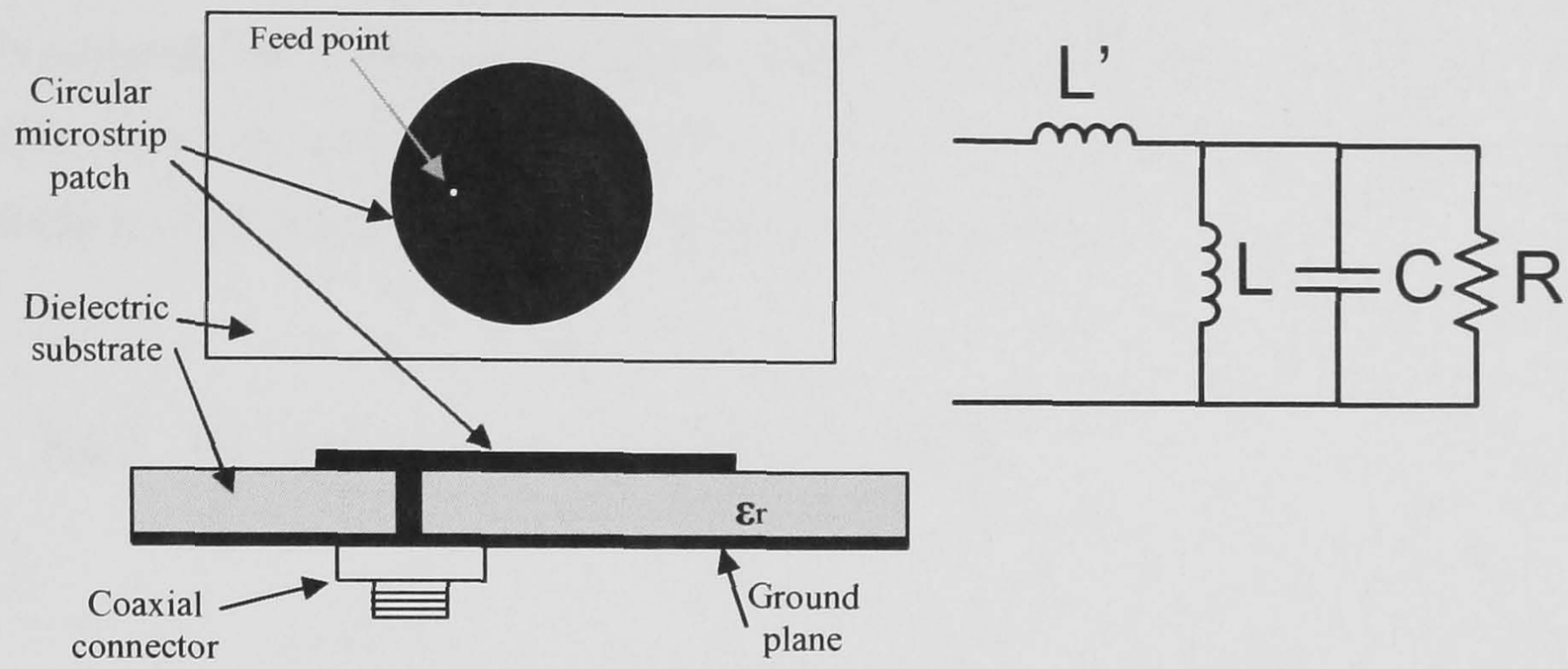

Figure 2.17 Coaxial line feed and the equivalent circuit.

Features [2, 4];

- First introduced in the1970s.
- Inner conductor of the coaxial cable is attached to the radiation patch and the outer conductor to the ground plane.
- Easy to fabricate and match (not as easy as planar)
- Low spurious radiation and narrow bandwidth.
- More difficult to model especially for thick substrates (h>0.05λ). As the inner conductor becomes longer, the input impedance becomes more inductive and more difficult to match.

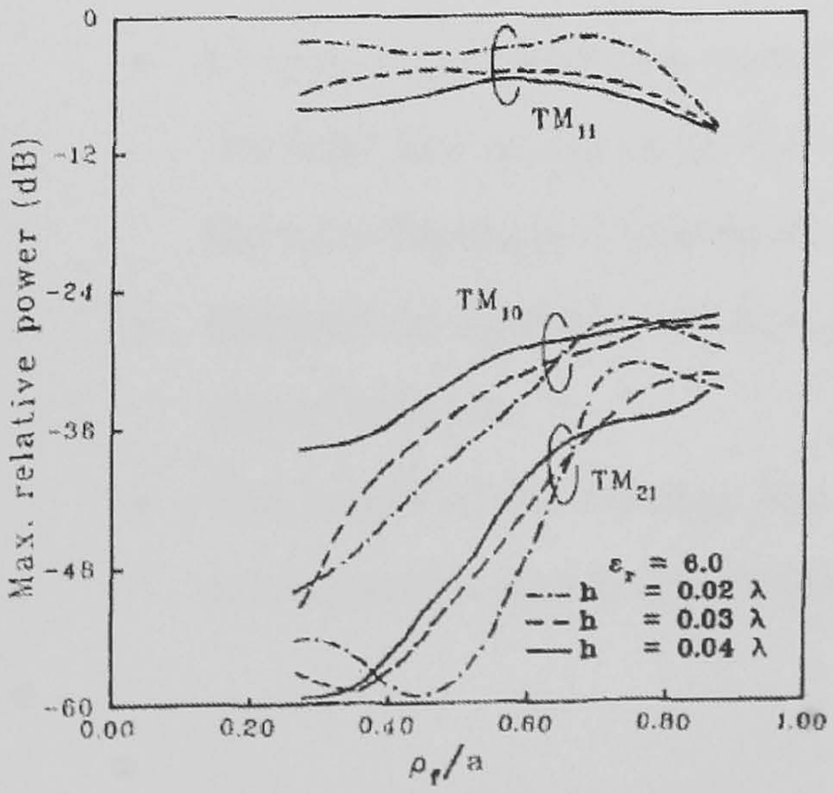

Figure 2.18 The effect of the feed position on the excitation efficiency of the TM_{mn} mode.

For coaxial feeds, the feed location is chosen to provide the desired impedance matching and proper excitation of the required mode. In particular, the excitation efficiency is affected by the feed position and the order mode. Figure 2.18 shows the power excited to the antenna from a coaxial feed along various positions on the antenna [40].

This shows that TM_{11} mode is the most efficient for this feeding technique. One main advantage of coaxial feed is that the inner conductor can be located across the antenna radius for good impedance matching. Since it is located under the ground plane and usually isolated, the coupling between the cable and ground plane is minimised. On the other hand, by using coaxial feed the structure becomes non-monolithic and potentially hard to integrate on microstrip circuits systems[16].

2.6.3. Proximity-coupled multi-layer feed

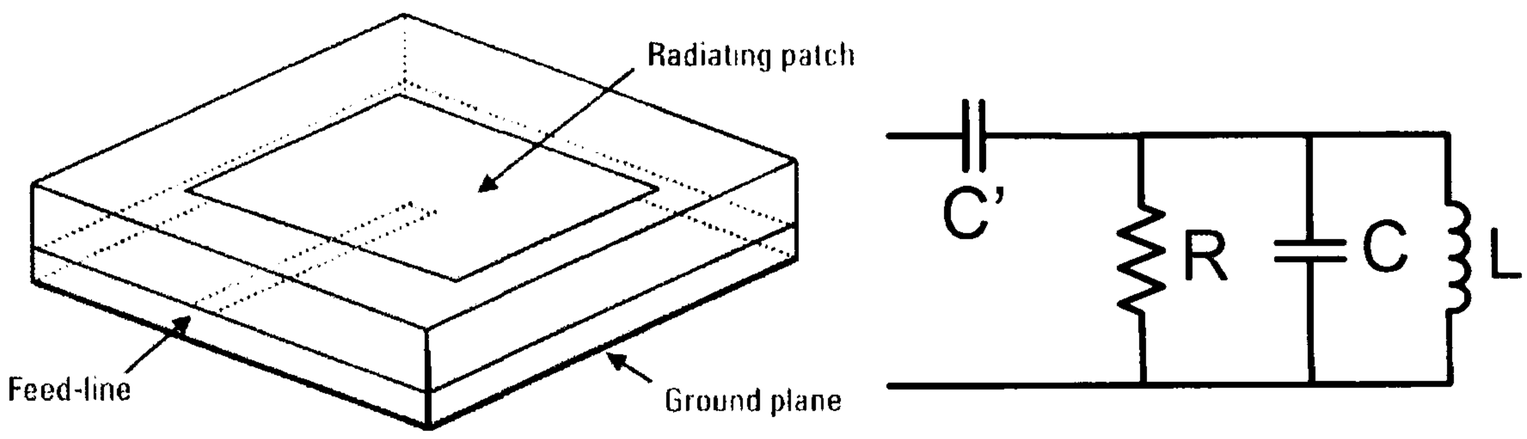

Figure 2.19 Proximity-coupled multi-layer feed and the equivalent circuit. [4].

Features [2, 4];

- It offer the largest bandwidth for the antenna. This method overcomes the problem of feed radiation or increased feed inductance when the substrate thickness increases.
- Easy to model.
- Choice of two dielectric materials, one for the antenna and the other for the feed line to optimise the performance. Increased bandwidth since the total thickness is increased.
- Difficult to fabricate, as accurate alignment is required and increased size of antenna.
- The length of the feeding stub and the width-to-line ratio of the patch can be used to match the circuit.

2.6.4. Aperture-Coupled feed

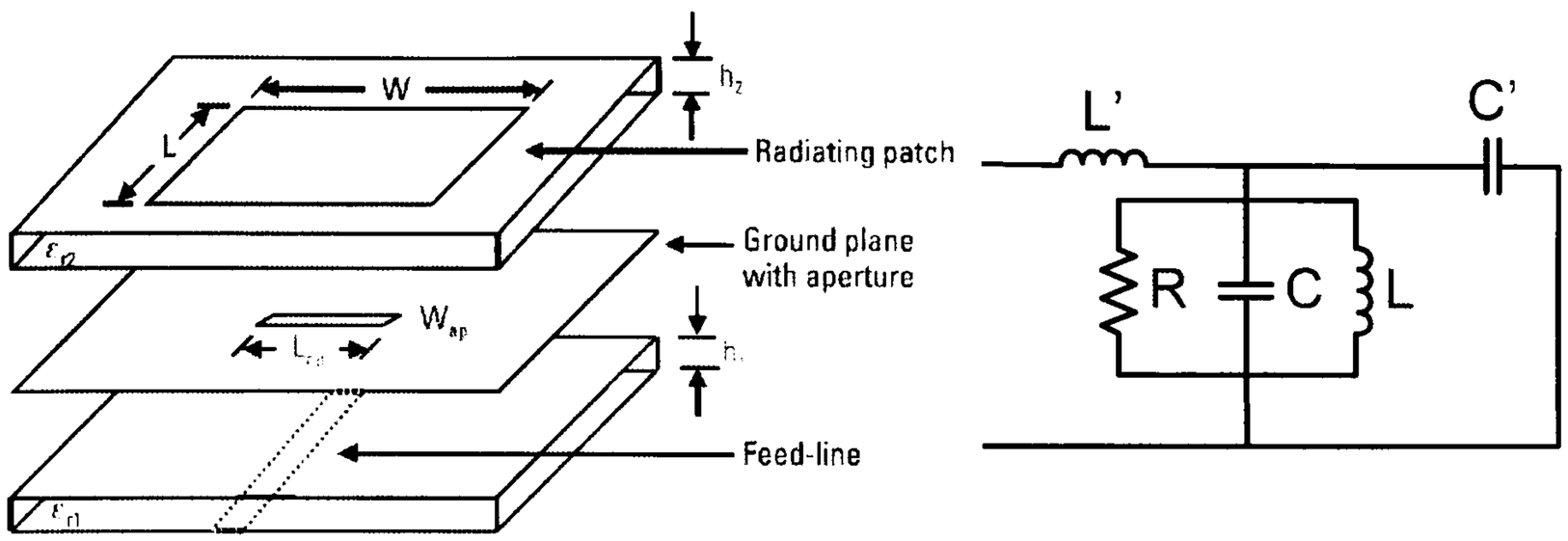

Figure 2.20 Aperture-Coupled feed and equivalent circuit. [4]

Features [2, 4, 25]:

- Overcomes the problem of generating higher order modes and offers an increased bandwidth for the antenna.
- Difficult to fabricate.
- Easier to model and has moderate spurious radiation.
- Energy is coupled through the slot from the feed line to the patch.
- ε_{r1} is high and ε_{r2} is low and the dielectric thick.
- The ground plane also isolates the feed line from the patch (radiation), and minimise the interference of spurious radiation for pattern formation and polarisation purity.
- The design can be optimised using the following factors.
    i. Substrate electrical parameters.
    ii. Feedline width.
    iii. Slot size.
    iv. Position.
- Matching is performed by controlling the width of the feed line and the length of the slot.
- The design can be modelled using the theory of Bethe.

2.7. Summary

The theory of the microstrip patch antenna was reviewed in this chapter. The structure, radiation and various analysis techniques were discussed. Microstrip antennas are naturally resonant, it was explained how the antenna can be modelled as a high quality cavity resonator, and therefore has a small bandwidth. The bandwidth can be improved by increasing the thickness at the expense of the antennas efficiency. The input impedance expression was derived and plotted to help designing antennas in the next two chapters. Various feeding techniques were discussed, however, the coaxial line feed is the one used for most of the designs described in this thesis.

Chapter 3. Broadband Matching Techniques

The word "bandwidth" might refer to three definitions, these are impedance, polarisation and pattern bandwidth. The impedance bandwidth defines the frequency band over which the antenna remains matched within a specified level (e.g. 6dB return loss or VSWR<2). The polarisation bandwidth defines the loss that can occur due to polarisation mismatch, while the pattern bandwidth states the frequency band at which the radiation pattern of an antenna is constant, or a measure of radiation from the antenna to free space [14, 44]. Ideally, the antenna is expected to meet both the impedance and pattern bandwidth for a particular polarisation. However, the pattern bandwidth is usually broader than the impedance bandwidth, which (as all resources agree) is usually a struggle to meet for broadband microstrip antennas [1, 45, 46]. The main reason for this is that microstrip antennas are modelled as cavity resonators which have a resonant nature and high quality factor [44]. Also, the quick change of the input impedance with respect to the frequency makes it difficult to obtain good matching over wide frequency bands [6].

The first and simplest way of increasing the bandwidth of the antenna is by increasing the thickness and reducing the dielectric constant, however, this technique only reduces the radiation quality factor and compromises the efficiency of the antenna [2, 15, 47]. With the increasing use of microstrip antennas, and the demand for more bandwidth and high speed applications, many techniques have been reported and studied over the last four decades to improve this drawback. Some of these

techniques are discussed in the next section. There are three main approaches for improving the bandwidth of microstrip antennas. Some techniques treated the antenna as a high quality circuit, and therefore tried to reduce the quality factor by increasing the thickness, changing the shape of the patch, using new material to lower the dielectric constant or introducing losses to the antenna on the expense of efficiency [14, 44-46]. The second approach is to use matching circuits employing a matching network, tuning elements, or slots and notches on patches [14, 45, 46]. The third technique is introducing multiple resonances by utilising additional resonant or parasitic elements [14, 44-46]. New original techniques for broadband matching of microstrip antennas using circuit theory are also discussed in this chapter.

3.1. Literature Review

The first real contributions to Microstrip patch antennas started to be given in the 1970s [2], two fundamental feeding techniques were introduced, these are the edge and the probe feeds. However, all the developed antennas had an extremely narrow impedance bandwidth of around 1-2% of the centre frequency [2]. In the 1980s, all the major contributions from the defence industry, R&D firms and government grants were focused on improving the inherent narrow impedance bandwidth of microstrip patch antennas [45]. The first two feeding techniques found, edge and probe feed, are both inductive in nature, and therefore dominating the frequency response of the antenna at frequencies below resonance [44, 45]. However, the microstrip patch antenna is resonant, and to make it efficient the reactance must be close to zero, where both the capacitive and the inductive factors must effectively cancel each other [8]. As explained earlier, the antenna bandwidth can be increased by increasing the substrate thickness. However, this will also increase the inductive component of the feeding probe [46]. Two significant feeding methods were introduced by Pozar and Kaufman in 1985 and 1987 to resolve this issue [48, 49], these are aperture-coupling and proximity coupling illustrated in Figure 3.1.

LEEDS UNIVERSITY LIBRARY

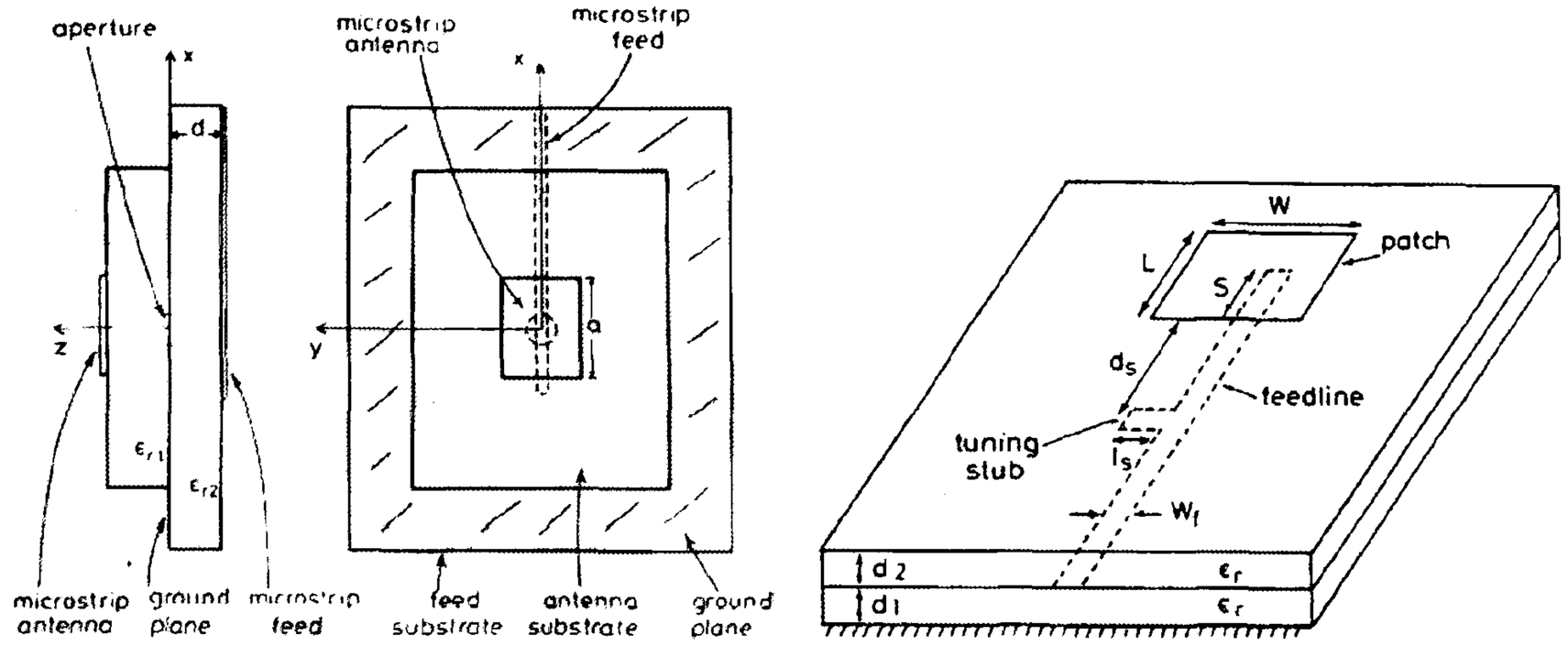

Figure 3.1 Aperture and proximity coupled microstrip antennas [49, 50].

These techniques are naturally capacitive and hence help to achieve a better impedance bandwidth. Impedance matching techniques were also used in the same design, and a few years later matching circuit techniques were developed to improve the impedance bandwidth of the antenna [51, 52]. The aperture-coupling was further developed in several ways utilising various substrates and various aperture shapes (shown in Figure 3.2) which achieve wider bandwidth, better coupling and allow for array configuration [50, 53, 54].

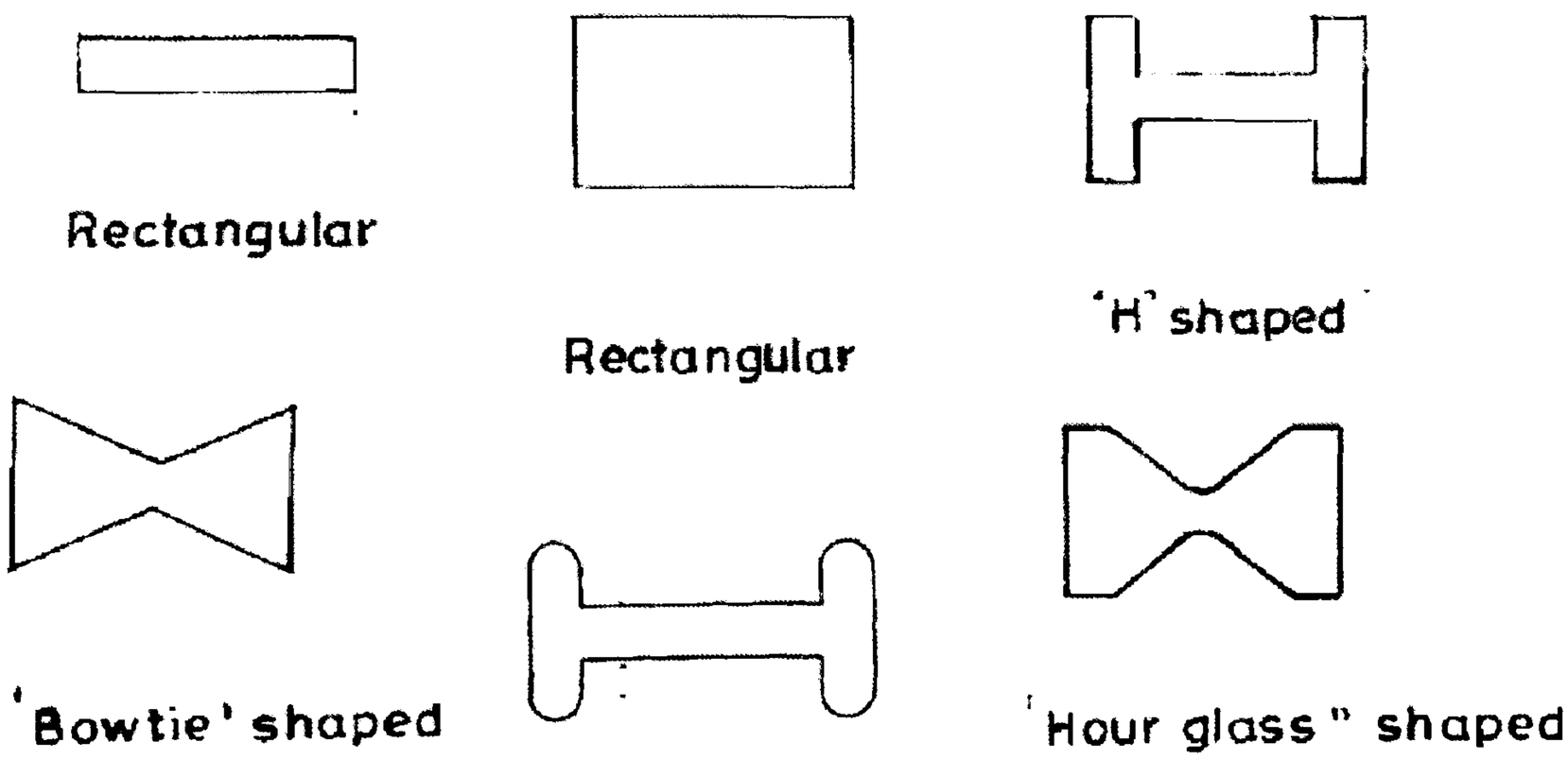

Figure 3.2 Various shapes of aperture used in aperture coupling feeds [50, 54].

One of the first attempts to improve the bandwidth by stacking patches was first proposed by Sanford in 1978 where a patent was issued [55]. His work was further developed a year later by Long and Walton [56] and another patent was issued for Jones et al for developing stacked or so called piggyback microstrip antennas for missiles applications [3, 57]. Hall et al combined the proximity coupling technique with multilayer design in that year, using different substrates and therefore making it efficient for circuit integration as well as achieving wider bandwidth [58]. In 1983, Sabban studied the bandwidth enhancement of stacking various shapes of microstrip antennas and the array configuration as well [59]. One year later, Chen et al explored the possibility of circular polarisation stacked microstrip antennas for space applications [60]. The topic of stacked resonators started to get more attention, different configurations, shapes, substrates, thicknesses and analysis were all investigated. Araki et al and Lee et al reported numerical analysis and characteristics of two layer circular disc antennas [61-64]. More efficient designs were developed in the nineties and 2000s [1, 8, 45, 65], shorted stacked patches achieved 30% bandwidth [66], and Targonski et al achieved impedance bandwidth of 67% [2, 44, 67]. However, the drawbacks for this technique are the increased height and manufacturing complication [2]. Various illustrations of stacked microstrip antennas are shown in Figure 3.3.

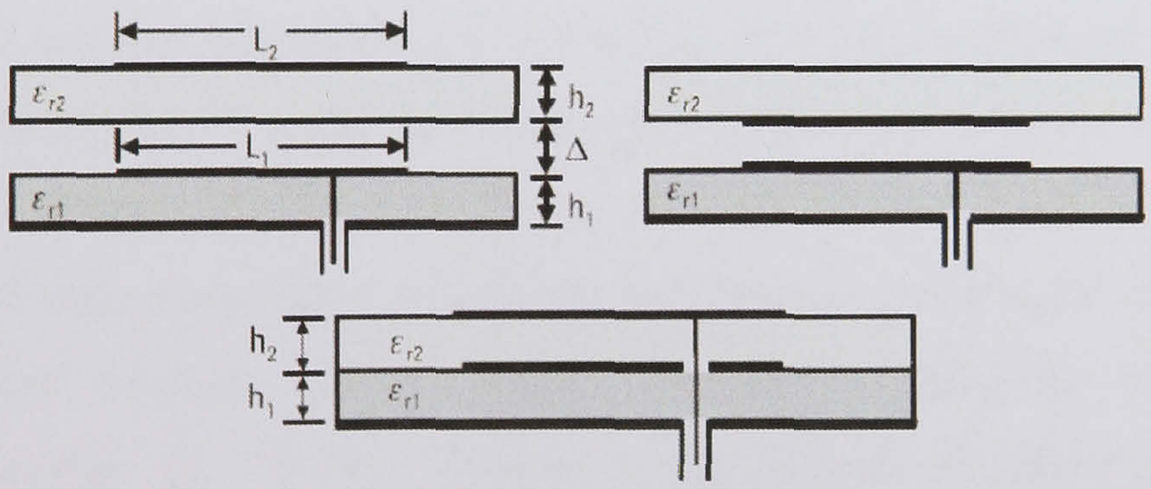

Figure 3.3 Various configurations of multilayer stacked microstrip antennas [2].

Another technique where the shape of the patch is modified to improve the efficiency and bandwidth of microstrip antennas was also introduced in the eighties. Bahl et al [68] introduced microstrip ring radiators shown in Figure 3.4, and later Weng [69] achieved wider bandwidth using ring microstrip antennas. The energy stored underneath the patch in this case is less when compared to the regular circular

patch. This also allows more radiation and therefore the quality factor of the patch resonator is reduced. Similar investigations were also reported for rectangular and other shapes of microstrip antennas [2]. Other techniques of reducing the energy stored underneath the patch, and hence the quality factor were published in the nineties. Cutting a U shaped slot inside the patch for example has shown approximately 40% impedance bandwidth [70-73]. This is also shown in Figure 3.4.

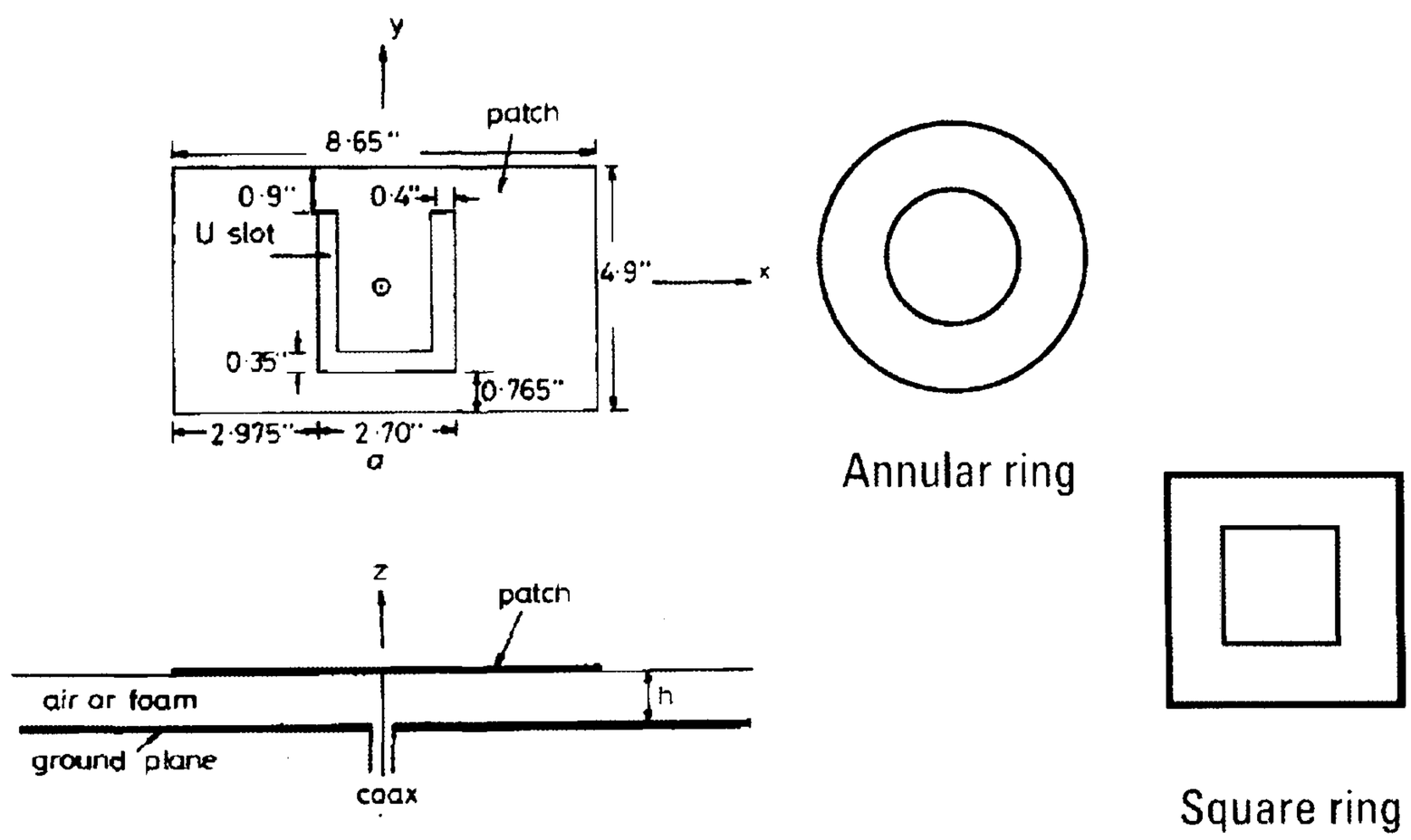

Figure 3.4 Microstrip antenna with U slot and microstrip ring antennas [2].

Planar multiresonator configuration and parasitic element techniques were also studied in the eighties [2]. Elements resonating at slightly different frequency are either parasitically excited or directly coupled to the antenna to achieve more than one resonance [14]. Wood was one of the first to study this in 1980 [74]. His idea attracted the attention of other researchers who later investigated various parasitic patches such as gap coupled patches, narrow strips, shorted and directly coupled quarter wavelength patches [7, 75-78]. Various configurations of planar multiresonator microstrip antennas are shown in Figure 3.5.

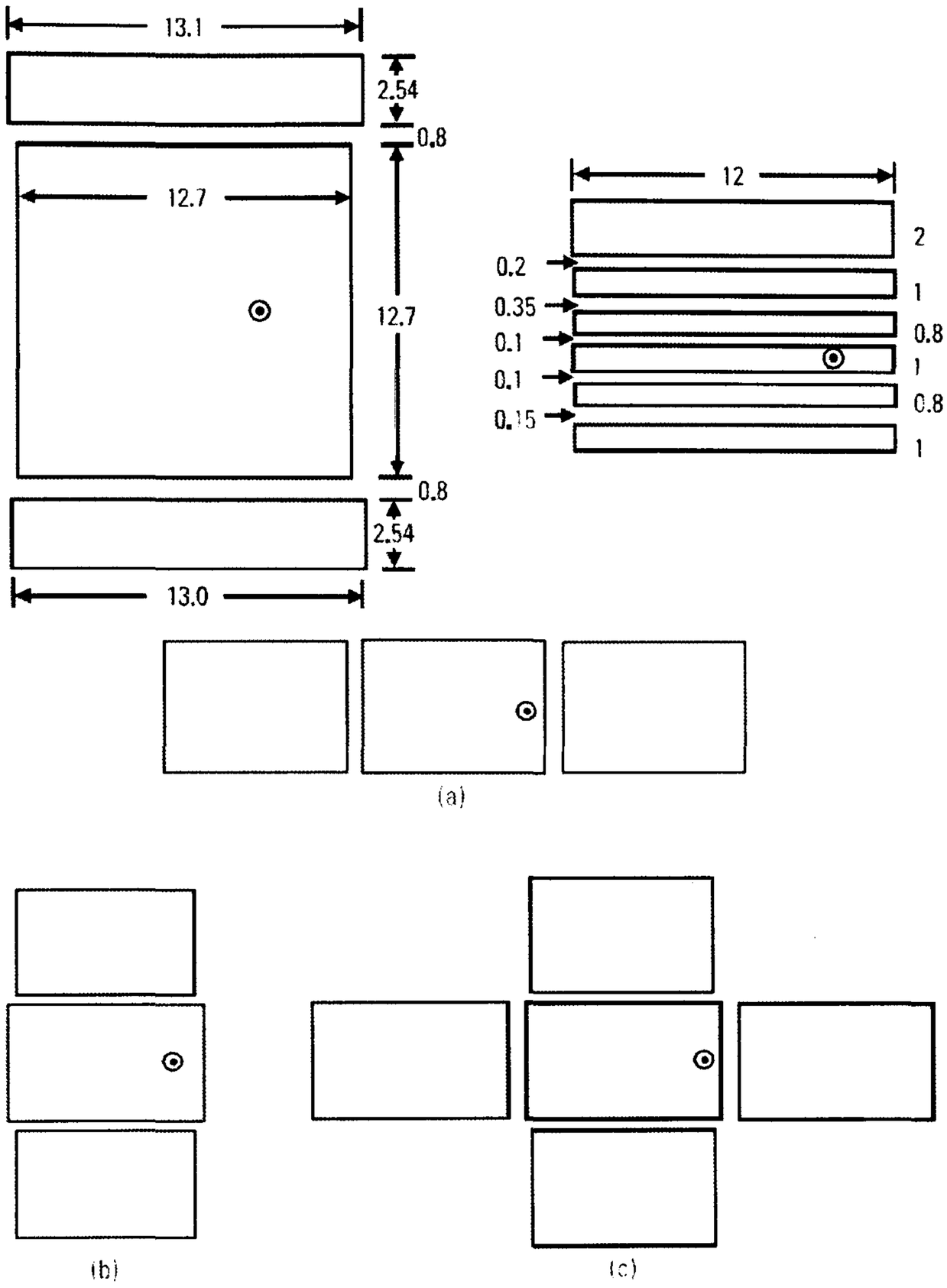

Figure 3.5 Various configurations of multi resonator microstrip antennas [2].

In the nineties, techniques were also reported on utilising the multi-resonator configuration in stacked patches, where a single-fed antenna is coupled to 2-6 others, achieving even wider bandwidth [79-81]. Examples of these configurations are shown in Figure 3.6. These configurations have achieved impedance bandwidth of around 5-25% of the centre frequency. However, the main disadvantage of this approach is the large space used, which makes it less favourable for arrays applications. Also there is a variation in the radiation pattern over the impedance bandwidth [2].

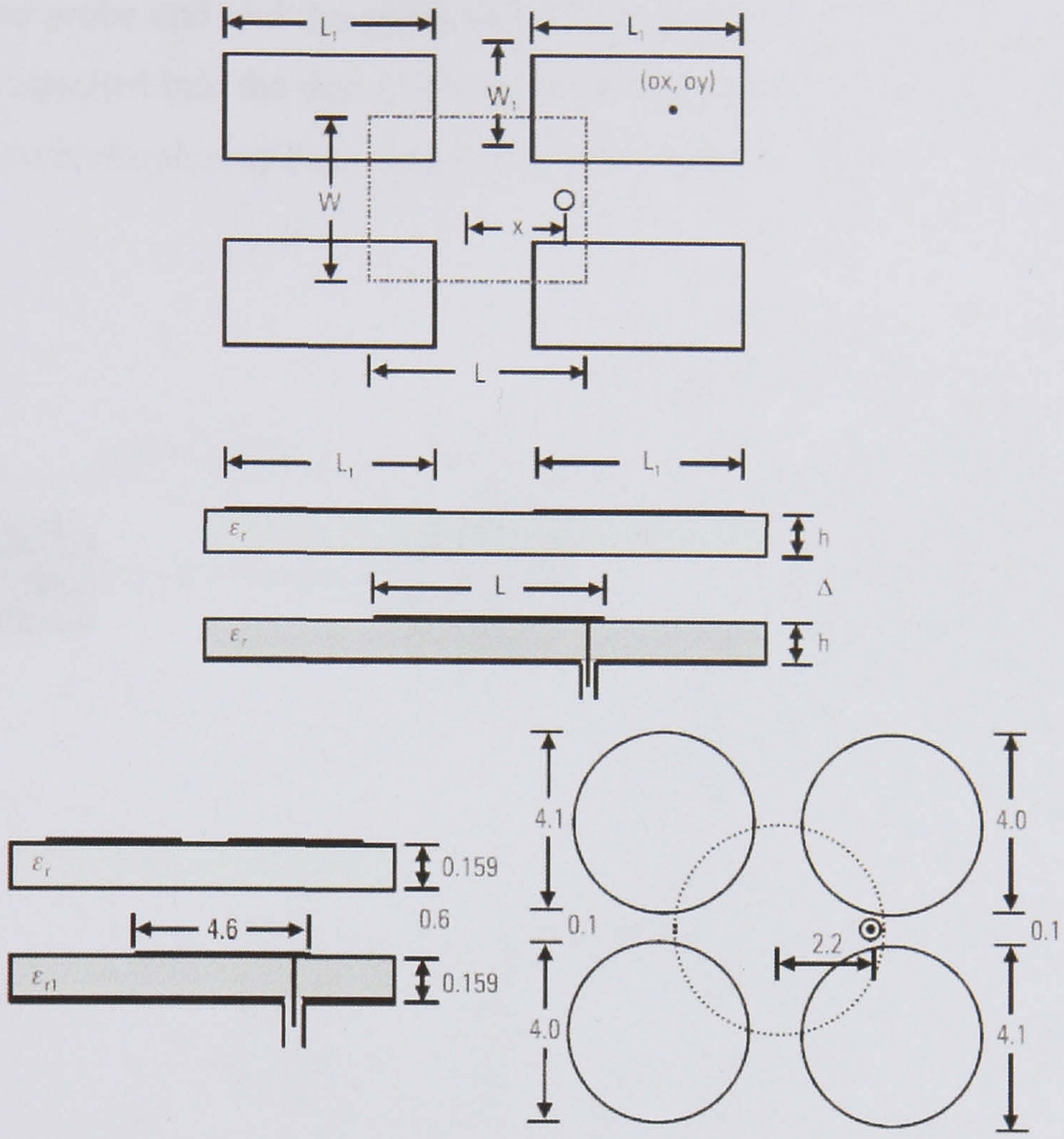

Figure 3.6 Various configurations of stacked multi-resonator microstrip patch antenna [2].

Impedance matching techniques have also been described in the literature [45]. An impedance matching network is introduced to achieve better matching between the source (which has a fixed impedance) and microstrip patch antenna (which has a frequency dependent impedance) [6]. In the late seventies, Derneryd reported one of the first designs for microstrip antenna with a separate matching network [6]. This essentially consisted of two section impedance transformer, and allowed the antenna to be matched at two distinct frequencies. In the eighties, Pues and Van de Capelle reported a comprehensive study about this [51]. They used open circuited stubs to obtain a better match for the antenna, achieving bandwidths of 10-12% of the centre frequency. Paschen applied a similar approach for GPS applications achieving bandwidth of 25% of the centre frequency [45]. In terms of probe fed thick microstrip antennas, matching techniques were also discussed by implementing a series capacitor to tune out the probe inductance. This was achieved by allowing a gap

between the probe end and the patch [82]. Hall proposed a similar technique, where the feed is attached into the disc in the typical manner but with a gap around the feed point to account for the capacitance [83], as illustrated in Figure 3.7.

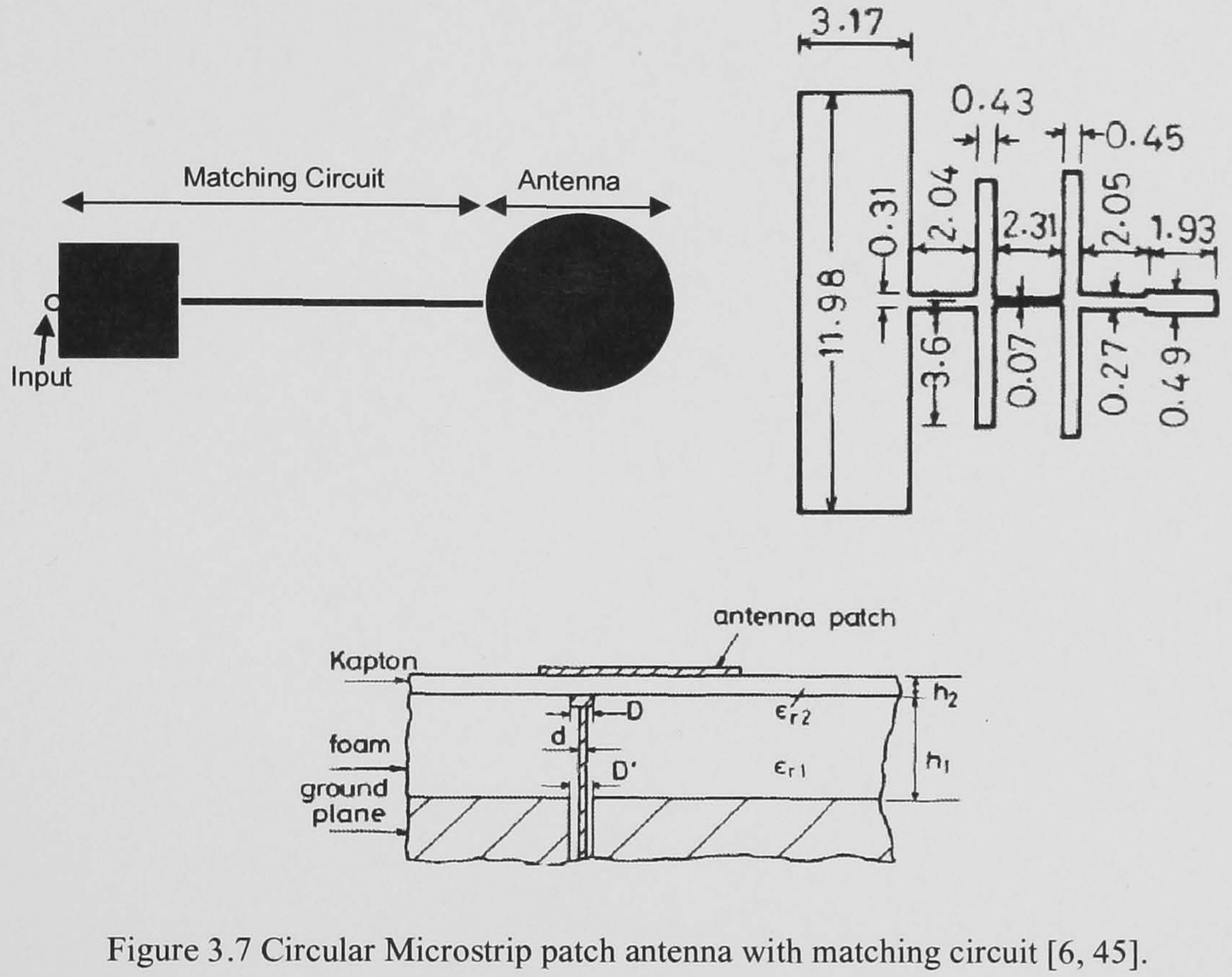

Figure 3.7 Circular Microstrip patch antenna with matching circuit [6, 45].

Systematic impedance matching techniques were also reported [1, 2, 9, 84, 85]. Circuit theory is used to design the equivalent circuit of microstrip antennas, where an *RLC* resonator network are introduced to model and improve the input impedance of one and multilayer microstrip patch antennas. The circuits systematically provide information that helps in designing the physical antenna, and therefore provide better understanding of the theory.

Other techniques such as log-periodic microstrip antennas were also reported [2, 12]. A set of patches are fed 180° out of phase with dimensions that are increased logarithmically. However, it was found that the radiation pattern varies significantly over the bandwidth. Also, Ferrite substrate based microstrip patch antenna were also explored, but shown to have poor efficiency [2].

Microstrip patch antennas are increasingly used in wireless applications, and the demand for high efficiency antennas with improved impedance bandwidth is

continuous. Recent researches are trying to use a combination of approaches in an attempt to reach an optimum design and performance [1, 2, 4, 44].

3.2. Single and Dual Mode Microstrip Antennas

In recent years, there has been a significant trend towards the use of internal antennas in cellular phones and other wireless communication devices. These antennas must fit into a very restricted space which generally causes significant reduction in system performance. There are fundamental limitations on the performance of electrically small antennas, these are the efficiency, impedance matching and frequency bandwidth [11, 86]. For example, a general expression for the bandwidth of the input reflection coefficient of a narrowband antenna can approximately be shown as [87]:

$$\Delta f = \left(\frac{2\pi r}{c}\right)^3 f^4 \qquad 3.1$$

where "r" is the radius of a sphere enclosing the antenna, "f" is the frequency of operation and "c" is the speed of light. Thus a small antenna working at low frequencies may have a very restricted bandwidth of operation. In practice it is usually a struggle to achieve a reasonable input match over the full 80MHz bandwidth required for a GSM phone operating at 900MHz [88]. Furthermore if a significant improvement in bandwidth were achievable, then the physical size of the antenna could be reduced. Broadband matching theory can be used to increase the bandwidth of a reactive load for a given return loss level [89, 90]. In the case of a resonant antenna an external resonator (or resonators) can be coupled to the antenna enabling a bandwidth improvement to be achieved. This is shown in Figure 3.8.

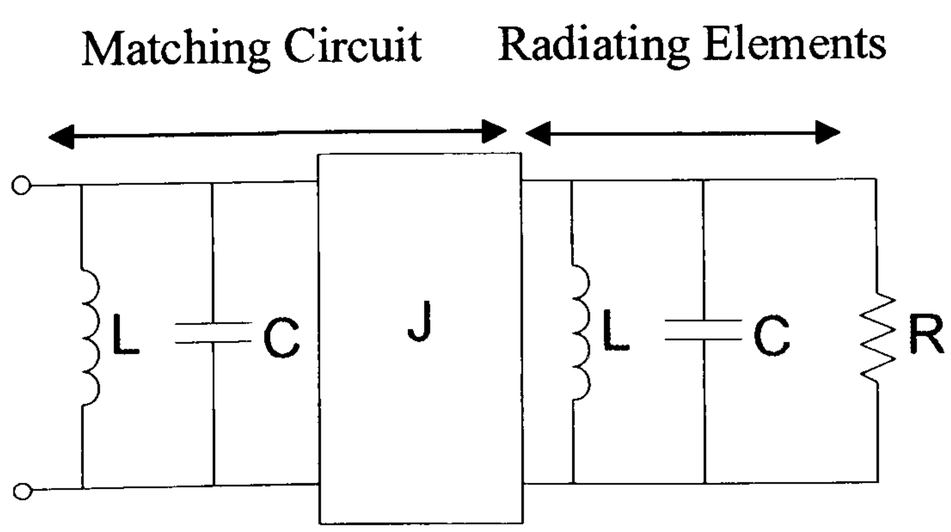

Figure 3.8 Conventional Broadband Matching of a Resonant Antenna.

Here the antenna is represented by a resonator coupled into a resistive load. The matching network is coupled into the antenna via an admittance inverter J. However the matching network requires physical volume which may be better employed by simply increasing the size of the antenna. Furthermore the matching network will have a finite unloaded Q factor, thus causing some resistive losses which will reduce the radiated power. This problem could be partially overcome if the matching network was also the last element in a bandpass filter, but such filters are not always required in radio transceivers. An alternative method of broadband matching, using a dual-mode antenna structure is described in the next section.

3.2.1. Single Mode Antenna

Consider the microstrip patch antenna and the equivalent circuit of a single mode patch antenna shown in Figure 3.9.

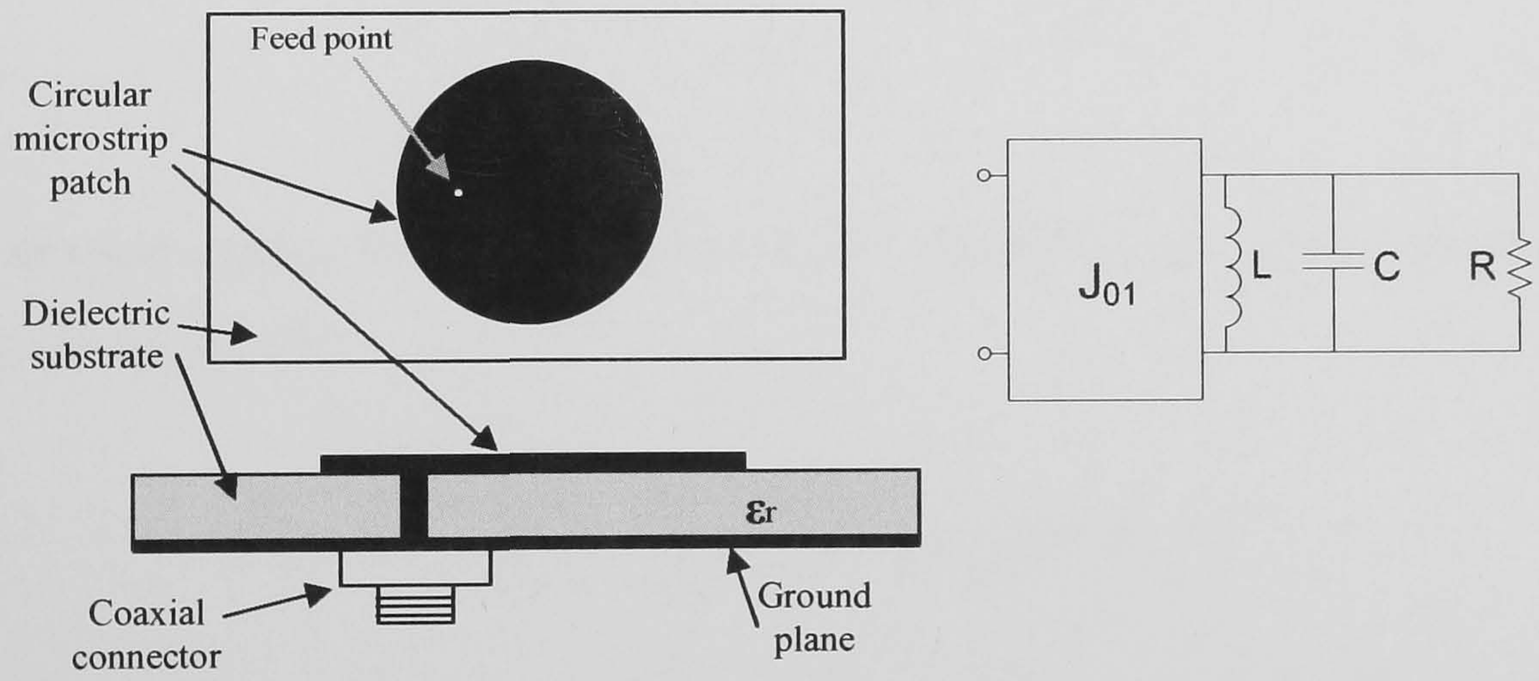

Figure 3.9 Single mode antenna structure and its equivalent circuit.

In Figure 3.9, the impedance inverter J_{01} represent the coupling between the probe and the antenna, the inductor L and the capacitor C represent resonance, and the resistance R represents the energy radiated. However, this can be replaced by a low pass prototype network for comparison purposes with other circuits shown in Figure 3.10.

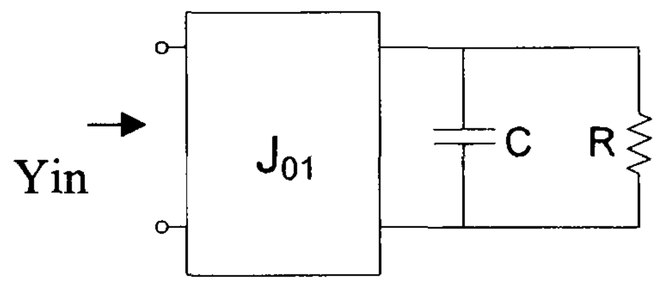

Figure 3.10 Single mode antenna equivalent circuit, R = C = 1.

The input admittance of this circuit can be expressed as

$$Y_{in} = \frac{J_{01}^2}{p+1} = \frac{1}{Z_{in}} \qquad 3.2$$

Where "p" is "jω", and the reflection coefficient of the circuit on Figure 3.10 is equal to:

$$S_{11(p)} = \frac{Z_{in} - Z_l}{Z_{in} + Z_l} = \frac{\frac{p+1}{J_{01}^{\ 2}} - 1}{\frac{p+1}{J_{01}^{\ 2}} + 1} = \frac{p+1-J_{01}^{\ 2}}{p+1+J_{01}^{\ 2}} \qquad 3.3$$

The simplest strategy for matching is to critically couple the circuit at zero frequency.

$S_{11(0)} = 0$, i.e. $J_{01} = 1$;

$$|S_{11(jw)}|^2 = \frac{1-2J_{01}^{\ 2}+J_{01}^{\ 4}+\omega^2}{1+2J_{01}^{\ 2}+J_{01}^{\ 4}+\omega^2} = \frac{\omega^2}{\omega^2+4} \text{ for } J_{01} = 1. \qquad 3.4$$

Considering 6dB return loss specification;

$$|S_{11(jw)}|^2 = \frac{\omega^2}{\omega^2+4} = \frac{1}{4} \qquad 3.5$$

giving $\omega = \pm\frac{2}{\sqrt{3}}$ and a 6dB bandwidth of $\frac{4}{\sqrt{3}} = 2.3094$.

This bandwidth can be improved by adjusting the input coupling J.

Thus, using equation (3.4) again at the 6dB frequencies for variable J_{01} value;

$$|S_{11(jw)}|^2 = \frac{1 - 2J_{01}^{\ 2} + J_{01}^{\ 4} + \omega^2}{1 + 2J_{01}^{\ 2} + J_{01}^{\ 4} + \omega^2} = \frac{1}{4} \qquad 3.6$$

this results in;

$$\omega^2 = -J_{01}^{\ 4} + 3.333J_{01}^{\ 2} - 1 \qquad 3.7$$

and $\Delta_{(6dB)}$, the 6dB return loss bandwidth is given by;

$$\Delta_{(6dB)} = 2\sqrt{-\left(J_{01}^{\ 2} - 3\right)\left(J_{01}^{\ 2} - 1/3\right)} \qquad 3.8$$

The bandwidth can be maximised by maximising the function $f(x)$ with reference to equation 3.8 above

$$f(x) = -x^2 + 3.333x - 1 \qquad \text{where } x = J_{01}^{\ 2} \qquad 3.9$$

The value of x which gives maximum result for $f(x)$ can be obtained by finding the first and second derivative of $f(x)$;

$$\text{Thus} \qquad \frac{df(x)}{dx} = -2x + 3.333 = 0 \qquad 3.10$$

$$\text{Giving } J_{01} = \sqrt{\frac{5}{3}} \qquad 3.11$$

And from (3.8)

$$\Delta_{(6dB)} = 2.666 \qquad 3.12$$

The coupling value in equation 3.11 above was used to simulate the circuit in Figure 3.10. The simulated return loss bandwidth S_{11} shown in Figure 3.11 agrees with the analysis and is approximately 15% greater than for the critically coupled case. Note that a 6dB return loss level is typical for handset antennas. If a 10dB return loss was required then the value of J_{01} would be $\sqrt{11/9}$ giving a 5% improvement over the

critically coupled case. These optimised bandwidths are used as the basis for comparison with other matching schemes.

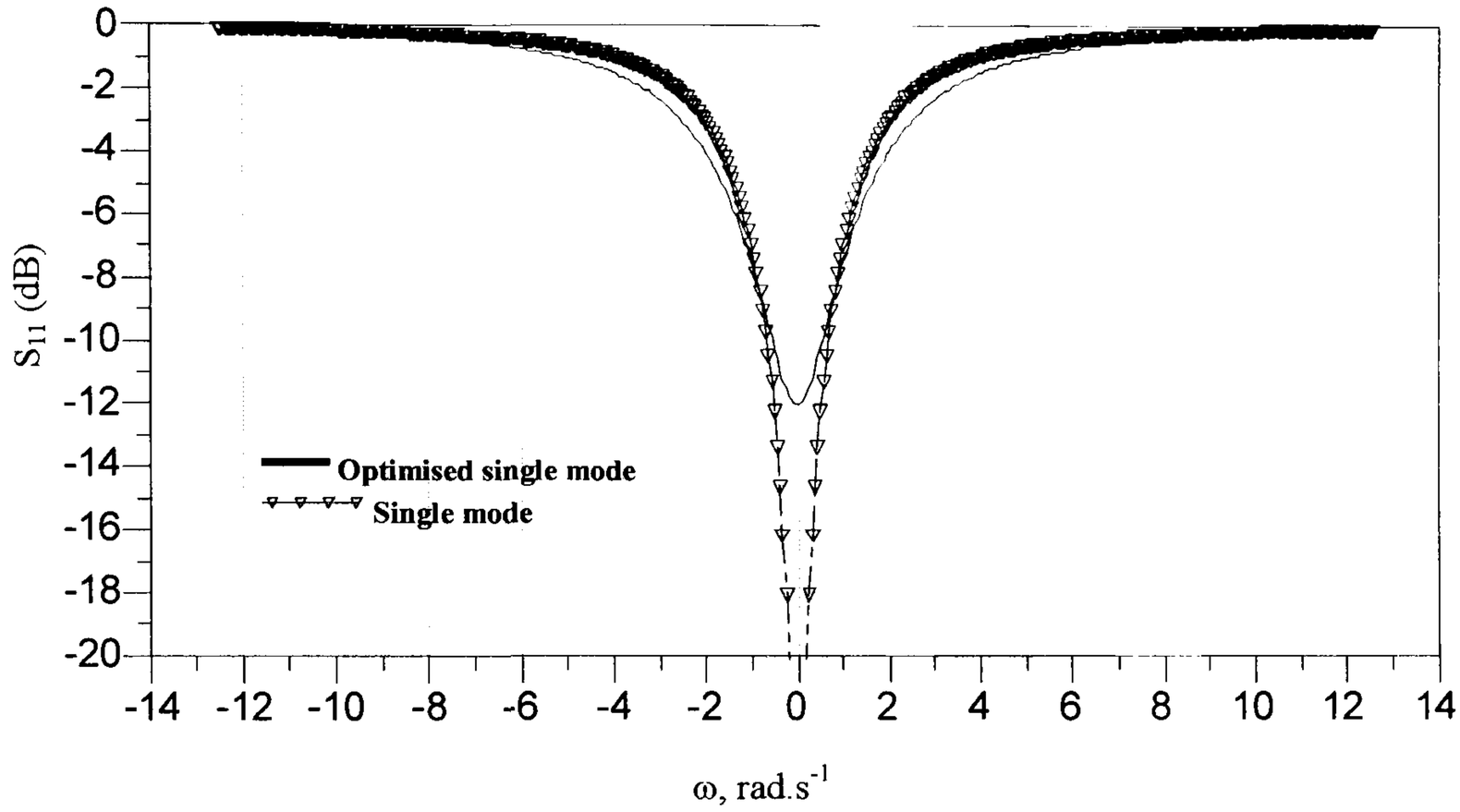

Figure 3.11 Circuit simulation results showing 15% optimised return loss bandwidth when $J_{01} = \sqrt{\frac{5}{3}}$,

3.2.2. Dual mode Microstrip Antennas

Structures such as circular, square and triangular microstrip patch antennas can support two orthogonal resonant modes, or two polarizations [3, 91]. For a dual mode antenna, the equivalent circuit can be anticipated as a second order low pass prototype shown in Figure 3.12.

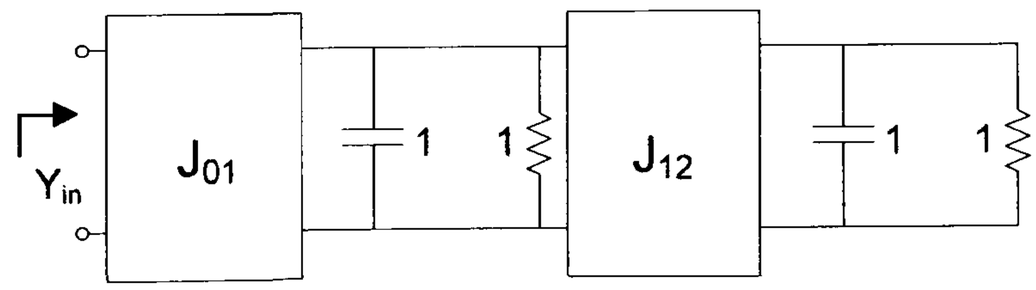

Figure 3.12 Dual-mode antenna low pass prototype.

Here, the resistor and capacitor values have been set to unity to enable direct comparison with the single-mode case. This also implies a symmetrical network structure. The input admittance of this circuit is given by equation (3.13).

$$Y_{in}(p) = \frac{J_{01}^{\,2}}{1+p+\dfrac{J_{12}^{\,2}}{1+p}} \qquad 3.13$$

$$= \frac{J_{01}^{\,2}p + J_{01}^{\,2}}{p^2+2p+1+J_{12}^{\,2}} \qquad 3.14$$

$$and\ S_{11}(p) = \frac{p^2+(2-J_{01}^{\,2})p+1+J_{12}^{\,2}-J_{01}^{\,2}}{p^2+\left(2+J_{01}^{\,2}\right)p+1+J_{12}^{\,2}+J_{01}^{\,2}} \qquad 3.15$$

The values of "J_{01}" and "J_{12}" can now be evaluated in order to obtain maximum bandwidth for a specified return loss level. As an example, a 6dB return loss will be considered. Now $S_{11}(p)$ is of degree 2, thus it can be arranged for the return loss to have a turning point between the two resonances of value 6dB (i.e. $S_{11} = ½$) at DC.

$$Then\ S_{11}(0) = \frac{1+J_{12}^{\,2}-J_{01}^{\,2}}{1+J_{12}^{\,2}+J_{01}^{\,2}} = \frac{1}{2} \qquad 3.16$$

$$\text{Or} \qquad J_{12}^{\,2} = 3J_{01}^{\,2} - 1 \qquad 3.17$$

Thus

$$S_{11}(p) = \frac{p^2+\left(2-J_{01}^{\,2}\right)p+2J_{01}^{\,2}}{p^2+\left(2+J_{01}^{\,2}\right)p+4J_{01}^{\,2}} \qquad 3.18$$

$$Giving\ \left|S_{11}(j\omega)\right|^2 = \frac{\omega^4+\omega^2\left(J_{01}^{\,4}-8J_{01}^{\,2}+4\right)+4J_{01}^{\,4}}{\omega^4+\omega^2\left(J_{01}^{\,4}-4J_{01}^{\,2}+4\right)+16J_{01}^{\,4}} \qquad 3.19$$

For a 6dB return loss $\left|S_{11}(j\omega)\right|^2 = \frac{1}{4}$. Applying this into equation 3.19;

$$3\omega^4+\omega^2\left[12-28J_{01}^{\,2}+3J_{01}^{\,4}\right]=0 \qquad 3.20$$

solutions of 3.20 are $\omega = 0$ (as already specified) and the band-edge frequencies, ω_1 and ω_2 that result in a 6dB return loss (or S_{11}=1/2). These are given by (3.21-3.22).

$$\omega_{1,2} = \pm\sqrt{-J_{01}{}^4 + \frac{28}{3}J_{01}{}^2 - 4} \qquad 3.21$$

$$\text{or } \Delta_{(6dB)} = \omega_2 - \omega_1 = 2\sqrt{-J_{01}{}^4 + \frac{28}{3}J_{01}{}^2 - 4} \qquad 3.22$$

To maximise the bandwidth, the value of J_{01} which maximises the function f(x) with reference to equation 3.22 is obtained.

$$f(x) = -x^2 + \frac{28}{3}x - 4 \quad \text{where } x = J_{01}{}^2 \qquad 3.23$$

$$\text{hence} \qquad \frac{df(x)}{dx} = -2x + \frac{28}{3} = 0 \qquad 3.24$$

$$x = J_{01}{}^2 = \frac{14}{3} \qquad 3.25$$

and using 3.17

$$J_{12}{}^2 = 13 \qquad 3.26$$

These values of "J_{01}" and "J_{12}" are then applied to equation 3.22 giving $\Delta_{(6dB)} = 8.4327$. This is a 3.16:1 improvement compared with the optimum single mode case. Furthermore, it may be shown that the improvement increases to 3.46:1 for a 10dB return loss design, although the overall bandwidth is less than for the 6dB case. Simulations of the analytical results obtained for the low pass prototype of the two schemes explained above are shown in Figure 3.13 and Figure 3.14, showing over 3 times wider 6dB return loss bandwidth.

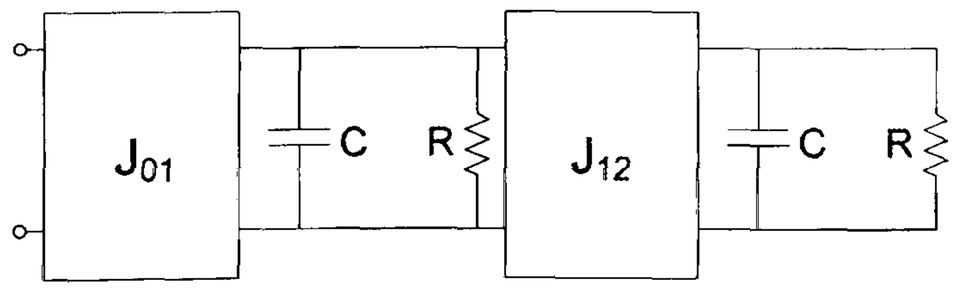

Figure 3.13 Dual Mode antenna equivalent circuit, where $J_{01}=(14/3)^{1/2}$, $J_{12}=(13)^{1/2}$ and R=C=1.

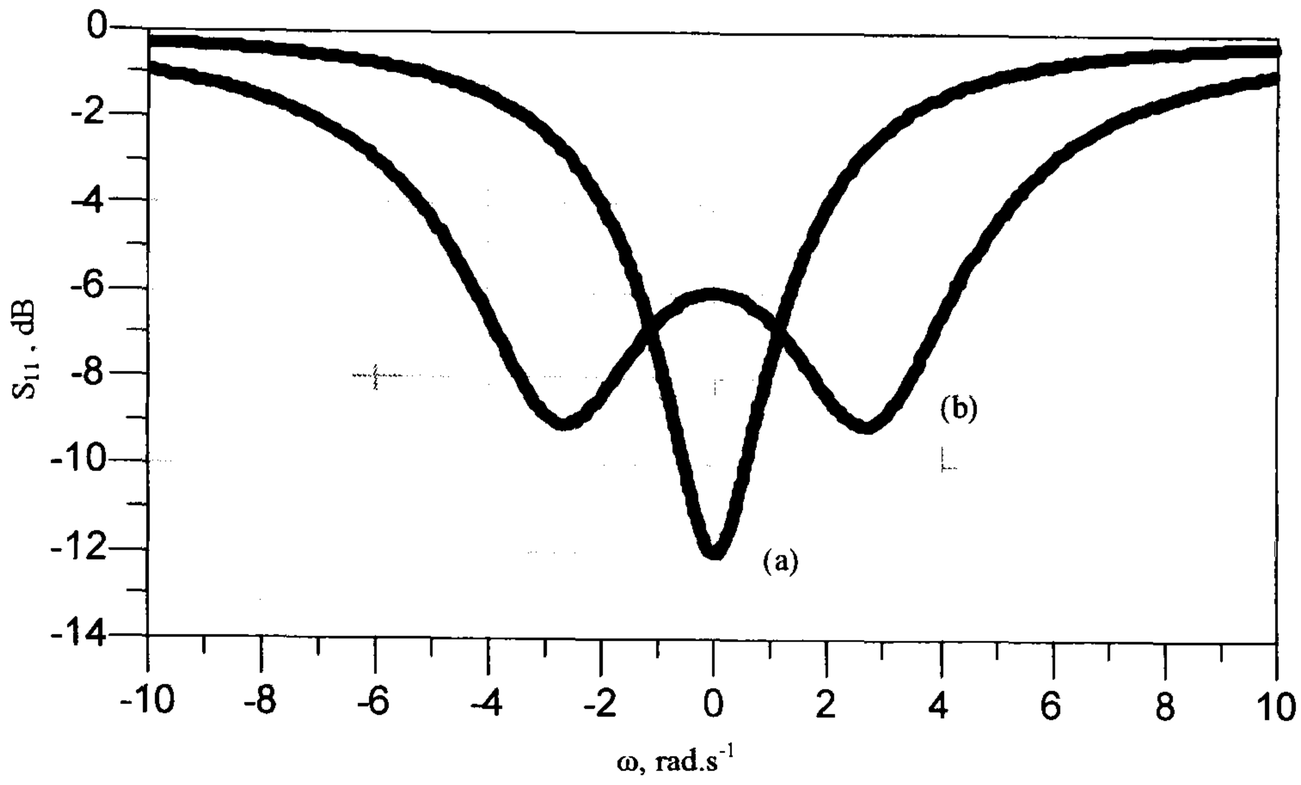

Figure 3.14 Simulation results, (a) Optimised single mode and (b) Dual mode showing 300% wider bandwidth.

3.2.3. Design and Practical Implementation.

In order to demonstrate the theory an experimental prototype antenna was designed and implemented. This was based on a dual-mode dielectric resonator structure originally developed for filtering applications [88, 92]. A circular patch microstrip antenna on a particular substrate has only one degree of freedom to control, i.e. the radius, and in turn, changing the radius affects the resonant frequency of the antenna. The equation that relates the radius to the resonant frequency in the dominant mode is [1, 4, 36, 37, 41];

$$f_r = \frac{c\chi'_{mn}}{2\pi a(\varepsilon_r)^{1/2}} \qquad 3.27$$

Where:

f_r is the resonant frequency.

χ'_{mn} are the zeros of the Bessel function of order "n", and equal to 1.8412 for the dominant TM_{110} mode.

a is the radius of the circular patch.

c is velocity of light

Therefore, considering the dominant mode, at 2GHz, the radius of the patch is 3 cm using the Duroid 5880 of permittivity 2.2, as equation 3.27 implies. A coaxial cable was used to feed the antenna, and moving the feed point along the radius controls the input match, as the resistance is maximum on the edge and drops to zero as the centre of the patch is approached [1, 4, 12, 31, 41]. Therefore it is fairly easy to locate the feed point for the critically coupled and the optimised single mode cases.

In the dual mode case, two couplings must be simultaneously optimised, and hence a specific design procedure must be followed. First the feed point location must be obtained, this is achieved by referring to the equivalent circuit in Figure 3.13, and evaluating the return loss when J_{12} is reduced to zero. This represents the coupling between the probe and the patch, at which point, the maximum value of return loss is 3.783dB. Hence the feed point on the antenna is situated to achieve this value of return loss when the two resonances are un-coupled, but coexist orthogonally.

Secondly, we introduce the coupling notch which in turn perturbs the fields, or in other words disturbs the symmetry, this can be used to couple the two orthogonal modes and achieve wider bandwidth. A similar approach was experimented within [9] using a microstrip square patch antenna, without the leading circuit analysis presented here. The notch position is very important, it should be located at an angle of 45°, 135°, 225° or 315° [91]. If the notch was located at another angle, it may not couple the two modes properly or it may even reduce one of the modes to zero [91]. To obtain the correct final return loss characteristics, in this particular example, EM simulations shows that the notch should be approximately ⅙ of the radius to meet the desired specifications, i.e. 6dB in the analysis above.

Optimised single mode and dual mode circular microstrip antennas were designed, operating at 2GHz using Duroid 5880 substrate ($\varepsilon_r = 2.2$), and a notch of dimensions 4.5mm x 5mm was introduced. The dual mode circular microstrip antenna is illustrated in Figure 3.15, both the simulation (using ADS-Momentum) and measured results are shown in Figure 3.16.

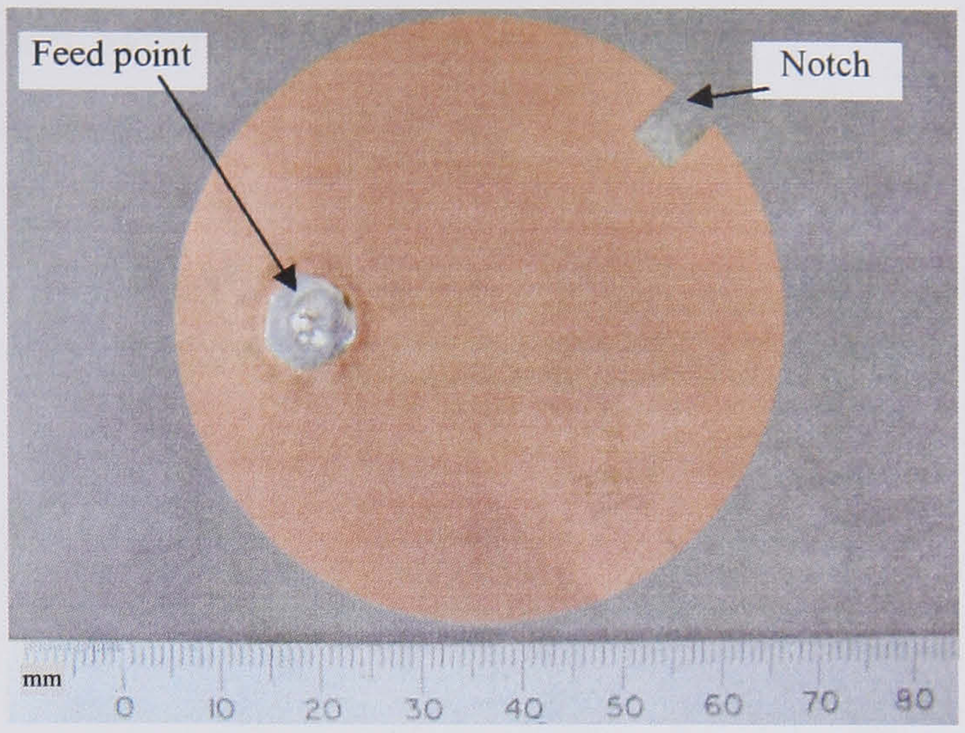

Figure 3.15 Dual-mode circular patch antenna designed at 2 GHz.

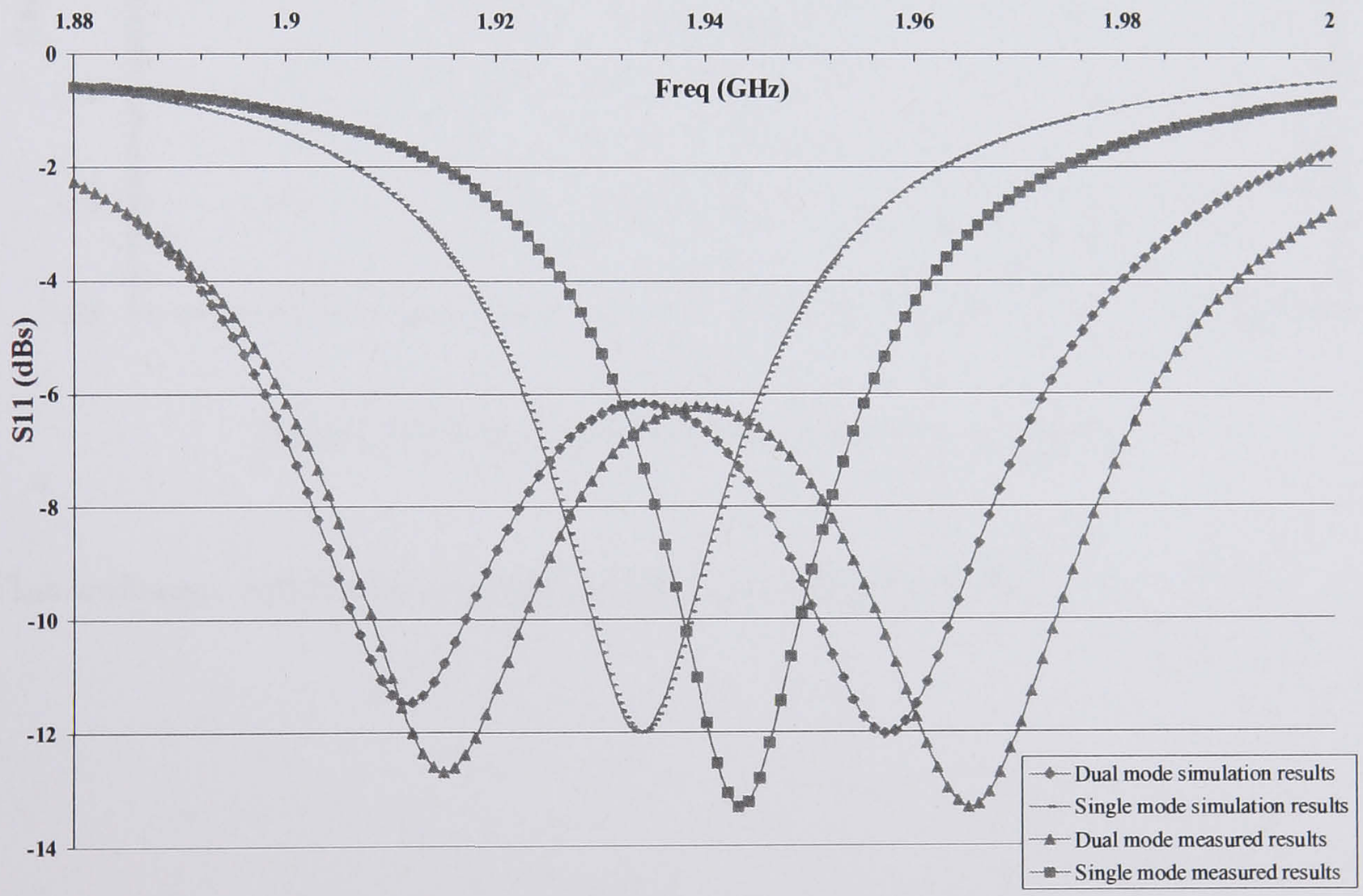

Figure 3.16 Electromagnetic simulations and measured results of circular patch antenna designed at 2 GHz showing optimized single-mode and dual-mode antenna results.

Clearly, the dual mode antenna has a 6dB bandwidth over 3 times wider compared to the optimised single mode case, and as expected the resonant frequency is slightly lower in the simulations results than the measured results [5, 36, 37, 41]. It is shown that the notch illustrated in Figure 3.15 resulted in coupling the two polarisation modes, and simulations shown that the degree of splitting the resonant frequency is dependent on the width and depth of the notch.

The far-field radiation pattern of the dual mode antenna is similar to a conventional single mode antenna, as shown in Figure 3.17.

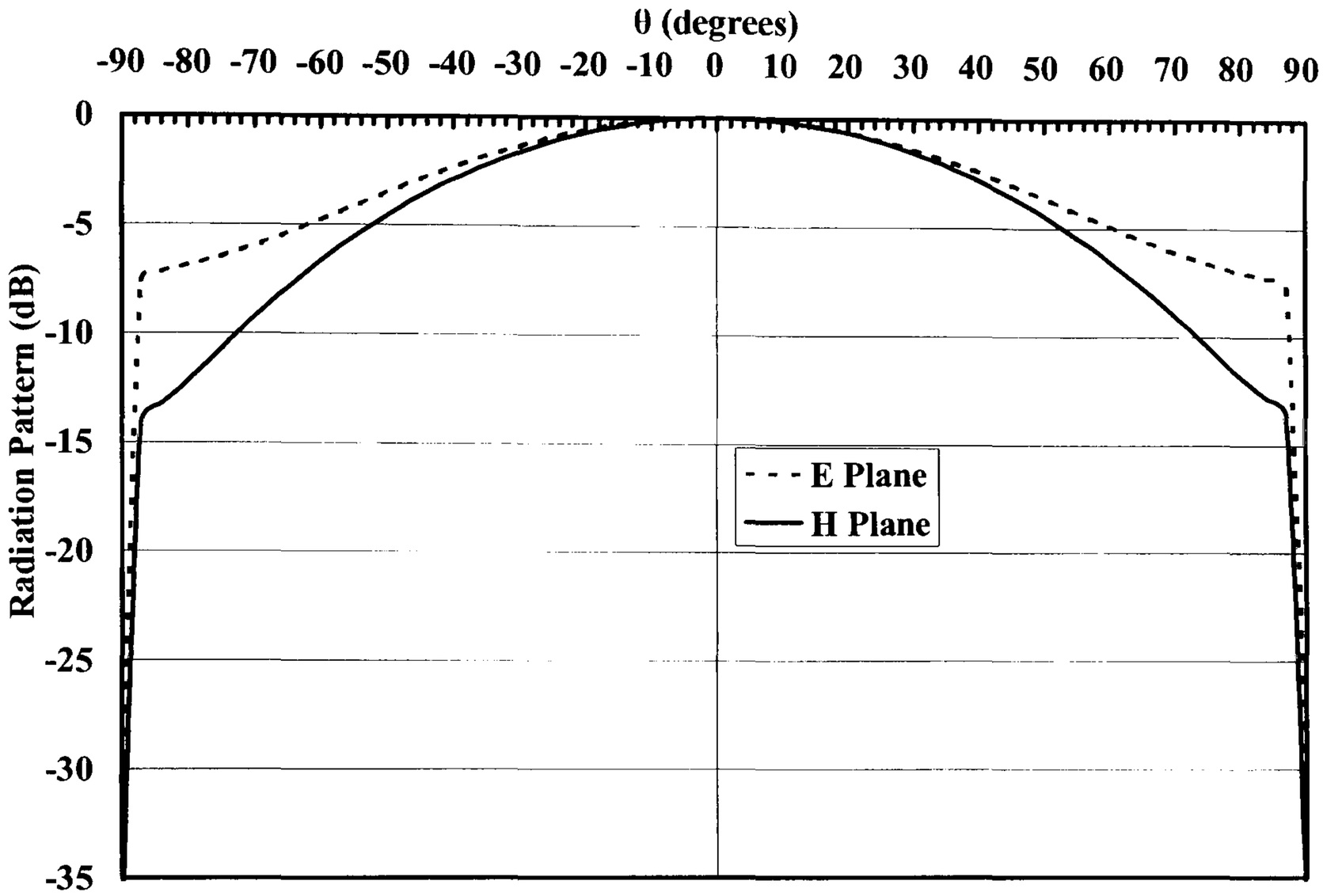

Figure 3.17 Far-field radiation pattern of the dual mode antenna.

This technique and results were published in [93] (Appendix B).

3.3. Quadruple Mode Patch Antenna

A novel method for the design of broadband patch antennas is described. The approach taken is to broadside couple two dual-mode patch antennas, resulting in an antenna with four resonances. The equivalent circuit of the antenna is similar to that of microwave filters, thus filter design techniques may be employed to synthesize the antenna to obtain maximum return loss bandwidth. This is the first time an increase in the bandwidth is achieved on a relatively thin substrate antenna as a result of coupling four resonant modes, using two stacked circular microstrip patches, without a significant increase in substrate height, reducing permittivity, or changing the patch radius. Electromagnetic simulation and measured results of the complete structure demonstrate bandwidth improvement of over 4 times compared with a single mode design. This is the first time that such an approach of designing antennas as multi-mode filters has been demonstrated.

3.3.1. Mathematical Analysis

Two or three layers of microstrip patches can provide a considerably wider antenna bandwidth. However, this increase in bandwidth is mainly due to an increase in the overall height of the substrate, utilising an air gap or foam to decrease the effective dielectric constant or implementing various feeding techniques, besides the multi-resonator effect [1, 2, 30, 45].

In the previous section it was shown that it is possible to design a dual-polarised patch antenna as if it was a dual-mode filter. This enabled the bandwidth of the antenna to be significantly improved. In this section, a new stacked two layer antenna is presented, where the theory has been extended to the design of a quadruple-mode antenna.

Consider the dual-mode antenna lowpass prototype shown in Figure 3.18.

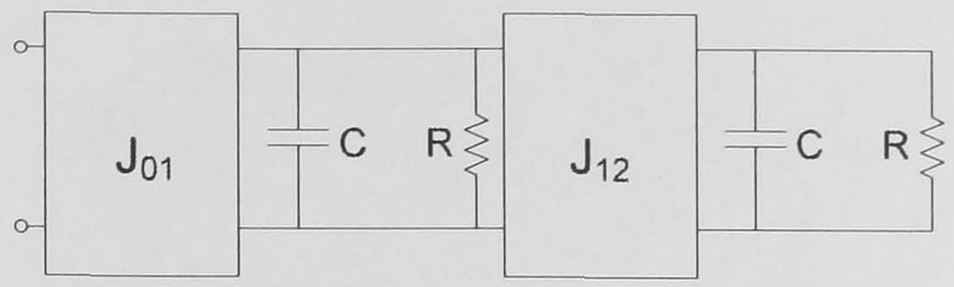

Figure 3.18 Dual-mode antenna lowpass prototype.

Each resistor represents the antenna radiation resistance of each mode (i.e. the first and the second resistance in the diagram represent the radiation resistance of the first and the second mode respectively). The admittance inverters represent the input matching to the antenna and the coupling between the two modes. By correct choice of J_{01} and J_{12} the input return loss bandwidth can be maximised [93]. The theory of coupling matrices in filter prototypes is further explained in [94, 95]. In theory, the dual-mode design approach may be extended by stacking two dual-mode antennas, as shown in Figure 3.19. Figure 3.19 shows the physical structure of the proposed design, and an analytical figure of the two dualmode antennas stacked on top of each other, with 2 resonant modes on each layer (1 and 2 on the lower layer and 3 and 4 on the top layer). A starting point for the physical realisation would be feeding the antenna using a coaxial connector as shown in Figure 2.17. This feeds into mode 1 which is then coupled to mode 2 via a discontinuity in the structure. However, couplings may then exist between all four resonant modes. Therefore, all couplings must be carefully considered.

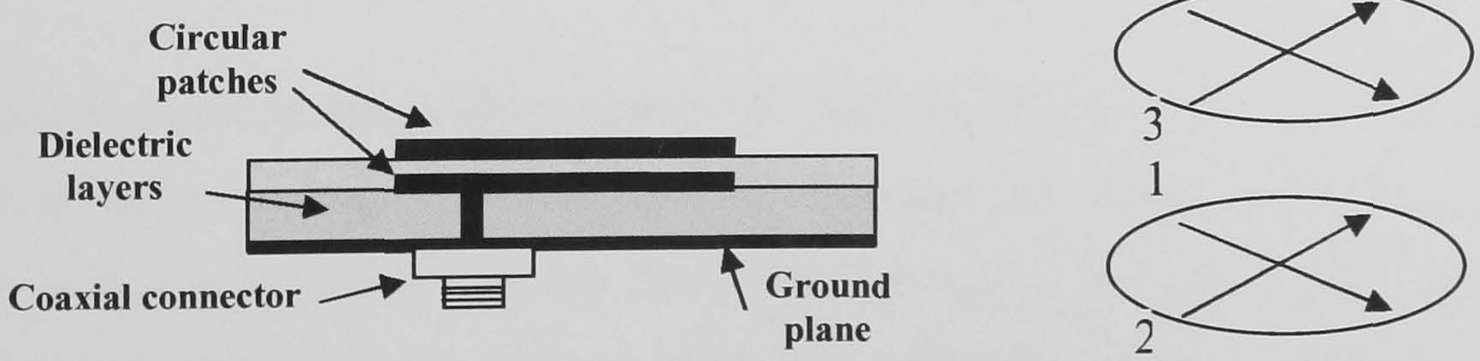

Figure 3.19 Quad-mode patch antenna physical design.

The field distribution in stacked microstrip patch antennas was reported in [1] and shown in Figure 3.20.

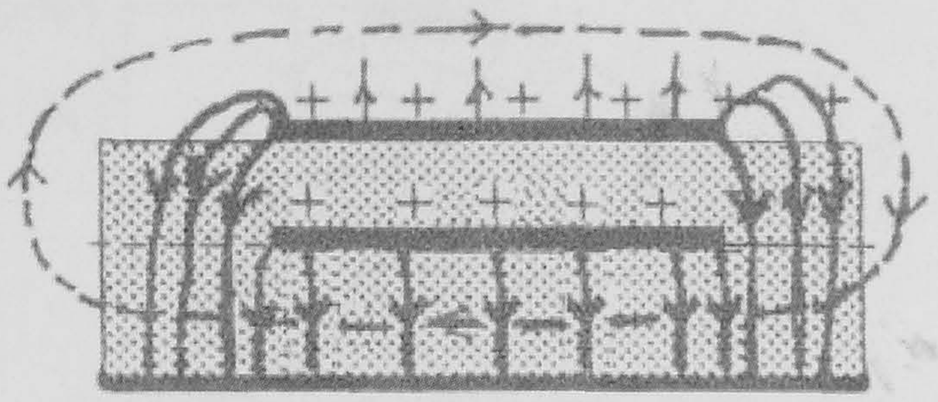

Figure 3.20 Electric and Magnetic field distribution in a stacked patch configuration [1].

The generalised equivalent circuit of the antenna in Figure 3.19 is shown in Figure 3.21. In a similar way to [93] it may be denormalised to lowpass prototype.

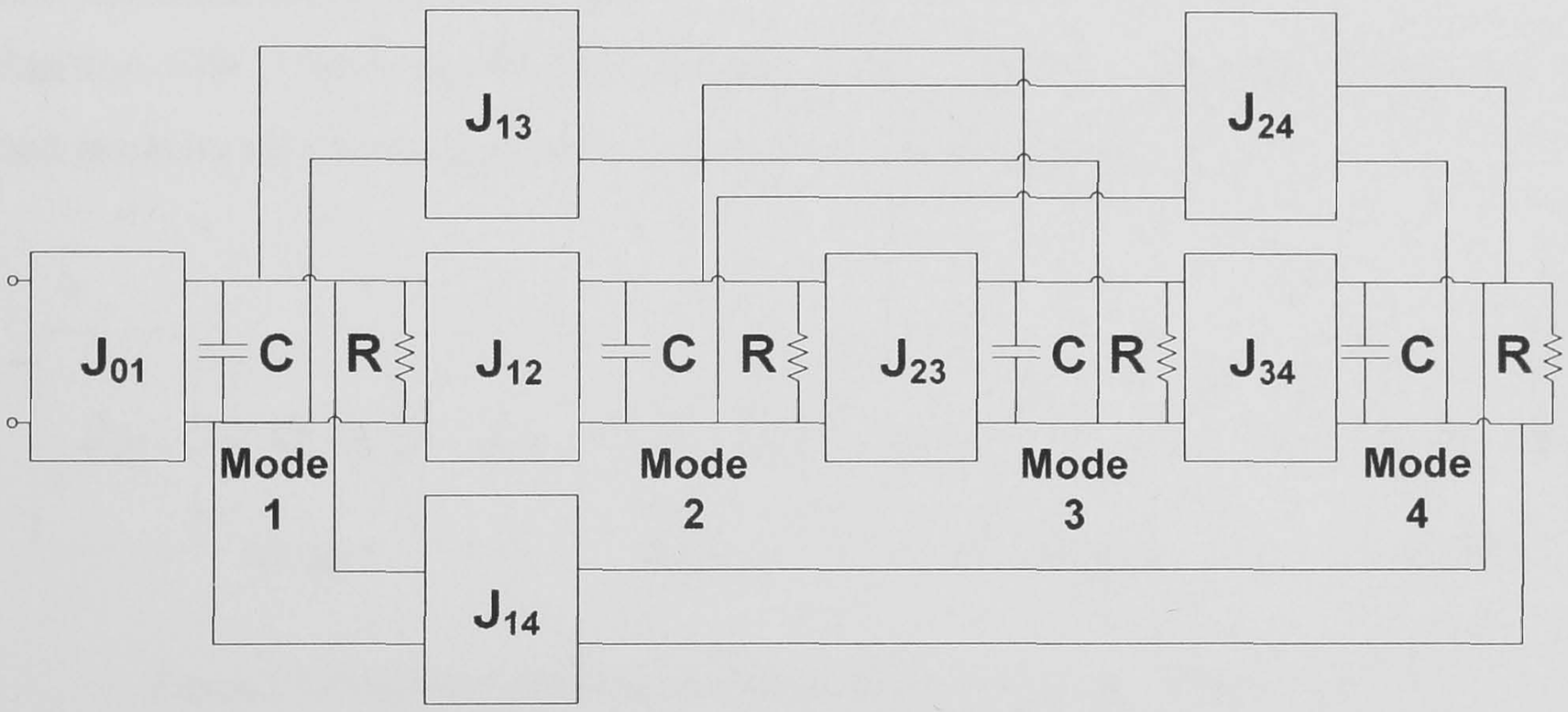

Figure 3.21 Quad-mode circular microstrip patch antenna lowpass prototype considering all the possible electromagnetic couplings between the 4 resonant modes in the physical model.

Furthermore, electromagnetic couplings through the dielectric layer are expected only to occur between modes 1-4, and modes 2-3 respectively if they are in line with each other as shown in Figure 3.19, but cross coupling is also possible. In theory couplings 3-1 and 4-2 are expected to reduce to zero. Therefore, the circuit in Figure 3.21 should in theory reduce to the one in Figure 3.22.

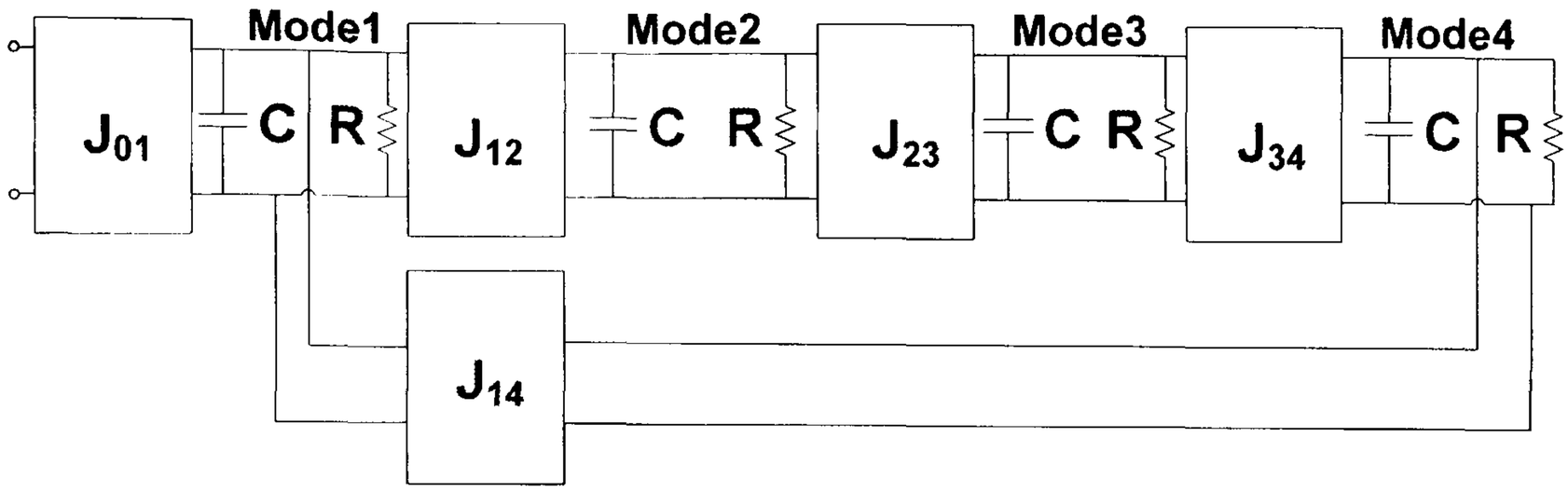

Figure 3.22 Quad-mode circular microstrip patch antenna lowpass prototype.

In the following analysis, it is shown how the prototype networks in Figure 3.21 and Figure 3.22 above can be derived analytically, reaching physical design dimensions and EM simulations of the antenna.

Starting with a basic fourth order lowpass ladder network, where all the capacitors and resistors may be normalised to unity as shown in Figure 3.23.

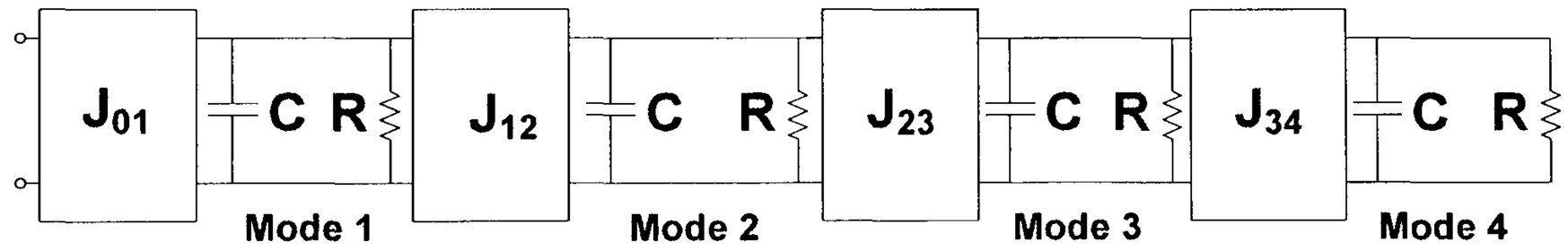

Figure 3.23 Equivalent Fourth order lowpass ladder network (N=4 and R = C = 1).

The expression for the reflection coefficient $S_{11}(p)$ of the network shown in Figure 3.23 can be derived using circuit analysis techniques in [95];

$$S_{11}(p)=\frac{p^4+p^3(4-J_{01}^2)+p^2(6-3J_{01}^2+J_{12}^2+J_{23}^2+J_{34}^2)+p(4-3J_{01}^2+2J_{12}^2+2J_{23}^2+2J_{34}^2-J_{01}^2J_{34}^2-J_{01}^2J_{23}^2)+(1-J_{01}^2+J_{12}^2+J_{23}^2+J_{34}^2+J_{12}^2J_{34}^2-J_{01}^2J_{34}^2-J_{01}^2J_{23}^2)}{p^4+p^3(4+J_{01}^2)+p^2(6+3J_{01}^2+J_{12}^2+J_{23}^2+J_{34}^2)+p(4+3J_{01}^2+2J_{12}^2+2J_{23}^2+2J_{34}^2-J_{01}^2J_{34}^2-J_{01}^2J_{23}^2)+(1+J_{01}^2+J_{12}^2+J_{23}^2+J_{34}^2+J_{12}^2J_{34}^2+J_{01}^2J_{34}^2+J_{01}^2J_{23}^2)}$$

3.28

However, the correct coupling values (J_{01}-J_{34}) are still to be found. This may be designed to have a quasi-equiripple return loss characteristic using techniques

described in [95, 96]. The theory of coupling matrices in filter prototypes is further explained in [94, 95]

The return loss function for lowpass equiripple prototype resonator of order "r" is given by [96, 97];

$$S_{11}(p) = \prod_{r=1}^{n} \frac{p - j\omega_r}{p - j\omega_r + 2/Q} \qquad 3.29$$

Where n represent the number of resonators used

$p = j\omega$

ω_r is the frequencies at which S_{11} is equal to zero.

and $Q = \omega CR$

Using optimisation, the values of ω_r for $r = 1 \rightarrow n$ can be found to achieve an equiripple response over a particular level (Matlab code can be found in Appendix A). In this case, n is equal to 4, Q is equal to 1 (assuming R=C=1) and therefore the expression of the reflection coefficient $S_{11}(p)$ can be computed to achieve a 6dB return loss ripple level (which is typical for handset antennas) and can be shown as:

$$S_{11}(p) = \frac{p^4 + 46.4425p^2 + 201.3561}{p^4 + 8p^3 + 70.4425p^2 + 217.77p + 403.1261} \qquad 3.30$$

where $\omega_1 = \pm 2.2$rad and $\omega_2 = \pm 6.25$rad.

The expression derived in equation 3.30 is plotted in Figure 3.24, showing a fourth degree equiripple response.

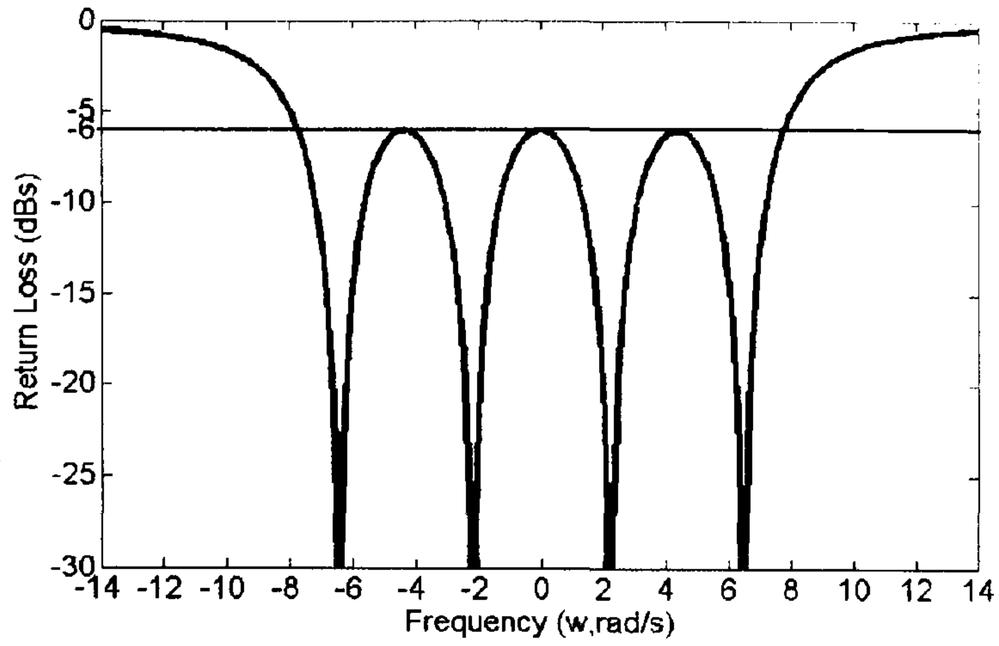

Figure 3.24 Graphical plot of the return loss response obtained by equation 3.30.

By equating the coefficients of equations 3.28 and 3.30; these are the reflection coefficients expressions $S_{11}(p)$ found with reference to Figure 3.23 (circuit analysis) and the result of equation 3.30, the coupling values (J_{01}-J_{34}) can be obtained. These are:

$$J_{01} = 2\ , \qquad J_{12} = 5.296, \quad J_{23} = 3.898 \quad \text{and} \quad J_{34} = 2.976 \qquad 3.31$$

Matlab was used for this rigorous mathematical analysis. The simulated response for the network in Figure 3.23 using the values for (J_{01}-J_{34}) found above is shown in Figure 3.25, where a comparison with a single mode design shows over 5.7 times 6dB bandwidth improvement.

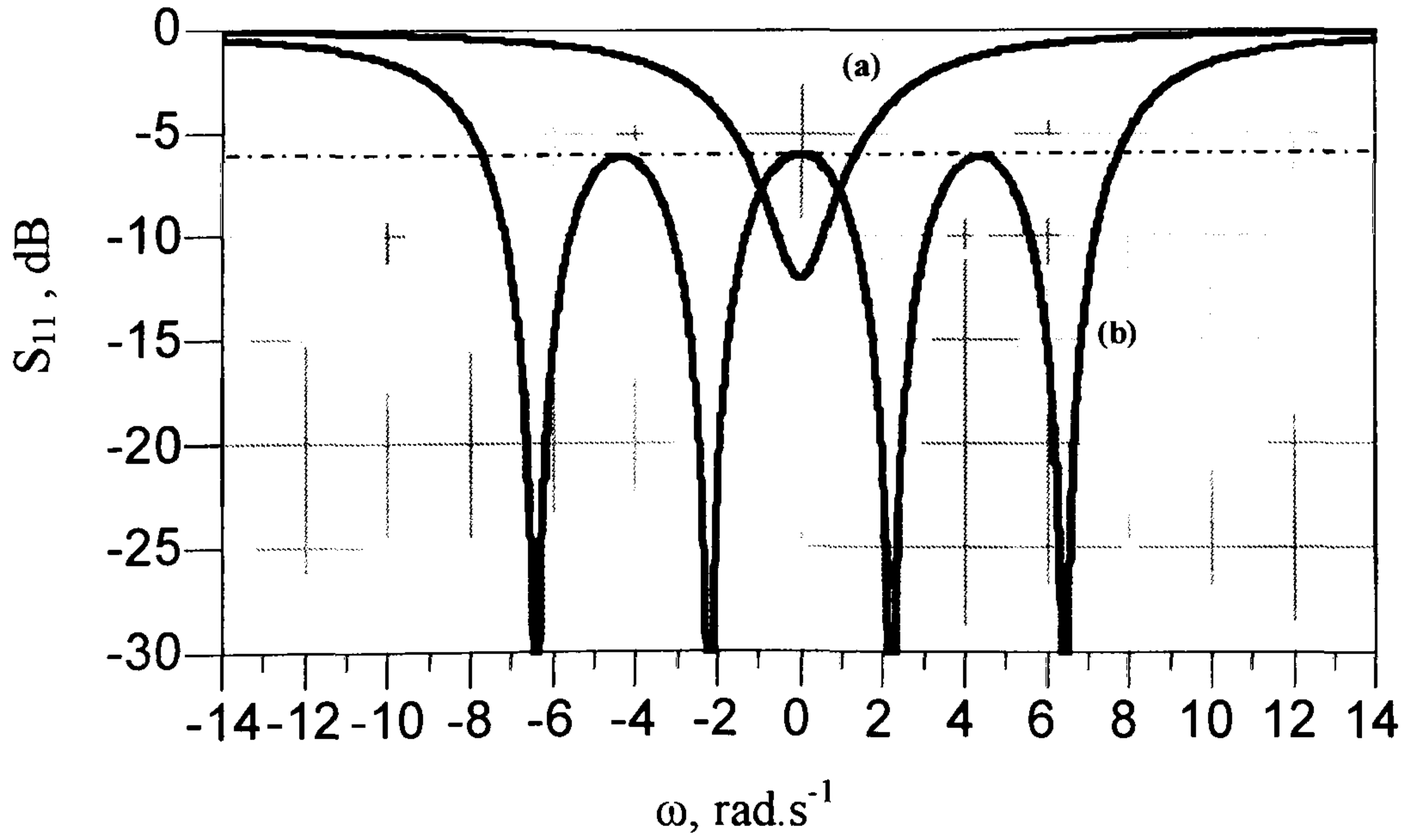

Figure 3.25 Simulation results of the equivalent lowpass circuit prototype of (a) single mode antenna and (b) quad-mode antenna.

However, the actual equivalent circuit of the practical antenna includes non-adjacent couplings between modes, as shown in Figure 3.21.

The admittance matrix of the lowpass prototype in Figure 3.25 is given by (3.32).

$$[y]=\begin{bmatrix} 0 & jJ_{01} & 0 & 0 & 0 \\ jJ_{01} & 1+p & jJ_{12} & 0 & 0 \\ 0 & jJ_{12} & 1+p & jJ_{23} & 0 \\ 0 & 0 & jJ_{23} & 1+p & jJ_{34} \\ 0 & 0 & 0 & jJ_{34} & 1+p \end{bmatrix} \quad 3.32$$

Or,

$$[y]=\begin{bmatrix} 0 & 0 & 0 & 0 & 0 \\ 0 & 1+p & 0 & 0 & 0 \\ 0 & 0 & 1+p & 0 & 0 \\ 0 & 0 & 0 & 1+p & 0 \\ 0 & 0 & 0 & 0 & 1+p \end{bmatrix} + \begin{bmatrix} 0 & jJ_{01} & 0 & 0 & 0 \\ jJ_{01} & 0 & jJ_{12} & 0 & 0 \\ 0 & jJ_{12} & 0 & jJ_{23} & 0 \\ 0 & 0 & jJ_{23} & 0 & jJ_{34} \\ 0 & 0 & 0 & jJ_{34} & 0 \end{bmatrix} \quad 3.33$$

Where the second part of equation 3.33 is known as the coupling matrix j[J] [94, 95].

It is well known from the theory of dual mode filters that the coupling matrix may be pre and post multiplied by rotational matrices without altering the input reflection coefficient of the network provided that these matrices do not operate on the first row and column of the coupling matrix. This process is known as matrix rotation [95]. Figure 3.26 below shows all the possible rotations that can produce couplings between the source (S), resonators 1, 2, 3 and 4

Rotation	**Induced Couplings**
1-2	S-2 and1-3
2-3	1-3 and 2-4
3-4	2-4
1-3	S-3 and 1-4
1-4	S-4, 1-3 and 2-4
2-4	1-4

Figure 3.26 Possible circuit rotation and result induced coupling

Scrutiny on Figure 3.26 shows that 2-4 rotation followed by 3-4 rotation will produce the network shown in Figure 3.21. However, one should be careful when doing this, as successive rotation might arise in different couplings (e.g. 2-4 rotation must be performed first and then 3-4 second, different results will be produced if 3-4 rotation was applied first).

So if we take the coupling matrix [J] from equation 3.33, apply 2-4 rotation, and then 2-3 rotation as shown in equations 3.34, 3.35 and 3.36.

$$[J_{2x4}]\rightarrow\begin{bmatrix}0&0&0&0&0\\0&0&0&0&0\\0&0&C_{2x4}&0&-S_{2x4}\\0&0&0&0&0\\0&0&S_{2x4}&0&C_{2x4}\end{bmatrix}\begin{bmatrix}0&J_{01}&0&0&0\\J_{01}&0&J_{12}&0&0\\0&J_{12}&0&J_{23}&0\\0&0&J_{23}&0&J_{34}\\0&0&0&J_{34}&0\end{bmatrix}\begin{bmatrix}0&0&0&0&0\\0&0&0&0&0\\0&0&C_{2x4}&0&S_{2x4}\\0&0&0&0&0\\0&0&-S_{2x4}&0&C_{2x4}\end{bmatrix} \quad 3.34$$

$$[J]\rightarrow\begin{bmatrix}0&0&0&0&0\\0&0&0&0&0\\0&0&C_{2x3}&-S_{2x3}&0\\0&0&S_{2x3}&C_{2x3}&0\\0&0&0&0&0\end{bmatrix}[J_{2x4}]\begin{bmatrix}0&0&0&0&0\\0&0&0&0&0\\0&0&C_{2x3}&S_{2x3}&0\\0&0&-S_{2x3}&C_{2x3}&0\\0&0&0&0&0\end{bmatrix} \quad 3.35$$

$$[J]\rightarrow\begin{bmatrix}0&J_{01}&0&0&0\\J_{01}&0&C_{2x3}.C_{2x4}.J_{12}&S_{2x3}.C_{2x4}.J_{12}&S_{2x4}.J_{12}\\0&C_{2x3}.C_{2x4}.J_{12}&-2S_{2x3}.C_{2x3}(C_{2x4}.J_{23}-S_{2x4}.J_{34})&-S_{2x3}^2.(C_{2x4}.J_{23}-S_{2x4}.J_{34})+C_{2x3}^2.(C_{2x4}.J_{23}-S_{2x4}.J_{34})&-S_{2x3}.(S_{2x4}.J_{23}+C_{2x4}.J_{34})\\0&S_{2x3}.C_{2x4}.J_{12}&-S_{2x3}^2.(C_{2x4}.J_{23}-S_{2x4}.J_{34})+C_{2x3}^2.(C_{2x4}.J_{23}-S_{2x4}.J_{34})&2S_{2x3}.C_{2x3}.(C_{2x4}.J_{23}-S_{2x4}.J_{34})&C_{2x3}.(S_{2x4}.J_{23}-C_{2x4}.J_{34})\\0&S_{2x4}.J_{12}&-S_{2x3}.(S_{2x4}.J_{23}+C_{2x4}.J_{34})&C_{2x3}.(S_{2x4}.J_{23}-C_{2x4}.J_{34})&0\end{bmatrix} \quad 3.36$$

Where

$$C_{2x3}=\cos(\theta_{2x3})$$
$$C_{2x4}=\cos(\theta_{2x4})$$
$$S_{2x3}=\sin(\theta_{2x3})$$
$$S_{2x4}=\sin(\theta_{2x4}) \quad 3.37$$

This mathematical result takes into account all the possible electromagnetic couplings in the physical structure in Figure 3.19. As shown in equation 3.36, the coupling between modes 1-3, 1-4, 2-3 and 2-4 are non zero anymore. This matrix now

describes the circuit in Figure 3.21, but the correct value of θ_{2x3} and θ_{3x4} are still to be found.

Now looking back at Figure 3.21 and Figure 3.25 again, in theory it can be assumed that the coupling between modes 2-3 and 1-4 are equal, as are the cross couplings between modes 2-4 and 1-3. This will help to obtain the value of θ in equation 3.36 and 3.37 that satisfies the conditions above, and hence find the correct values of the couplings that achieves the quad-ripple response. With reference to equation 3.36, the value of θ_{2x3} and θ_{2x4} can be found by equating the values for the coupling between modes 2-3 and 1-4, and coupling between modes 1-2 and 2-4 in the matrix

$$jS_{2x3}.C_{2x4}J_{12} = -jS_{2x3}.(S_{2x4}J_{23} + C_{2x4}J_{34}) \tag{3.38}$$

$$jS_{2x4}J_{12} = -jS_{2x3}^2.(C_{2x4}J_{23} - S_{2x4}J_{34}) + jC_{2x3}^2.(C_{2x4}J_{23} - S_{2x4}J_{34}) \tag{3.39}$$

The equation above was computed, and the values of θ_{2x3} and θ_{2x4} that satisfy equations 3.27 and 3.28 were found:

$$\theta_{2x3} = \pi \text{ and } \theta_{2x4} = 0.44029 \tag{3.40}$$

As expected, those values will force cross couplings (i.e. J_{13} and J_{24}) to zero and equalise the adjacent couplings (i.e. J_{14} and J_{23}) to reach a response similar to the one shown in Figure 3.22.

Those values alongside the coupling values found in equation 3.31 were used to evaluate [J] in equation 3.36 and the result is shown in equation 3.41.

$$[J] \rightarrow \begin{bmatrix} 0 & 2 & 0 & 0 & 0 \\ 2 & 0 & -4.793 & 0 & 2.26 \\ 0 & -4.793 & 0 & 2.26 & 0 \\ 0 & 0 & 2.26 & 0 & -4.354 \\ 0 & 2.26 & 0 & -4.354 & 0 \end{bmatrix} \tag{3.41}$$

Figure 3.27 shows the final equivalent circuit as a result of matrix rotation.

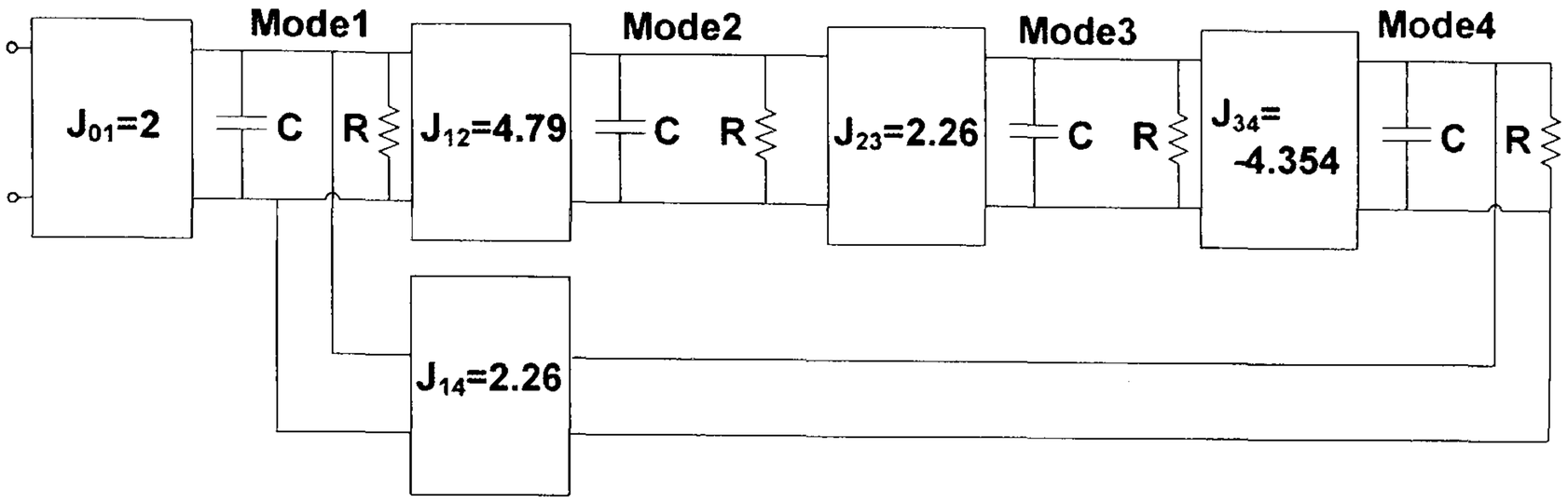

Figure 3.27 Quad-mode circular microstrip patch antenna lowpass prototype.

Here it can be clearly seen that there will definitely be couplings between modes 1-4, and 2-3. These couplings are equal in magnitude as expected. The other couplings between modes 1-3 and 2-4 are zero as expected.

3.3.2. EM Simulation and Practical Implementation

The resonant frequency of a circular microstrip patch antenna at a particular mode is governed by the radius and the substrate used to make the antenna, the relation between these parameters is given approximately by [4, 12, 37]:

$$f_r = \frac{c\chi'_{mn}}{2\pi a(\varepsilon_r)^{1/2}} \qquad 3.42$$

Where f_r is the resonant frequency, χ'_{mn} are the zeros of the Bessel function of order "n", and equal to 1.8412 for the dominant TM_{110} mode and a is the radius of the circular patch. The radius of quadruple-mode antenna can be calculated using equation 3.42. Couplings between adjacent modes in each patch can be introduced using a notch. The most logical procedure is to start with the first patch and obtain the dimensions of the slot by electromagnetic simulation with reference to the circuit simulation. If the circuit in Figure 3.27 is simulated with couplings J_{12}, J_{23}, J_{34} and J_{14} are reduced to zero, this would leave us with the first patch only. The simulated return loss at the centre frequency is -4.4dB. This result represents the coupling between the port and the first patch, and therefore enables us to locate the position of the feed point [1]. The second step is to account for the coupling between the first two modes, i.e. J_{01} and J_{12}. If the circuit in Figure 3.27 is simulated with all couplings reduced to zero apart from J_{01} and J_{12}, the result indicates the return loss bandwidth of modes 1

and 2 only. The coupling between them is found to be approximately 3dB, hence, a notch can be introduced at the lower layer and with the aid of computer simulations, it can be designed to achieve a coupling of 3dB between modes 1 and 2. At this stage, the lower patch is designed.

The second step is to introduce the coupling between the first two modes on the bottom patch, i.e. J_{12}. If the circuit in Figure 3.27 is simulated with all couplings reduced to zero apart from J_{01} and J_{12}, the result indicates the return loss bandwidth of modes 1-2 only. The coupling level between them is found to be approximately 3 dB. A notch 6.17x5 mm placed at 135° from the feed line is introduced at the bottom patch, and with the aid of computer simulations, it can be designed to achieve a coupling of 3 dB between modes 1-2 in the same manner as [93].

At this stage, the bottom patch is now designed. The top patch may now be introduced and the dimensions of the second notch may be evaluated. Three tuning parameters were found useful to achieve the overall maximum 6 dB return loss bandwidth, these are the thickness of the substrate between the two patches which controls the coupling strength between the two layers, a notch at one mode and a metal extension on the other mode controlling the couplings J_{23} and J_{14} respectively. By tuning the circuit using computer simulation, a 5.55x5 mm notch is placed at 135° from the feed line on the upper patch and a metal extension of 3.87x5 mm placed at 225° from the feed line on the top patch, where the top substrate thickness is 0.381 mm. A quadruple-mode antenna (Figure 3.28 and Figure 3.29) has been designed on Duroid 5880, εr =2.2, with total thickness 1.168 mm.

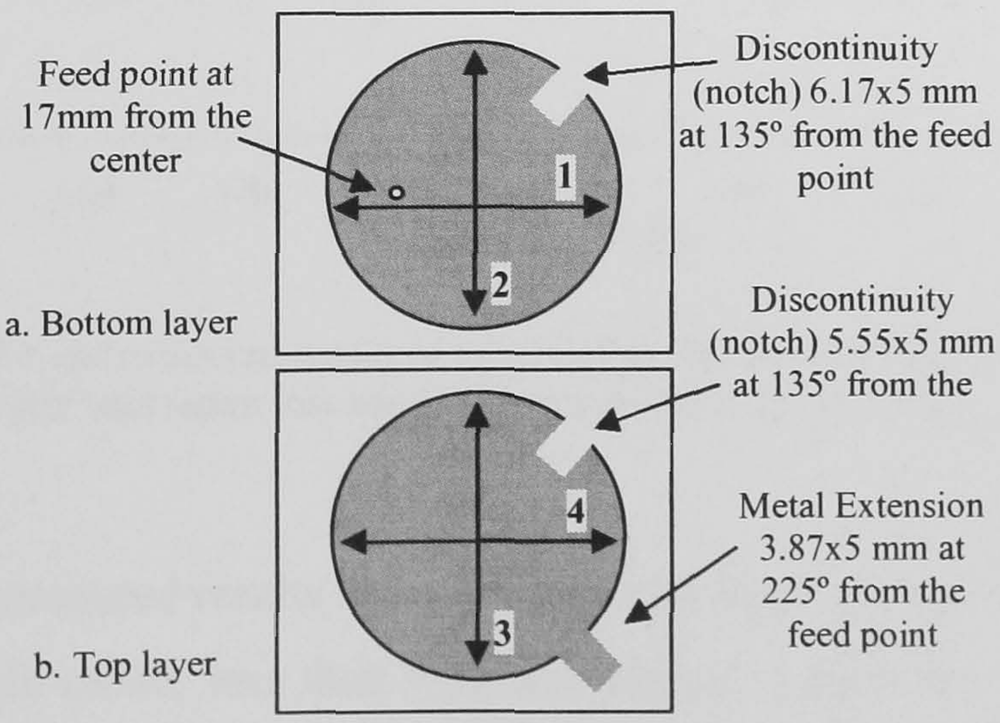

Figure 3.28 The physical dimensions of the antenna.

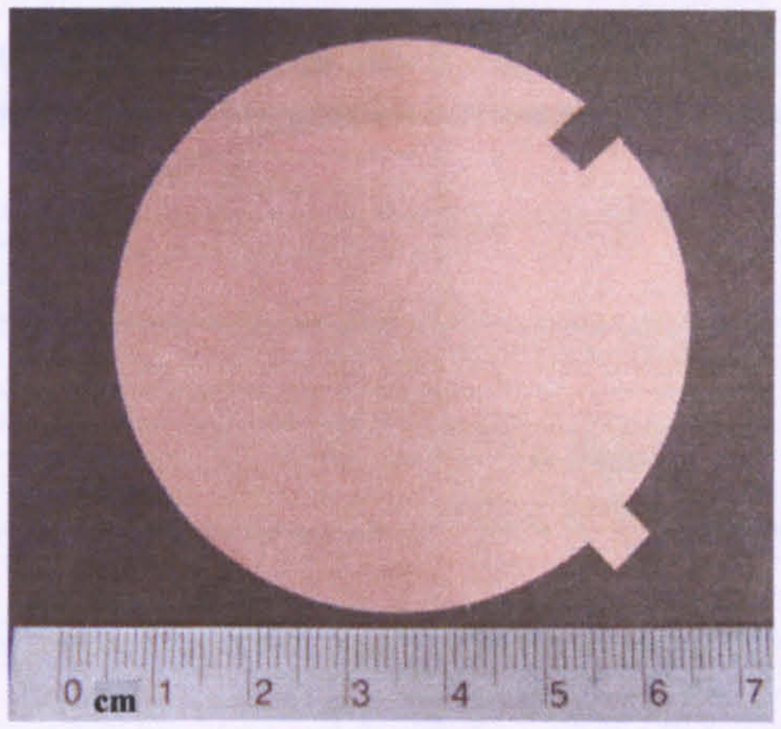

Figure 3.29 Quad-mode patch antenna prototype (Top layer view).

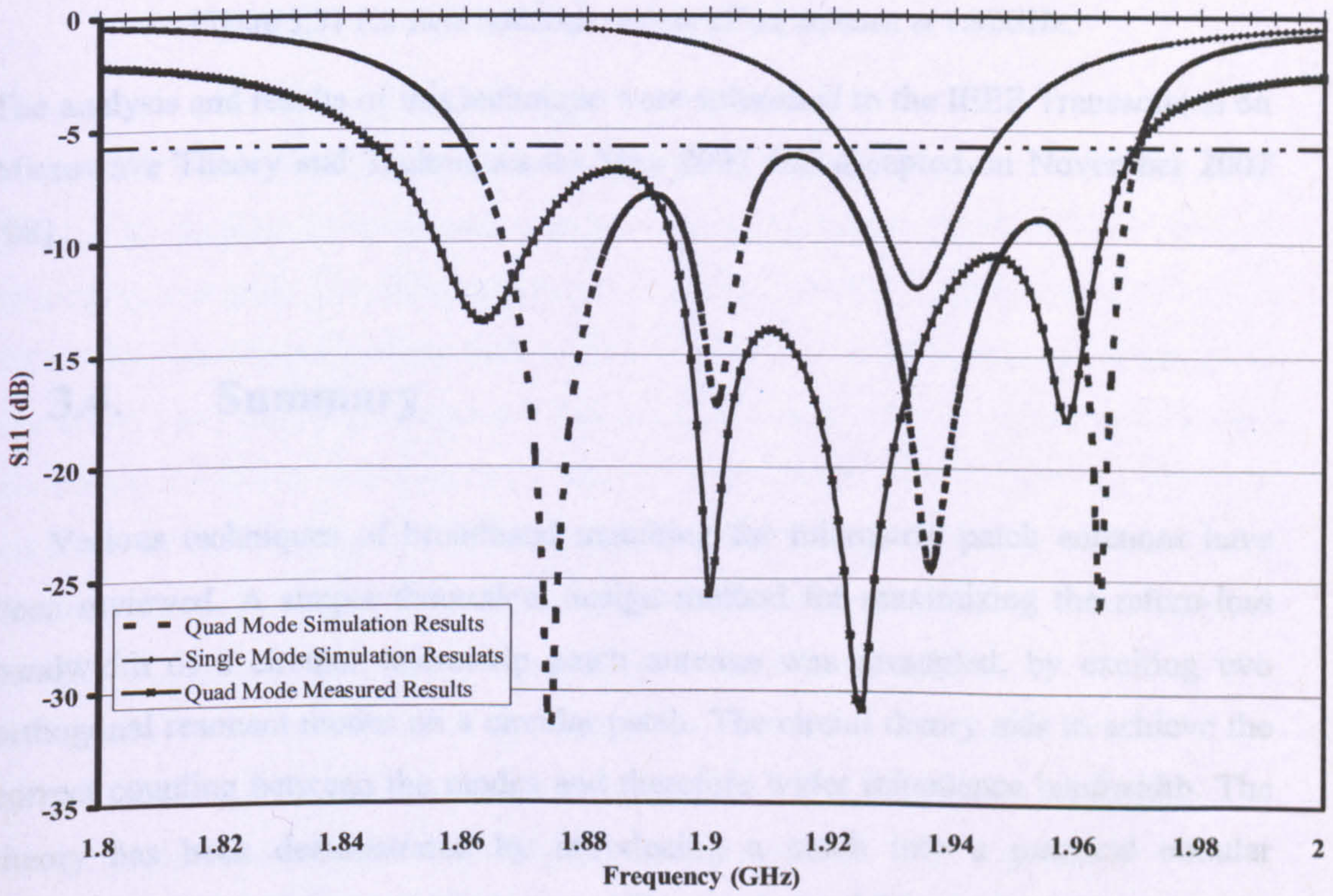

Figure 3.30 Simulation and measured results of the Quad-mode antenna design showing 4.2 times wider 6dB return loss bandwidth compared to single mode.

The simulated and measured results show a bandwidth improvement of over 4.2 times compared to a single mode, less than what the circuit simulations anticipated. The radiation patterns of this antenna at 1.92GHz are shown in Figure 3.31. This is quite similar to a single mode patch antenna.

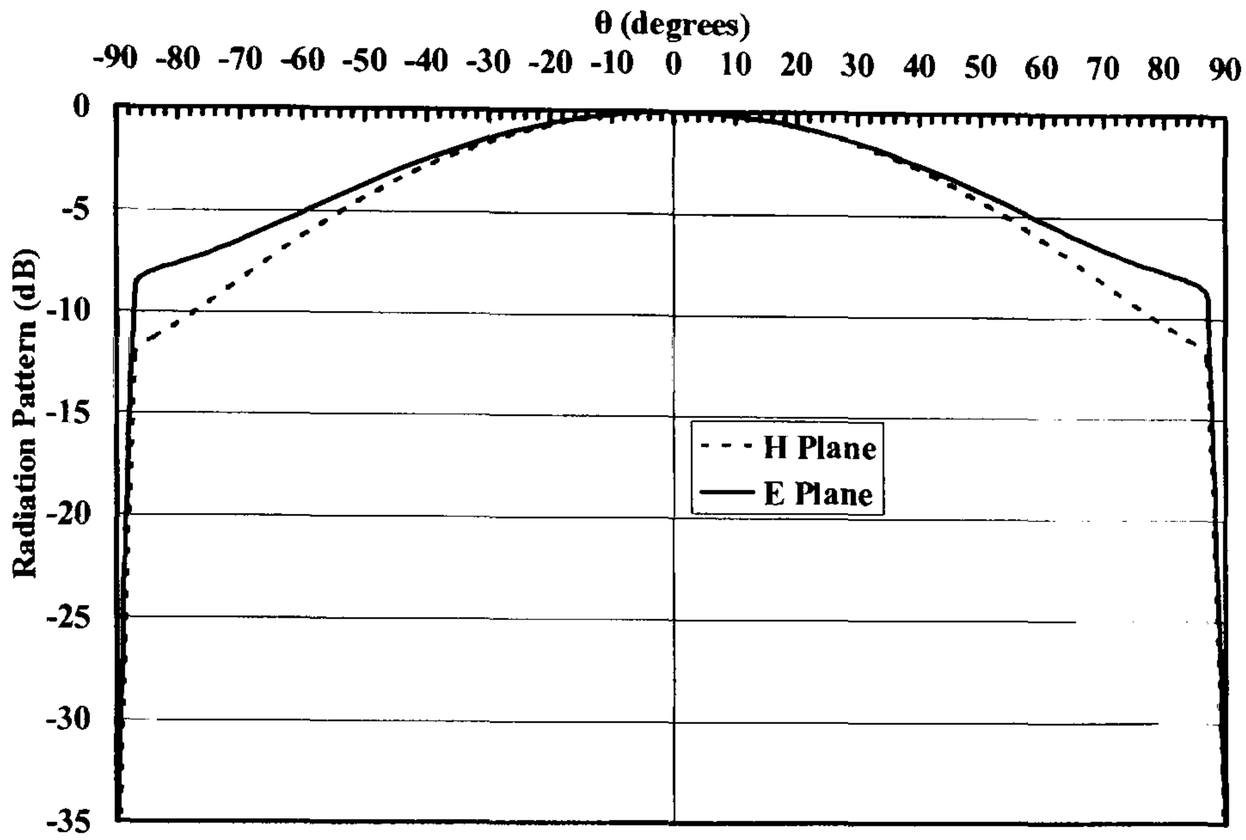

Figure 3.31 Far field radiation pattern of the antenna at 1.92GHz.

The analysis and results of this technique were submitted to the IEEE Transactions on Microwave Theory and Techniques on May 2007 and accepted on November 2007 [98].

3.4. Summary

Various techniques of broadband matching for microstrip patch antennas have been reviewed. A simple theoretical design method for maximizing the return-loss bandwidth of a circular microstrip patch antenna was presented, by exciting two orthogonal resonant modes on a circular patch. The circuit theory aids to achieve the correct coupling between the modes and therefore wider impedance bandwidth. The theory has been demonstrated by introducing a notch into a practical circular microstrip patch antenna, which in turn will perturb the fields and couple the modes. This technique was then extended into a quadmode circuit, where two dualmode circular microstrip patches are broadside coupled, achieving an even wider impedance bandwidth of over 4 times compared to the single mode case.

Chapter 4. Multiband Matching Techniques

From the seventies through until the mid eighties, most research in the field of microstrip antennas developments was addressing the narrow bandwidth property of microstrip antennas, and little attention was given to multi-frequency operation [99, 100]. The rise of applications such as GSM, WLAN and GPS required antennas to operate at more than one frequency. The main challenge when it comes to designing multiband microstrip antennas is to obtain a good match with the feeding network, maintain the radiation pattern and keeping the design simple while operating at more than one frequency [2, 100]. Three different approaches were reported in the literature to achieve multiband operation of microstrip antenna, these are [100]:

a) Orthogonal-mode dual frequency patch antennas.

b) Multi-patch dual frequency antennas.

c) Reactively loaded dual-frequency patch antennas.

These approaches are summarised in Figure 4.1 showing different techniques of multiband matching. However, only the first approach will be discussed in further details in this section.

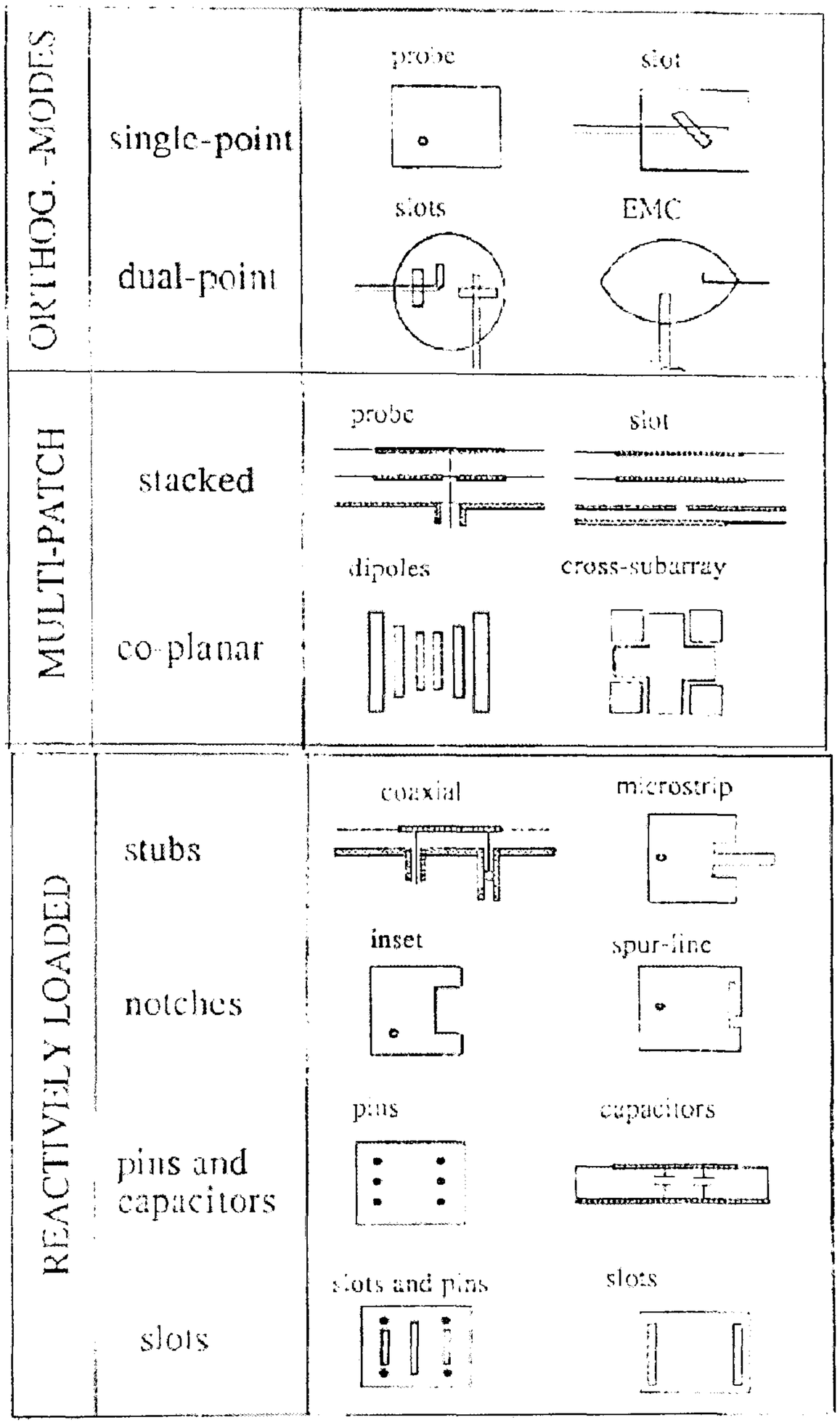

Figure 4.1 Dual-frequency techniques for patch antennas [100].

The idea of designing microstrip antennas with multiple resonances began in the late seventies. Sanford filed one of the first patents on multiband microstrip antennas in 1978 [55]. In the same year, Derneryd studied microstrip antennas that covers multiple frequencies by integrating a two section impedance transformer [6]. In the following year, Long and Walton further developed Sanford's work and designed a dual frequency circular disc antenna [56], by stacking two discs with different radiuses and therefore radiating at different frequencies. At that time there were not many applications that required multiple frequency operation, not until the mid eighties, when the research on muiltiband microstrip antennas started to become more

active [2, 100]. Microstrip patch antennas, like cavity resonators, resonate at different resonant modes, and therefore, these modes can be used for dual frequency operation. Also by varying the dimensions of a rectangular microstip antenna or using an elliptical microstrip antenna, dual frequency operation with orthogonal polarisation can be achieved as discussed in [2, 101]. Reactive loading to the patch by cutting a notch can also be used to obtain dual band resonance [102]. Other techniques derived from filter designs, achieving circular polarisation [103] and aperture coupling [2, 99, 100] were also reported. Many of the broadband matching techniques were used for dual band matching as well.

4.1. Dual-band Microstrip Antenna

Microstrip antennas are widely used in modern microwave systems, supporting the trend towards utilisation of internal antennas in wireless systems. During the last decade, there has been research on frequency agility and multi-band matching for microstrip antennas where an increase in length or height of the antenna were expected or the use of multilayer design has been adopted [103, 104]. However, space is usually limited, and this may significantly reduce the system performance. Small antennas working at low frequencies may have a very restricted bandwidth of operation, sometimes even being required to operate on more than one frequency. For example, antennas are usually expected to achieve a reasonable input match over more than one of the assigned frequencies of GSM devices and for Global Positioning Systems (GPS). In an antenna workshop at the IMS2007 [105], it was pointed that the next generation of mobile phones handset are expected to operate on 9 different frequencies.

In this section, a new circuit-theoretic method of multi-band matching for circular microstrip patch antennas is presented. The input impedance of a patch antenna may be represented as a second order ladder network of coupled resonators where each resonator is coupled to a load resistor as shown in Chapter 3. Analysis based on circuit theory shows that the antenna can be used as a dual-band antenna, exploiting the fact that circular microstrip patch antennas can support two orthogonal resonant

modes. A theoretical method for evaluating the coupling values in the network is discussed, enabling the antenna to be matched at two distinct frequencies. This is confirmed with an experimental dual-band circular microstrip patch antenna. The antenna is then further developed, providing designs for a self diplexing patch antenna. The designs are all developed with techniques used in microwave filter theory and single layer layouts.

4.1.1. Mathematical Analysis – Dual-mode to Dual-band Transformation

In chapter 3, it was shown that the input can feed into one mode of the antenna and then couple to the second mode via a discontinuity in the structure as shown in Figure 4.2.

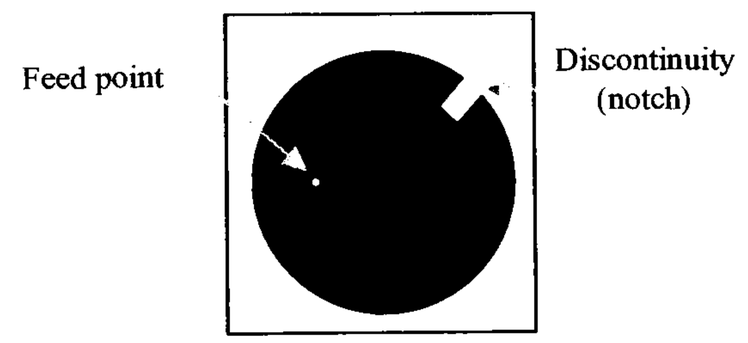

Figure 4.2 Dual mode circular microstrip patch antenna

The equivalent circuit of this structure is a second order ladder network shown in Figure 4.3. Figure 4.4 shows the simulation results of this circuit [93].

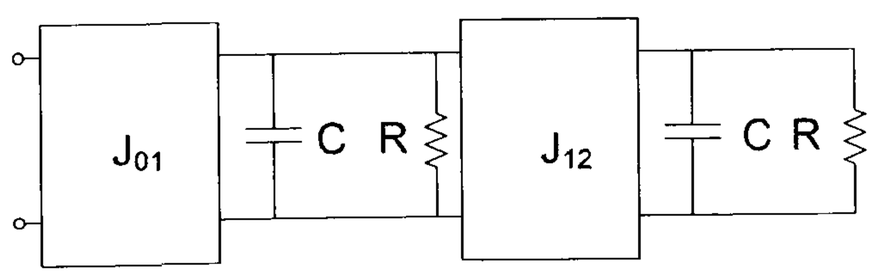

Figure 4.3 Equivalent lowpass circuit of dual-mode Antenna.

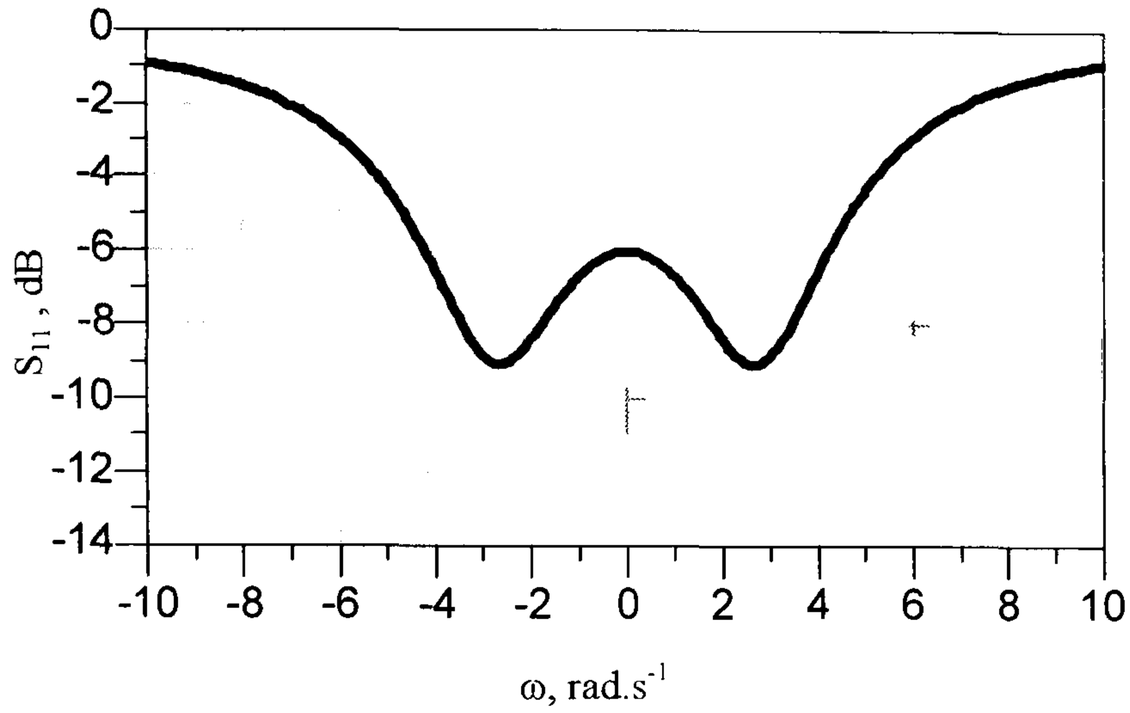

Figure 4.4 Dual mode antenna equivalent circuit simulated results.

The antenna can be considered in terms of two distinct transfer functions, these are S_{12A} and S_{12B} each presenting the coupling into the two polarisation modes [95]. The squared total transfer function is given by the sum of the magnitude squared of S_{12A} and S_{12B} [95], i.e.;

$$\left|S_{12\text{Total}}(j\omega)\right|^2 = \left|S_{12\text{A}}(j\omega)\right|^2 + \left|S_{12\text{B}}(j\omega)\right|^2 \qquad 4.1$$

And from unitary conditions for a lossless network [95]:

$$\left|S_{12\text{Total}}(j\omega)\right|^2 = 1 - \left|S_{11}(j\omega)\right|^2 \qquad 4.2$$

The return loss expression for the circuit in Figure 4.3 was derived in chapter 3 [93] and shown as:

$$\left|S_{11}(j\omega)\right|^2 = \frac{\omega^4 + \omega^2\left({J_{01}}^4 - 8{J_{01}}^2 + 4\right) + 4{J_{01}}^4}{\omega^4 + \omega^2\left({J_{01}}^4 - 4{J_{01}}^2 + 4\right) + 16{J_{01}}^4} \qquad 4.3$$

It was also shown that if a 6dB return loss bandwidth is considered, $J_{01}^{\ 2} = 1\frac{4}{3}$, and therefore equation 4.3 becomes;

$$|S_{11}(j\omega)|^2 = \frac{\omega^4 - 11\frac{5}{9}\omega^2 + 87\frac{1}{9}}{\omega^4 + 7\frac{1}{9}\omega^2 + 348\frac{4}{9}} \qquad 4.4$$

And using 4.3,

$$|S_{12}(j\omega)|^2 = 1 - \frac{\omega^4 - 11\frac{5}{9}\omega^2 + 87\frac{1}{9}}{\omega^4 + 7\frac{1}{9}\omega^2 + 348\frac{4}{9}} \qquad 4.5$$

$$= \frac{18\frac{6}{9}\omega^2 + 261\frac{1}{3}}{\omega^4 + 7\frac{1}{9}\omega^2 + 348\frac{4}{9}} \qquad 4.6$$

This result assumes a lossless antenna, considering the lowpass prototype for 6dB return loss (i.e. at ω=0) then $|S_{12}|^2 = 0.75$.

It is interesting to note that there are different network realisations each with a different transfer function into the two polarisations. For instance, once again let us consider the dual mode antenna lowpass prototype shown in Figure 4.3, the resistor and capacitor values were set to unity in previous studies to enable direct comparison with the single-mode case, and the admittance matrix of the lowpass prototype can be shown as;

$$[Y] = \begin{bmatrix} 0 & jJ_{01} & 0 \\ jJ_{01} & 1+p & jJ_{12} \\ 0 & jJ_{12} & 1+p \end{bmatrix} \qquad 4.7$$

and can also be re-written as;

$$[Y] = \begin{bmatrix} 0 & 0 & 0 \\ 0 & 1+p & 0 \\ 0 & 0 & 1+p \end{bmatrix} + \begin{bmatrix} 0 & jJ_{01} & 0 \\ jJ_{01} & 0 & jJ_{12} \\ 0 & jJ_{12} & 0 \end{bmatrix} \qquad 4.8$$

The second part of equation 4.8 is known as the coupling matrix j[J]. The theory of coupling matrix in filter prototype is further explained in [94, 95]. However, from the theory of dual mode filters, the coupling matrix can be pre and post multiplied by

rotational matrices without altering the input reflection coefficient of the network, providing that they do not operate on the first row or column [95]. As shown in Figure 4.3, the capacitors only exist between nodes and ground, therefore the complex frequency variable "p" only exists on the main diagonal of the identity matrix. Thus if the matrix is pre and post multiplied by a matrix $[T]$ an infinite number of new matrices may be generated all with the same transfer function, and this will not affect the capacitors as the theory indicates in equation 4.9-10 [95]:

$$[Y]=[T]^{-1}p[I][T]+j[T]^{-1}[J][T] \tag{4.9}$$

$$=p[I]+j[T]^{-1}[J][T] \tag{4.10}$$

the new coupling matrix is given by:

$$[M]=[T]^{-1}[J][T] \tag{4.11}$$

Since the theory only allows matrices that do not operate on the first row and column, The only possible transformation is 2-3. Thus if a 2, 3 rotation of angle θ is performed as follows [95]:

$$[J]\rightarrow\begin{bmatrix}1&0&0\\0&C&S\\0&-S&C\end{bmatrix}\text{x}\begin{bmatrix}0&\text{jJ}_{01}&0\\\text{jJ}_{01}&0&\text{jJ}_{12}\\0&\text{jJ}_{12}&0\end{bmatrix}\text{x}\begin{bmatrix}1&0&0\\0&C&-S\\0&S&C\end{bmatrix} \tag{4.12}$$

Where $C=\cos(\theta), S=\sin(\theta)$; thus $[J]$ becomes;

$$[J]=\begin{bmatrix}0&\text{jJ}_{01}C&-\text{jJ}_{01}S\\\text{jJ}_{01}C&2\text{jJ}_{01}SC&\text{jJ}_{12}(C^2-S^2)\\-\text{jJ}_{01}S&\text{jJ}_{12}(C^2-S^2)&-2\text{jJ}_{01}SC\end{bmatrix} \tag{4.13}$$

And hence $[Y]$ becomes:

$$[Y]=\begin{bmatrix}0&\text{jJ}_{01}C&-\text{jJ}_{01}S\\\text{jJ}_{01}C&1+2\text{jJ}_{01}SC+p&\text{jJ}_{12}(C^2-S^2)\\-\text{jJ}_{01}S&\text{jJ}_{12}(C^2-S^2)&1-2\text{jJ}_{01}SC+p\end{bmatrix} \tag{4.14}$$

As shown, the capacitor values are not affected by this transformation, however, new couplings were introduced. The equivalent circuit after this transformation is shown in Figure 4.5.

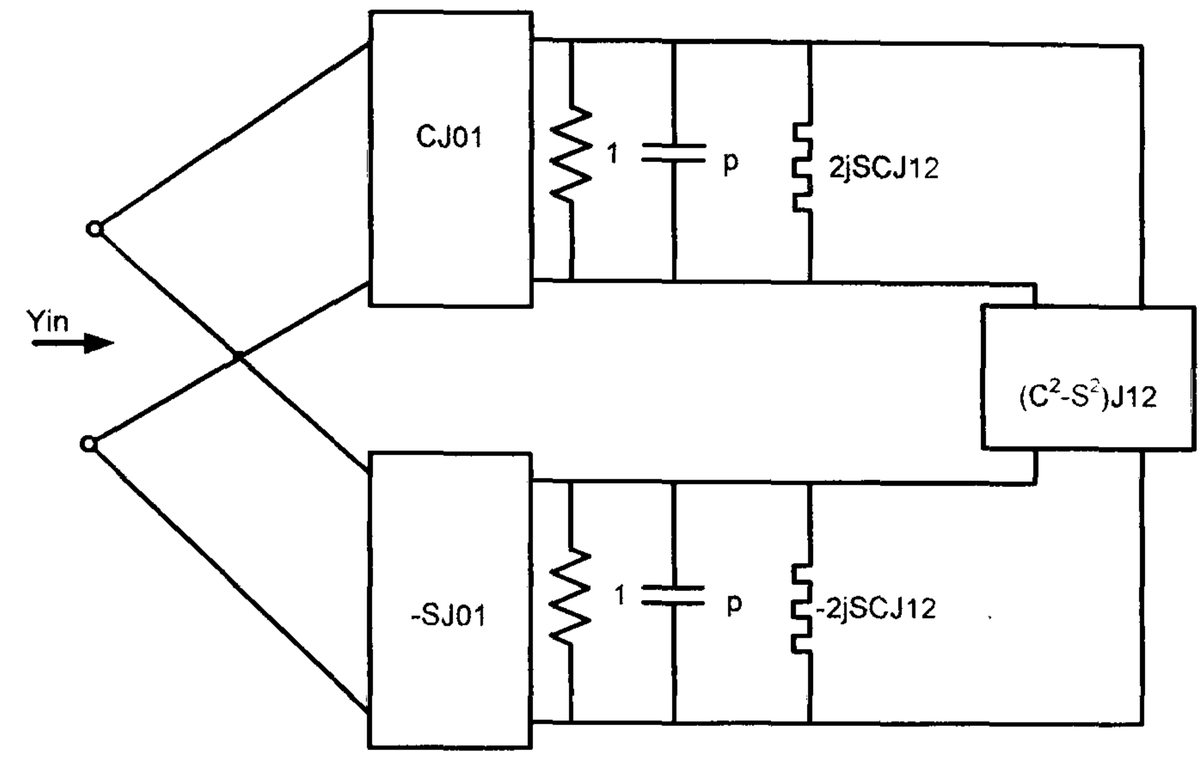

Figure 4.5 The equivalent circuit of the dual-mode antenna after pre/post multiplying it by rotational matrix.

Here we see that the input is now coupled to both resonant modes individually, which are detuned by frequency invariant reactances, one up and one down in frequency. However, the modes are still coupled to each other as shown in Figure 4.5, and in order to reach a dual mode antenna equivalent circuit, this coupling must be eliminated. Looking at this coupling value, one possible solution is that:

$$C^2 - S^2 = 0 \quad \rightarrow \qquad \cos^2(\theta) - \sin^2(\theta) = 0 \tag{4.15}$$

and this can achieved by adjust the value of θ to;

$$\theta = -45^\circ \text{ giving } C = \tfrac{1}{\sqrt{2}} \;\&\; S = \tfrac{-1}{\sqrt{2}} \tag{4.16}$$

This value of θ can be used in equation 4.14 to evaluate the coupling values as shown in equation 4.17, and as a result, the circuit reduces to the one shown in Figure 4.6. The coupling into each mode is equal and detuned by equal frequency invariant reactances up and down in frequencies. These couplings from the source to each mode represent the transfer functions S_{12A} & S_{12B} of the dual mode antenna [88, 95] with rotation angle $\theta = -45^\circ$.

$$[Y]=\begin{bmatrix} 0 & \frac{jJ_{01}}{\sqrt{2}} & \frac{jJ_{01}}{\sqrt{2}} \\ \frac{jJ_{01}}{\sqrt{2}} & 1-jJ_{01}+p & 0 \\ \frac{jJ_{01}}{\sqrt{2}} & 0 & 1+jJ_{01}+p \end{bmatrix} \qquad 4.17$$

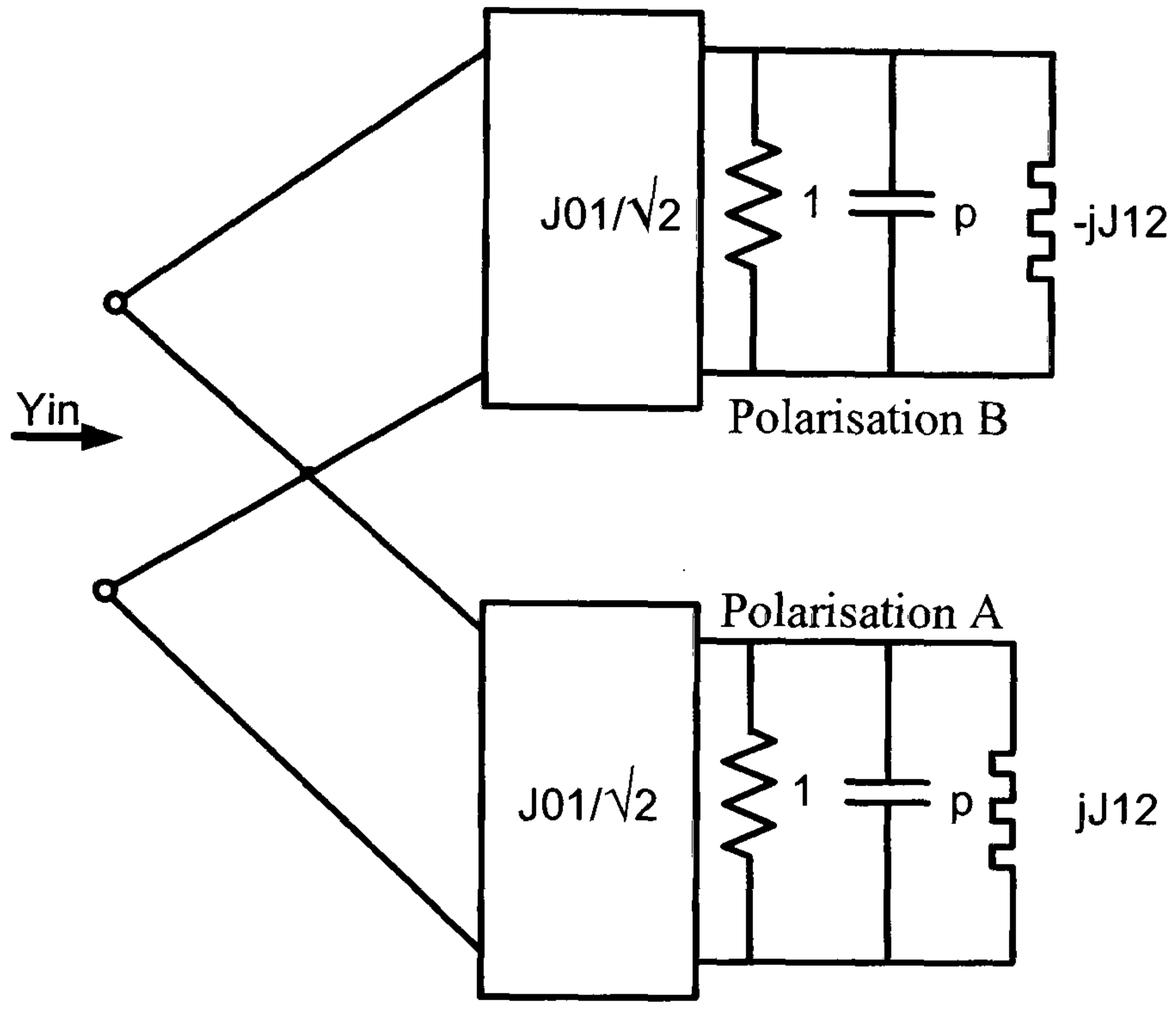

Figure 4.6 The equivalent circuit of the Dual-band antenna as a result of 2-3 rotation to the dual-mode network.

The simulation results of the circuit in Figure 4.6 are shown in Figure 4.7. As expected, the return loss response of the antenna is the same, however, it is clear that the antenna now behaves like a multimode transmitter/receiver, with lower frequencies radiating in polarisation B and higher frequencies in polarisation A.

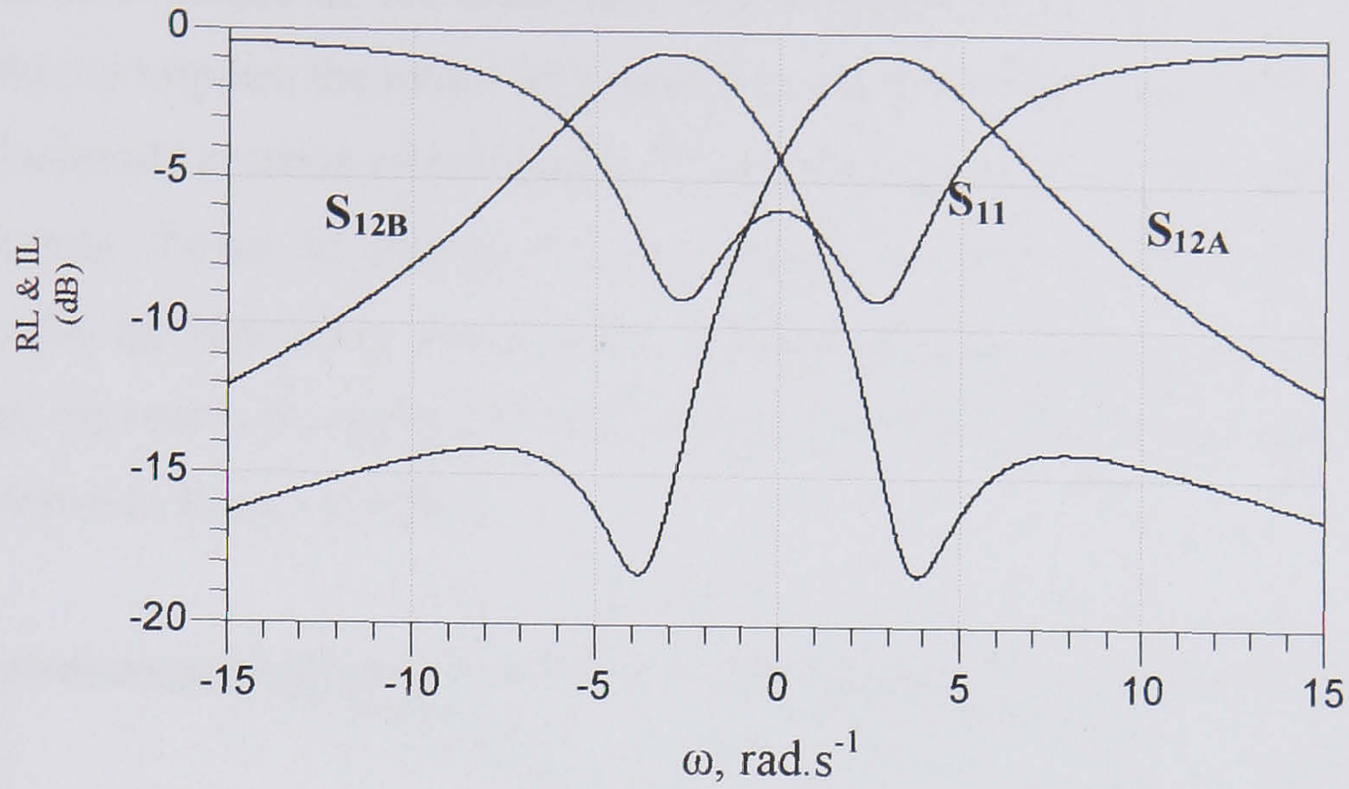

Figure 4.7 Dual-band antenna equivalent circuit simulation results, showing the coupling into the two polarisation modes (A&B) at two different frequencies.

4.1.2. Simulation and Practical Implementation.

In order to demonstrate the theoretical results derived earlier, the experimental prototype antenna designed in section 3 can be used again here.

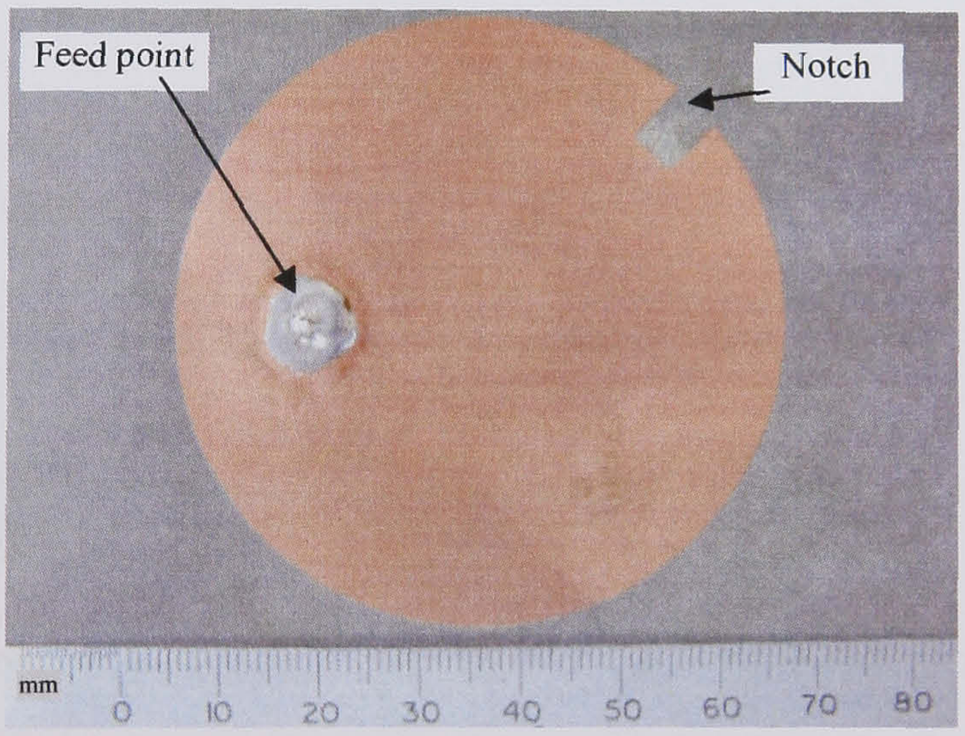

Figure 4.8 Dual-mode circular patch antenna designed at 2 GHz.

For the antenna to operate at two distinct frequencies, the two modes must be split, one up and the other down from the centre frequency. To achieve this, a coupling notch which perturbs the fields on the patch disturbing the symmetry is introduced. This has been used to couple the two orthogonal modes in [88, 93] and achieve a wider bandwidth accordingly. A dual-band circular microstrip antenna, with exactly

the same dimensions of the dualmode one in chapter 3 is fabricated. Now as the circuit theory implies, the return loss response of the dualband one should be the same as the dualmode antenna after transformation, however, the insertion loss is different. The antenna shown in Figure 4.8 can radiate at each of the two polarisations individually by physically rotating the antenna through 90°, or facing it with two antennas, one vertically polarised and another horizontally polarised, and the result of this is shown in Figure 4.9 [93].

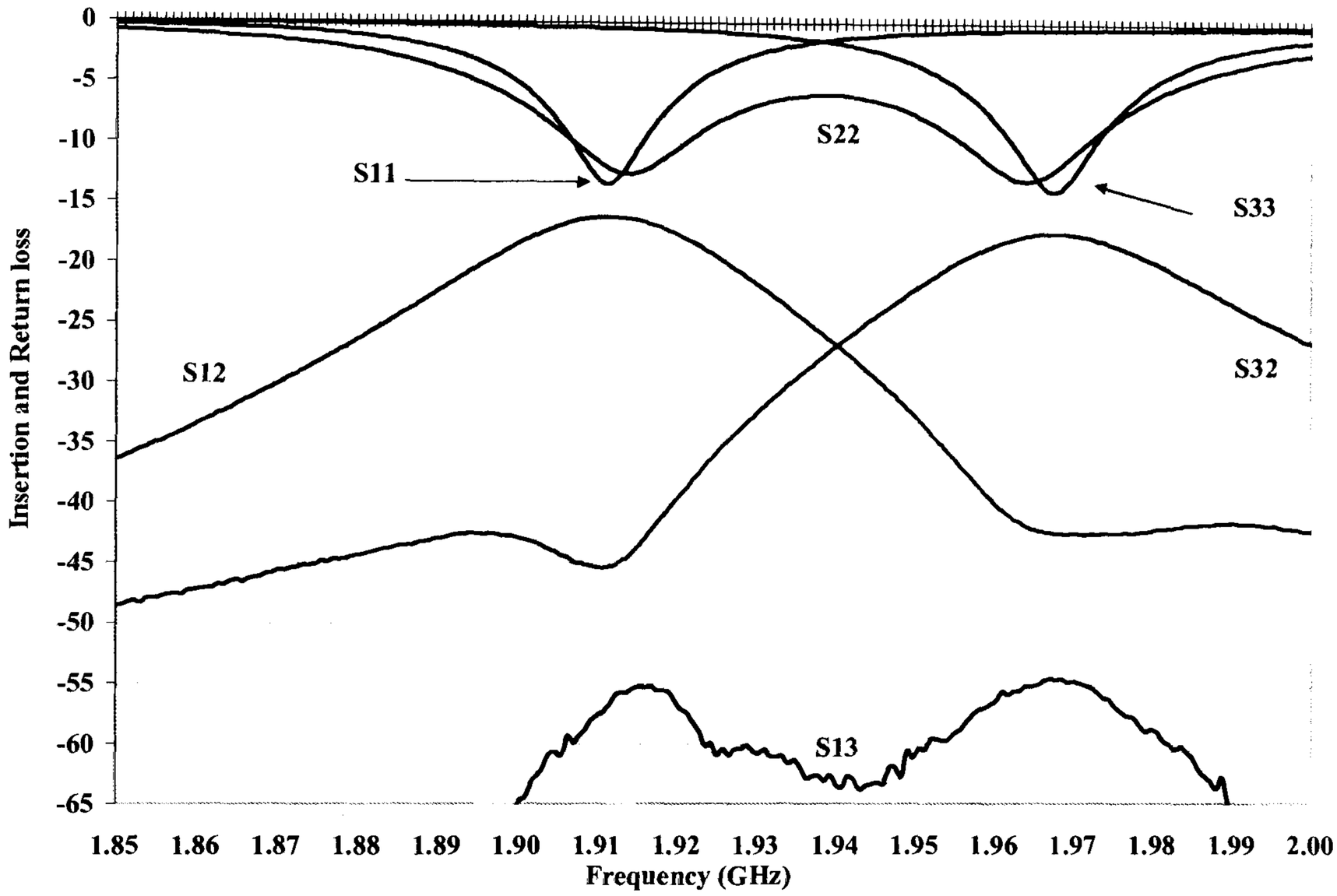

Figure 4.9 Measured results of circular patch antenna designed at 2 GHz showing dual band antenna results; where:

- The dual-band antenna is port 2.
- The single mode antenna with vertical polarisation is port 1.
- The single mode antenna with horizontal polarisation is port 3.

As expected, the return loss response does not change. However, the insertion loss response is similar to the one anticipated in the circuit analysis in Figure 4.7. From a different prospective, if a notch is introduced into one mode, this will reduce the amount of metallization on that mode and therefore increase its resonant frequency. Conversely if the metal area is extended on the orthogonal mode, this results in lowering the resonant frequency of that mode. The position of the metal indentation/extension is very important, it should be located at an angle of 45°, 135°, 225° or 315° as otherwise it may reduce one of the modes to zero [91]. Increasing the

size of the indentation or extension of the metallization at each mode, causes the resonant frequencies to move further apart from the central frequency. In principle if the notch in Figure 4.8 is further extended in and an extra metallization is extended out on the orthogonal mode, the two resonant modes will move further apart. Another dual-band antenna that radiates at 1.82GHz and 1.96GHz was designed. The fabricated antenna, simulated and practical results are shown in Figure 4.10 and Figure 4.11 .

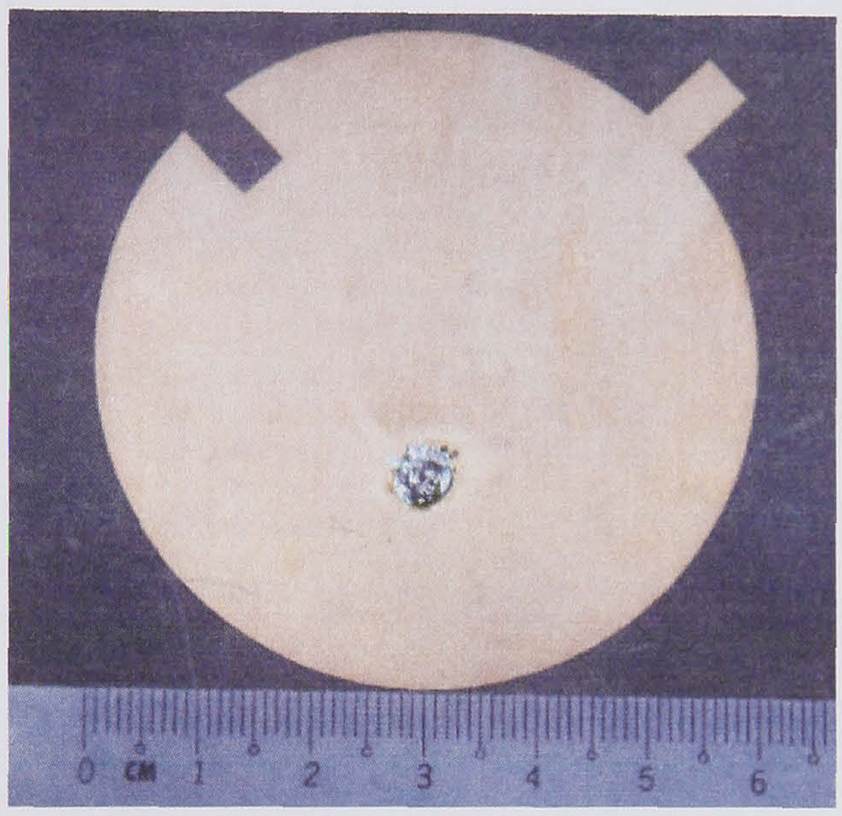

Figure 4.10 Dual-band circular patch antenna designed at 1.82 GHz & 1.96 GHz.

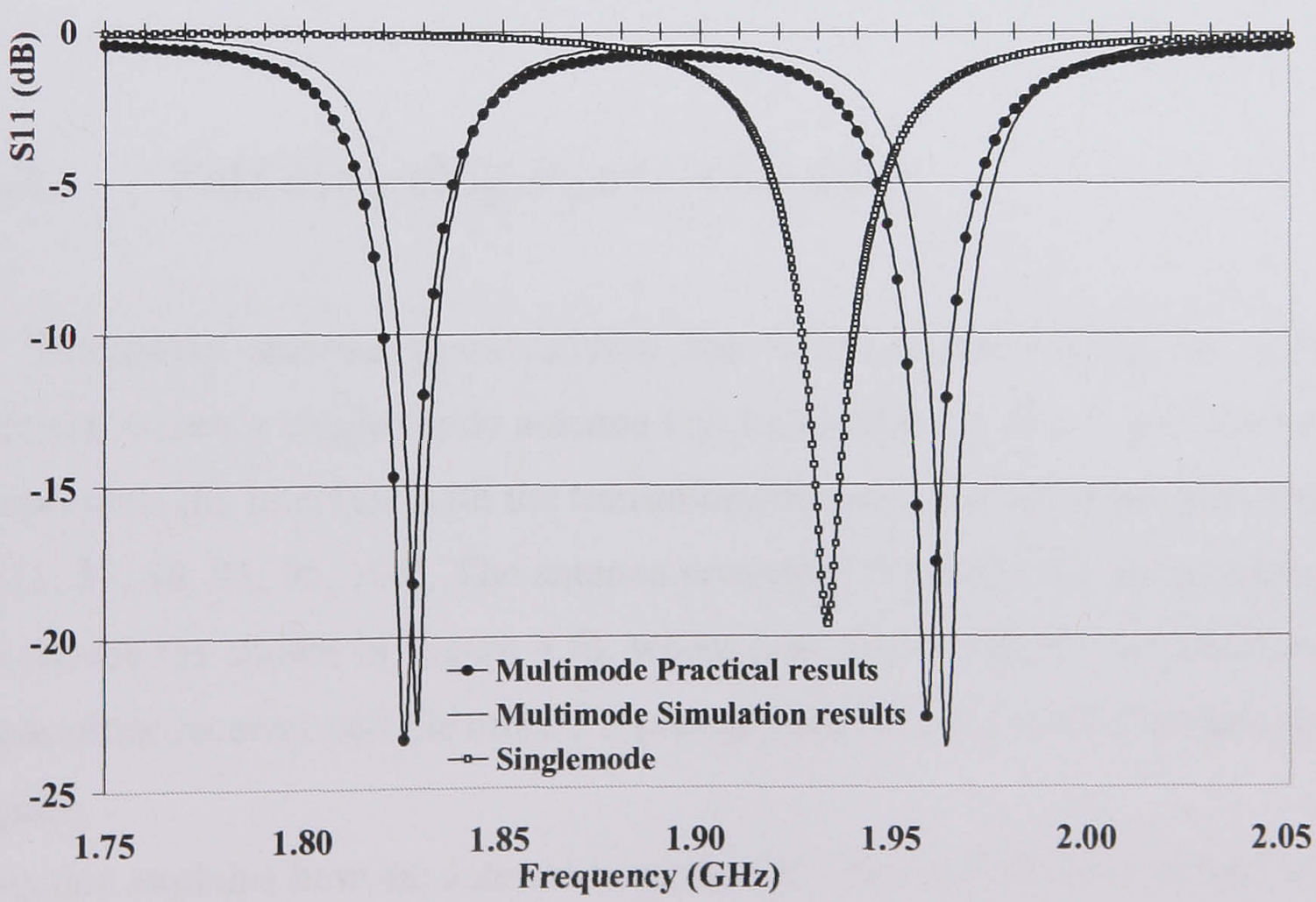

Figure 4.11 Electromagnetic simulations and measured results of circular patch antenna designed at 1.82 GHz & 1.96 GHz showing optimised single mode and multimode antenna results where the two modes are moved further apart by extending out the metallization on one mode and extending the notch in for the orthogonal mode.

The results show that the antenna can be used at 2 distinct frequencies, and therefore can be utilised as a dual band antenna for communication systems. Figure 4.12 shows the far field pattern of the antenna, which is similar at both frequencies.

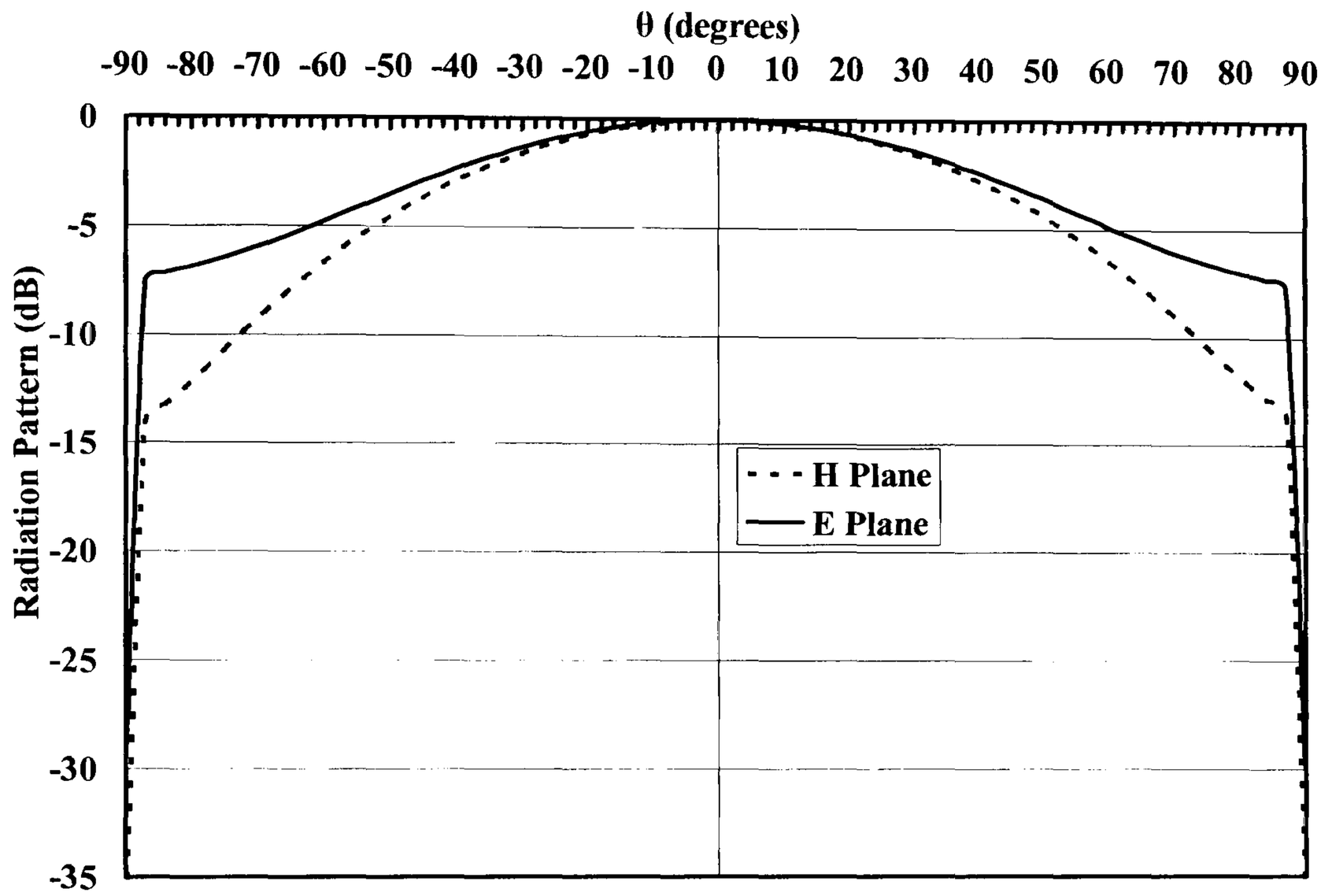

Figure 4.12 Far field radiation pattern of the antenna.

4.2. Self diplexing Patch Antenna

Microstrip antenna characteristics can be represented using the scattering parameters, where a single mode antenna can be considered as a 2 port device. One port represents the interface with the transmitter/receiver, and the other port with free space [1, 37, 88, 91, 95, 106]. The antenna presented in section 4.1 is considered as a 3-port device (as shown in Figure 4.6), where one port represents the interface with the transmitter/receiver and the other 2 represent radiation at 2 distinct polarisations in free space.

This section explains how the antenna in section 4.1 can be further developed to be an antenna transceiver utilising four-ports. Two of these represent the interface with free

space at two distinct polarisations, one port represents the interface with the transmitter and one other port with the receiver.

4.2.1. Circuit Analysis

For two port devices, the S-parameters only involve the insertion and return loss of the antenna, i.e. S_{11} and S_{12}. However, the dual-mode antenna discussed in this section comprises a transmitter and a receiver, therefore the device may be treated as a four-port network. Hence, other crucial parameters become evident, i.e. S_{21}, S_{14} & S_{23}, these are the isolation (or the coupling) between the two input (or output) ports as shown in Figure 4.13 [106].

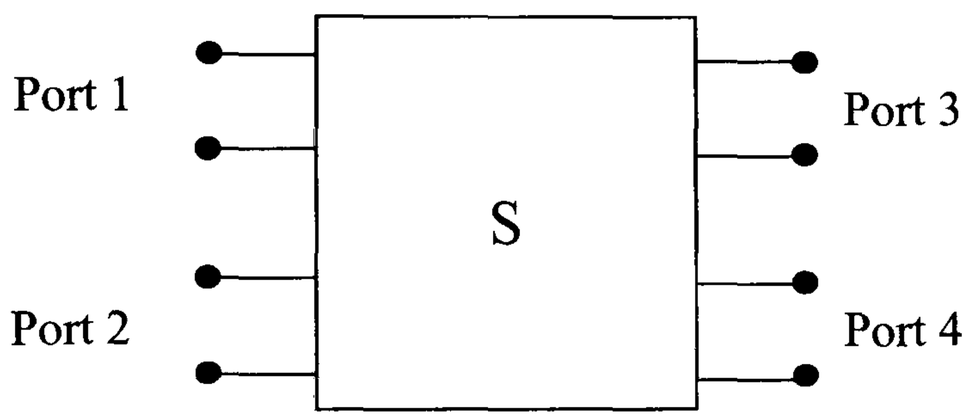

Figure 4.13 S-parameters representation of dual mode antenna transceiver comprising 4 ports, where ports 1 and 2 are transmitter/receiver and ports 3 and 4 are 2 distinct polarizations in free space.

S_{21} corresponds to the part of the signal to be transmitted at port 1 that is coupled into port 2. S_{14} and S_{23} correspond to the parts of the signal to be transmitted at port 1 that is coupled into port 4 or to be transmitted at port 2 that is coupled into port 3. In this case, S_{21} & S_{12} are known as 'Isolation parameters', and S_{14} & S_{23} are known as 'cross polarisation' [106]. Taking these issues into consideration brings attention to the fact that diplexing between the ports is essential.

As explained earlier, microstrip antennas can support two orthogonal resonant modes, therefore, it is possible for one mode to be utilised for transmission and the other for reception. The antenna in section 4.1 comprises one feed for both resonant modes, however, if the assumptions above are applied, then one port can be employed for each mode and hence the equivalent circuit in Figure 4.6 changes to the one shown in Figure 4.14.

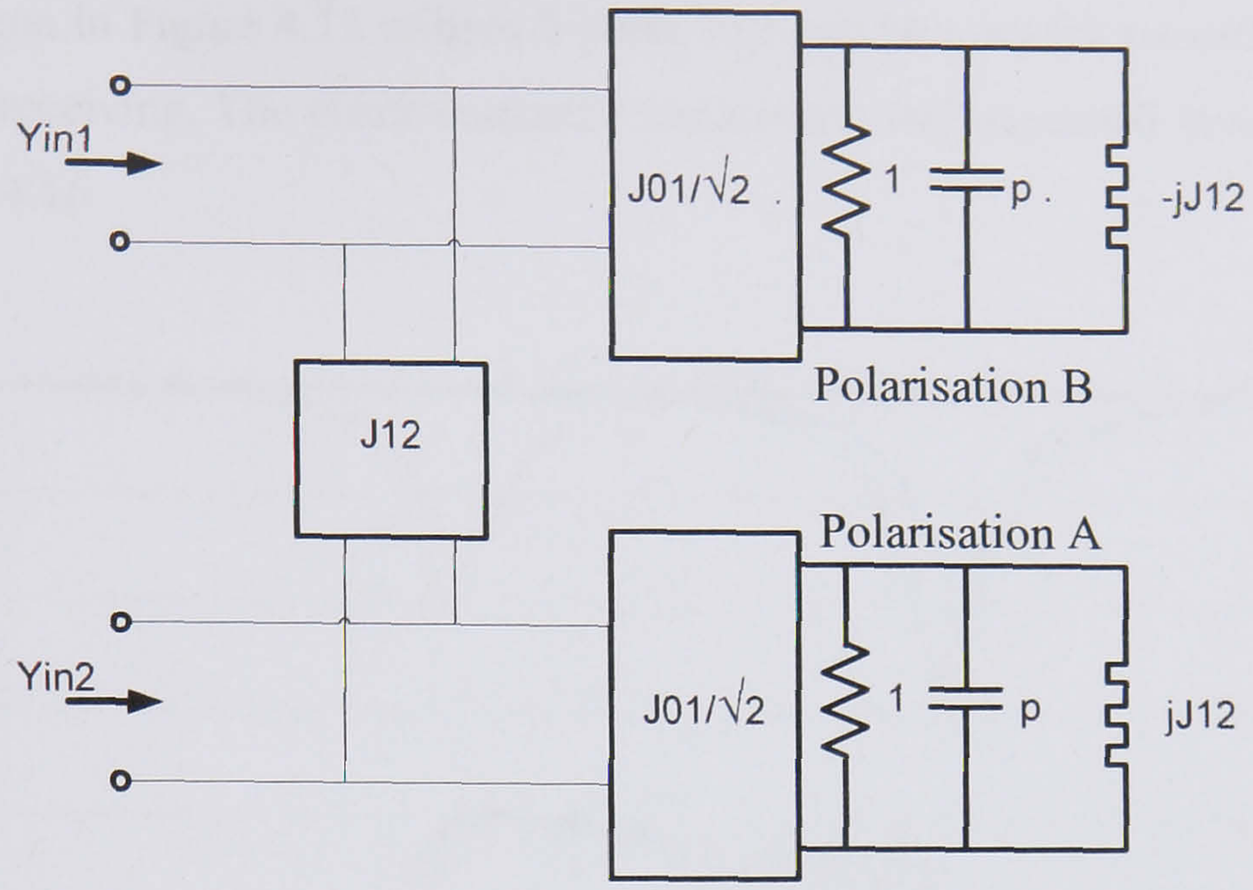

Figure 4.14 The equivalent circuit of the self diplexing patch antenna transceiver

Here, we see the antenna now behaves like a multimode antenna. There are 2 ports now coupled to each mode respectively, which are detuned by frequency invariant reactances, one up and one down in frequency, the lower frequencies radiating in polarisation B and higher frequencies in polarisation A. It is difficult to anticipate the coupling value between the ports in the circuit simulation, therefore, it was decided to study this using EM simulations and find out the coupling between the ports. The circuit above can be applied to the antenna design, this is depicted in Figure 4.15.

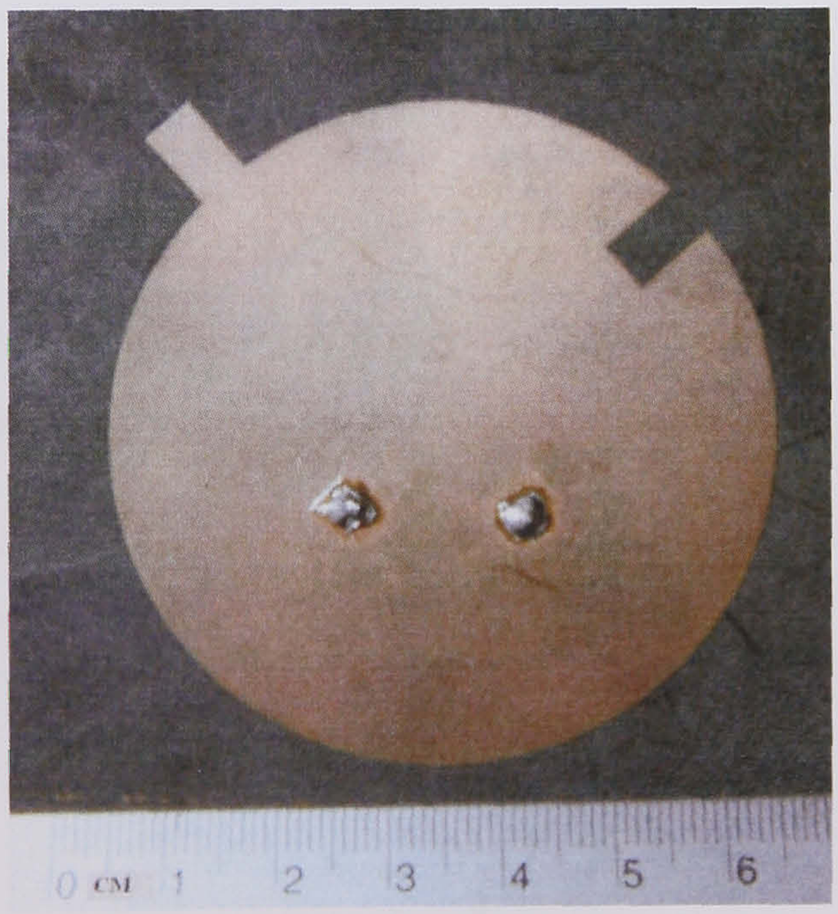

Figure 4.15 Dual-band antenna designed at 1.84GHz and 1.97GHz.

The antenna in Figure 4.15 utilises 2 ports, one can be used for transmitting and the other for receiving. The electromagnetic simulations and measured results are shown in Figure 4.16.

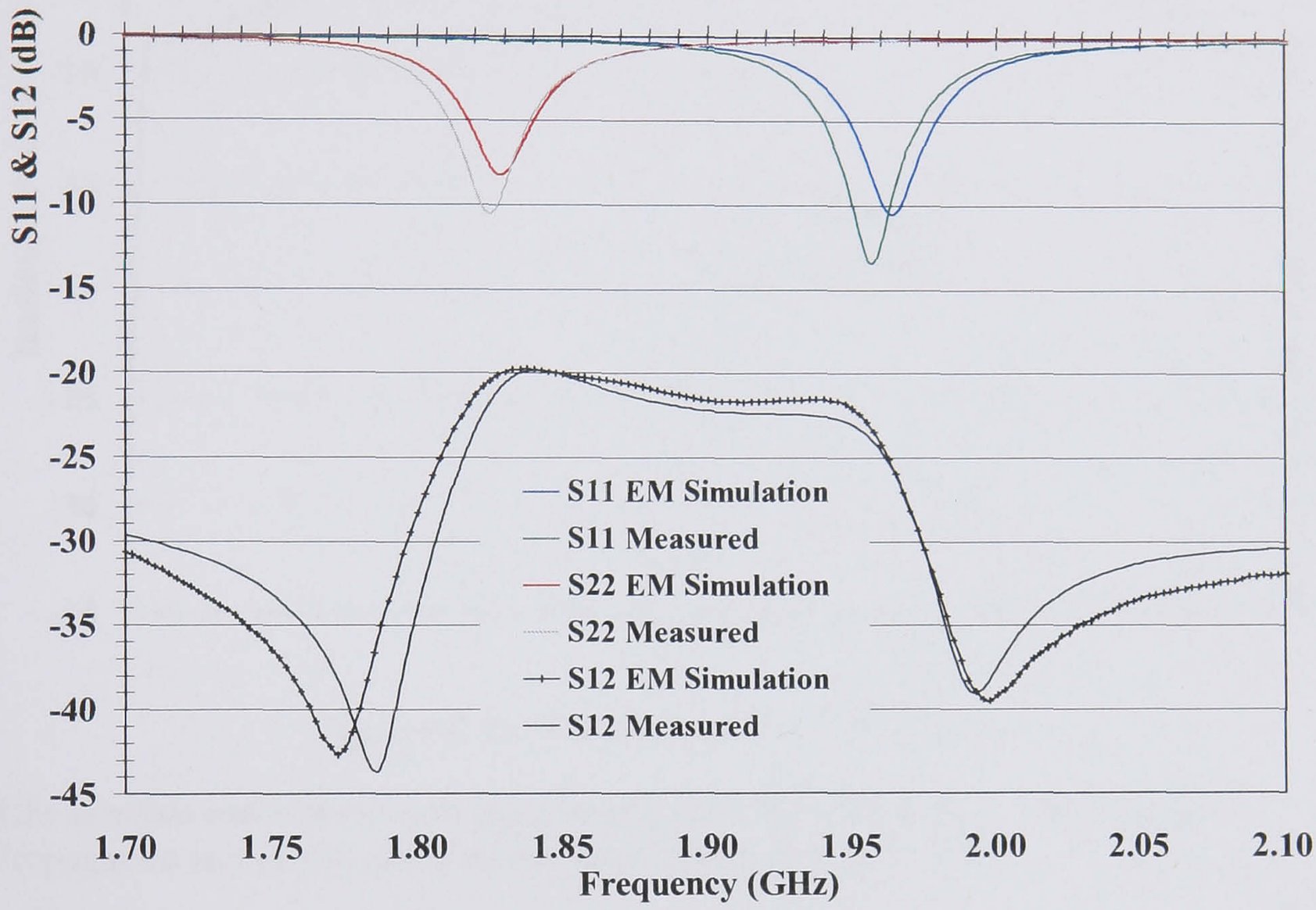

Figure 4.16 Electromagnetic simulations and experimental results of the dual-band antenna.

The isolation between the two ports is over 20dB (this is represented by J_{12} in Figure 4.14) which is satisfactory for diplexing the transmitted/received signals. The simulation results agree with the experimental results, and accordingly, this achieves a self diplexing dual band antenna with isolation of over 20dB between the ports but fairly narrow bandwidth. Figure 4.17 shows the far-field radiation pattern.

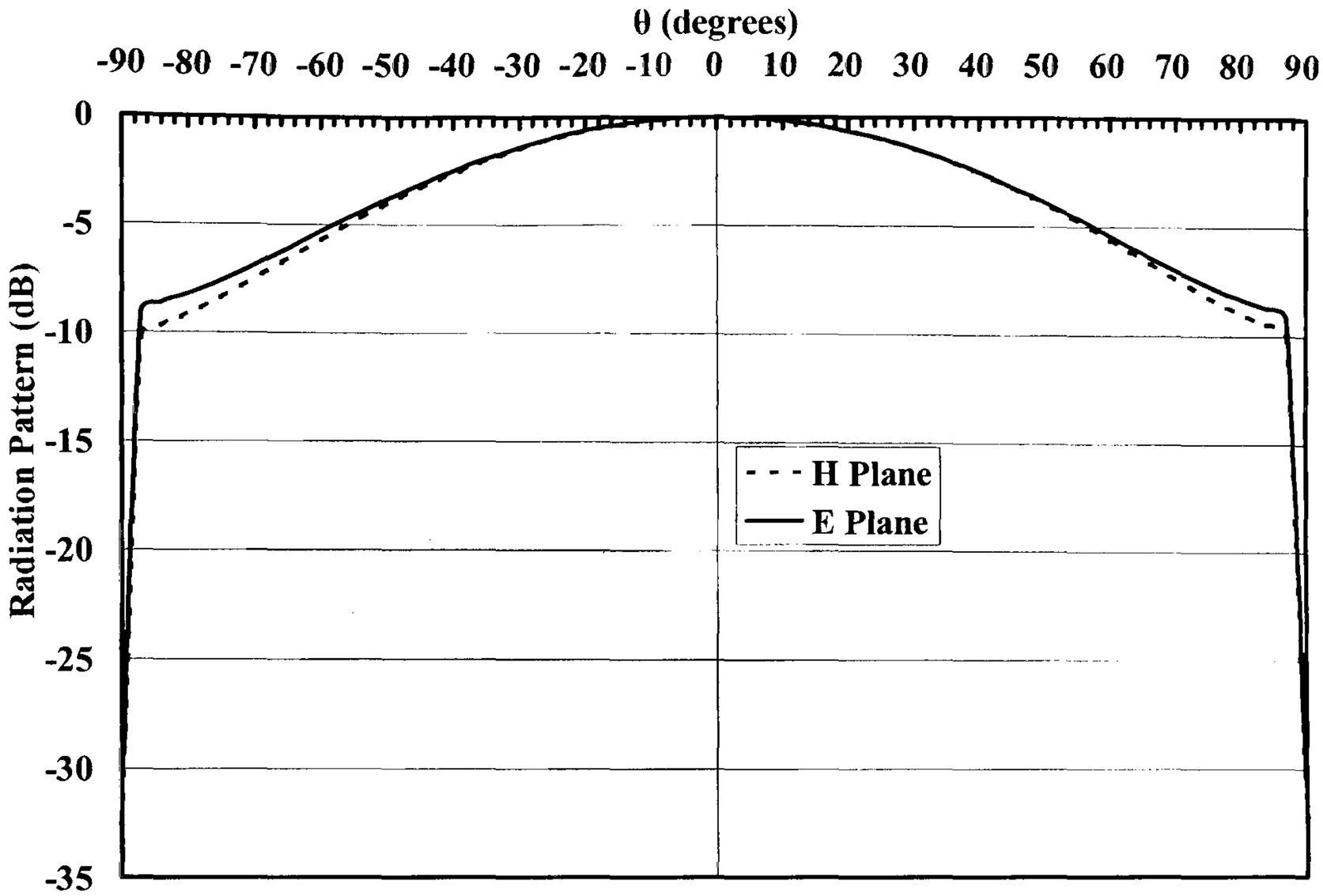

Figure 4.17 Far field radiation pattern of the antenna.

This analysis and results were submitted to the IEEE Transactions on Antennas Propagation and is still under review as of November 2007 [98].

4.3. Multiband Patch Antenna

The on-going development of wireless applications ranging from Bluetooth, WLANs, GSM, GPS and aerospace applications requires more efficient, low profile and flexible antennas. In particular, the need for multiband operation, e.g. multi-band antennas for global navigation systems (e.g. GPS). Other techniques were proposed to overcome this problem, such as electrically thick elements, stacked multipatch and multilayer elements [1]. However, these techniques increase the complexity and the size of the antenna.

A new method of multi-band matching for circular microstrip patch antennas is presented in this section. The analysis in the previous section enabled the antenna to be used as a dual-band antenna, in this section a theoretical method of incorporating an external matching network with the dual-mode polarisation property of a microstrip patch antenna network is presented. This enables an antenna fed by two ports to be matched at four distinct frequencies, and achieve good isolation between the two feeding ports. This is the first time where the dual-mode polarisation property of circular microstrip patch antennas is successfully utilized with a matching network to maximise the performance of single layer microstrip patch antennas. The simulation results are confirmed with an experimental quad-band circular microstrip patch antenna realisation.

4.3.1. Analysis, Simulation and Practical Implementation.

Microstrip patch antennas have relatively narrow bandwidth due to the quick change of the input impedance with respect to frequency and the high quality factor [6]. Derneryd has shown that the antenna can be excited at two different frequencies off resonance, using a two-section impedance transformer as shown in Figure 4.18 and Figure 4.19 [6].

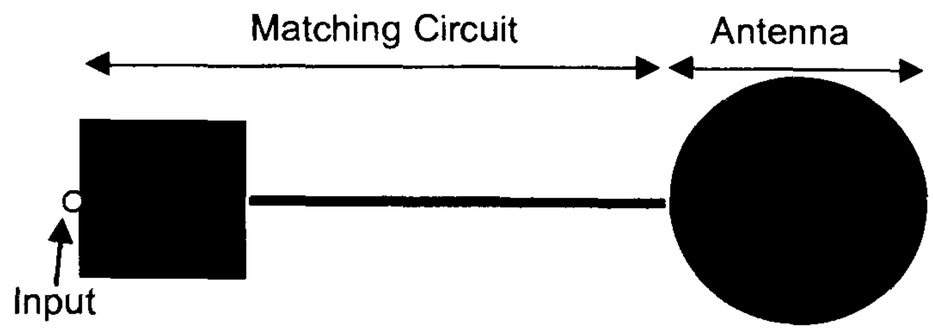

Figure 4.18 Circular Microstrip patch antenna with a matching circuit.

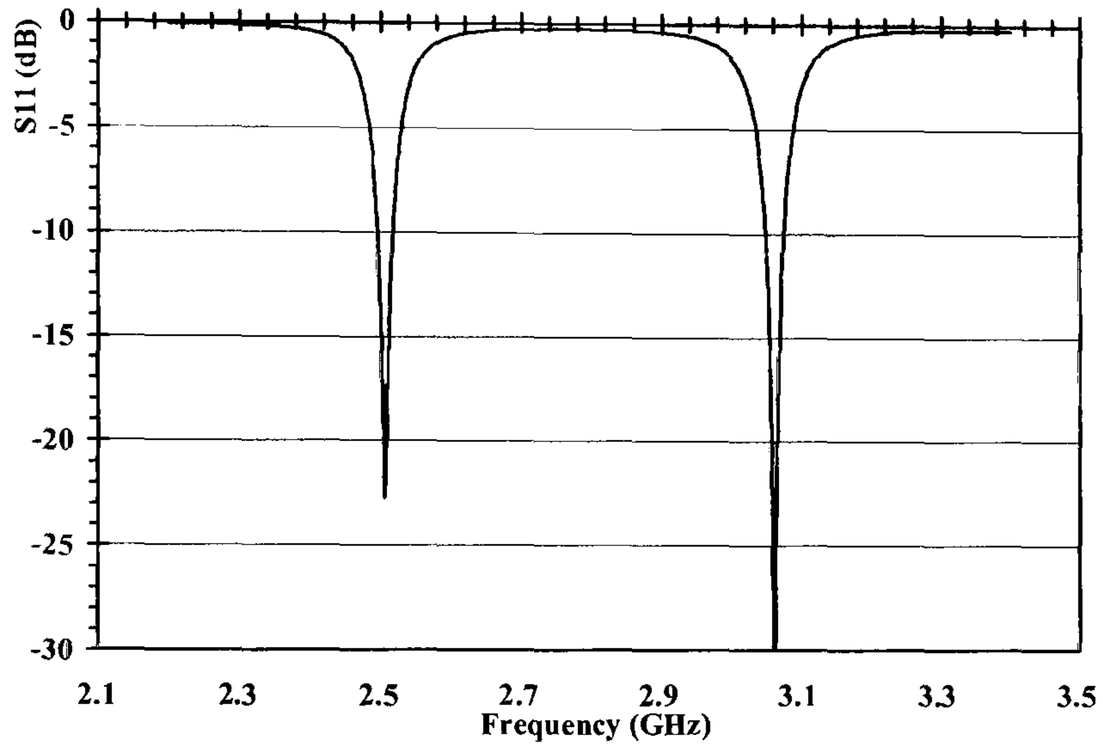

Figure 4.19 Circular Microstrip patch antenna response matched at two frequencies using matching network.

Though the dimensions of the matching network can be computed, it essentially consists of an open circuited stub (capacitive) and a transmission line (inductive) elements, together allowing the antenna to radiate at frequencies off resonance.

The dualmode property of patch antennas and the dualband matching technique presented earlier can now be both integrated to a single design. If two inputs are connected to two matching circuits and then coupled to both resonant modes of the antenna, which are detuned by frequency invariant reactances, one up and one down in frequency, then in theory, each input can be matched at two distinct frequencies different from those matched at the other port, as shown in Figure 4.20.

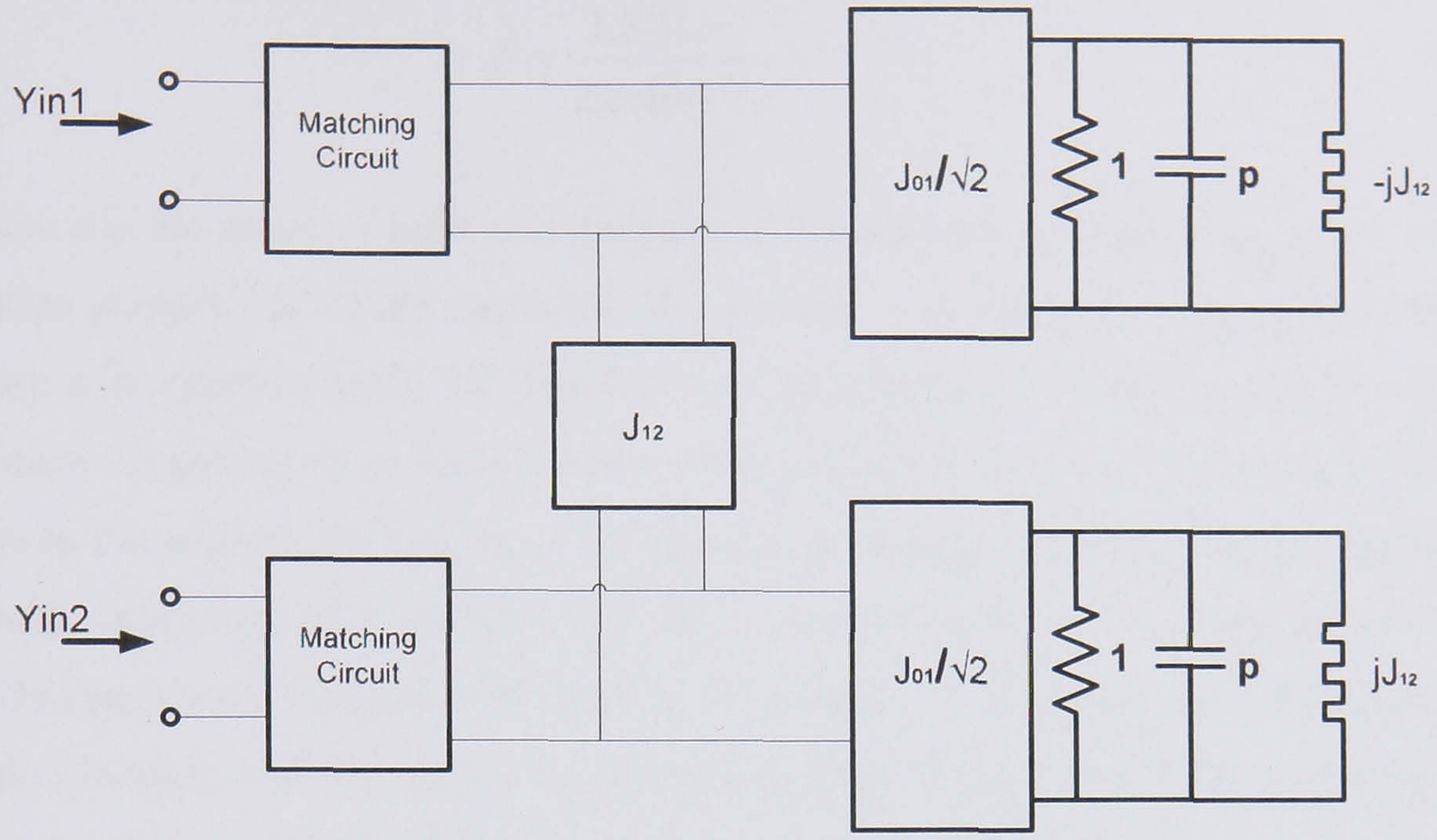

Figure 4.20 The equivalent circuit of the multimode patch antenna.

It is rather difficult to anticipate the cross coupling between the ports in circuit simulation, however, EM simulation is helpful for such design. If two matching circuits such as the ones used in [6], are employed 90° apart to feed the antenna and a notch was introduced at one mode and the metal was extended at the orthogonal mode, hence the circuit in Figure 4.20 can be realised in practice as shown in Figure 4.21.

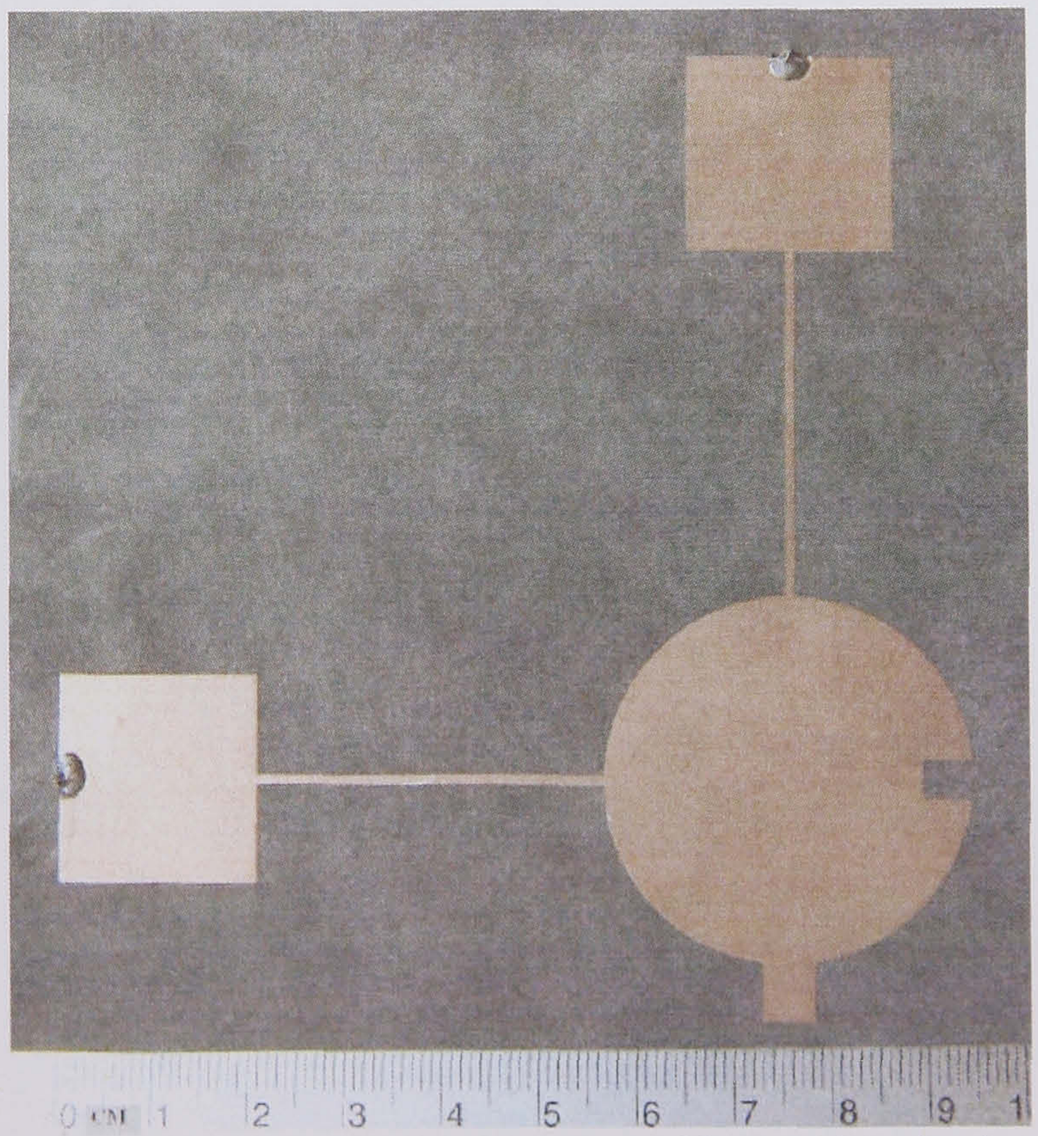

Figure 4.21 Multimode patch antenna with matching circuits.

The radius of the antenna can be found using equation 4.18 [4].

$$f_r = \frac{1.841.c}{2\pi a(\varepsilon_r)^{1/2}} \qquad 4.18$$

Where c is the speed of light, a is the radius, f_r is the resonant frequency and ε_r is the relative permittivity of the substrate. The antenna was designed using Duroid 5880, where ε_r is approximately 2.2, the radius of the antenna is 1.897cm and the central resonant frequency is around 2.8GHz. A matching circuit was then designed that allowes the antenna to resonate at frequencies off resonance. Two identical matching circuits consisting of a short circuit stub (21.5x20.5mm) and a transmission line (35.5x1mm) were integrated 90° apart to the antenna. A notch was introduced at one mode (5x4mm) and the metal was extended (5.4x6.13mm) on the orthogonal mode. The antenna was fabricated and the results are shown in Figure 4.22.

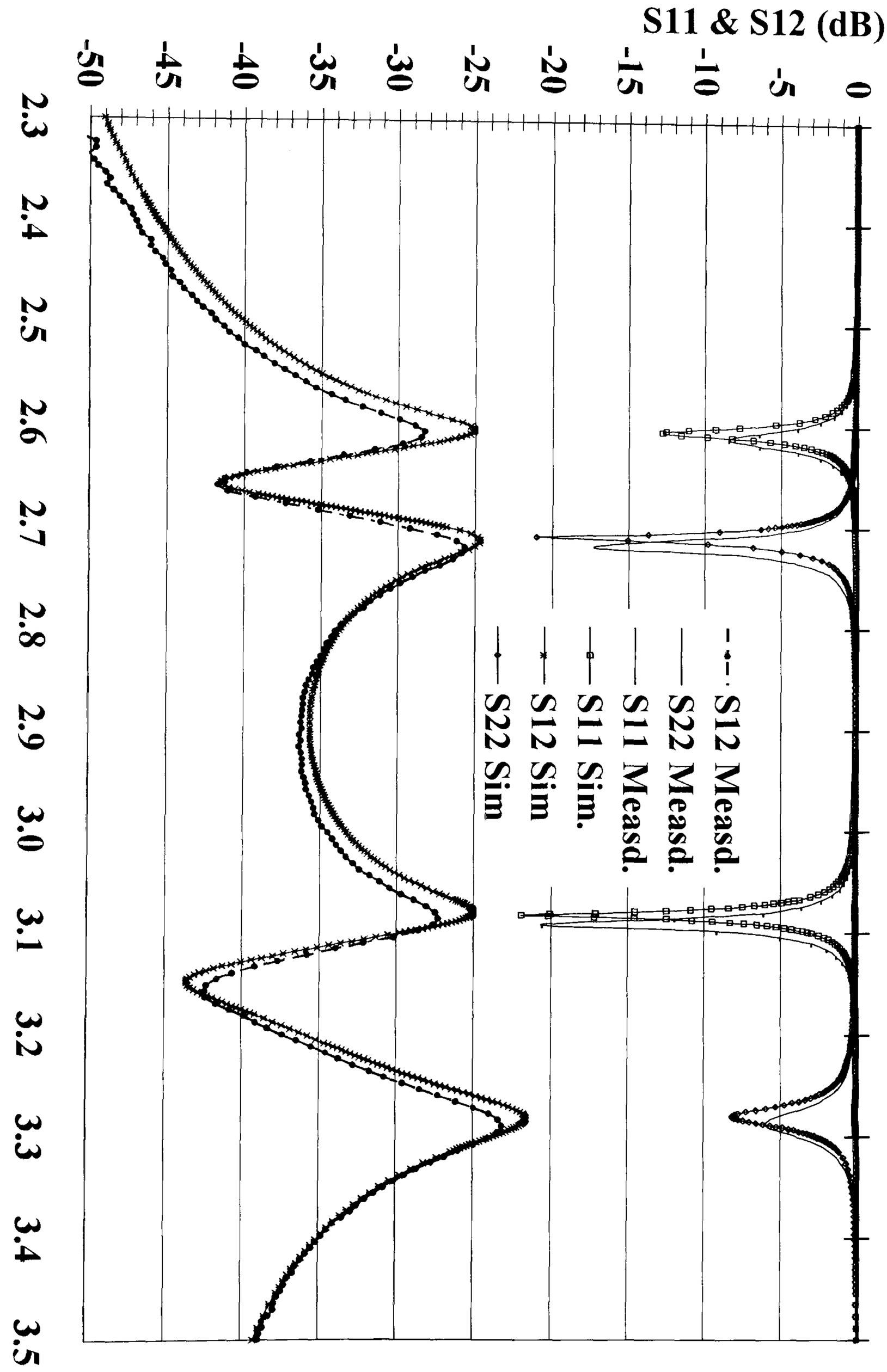

Figure 4.22 Simulation and measured results of the multimode antenna.

The simulation and measured results in Figure 4.22 show that the antenna is now matched at 4 distinct frequencies and fed by two ports. A crucial point here is the

isolation between the ports, which is shown to be over 22dB. The separation between the resonant modes is highly dependent on the notch and the extended metal at each mode, the bigger they are the more separation achieved. However, as the resonant frequencies moves away from the central resonance, the matching into the network becomes weaker and therefore parts of the signal start to be reflected. Figure 4.23, Figure 4.24, Figure 4.25 and Figure 4.26 show the radiation pattern of the antenna at the four frequencies.

This technique and results were presented at the European Microwave Conference in Munich 2007 [107].

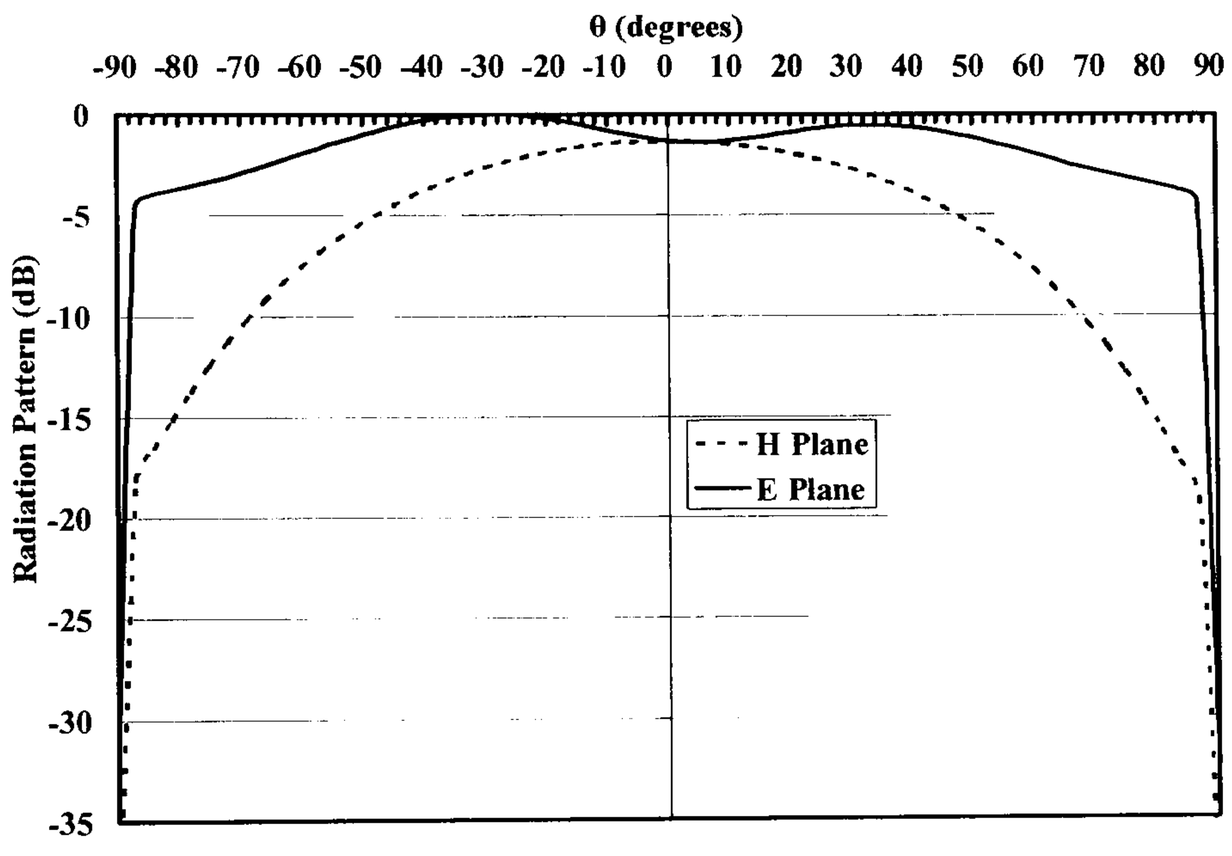

Figure 4.23 Far field radiation pattern of the antenna at 2.6GHz.

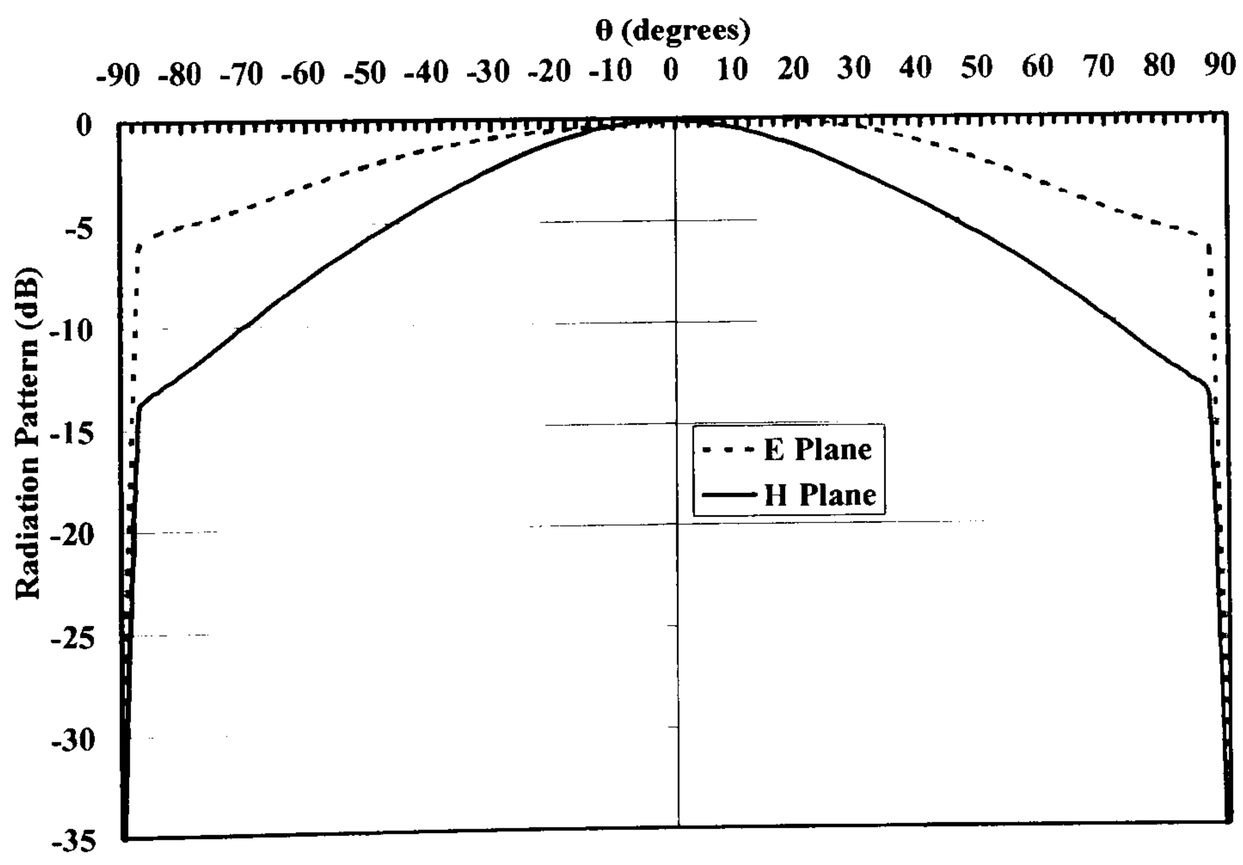

Figure 4.24 Far field radiation pattern of the antenna at 2.75GHz.

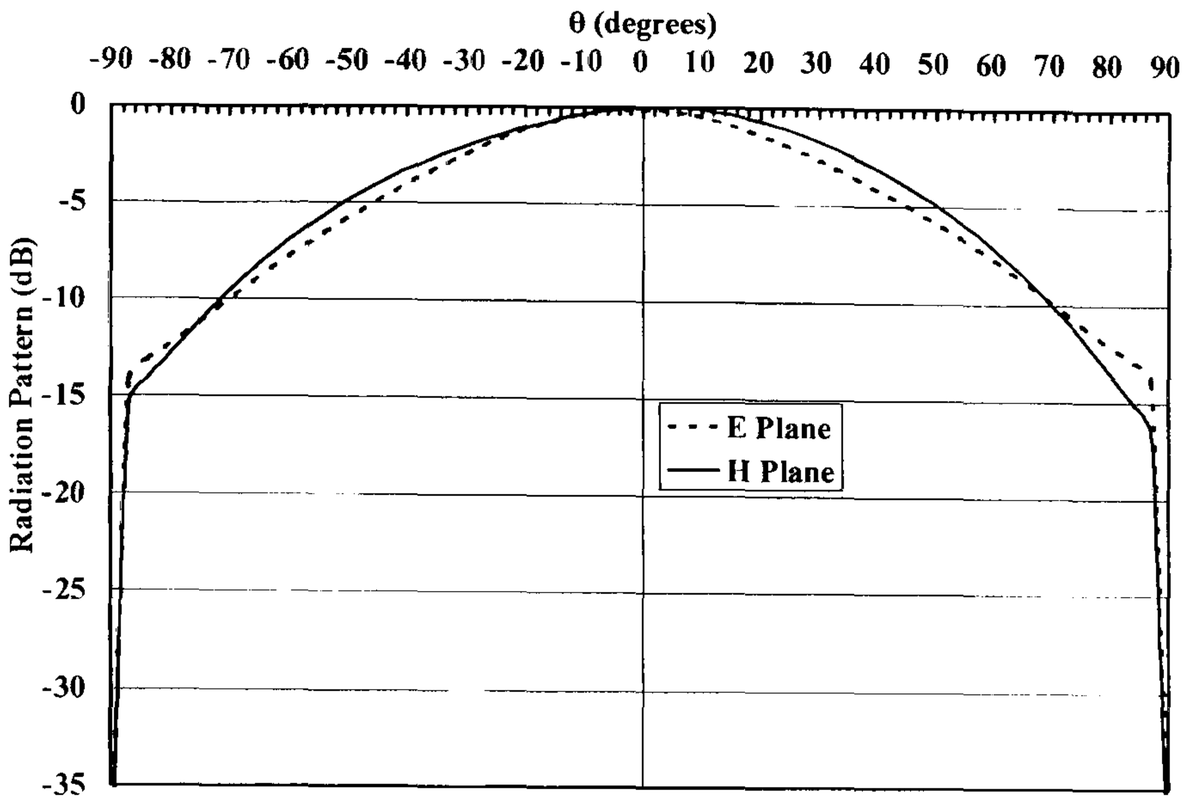

Figure 4.25 Far E-Field pattern of the antenna at 3.1GHz.

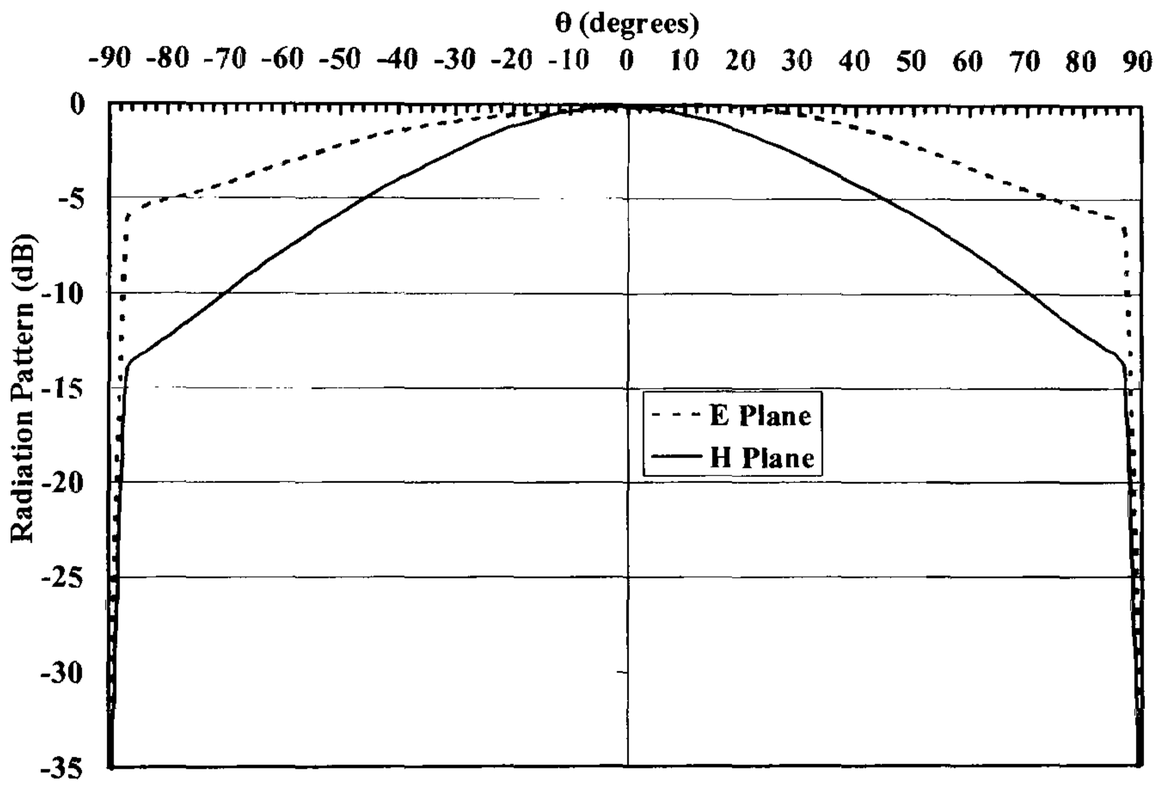

Figure 4.26 Far E-Field pattern of the antenna at 3.27GHz.

4.4. Summary

This chapter explained how the dual-mode antenna can be used as a dual-band antenna. Circuit transformations were also presented showing how the insertion loss transforms from dual-mode to dual-band. This was further developed by adjusting the separation between the bands, integrating two ports and external matching networks to reach the design of a multimode microstrip patch antenna transceiver with 20dB isolation between the ports.

Chapter 5. Conclusion and Future Work

The driving force for microstrip antennas is the desire for lower-cost, lighter weight, lower profile antennas for modern system requirements and the trend is likely to continue, mainly because of their mechanical features and ease of fabrication. Development and research in recent years have been focussed on improving electrical characteristics of microstrip antennas, primarily increasing the bandwidth and developing more efficient feeding techniques.

The equivalent circuits for the antennas presented in this thesis are based on simple lumped-element circuit models. Once the optimum equivalent circuit is reached for an antenna it can be used to aid the systematic design of the physical antenna, in particular the coupling between the resonant modes in a multi-resonant antenna. This shows how the antenna dimensions can be designed with reference to their circuit component counterparts. Thus, the number of optimisation iterations required to achieve the optimum bandwidth is reduced.

The motivation behind this work is to improve the narrow impedance bandwidth of microstrip patch antennas. A simple theoretical design method for maximising the return-loss bandwidth of a circular microstrip patch antenna is presented in chapter 2, and theoretical bandwidth improvement of up to 3:1 is achieved when compared to a single-mode antenna. By considering a dual-mode antenna as a filter network, it is shown that a significant improvement in bandwidth may be obtained when compared with a single mode device, this can be achieved by adjusting the coupling values. The theory has been demonstrated by introducing a

notch into a practical circular microstrip patch antenna. The dual mode design has been extended in different directions. In an attempt to improve the impedance bandwidth, a new approach for the exact synthesis of dual layer quadruple mode circular microstrip patch antennas is presented, using techniques normally employed in filter design. This has led to an increase in the return loss bandwidth of over 4.2 times compared to a single mode design. A quadruple-mode antenna was designed by adjusting the coupling values of two dual mode antennas stacked on top of each other with total thickness of 1.168mm. Electromagnetic simulation shows excellent results, and the measured results agree well with these.

Another extension to the dual-mode design is the dual band microstrip antenna. By theoretical study, the antenna was represented as a filter network. It was shown that the use of matrix rotations enable different transfer functions into the two radiation polarizations to be obtained. Accordingly, the input is then coupled to both resonant modes, which are detuned one up and one down in frequency. Hence, the antenna may operate as a multimode antenna transmitter/receiver, with two distinct frequencies radiating in the two orthogonal polarizations supported by a circular patch. The theory has been demonstrated by introducing a notch into a practical circular microstrip patch antenna, and compensates by extending the metallization on the orthogonal mode. The theoretical derivation presented has practically shown that the antenna can efficiently operate at two bands. The fact that circular microstrip patch antennas can support two orthogonal modes has allowed the antenna to be used as a self diplexing patch antenna transceiver with a port for each mode, and the isolation between the ports is found to exceed 20dB.

Several wireless applications require separate bands for transmitting and receiving, as well as multi-band transmission. The dual-band antenna is further developed into a quad-band design. Using the two orthogonal resonant modes, alongside simple matching techniques to separate the modes, has allowed the antenna to be matched at four distinct frequencies. Hence the antenna can operate as a multimode patch antenna, where the isolation between the ports was found to exceed 22dB. This technique can be adopted and further developed for applications such as GPS navigation and GSM communication systems where multi-band operation is required.

5.1. Future Work

The work in this thesis can be further developed in several directions. First of all, the quadruple mode antenna can be further optimised to achieve the result reached in the circuit analysis. This can possibly be done by using different thicknesses/dielectric constants for the two layers, or patches with different dimensions.

From a different perspective, the equivalent circuit can be transformed into a quadband antenna, and possibly utilising two or four ports for transmission. Also, an external network can be integrated into the circuit, achieving even more bands.

It was noticed that the radiation pattern was affected by the matching network in section 4.3. A solution for this is to embed the matching network underneath the ground plane of the antenna in a multilayer design.

The dual layer quadruple mode antenna can be further expanded to more than two layers. No doubt the conduction and dielectric losses will increase, however, a significant impedance bandwidth improvement is possible. The equivalent circuit of three or four layers microstrip antenna can be reached by starting with a sixth or eighth order ladder network. The circuit transformation could be rigorous, but this can potentially achieve outstanding improvements.

Size reduction for the antennas is also an interesting possibility [108]. This may be achieved by using a high dielectric constant substrate, and therefore, reducing the size of the disc. This however will be at the expense of the efficiency and bandwidth.

Another idea is to integrate an external ring resonator built on a different dielectric constant and coupled with a circular patch inside the ring. If each is designed to have dualmode resonance, this can achieve a quadruple mode antenna. If this idea works, then another ring and disc can be stacked on top to further expand the bandwidth.

Tunable antennas can also be investigated. The notch and the metal extension in the dualband design can be broken into smaller stripes connected with varactor diodes. Connecting more metallisation to the structure changes the resonant frequency at each mode, and makes the antenna look electrically smaller/longer at each mode.

Planar and stacked multiresonator configurations can be improved. Instead of coupling four patches to a central one, two dualmode patches can be used, thus reducing the size and number of resonators needed.

In terms of integrating the antenna to the circuit in a system, the quadruple mode patch antenna designed in chapter 3, can be integrated to be the last part of a filter and miniaturised using multilayer substrates.

References & Appendices

[1] R. Garg, *Microstrip Antenna Design Handbook* Artech House, 2001.

[2] G. Kumar and K. P. Ray, *Broadband Microstrip Antennas*: Artech House London, 2003.

[3] J. T. Bernhard, P. E. Mayes, D. Schaubert, and R. J. MAilloux, "A Commemoration of Deschamp's and Sichak's "Microstrip Microwave Antennas": 50 years of Development, Divergence, and New Directions," *Proceedings of the Antenna Applications*, 2003.

[4] C. A. Balanis, *Antenna theory : analysis and design*, 2nd ed: Wiley, 1997.

[5] D. M. Pozar, "Microstrip antennas," *Proceedings of the IEEE*, vol. 80, pp. 79, 1992.

[6] A. Derneryd, "Microstrip Disc Antenna Covers Multiple Frequencies," *Microwave Journal*, vol. 21, pp. 77-9, 1978.

[7] G. Kumar and K. Gupta, "Directly coupled multiple resonator wide-band microstrip antennas," *Antennas and Propagation, IEEE Transactions on [legacy, pre - 1988]*, vol. 33, pp. 588-593, 1985.

[8] R. B. Waterhouse, *Microstrip Patch Antennas: A Designer's Guide*: Kluwer Academic Publishers, 2003.

[9] J. Ollikainen et. al., "Design and bandwidth optimization of dual-resonant patch antennas," *Helsinki University of Technology Radio Laboratory Publications, Espoo*, March, 2002.

[10] S. Pritchard, "In the Lab: Nokia Research Center," in *Financial Times*. London, Feb. 13th, 2006, pp. 13.

[11] H. Wheeler, "Small antennas," *Antennas and Propagation, IEEE Transactions on [legacy, pre - 1988]*, vol. 23, pp. 462-469, 1975.

[12] I. J. Bahl and P. Bhartia, *Microstrip antennas*: Artech House 1980.

[13] G. A. Deschamps and W. Sichak, "Microstrip Microwave Antenna," presented at Third USAF Symposium on Antennas, 1953.

[14] D. M. Pozar, "An Update on Microstrip Antenna Theory and Design Including Some Novel Feeding Techniques," *IEEE Antennas and Propagation Socity Newsletter*, pp. 4-9, 1986.

[15] K. Carver and J. Mink, "Microstrip antenna technology," *Antennas and Propagation, IEEE Transactions on [legacy, pre - 1988]*, vol. 29, pp. 2, 1981.

[16] P. S. Hall, *Handbook of microstrip antennas*: Peregrinus, 1989.

[17] R. H. Collings, "Current Sheet Antenna," in *United States Patents*, U. S. Patents, Ed. USA, July 25, 1972.

[18] J. Watkins, "Circular Resonant Structures in Microstrip," *Electronics Letters*, vol. 5, pp. 524-525, 1969.

[19] P. Troughton, "High Q factor resonators in microstrip," *Electronics Letters*, vol. 4, pp. 520-522, 1968.

[20] R. Munson, "Conformal microstrip antennas and microstrip phased arrays," *Antennas and Propagation, IEEE Transactions on [legacy, pre - 1988]*, vol. 22, pp. 74, 1974.

[21] J. Howell, "Microstrip antennas," *Antennas and Propagation, IEEE Transactions on [legacy, pre - 1988]*, vol. 23, pp. 90, 1975.

[22] J. Mink, "Circular ring microstrip antenna elements," presented at Antennas and Propagation Society International Symposium, 1980, 1980.

[23] W. Richards, L. Yuen, and D. Harrison, "An improved theory for microstrip antennas and applications," *Antennas and Propagation, IEEE Transactions on [legacy, pre - 1988]*, vol. 29, pp. 38-46, 1981.
[24] D. M. Pozar, "Considerations for Millimetre Wave Printed Antennas," *IEEE Transactions on Antennas And Propagation*, vol. AP-31, pp. 740-747, 1983.
[25] D. Pozar and B. Kaufman, "Increasing the bandwidth of a Microstrip Antenna by Proximity Coupling," *Electronics Letters*, vol. 23, pp. 368-369, April 1987.
[26] R. Mailloux, J. McIlvenna, and N. Kernweis, "Microstrip array technology," vol. 29, pp. 25-37, 1981.
[27] Y. Qian and T. Itoh, "Progress in active integrated antennas and their applications," *IEEE Transactions on Microwave Theory and Techniques*, vol. 46, pp. 1891-1900, 1998.
[28] R. Waterhouse, "Small microstrip patch antenna," vol. 31, pp. 604-605, 1995.
[29] M. Lech, A. Mitchell, and R. Waterhouse, "Optimization of broadband microstrip patch antennas," 2000.
[30] K. Lee and W. Chen, *Advances in Microstrip and Printed Antennas*: John Whiley & Sons, Inc, 1997.
[31] A. Derneryd, "Analysis of the microstrip disk antenna element," *Antennas and Propagation, IEEE Transactions on [legacy, pre - 1988]*, vol. 27, pp. 660, 1979.
[32] C. A. Balanis, *Advanced engineering electromagnetics* Wiley, 1989.
[33] P. Agrawal and M. Bailey, "An analysis technique for microstrip antennas," *Antennas and Propagation, IEEE Transactions on [legacy, pre - 1988]*, vol. 25, pp. 756-759, 1977.
[34] S. Drabowitch, *Modern antennas*: Chapman & Hall, 1998.
[35] D. M. Pozar, *Microwave Engineering*, International Edition ed: Wiley, 2005.
[36] S. Long and L. Shen, "The circular disc, printed circuit antenna," 1977.
[37] N. Kumprasert and W. Kiranon, "Simple and accurate formula for the resonant frequency of the circular microstrip disk antenna," *Antennas and Propagation, IEEE Transactions*, vol. 43, pp. 1331, 1995.
[38] J. D. Kraus, *Antennas : for all applications*: McGraw-Hill, 2002.
[39] K. Saeed, "Study of Suspended Substrate Stripline Dual-mode and Combline Filters," in *Electronic and Electrical Engineering*: University of Leeds, 2004.
[40] A. Kishk and L. Shafai, "The effect of various parameters of circular microstrip antennas on their radiation efficiency and the mode excitation," vol. 34, pp. 969, 1986.
[41] L. Shen, S. Long, M. Allerding, and M. Walton, "Resonant frequency of a circular disc, printed-circuit antenna," *Antennas and Propagation, IEEE Transactions on [legacy, pre - 1988]*, vol. 25, pp. 595, 1977.
[42] J. Y. Siddiqui and G. Debatosh, "Improved Formulas for the Input Impedance of Probe-Fed Circular Microstrip Antenna " *IEEE Transactions on Antennas And Propagation*, 2003.
[43] S. A. Long, L. C. Shen, M. Walton, and M. Allerding, "Impedance of a Circular-Disc Printed-Circuit Antenna," *Electronics Letters*, vol. 14, pp. 684-686, 1978.
[44] Z. Chen and M. Chia, *Broadband Planar Antennas*: Wiley, 2006.
[45] D. M. Pozar and D. Schaubert, *Microstrip Antennas*. New Jersey: John Wiley & Sons, Inc, 1995.

[46] D. M. Pozar, "A Review of Bandwidth Enhancement Techniques for Microstrip Antennas," *ECE Department, University of Massachusetts At Amherst*, 1995.
[47] C. Weng and K. Jin, "Analysis of a circular microstrip disk antenna with a thick dielectric substrate," *Antennas and Propagation, IEEE Transactions on [legacy, pre - 1988]*, vol. 29, pp. 68-76, 1981.
[48] D. M. Pozar, "Microstrip antenna aperture-coupled to a microstripline," *Electronics Letters*, vol. 21, pp. 49-50, 1985.
[49] D. M. Pozar and B. Kaufman, "Increasing the bandwidth of a microstrip antenna by proximity coupling," *Electronics Letters*, vol. 23, pp. 368-369, 1987.
[50] D. M. Pozar and S. D. Targonski, "Improved coupling for aperture coupled microstrip antennas," *Electronics Letters*, vol. 27, pp. 1129-1131, 1991.
[51] H. F. Pues and A. R. Van de Capelle, "An impedance-matching technique for increasing the bandwidth of microstrip antennas," *Antennas and Propagation, IEEE Transactions on*, vol. 37, pp. 1345-1354, 1989.
[52] P. Bhattacharjee, "An impedance matching technique for increasing bandwidth of a circular microstrip antenna," presented at Geoscience and Remote Sensing Symposium, 1993. IGARSS '93. Better Understanding of Earth Environment., International, 1993.
[53] J. F. Zurcher, "The SSFIP: a global concept for high-performance broadband planar antennas," *Electronics Letters*, vol. 24, pp. 1433-1435, 1988.
[54] V. Rathi, G. Kumar, and K. P. Ray, "Improved coupling for aperture coupled microstrip antennas," *Antennas and Propagation, IEEE Transactions on*, vol. 44, pp. 1196-1198, 1996.
[55] G. Sanford, "Multiple Resonance Radio Frequency Microstrip Antenna Structure," vol. 4070676, U. S. Patent, Ed. USA: Ball Corporation, Muncie, Ind., 1978.
[56] S. A. Long and M. D. Walton, "A Dual-Frequency Stacked Circular-Disc Antenna," *IEEE Transactions on Antennas And Propagation*, vol. AP-27, , pp. 270-273, 1979.
[57] J. Jones et al, "Flush-mounted piggyback microstrip antenna," in *United States Patent*: USA, 1979.
[58] P. S. Hall, C. Wood, and C. Garrett, "Wide bandwidth microstrip antennas for circuit integration," *Electronics Letters*, vol. 15, pp. 458-460, 1979.
[59] A. Sabban, "A new broadband stacked two-layer microstrip antenna," presented at Antennas and Propagation Society International Symposium, 1983.
[60] C. Chen, A. Tulintseff, and R. Sorbello, "Broadband two-layer microstrip antenna," presented at Antennas and Propagation Society International Symposium, 1984, 1984.
[61] K. Araki, H. Ueda, and T. Masayuki, "Numerical analysis of circular disk microstrip antennas with parasitic elements," *Antennas and Propagation, IEEE Transactions on [legacy, pre - 1988]*, vol. 34, pp. 1390-1394, 1986.
[62] R. Q. Lee, K. F. Lee, and J. Bobinchak, "Two-layer electromagnetically coupled rectangular patch antenna," presented at Antennas and Propagation Society International Symposium, 1988. AP-S. Digest, 1988.
[63] R. Q. Lee, K. F. Lee, and J. Bobinchak, "Characteristics of a two-layer electromagnetically coupled rectangular patch antenna," *Electronics Letters*, vol. 23, pp. 1070-1072, 1987.

[64] A. N. Tulintseff, S. M. Ali, and J. A. Kong, "Input impedance of a probe-fed stacked circular microstrip antenna," *Antennas and Propagation, IEEE Transactions on*, vol. 39, pp. 381-390, 1991.

[65] R. B. Waterhouse, "Design of probe-fed stacked patches," *Antennas and Propagation, IEEE Transactions on*, vol. 47, pp. 1780-1784, 1999.

[66] L. Gwo-Yun, C. Tzung-Wern, and W. Kin-Lu, "Broadband stacked shorted patch antenna for mobile communication handsets," presented at Microwave Conference, 2001. APMC 2001. 2001 Asia-Pacific, 2001.

[67] S. D. Targonski, R. B. Waterhouse, and D. M. Pozar, "Design of wide-band aperture-stacked patch microstrip antennas," *Antennas and Propagation, IEEE Transactions on*, vol. 46, pp. 1245-1251, 1998.

[68] I. J. Bahl, S. S. Stuchly, and M. A. Stuchly, "A New Microstrip Radiator For Medical Applications," *Microwave Theory and Techniques, IEEE Transactions on*, vol. 28, pp. 1464-1469, 1980.

[69] C. Weng, "A broad-band annular-ring microstrip antenna," *Antennas and Propagation, IEEE Transactions on [legacy, pre - 1988]*, vol. 30, pp. 918-922, 1982.

[70] T. Huynh and K. F. Lee, "Single-layer single-patch wideband microstrip antenna," *Electronics Letters*, vol. 31, pp. 1310-1312, 1995.

[71] K. F. Lee, K. M. Luk, K. F. Tong, Y. L. Yung, and T. Huynh, "Experimental study of the rectangular patch with a U-shaped slot," presented at Antennas and Propagation Society International Symposium, 1996. AP-S. Digest, 1996.

[72] K. M. Luk, K. F. Lee, and W. L. Tam, "Circular U-slot patch with dielectric superstrate," *Electronics Letters*, vol. 33, pp. 1001-1002, 1997.

[73] K.-L. Wong and W.-H. Hsu, "Broadband triangular microstrip antenna with U-shaped slot," *Electronics Letters*, vol. 33, pp. 2085-2087, 1997.

[74] C. Wood, "Improved Bandwidth of Microstrip Antennas Using Parasitic Elements," *IEE Proceedings*, vol. 127 Pt H, 1980.

[75] P. S. Bhatnagar, J. P. Daniel, K. Mahdjoubi, and C. Terret, "Hybrid edge, gap and directly coupled triangular microstrip antenna," *Electronics Letters*, vol. 22, pp. 853-855, 1986.

[76] G. Kumar and K. Gupta, "Broad-band microstrip antennas using additional resonators gap-coupled to the radiating edges," *Antennas and Propagation, IEEE Transactions on [legacy, pre - 1988]*, vol. 32, pp. 1375-1379, 1984.

[77] G. Kumar and K. Gupta, "Nonradiating edges and four edges gap-coupled multiple resonator broad-band microstrip antennas," *Antennas and Propagation, IEEE Transactions on [legacy, pre - 1988]*, vol. 33, pp. 173-178, 1985.

[78] C. K. Aanandan and K. G. Nair, "Compact broadband microstrip antenna," *Electronics Letters*, vol. 22, pp. 1064-1065, 1986.

[79] H. Legay and L. Shafai, "New stacked microstrip antenna with large bandwidth and high gain," *Microwaves, Antennas and Propagation, IEE Proceedings* -, vol. 141, pp. 199-204, 1994.

[80] H. Legay and L. Shafai, "A new stacked microstrip antenna with large bandwidth and high gain," presented at Antennas and Propagation Society International Symposium, 1993. AP-S. Digest, 1993.

[81] B. Balakrishnan and G. Kumar, "Wide band and high gain electromagnetically coupled circular microstrip antennas," presented at Antennas and Propagation Society International Symposium, 1998. IEEE, 1998.

[82] K. S. Fong, H. F. Pues, and M. J. Withers, "Wideband multilayer coaxial-fed microstrip antenna element," *Electronics Letters*, vol. 21, pp. 497-499, 1985.
[83] P. S. Hall, "Probe compensation in thick microstrip patches," *Electronics Letters*, vol. 23, pp. 606-607, 1987.
[84] J. Anguera, C. Puente, and C. Borja, "A procedure to design stacked microstrip patch antennas based on a simple network model," *Microwave and Optical Technology Letters*, vol. 30, pp. 149-151, Aug 5, 2001.
[85] J. Anguera, C. Puente, and C. Borja, "A procedure to design wide-band electromagnetically-coupled stacked microstrip antennas based on a simple network model," presented at Antennas and Propagation Society International Symposium, 1999. IEEE, 1999.
[86] H. A. Wheeler, "Fundamental Limitations of Small Antennas," *Proceedings of the IRE*, vol. 35, pp. 1479-1484, 1947.
[87] J. S. McLean, "A re-examination of the fundamental limits on the radiation Q of electrically small antennas," *Antennas and Propagation, IEEE Transactions on*, vol. 44, pp. 672, 1996.
[88] I. Hunter, "Broad-band matching of antennas using dual-mode radiators," presented at 33rd European Microwave Conference, 2003.
[89] R. M. Fano, "Theoretical Limitations on the Broadband Matching of Arbitrary Impedances," *Journal of the Franklin Institute, MIT*, vol. 249, pp. 57-84, June 1947.
[90] G. Matthaei, *Microwave Filters, Impedance-Matching Networks, and Coupling Structures*: Artech House, 1980.
[91] K. Chang, *Microwave Ring Circuits and Antennas*: Wiley, 1996.
[92] I. C. Hunter, J. D. Rhodes, and V. Dassonville, "Dual-mode filters with conductor-loaded dielectric resonators," vol. 47, pp. 2304, 1999.
[93] A. I. Abunjaileh, I. C. Hunter, and A. H. Kemp, "Application of dual-mode filter techniques to the broadband matching of microstrip patch antennas," *Microwaves, Antennas & Propagation, IET*, vol. 1, pp. 273, 2007.
[94] H. C. Bell, "The Coupling Matrix in Low-Pass Prototype Filters," in *Microwave Magazine, IEEE*, vol. 8, 2007, pp. 70-76.
[95] I. Hunter, *Theory and Design of Microwave Filters*. London: IEE, 2001.
[96] J. D. Rhodes, "Microwave Reflection Filter Including A Ladder Network Of Resonators Having Progressively Smaller Q Values," vol. 5781084, U. S. Patent, Ed. USA: Filtronic Comtek PLC, West Yorkshire England, 1998, pp. 12.
[97] A. C. Guyette, "Optimum Design of Microwave Filters with Finite Dissipation," in *School of Electronic and Electrical Engineering*, vol. PhD thesis: The University of Leeds, July 2006.
[98] A. I. Abunjaileh, I. C. Hunter, and A. H. Kemp, "A Circuit-Theoretic Method of Multi-band Matching for Microstrip Patch Antennas," *Submitted to IEEE Transactions on Microwave Theory and Techniques* Submitted on May 2007.
[99] F. Croq and D. M. Pozar, "Multifrequency operation of microstrip antennas using aperture-coupled parallel resonators," *Antennas and Propagation, IEEE Transactions on*, vol. 40, pp. 1367-1374, 1992.
[100] S. Maci and G. B. Gentili, "Dual-frequency patch antennas," *Antennas and Propagation Magazine, IEEE*, vol. 39, pp. 13-20, 1997.
[101] J. S. Chen and K. L. Wong, "A single-layer dual-frequency rectangular microstrip patch antenna using a single probe feed," *Microwave and Optical Technology Letters*, vol. 11, pp. 83-84, 1998.

[102] H. Nakano and K. Vichien, "Dual-frequency square patch antenna with rectangular notch," *Electronics Letters*, vol. 25, pp. 1067-1068, 1989.
[103] D. Sanchez-Hernandez and I. D. Robertson, "Analysis and design of a dual-band circularly polarized microstrip patch antenna," *IEEE Transactions on Antennas and Propagation*, vol. 43, pp. 201-205, 1995.
[104] S. U. Xiang-Fei Peng (Sch. of Commun. & Inf. Eng., China); Shun-Shi Zhong; Sai-Qing Xu; Qiang Wu, "Compact dual-band GPS microstrip antenna," *Microwave and Optical Technology Letters*, vol. 44, pp. 58-61, 2005.
[105] S. M. El-Ghazaly, "Reconfigurable Antennas for Universal Wireless Receivers," in *Reconfigurable and Smart Antennas Workshop, IEEE International Microwave Symposium*. Hawaii, 2007.
[106] D. Pozar, D. Schaubert, and P. Hall, "Review of Techniques for Dual and Circularly Polarised Microstrip Antennas," *Microstrip Antennas The Analysis and Design of Microstrip Antennas and Arrays*, pp. 107-116, 1995.
[107] A. I. Abunjaileh, I. C. Hunter, and A. H. Kemp, "Multi-band Matching Technique for Microstrip Patch Antenna Transceivers," presented at The 37th European Microwave Conference (EuMC), Munich, Oct. 2007.
[108] K. L. Wong, *Compact and Broadband Microstrip Antennas*: John Wiley & Sons Inc., 2002.

Appendix A MATLAB Codes

```
% This Code computes the radius, conductivity, directivity, Antennas input resistance,
% quality factor, bandiwdth and far fields for circular microstrip patch antennas
clear
clc

c=3*10^8;                    % Speed of light in free space
eo=8.8541878*10^-12;         % Permitivity of Vacuum
er=2.2                       % Permitivity of Duriod 5880
uo=400*pi*10^-9;             % Permeabilty of Vacuum
th=0.0787                    % Substrate thickness
rho = 5.96*10^7;             % Copper Conductivity
tandel =0.0009               % Loss tangent
vswr=2;                      % Standing Wave Ratio(VSWR)
fr=2*10^9;                   % Operating Frequency
zo=50                        % Char Impedance
m = 1;                       % Resonant mode
n = 1;

lamda=(100*c)/(fr);          % Wavelength in cm
beta=(2*pi)/lamda;       % Wave number (k)
k=beta*(er)^0.5;             % Propagation constant Assuming alpha is zero, i.e. lossless

%  Roots of the Bessel Function
if m==0
   emo=2;
else
   emo=1;
end
xmn=BSL(m,n,emo);
% ---------------

% ANTENNA RADIUS
[a,ae,aecm]=rad(fr,er,th,xmn,c);
% --------------

% Antennas Radius Function
function [a,acm,aecm] = rad(fr,er,th,xmn,c)
a=(xmn*c)/(2*pi*fr*(er^0.5));      % Patch radius
acm=a*100;                         % change to cms for consistancy with other eqns
aecm=acm*(1+(2*th/(pi*er*acm))*(log(pi*acm/(2*th))+1.7726))^0.5;
                                   % Real Antenna Root
```

```
%    Conductance AND Directivity
for i=1:1000
aew=(i*lamda)/1000;                          % Breaking lamda into an array
GRadiation(i)=funGr(aew,m,emo,er,beta);      % find the integration value
Dir(i)=(beta*aew)^2./(120*GRadiation(i));    % Directivity
end

Grad=funGr(aecm,m,emo,er,beta);                          % G radiation
Gc=emo*pi*(pi*uo*fr)^(-3/2)*((k*aecm)^2-m^2)/(4*th^2*rho^0.5);  % G conduction
Gd=emo*tandel*((k*aecm)^2-m^2)/(4*uo*th*fr);             % G dielectric
Gt=Grad+Gc+Gd;
Rin_edge = 1/Gt                              % Input resistance at the edge of the patch

DirdB=10*log10(Dir);                         % Directivity (dBs) Vs radius
nr=0.001:0.001:1;                            % Normalised radius

figure(1)
plot(nr,abs(DirdB))                  % Directivity Vs. radius
title('Directivity Vs Normalised Radius');
xlabel('Radius/Wavelength')
ylabel('Directivity (dB)')

figure(2)
plot(nr,abs(GRadiation))                     % Radiation Conductance Vs. radius
title('Radiation Conductance Vs Normalised Radius');
xlabel('Effective Radius/Wavelength')
ylabel('Radiation Conductance')

% --------------

% G Radiation Integration Function
function Grad=funGr(ae,m,emo,er,beta)
an=0:0.1:90;                                 % Angle accross the antenna from 0-pi/2
tt=an.*pi/180;                       % Convert to radians
tlen=length(tt);                     % Number of values in the Array
mmm=beta*ae*sin(tt);
ji0mp=besselj(m-1,mmm)- besselj(m+1,mmm);            % Bp(X)=Jn-1(X)+Jn+1(X)
j0mp =besselj(m-1,mmm)+ besselj(m+1,mmm);            % Bm(X)=Jn-1(X)-Jn+1(X)
xxx=(((ji0mp.^2)+(cos(tt).^2).*(j0mp.^2)).*sin(tt)*pi/2)/tlen;
intr1=sum(xxx);
Grad=(emo*((beta*ae)^2)/480)*intr1;
```

```
% Antennas Input Resistance
radius=aecm*(1:1000)./1000;

Rin=(1/Gt).*((besselj(m,k*radius)).^2)/(besselj(m,k*aecm).^2);
x=1;
while  abs(Rin(x)) < zo
x=x+1;
end
po=(x/length(Rin))*aecm
figure(3)                                   %Input Resistance against effective radius
plot(radius,Rin)
title('Input Resistance accross the Radius');
xlabel('Radius')
ylabel('Input Resistance')
% --------------------



function xmn=BSL(m,n,emo,er)
%   Determining Roots of Bessel functions' differential root
x=15;                       % Max value at the x-axis
b=0.001;
nn=0:b:x;
jm=besselj(m,nn);           % Bessel function of the first kind of order m

abjm=abs(jm);               % IN ORDER TO FIND THE DIFFERENTIAL, THE MAX OR MIN
VALUES MUST BE FOUND
                            % THIS PLOT THE ABSOLUTE VALUES OF THE FUNCTION
                            % ALLOWING ALL MXIMUMS TO BE AT POSITIVE VALUES TO
                            % MAKE IT EASIER TO FIND THEM
for i= 3:length(jm);        % THIS FUNCTION SIMPLY COMPARES ALL THE FUNCTION
   if (abjm(i-1)>abjm(i-2)) & (abjm(i-1)>abjm(i));     % VALUES, IF THE VALUE IS X, IT
COMPARES IT WITH
      rtmat(i)=i-2;         % THE PREVIOUS AND NEXT VALUE IN ORDER TO POINT
   else                      % MAXIMUMS.
      rtmat(i)=0;           % "rtmat" will only equal max root value representing
   end                       % a "ZERO" or will have the value zero
end
roots=b*(nonzeros(rtmat));  %  SINCE THE X AXIS WAS magnified FROM 20 INTO 2000 (i.e.
by 1000) AS SHOWN IN
                    %  x, b & nn values, it must be reduced again by multiplying the
                    %  values with the factor b, i.e. 0.001
                    %  Bessel functions' differential root
xmn=roots(n,1)              %   Selecting relevant root/zero based on antenna mode
```

```
%   Far E-Field Pattern
phi=0;      % Far E-Fields at E plane
for i=1:1000;
   the=i*((pi/2)/1000);              %  theta from 0 to 90deg (pi/2)
   bas=beta*aecm*sin(the);
   jmi2=besselj(m-1,bas)-bessel(m+1,bas);
   ef(i)=cos(m*phi).*jmi2;
end
ef=ef/max(abs(ef));                  %  Normalizing the Field
efa=fliplr(ef);                      % Applying Field Symmetry
ll=linspace(-100,-100,(2*length(ef)));
efdd=[efa ef]./max(abs(ef));

phi=pi/2;   % Far E-Fields at H plane
for i=1:1000;
   the=i*((pi/2)/1000);              % From angle zero to 90deg (perpendicular to the antenna)
   bas=beta*aecm*sin(the);
   jm2=besselj(m-1,bas)+bessel(m+1,bas);
   efph(i)=cos(the)*sin(m*phi).*jm2;
end
efph=efph/max(abs(efph));                  % Normalizing the Field
efaph=fliplr(efph);                  % Applying Field Symmetry
ll=linspace(-40,-40,(2*length(efph)));
efddph=[efaph efph]./max(abs(efph));

cc=length(efdd);
lll=(1:cc)*pi/cc;

%   Plotting Electric Field
figure(4)
polar(lll,abs(efdd))
title('Far E-Field at phi=0 or 180deg and 0<theta<90deg (E-Plane)');

figure(5)
polar(lll,abs(efddph))
title('Far E-Field at phi=90 or 270deg and 0<theta<90deg (H-Plane)');


% --------------------
```

```
% Quality factor and Bandwidth
an=0.1:0.01:90;
tt=an.*pi/180;
tlen=length(tt);

mmm=beta*aecm*sin(tt);                          % I1 factor in Qr
jmpx=besselj(m,(mmm/mmm.^2));
jmp=besselj(m,mmm);
jmpd=gradient(jmp)*(2*tlen/pi);

xx=((jmpd.^2+((jmpx^2).*cos(tt).^2).*sin(tt))*pi/(2*tlen) );
I1=sum(xx);

hm=th/100;                                      % Thickness from cm to meters
Qr=(30*((k*aecm)^2-n^2))/(hm*fr*uo*((beta*aecm)^2)*I1); % Q Radiation
Qd=1/tandel;                                    % Q Dielectric
Qc=hm*(pi*fr*uo*rho)^0.5;                       % Q Conduction
Qt=((Qr^-1)+(Qd^-1)+(Qc^-1))^-1;                % Q total

BW=(fr*(vswr-1))/(Qt*vswr^0.5);                 %  Bandwidth in Hz
BWGHz=BW/10^9                                   %  Bandwidth in GHz
effi=Qt/Qr                                      %  Efficiency
% --------------------


%this program finds the optimum values of omega for the return loss function of
%lowpass prototype
clc
clear all
w1=2.2;                         % First pole
w2=6.45;                        % Second Pole
w=-15:0.05:15;
Q=1;                            % Assuming R=C=1
for x=1:601;
S11(x) = ((j*w(x)-j*(-w2))/(j*w(x)-j*(-w2)+2/Q))*((j*w(x)-j*(-w1))/(j*w(x)-j*(-w1)+2/Q))*( (j*w(x)-
j*(w1))/(j*w(x)-j*(w1)+2/Q))*( (j*w(x)-j*(w2))/(j*w(x)-j*(w2)+2/Q));
end
plot (w,20*log10(abs(S11)));
syms p
S1 = ((p-j*(-w2))/(p-j*(-w2)+2/Q))*((p-j*(-w1))/(p-j*(-w1)+2/Q))*( (p-j*(w1))/(p-j*(w1)+2/Q))*( (p-
j*(w2))/(p-j*(w2)+2/Q));
pretty(simple(expand(S1)))
pretty(simple(expand(1-(S1^2)^.5)))
```

Appendix B Publications

1. A. I. Abunjaileh, I. C. Hunter, and A. H. Kemp, "Application of Dual-mode Filter Techniques to the Broadband Matching of Microstrip Patch Antennas," *Microwaves, Antennas & Propagation, IET*, vol. 1, pp. 273, 2007.
2. A. I. Abunjaileh, I. C. Hunter, and A. H. Kemp, "Multi-band Matching Technique for Microstrip Patch Antenna Transceivers," presented at The 37th European Microwave Conference (EuMC), Munich, Oct. 2007.
3. A. I. Abunjaileh, I. C. Hunter, and A. H. Kemp, " A Circuit-theoretic Approach to the Design of Quadruple-Mode Broadband Microstrip Patch Antenna," IEEE Transactions of Microwave Theory and Techniques, accepted and to be published, 2008.
4. A. I. Abunjaileh, I. C. Hunter, and A. H. Kemp, "A Circuit-Theoretic Method of Multi-band Matching for Microstrip Patch Antennas", submitted to the IEEE Transactions on Antennas and Propagation, November 2007.

Application of dual-mode filter techniques to the broadband matching of microstrip patch antennas

A.I. Abunjaileh, I.C. Hunter and A.H. Kemp

Abstract: Structures such as square or circular microstrip patch antennas may support two orthogonal resonant modes. The paper presents a new method of utilising the dual-mode property to increase the bandwidth of microstrip antennas. The input impedance of such a dual-mode antenna may be represented as a second-order ladder network of coupled resonators, where each resonator is coupled to a load resistor. A theoretical method for evaluating the coupling values in the network is presented, enabling the bandwidth of a dual-mode antenna to be maximised. A theoretical bandwidth improvement of up to 3:1 is achieved when compared to a single-mode antenna. This is confirmed with an experimental dual-mode circular microstrip patch antenna.

1 Introduction

In recent years, there has been a significant trend towards the use of internal antennas in cellular phones and other wireless communication devices. These antennas must fit into a very restricted space which generally causes significant reduction in system performance. There are well known fundamental limitations on the performance of electrically small antennas [1]. For example the 3 dB bandwidth of the input reflection coefficient of an antenna is given by

$$\Delta_{(3\ dB)} = \left(\frac{2\pi r}{v}\right)^3 f^4 \tag{1}$$

where r is the radius of the antenna, f is the frequency of operation and v is the velocity of light. Thus, a small antenna working at low frequencies may have a very restricted bandwidth of operation. In practice, it is usually a struggle to achieve a reasonable input match over the full 80 MHz of bandwidth required for a GSM phone operating at 900 MHz. Furthermore, should a significant improvement in bandwidth be achievable, then the physical size of the antenna could be reduced. It is well known that broadband matching theory can be used to increase the bandwidth of a reactive load for a given return loss level [2]. In the case of a resonant antenna, an external resonator (or resonators) can be coupled to the antenna, enabling a bandwidth improvement of approximately 2:1 to be achieved, as is shown in Fig. 1.

In the Figure, the antenna is represented by a resonator coupled into a resistive load. The matching network is coupled into the antenna via an impedance inverter K. However, the matching network requires physical volume which may be better employed by simply increasing the size of the antenna. Also the matching network will have a finite unloaded Q factor, thus causing some resistive losses which will reduce the radiated power. This problem could be partially overcome, if the matching network was also the last element in a bandpass filter, but such filters are not always required in radio transceivers. An alternative method of broadband matching, using a dual-mode antenna structure is described in this paper. Consider the circular microstrip patch antenna in Fig. 2.

This forms the basis for the antenna described in this paper, shown in Fig. 3. The fundamental resonant mode of this structure is the dual degenerate TM_{110} mode, where each of the resonant modes radiates and can be represented by a resonant circuit terminated in a resistor. It is simple to arrange for the input feed to the antenna to couple into one mode, which is then coupled to the second mode via a discontinuity in the structure.

The equivalent circuit of this structure is a second-order ladder network where each resonant circuit is terminated in a resistor R, representing its own internal losses and radiation. This is shown in Fig. 4, where J_{01} and J_{12} are admittance inverters.

The similarities between this circuit and the conventional broadband matching approach shown in Fig. 1 are obvious. The fundamental difference is that there is resistive loss in both resonators in the dual-mode case. This loss may be used to broaden the input match of the dual-mode antenna.

A simple theoretical method for calculating the coupling required into a single mode antenna to achieve maximum bandwidth will be described in the next section. This will be used as the basis of comparison. It is then followed by a similar procedure for dual-mode antennas, showing the theoretical improvement obtained. Finally, the design of an experimental antenna will be demonstrated, showing the bandwidth improvement.

2 Optimum bandwidth for a single-mode antenna

The equivalent circuit of a single-mode antenna is shown in Fig. 5. This can be replaced by a lowpass prototype network shown in Fig. 6. The simplest strategy for matching is to critically couple the circuit at zero frequency, i.e.

$$S_{11}(0) = 0 \tag{2}$$

Hence, J = 1 and

$$|S_{11}(j\omega)|^2 = \frac{\omega^2}{4 + \omega^2} \tag{3}$$

© The Institution of Engineering and Technology 2007

doi:10.1049/iet-map:20060049

Paper first received 8th March and in revised form 1st June 2006

The authors are with the School of Electronic and Electrical Engineering, University of Leeds, West Yorkshire, LS2 9JT, UK

E-mail: aabunjaileh@yahoo.co.uk

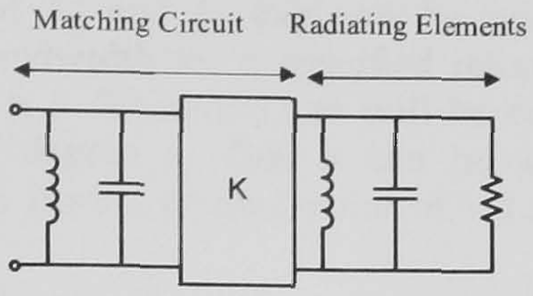

Fig. 1 *Conventional broadband matching of a resonant antenna*

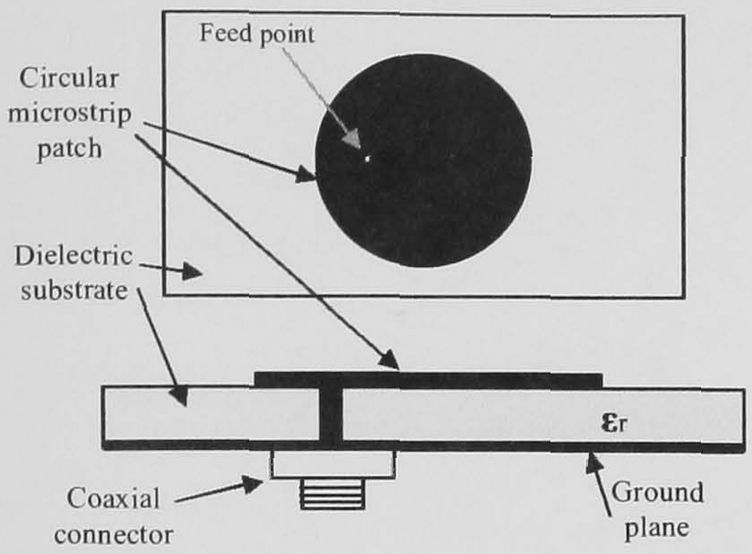

Fig. 2 *Circular patch microstrip antenna fed by a coaxial cable*

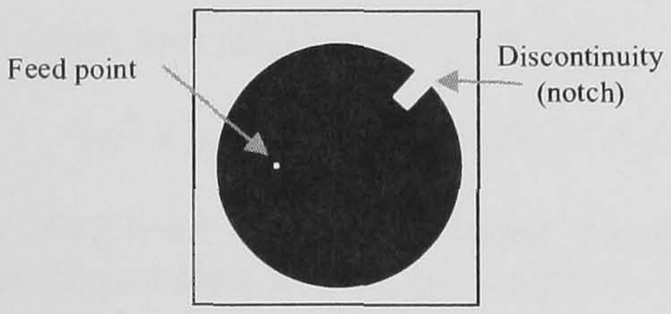

Fig. 3 *Dual-mode circular microstrip patch antenna*

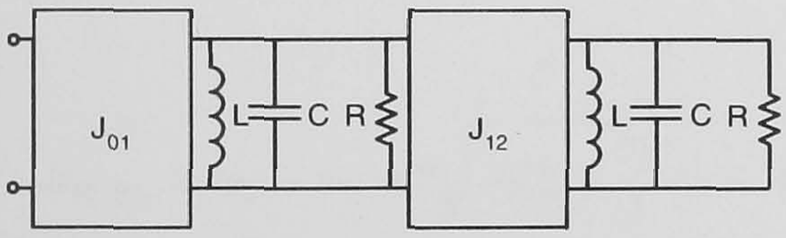

Fig. 4 *Equivalent circuit of dual-mode antenna*

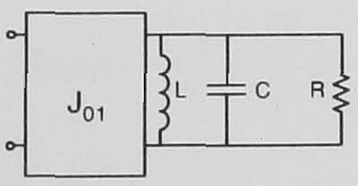

Fig. 5 *Single-mode antenna equivalent circuit*

For a 6 dB return loss specification, for example, we have

$$|S_{11}(j\omega)|^2 \frac{\omega^2}{4+\omega^2} = \frac{1}{4}, \text{ at the 6 dB frequency} \quad (4)$$

giving

$$\omega = \pm \frac{2}{\sqrt{3}} \quad (5)$$

and a 6 dB bandwidth of $4/\sqrt{3} = 2.3094$.

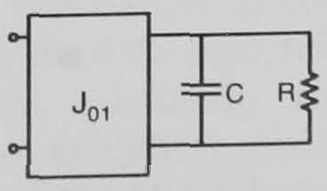

Fig. 6 *Single-mode antenna equivalent circuit $R = C = 1$*

This bandwidth can be improved by adjusting the input coupling J. Thus, at the 6 dB frequency

$$|S_{11}(j\omega)|^2 \frac{(1-J^2)^2+\omega^2}{(1+J^2)^2+\omega^2} = \frac{1}{4} \quad (6)$$

or

$$\omega^2 = -J^4 + 3.333J^2 - 1 \quad (7)$$

and

$$\Delta_{(6\text{dB})} = 2\sqrt{-(J^2-3)(J^2-1/3)} \quad (8)$$

where $\Delta_{(6\text{dB})}$ is the 6 dB return loss bandwidth. To maximise the bandwidth we maximise the function

$$f(x) = -x^2 + 3.333x - 1, \quad \text{where } x = J^2 \quad (9)$$

Thus

$$\frac{df(x)}{dx} = -2x + 3.333 = 0 \quad (10)$$

Giving

$$J = \sqrt{\frac{5}{3}} \quad (11)$$

And, from (8),

$$\Delta_{(6\text{dB})} = 2.666 \quad (12)$$

This is approximately 15% greater than for the critically coupled case. This is the overcoupled case described in (6). There is another value of $J = \sqrt{3}/5$ which minimises the 6 dB bandwidth.

Note that a 6 dB return loss level was chosen arbitrarily. Should a 10 dB return loss be required then the value of J would be $\sqrt{11/9}$, giving a 5% improvement over the critically coupled case. These optimised bandwidths are the ones which should be used as the basis for comparison with other matching schemes.

3 Optimisation of the return loss bandwidth of a dual-mode antenna

The lowpass prototype for the dual-mode antenna is shown in Fig. 7, where, the resistor and capacitor values have been set to unity, to enable direct comparison with the single-mode case. This also implies a symmetrical antenna structure, the input admittance of this circuit is given by

$$Y_{\text{in}}(p) = \frac{J_{01}^2}{1+p+\dfrac{J_{12}^2}{1+p}} \quad (13)$$

$$= \frac{J_{01}^2 p + J_{01}^2}{p^2 + 2p + 1 + J_{12}^2} \quad (14)$$

and

$$S_{11}(p) = \frac{p^2 + (2-J_{01}^2)p + 1 + J_{12}^2 - J_{01}^2}{p^2 + (2+J_{01}^2)p + 1 + J_{12}^2 + J_{01}^2} \quad (15)$$

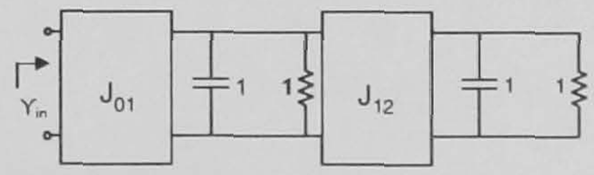

Fig. 7 *Dual-mode antenna lowpass prototype*

The values of J_{01} and J_{12} can now be evaluated to obtain maximum bandwidth for a specified return loss level. As an example, a 6 dB return loss will be considered. Now, $S_{11}(p)$ is of degree 2, thus it can be arranged for the return loss to have a turning point of value 6 dB at direct current, then

$$S_{11}(0) = \frac{1 + J_{12}^2 - J_{01}^2}{1 + J_{12}^2 + J_{01}^2} = \frac{1}{2} \tag{16}$$

or

$$J_{12}^2 = 3J_{01}^2 - 1 \tag{17}$$

Thus

$$S_{11}(p) = \frac{p^2 + (2 - J_{01}^2)p + 2J_{01}^2}{p^2 + (2 + J_{01}^2)p + 4J_{01}^2} \tag{18}$$

giving

$$|S_{11}(j\omega)|^2 = \frac{\omega^4 + \omega^2(J_{01}^4 - 8J_{01}^2 + 4) + 4J_{01}^4}{\omega^4 + \omega^2(J_{01}^4 - 4J_{01}^2 + 4) + 16J_{01}^4} \tag{19}$$

For 6 dB return loss $|S_{11}(j\omega)|^2 = \frac{1}{4}$, giving

$$3\omega^4 + \omega^2[12 - 28J_{01}^2 + 3J_{01}^4] = 0 \tag{20}$$

Solutions of (20) are $\omega = 0$ (as already specified) and the band-edge frequencies, ω_1 and ω_2, are given by

$$\omega_{1,2} = \pm\sqrt{-J_{01}^4 + \frac{28}{3}J_{01}^2 - 4} \tag{21}$$

or

$$\Delta_{(6\text{ dB})} = \omega_2 - \omega_1 = 2\sqrt{-J_{01}^4 + \frac{28}{3}J_{01}^2 - 4} \tag{22}$$

To maximise the bandwidth, the value of J_{01} which maximise the function is obtained.

$$f(x) = -x^2 + \frac{28}{3}x - 4 \tag{23}$$

hence

$$\frac{df(x)}{dx} = -2x + \frac{28}{3} = 0 \tag{24}$$

yielding

$$x = J_{01}^2 = \frac{14}{3} \tag{25}$$

and using (17)

$$J_{12}^2 = 13 \tag{26}$$

giving $\Delta_{(6\text{ dB})} = 8.4327$. This is a 3.16:1 improvement compared with the optimum single mode case. Furthermore, it may be shown that the improvement increases to 3.46:1 for a 10 dB return loss design, although the overall bandwidth is less than for the 6 dB case, this was also experimented in [3] using a microstrip square patch antenna. Simulations of the analytical results obtained for the lowpass prototype of the two schemes explained here are shown in Figs. 8 and 9.

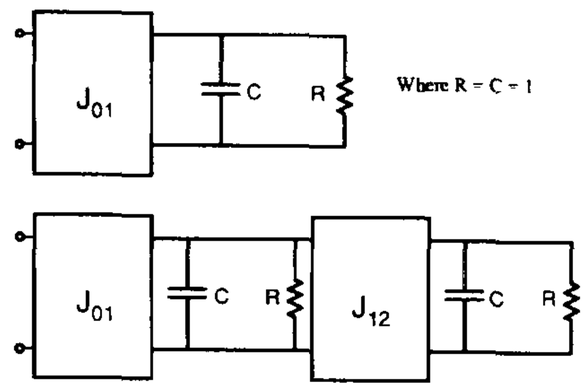

Fig. 8 *Circuit simulation*
a Optimised single mode ($J_{01} = (5/3)^{1/2}$)
b Dual mode ($J_{01} = (14/3)^{1/2}$ and $J_{12} = (13)^{1/2}$)

4 Electromagnetic simulation and practical implementation

To demonstrate the theory, an experimental prototype antenna was designed. This was based on a dual-mode dielectric resonator structure originally developed for filtering applications [4, 5]. A circular patch microstrip antenna on a particular substrate has only one degree of freedom to control, i.e. the radius, and, in turn, changing the radius affects the resonant frequency of the antenna. The equation that relates the radius to the resonant frequency in the dominant mode is [1, 6, 8, 10–12, 14]

$$f_r = \frac{\chi'_{mn}}{2\pi a(\mu\varepsilon_r)^{1/2}} \tag{27}$$

Where f_r is the resonant frequency, χ'_{mn} are the zeros of the Bessel function of order n, and equal to 1.8412 for the dominant TM_{110} mode, and a is the radius of the circular patch.

Hence, considering the dominant mode, at 2 GHz, the radius of the patch is around 3 cm using the Duroid 5880, of permittivity 2.2, as equation (27) implies. A coaxial cable was used to feed the antenna, and moving the feed point along the radius changes the return loss accordingly, as the resistance is maximum on the edge and drops to zero as the centre of the patch is approached [1, 6–9, 13]. It is therefore fairly easy to locate the feed point for the critically coupled and the optimised single-mode cases.

In the dual-mode case, two couplings must be optimised simultaneously and hence a specific design procedure must be followed. First, the feed point location must be obtained, this is achieved by referring to the equivalent circuit in Fig. 8, and evaluating the return loss when J_{12} is reduced to zero. At which point, the maximum value of return loss is 3.783 dB. Hence, the feed point is situated to achieve this value of return loss when the two resonances are uncoupled, but coexist orthogonally.

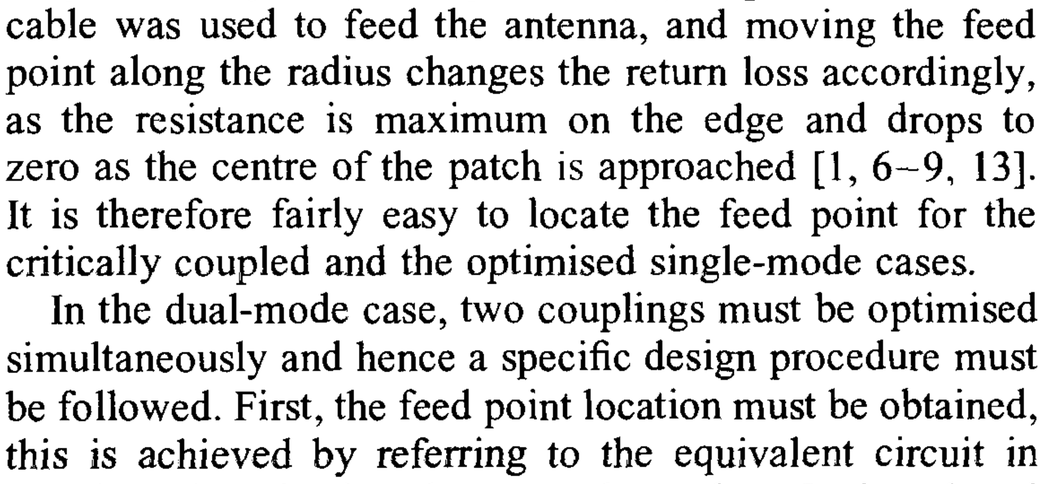

Fig. 9 *Simulation results*
a Optimised single-mode and *b* dual-mode showing 300% wider bandwidth

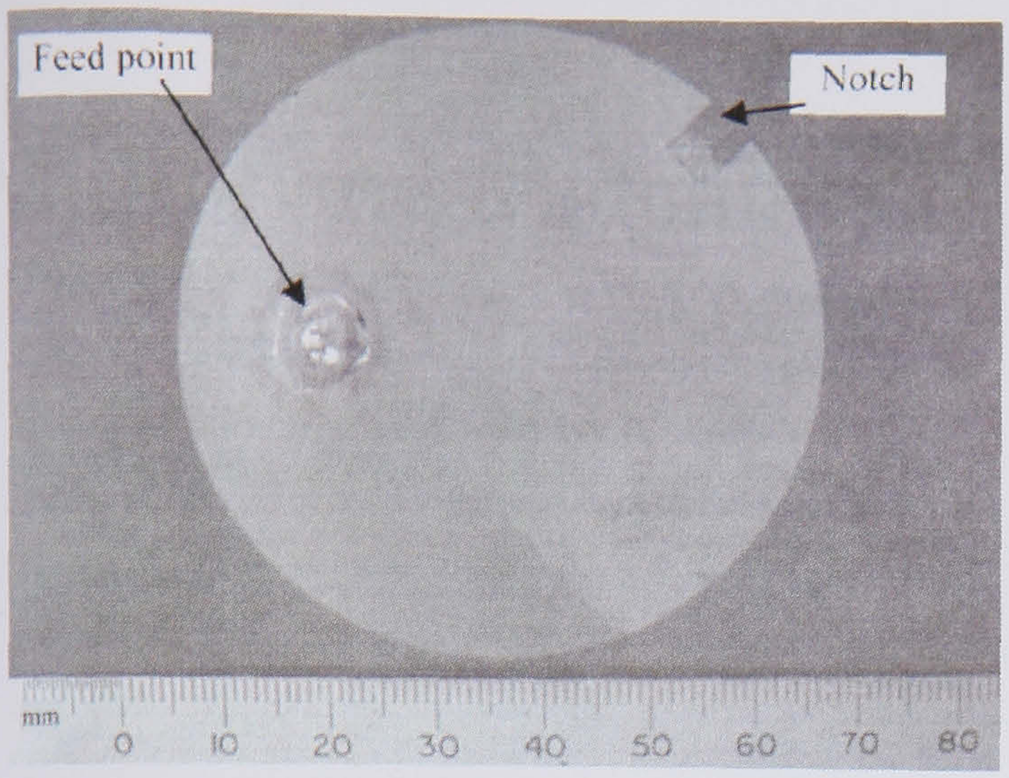

Fig. 10 *Dual-mode circular patch antenna designed at 2 GHz*

Secondly, we introduce the coupling notch which, in turn, perturb the fields, or in other words disturb the symmetry, this can be used to couple the two orthogonal modes and achieve wider bandwidth. The notch position is very important, it should be located at an angle of 45°, 135°, 225° or 315°[15], otherwise, if the notch was located at any other angle, it may not couple the two modes properly or even reduce one of the modes to zero [15]. To obtain the correct final return loss characteristic, in this particular example, simulations show that the notch should be approximately 1/6 of the radius to meet the desired specifications, i.e. 6 dB in the analysis given here.

Optimised single-mode and dual-mode circular microstrip antennas were designed, operating at 2GHz using Duriod 5880 substrate ($\varepsilon_r = 2.2$), and a notch of dimensions 4.5mm × 5mm was introduced, both the simulation (using ADS-Momentum) and measured results are shown in Figs. 10 and 11.

Clearly, the dual-mode antenna has a 6 dB bandwidth 3 times wider compared to the optimised single-mode case, and, as expected, the resonant frequency is lower in the simulation results than the measured results [11–14]. It is shown that the notch in Fig. 10 resulted in splitting the two resonant modes, and the simulations show that the degree of splitting is dependent on the width and depth of the notch.

The far-field radiation pattern of the antenna is essentially similar to a conventional single mode antenna, as shown in Fig. 12.

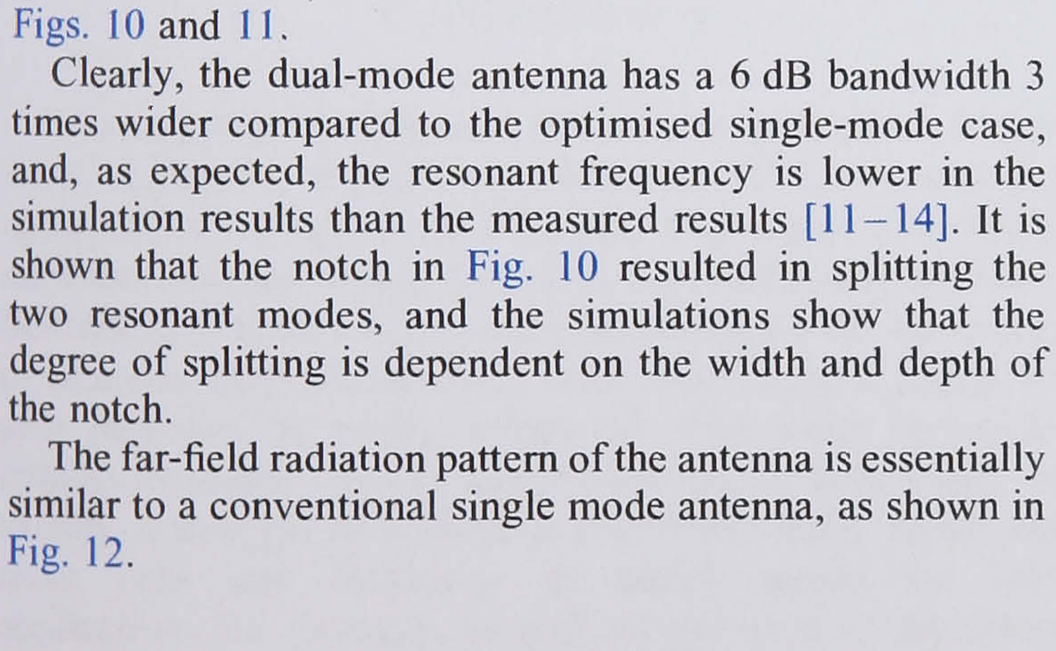

Fig. 11 *Electromagnetic simulations and measured results of circular patch antenna designed at 2 GHz showing optimised single-mode and dual-mode antenna results*

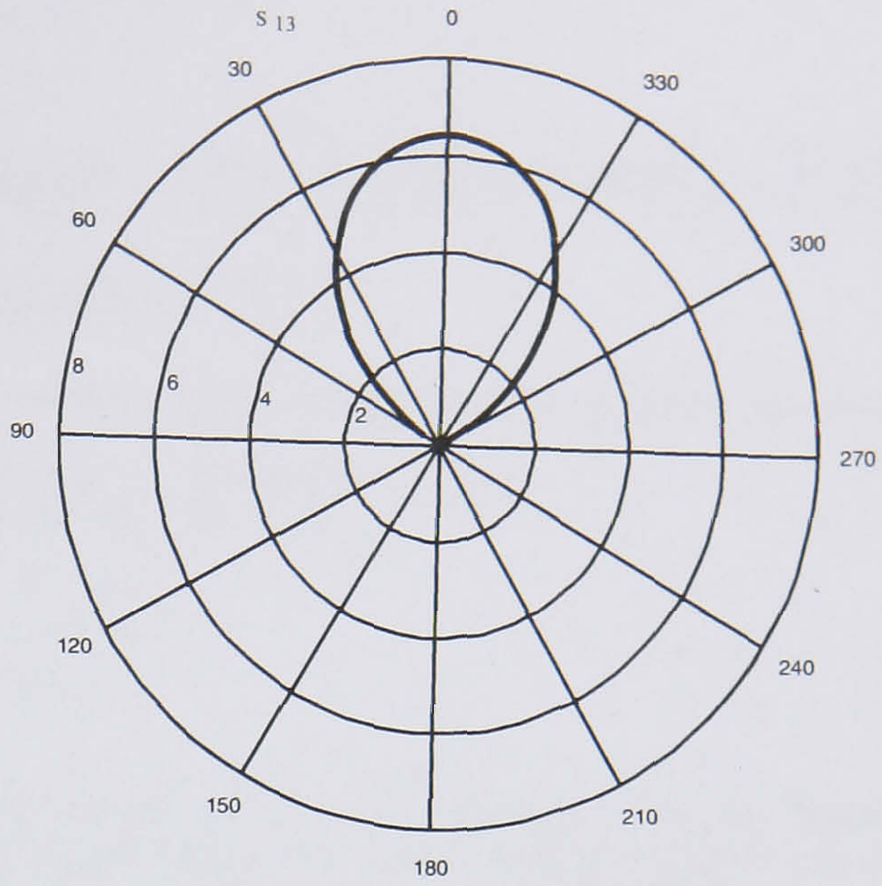

Fig. 12 *Far-field radiation pattern of the antenna*

5 Conclusion

The motivation behind this work is to improve the performance of microstrip patch antennas. A simple theoretical design method for maximising the return-loss bandwidth of a circular microstrip patch antenna is presented, and theoretical bandwidth improvement of up to 3:1 is achieved when compared to a single-mode antenna. By considering a dual-mode antenna as a filter network, it is shown that a significant improvement in bandwidth may be obtained when compared with a single mode device, this can be achieved by adjusting the coupling values. The theory has been demonstrated by introducing a notch into a practical circular microstrip patch antenna, without the need for complicated multilayer design or complicated feeding techniques, and is shown practically to achieve a 3:1 bandwidth improvement.

6 References

1 Balanis, C.A.: 'Antenna theory: analysis and design' (Wiley, New York, 2nd edn.), 1997, pp. 752–767
2 Fano, R.M.: 'Theoretical limitations on the broadband matching of arbitrary impedances', *J. Franklin Inst., MIT*, 1947, **249**, pp. 57–84
3 Ollikainen, J. *et al.*: 'Design and bandwidth optimization of dual-resonant patch antennas' (Helsinki University of Technology Radio Laboratory Publications, Espoo, March 2002)
4 Hunter, I.C., Rohdes, J.D., and Dassonville, V.: 'Dual mode filters with conductor-loaded dielectric resonators', *IEEE Trans.*, 1999, **47**, (12), pp. 2304–2311
5 Hunter, I.: 'Broad-band matching of antennas using dual-mode radiators'. Presented at 33rd European Microwave Conference, October 2003, pp. 43–434
6 Bhartia, P.: 'Microstrip antennas' (Artech House, Massachusetts, 1980), pp. 85–126
7 Derneryd, A.: 'Analysis of the microstrip disk antenna element', *IEEE Trans. Antennas Propag.*, 1979, **27**, p. 660
8 Garg, R.: 'Microstrip antenna design handbook' (Artech House, Massachusetts, 2001), pp. 317–353
9 Hall, P.S.: 'Handbook of microstrip antennas' (Peregrinus, 1989)
10 Howell, J.: 'Microstrip antennas', *IEEE Trans. Antennas Propag.*, 1975, **23**, p. 90
11 Kumprasert, N., and Kiranon, W.: 'Simple and accurate formula for the resonant frequency of the circular microstrip disk antenna', *IEEE Trans. Antennas Propag.*, 1995, **43**, p. 1331
12 Long, S., and Shen, L.: 'The circular disc, printed circuit antenna'. Antennas Propag. Soc. Int. Symp., 1977, **15**, pp. 100–103
13 Pozar, D.M.: 'Microstrip antennas', *Proc. IEEE*, 1992, **80**, p. 79
14 Shen, L., Long, S., Allerding, M., and Walton, M.: 'Resonant frequency of a circular disc, printed-circuit antenna', *IEEE Trans. Antennas Propag.*, 1977, **25**, p. 595
15 Chang, Kai: 'Microwave ring circuits and antennas' (Wiley, 1996), Chap. 3

Multi-band Matching Technique for Microstrip Patch Antenna Transceivers

Alaa I. Abunjaileh, *Student member IEEE*, Ian C. Hunter, *Fellow IEEE,* Andrew H. Kemp, *Member IEE*

School of Electronic and Electrical Engineering, The University of Leeds
Woodhouse lane, Leeds, LS2 9JT, The United Kingdom

een1aian@leeds.ac.uk
i.c.hunter@leeds.ac.uk
a.h.kemp@leeds.ac.uk

Abstract— **A new method of multi-band matching for circular microstrip patch antennas is presented. The input impedance of circular patch antennas can be represented as a second order ladder network of coupled resonators where each resonator is coupled to a load resistor. Using analysis based on microwave filter theory, the antenna can also be used as a dual-band antenna exploiting the fact that structures such as circular, square or triangular microstrip patch antennas can support two orthogonal resonant modes. A theoretical method of incorporating an external matching network with the dual-mode polarisation property of a microstrip patch antenna network is presented. This enables an antenna fed by two ports to be matched at four distinct frequencies, and achieve good isolation between the two feeding ports. This is the first time where the dual-mode polarisation property of circular microstrip patch antennas is successfully utilized with a matching network to maximise the performance of single layer microstrip patch antennas. The simulation results are confirmed with an experimental quad-band circular microstrip patch antenna realisation.**

I. INTRODUCTION

The on-going development of wireless applications ranging from Bluetooth, WLANs and GSM to GPS and aerospace applications requires more efficient, low profile and flexible antennas. In particular, the need for multiband operation. Microstrip antennas enjoy many advantages over other types of antennas, they are relatively small, light weight, strong, low cost and can be easily integrated with other microwave circuits. However, they do suffer from narrow bandwidth. It is usually a struggle to achieve a reasonable input match over more than one frequency to satisfy needs for GSM applications for example, as well as the need of multi-band antennas for global navigation systems (e.g. GPS). Other techniques were proposed to over come this problem, such as electrically thick elements, stacked multipatch and multilayer elements [1], however, these techniques increase the complexity and the size of the antenna, and also do not fully make use of techniques that allow single layer antennas to perform better. A circular microstrip patch antenna fed using a coaxial cable from the ground plane is shown in Figure 1. The dominant mode of this antenna is the TM_{110} mode [2]. Each of the resonant modes radiate and can be represented using circuit theory by a resonant circuit terminated in a resistor [3]. Figure 2 shows the equivalent circuit of this antenna, where the admittance matrix J_{01} represents the coupling between the input and the antenna, an inductor and a capacitor representing resonance and a resistor representing power loss due to radiation from the antenna.

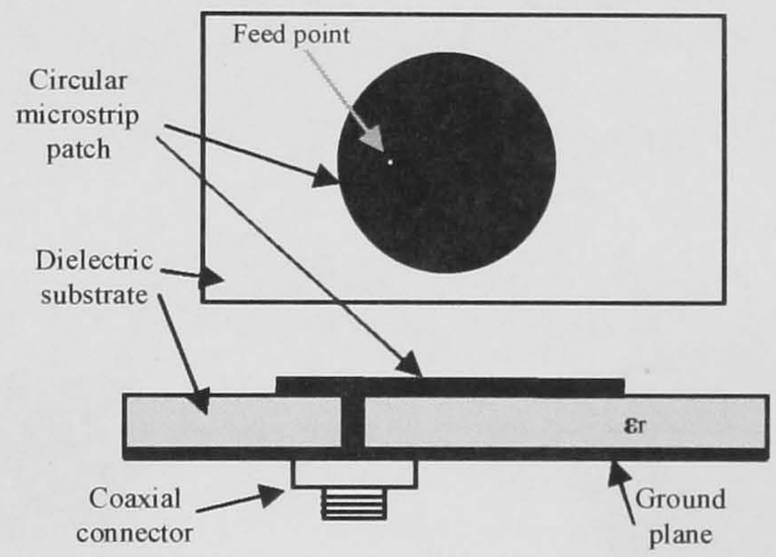

Fig. 1 Circular microstrip patch antenna fed by a coaxial cable.

However, the low pass prototype network shown in figure 3 can be used instead for comparison purposes [3, 4].

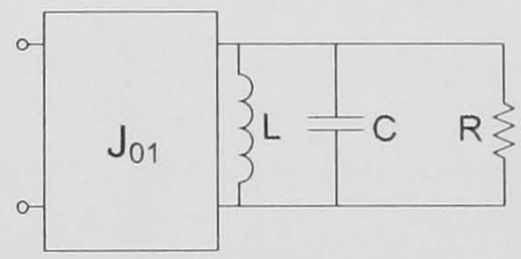

Fig. 2 Single mode antenna equivalent circuit.

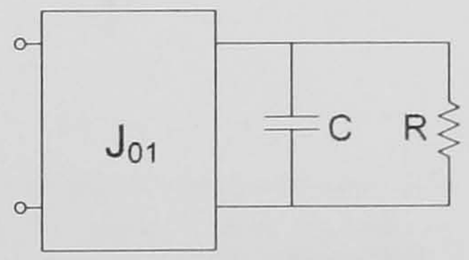

Fig. 3 Single mode antenna Lowpass equivalent circuit, where R = C = 1.

II. PREVIOUS WORK

In previous work, it was proved that the antenna's return loss bandwidth can be significantly improved by exploiting the fact that circular microstrip patch antenna can support two orthogonal polarisation modes [5, 6], where the input couples

into one mode, which is then coupled into a second mode via a discontinuity in the structure [7]. The equivalent circuit for the dual mode antenna is the second order ladder network shown in figure 4, and the simulated results are shown in figure 5 [7].

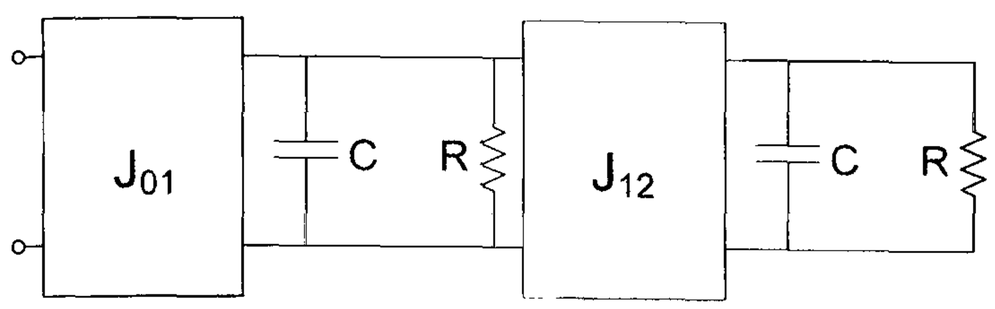

Fig. 4 Equivalent Lowpass circuit of Dual-Mode Antenna.

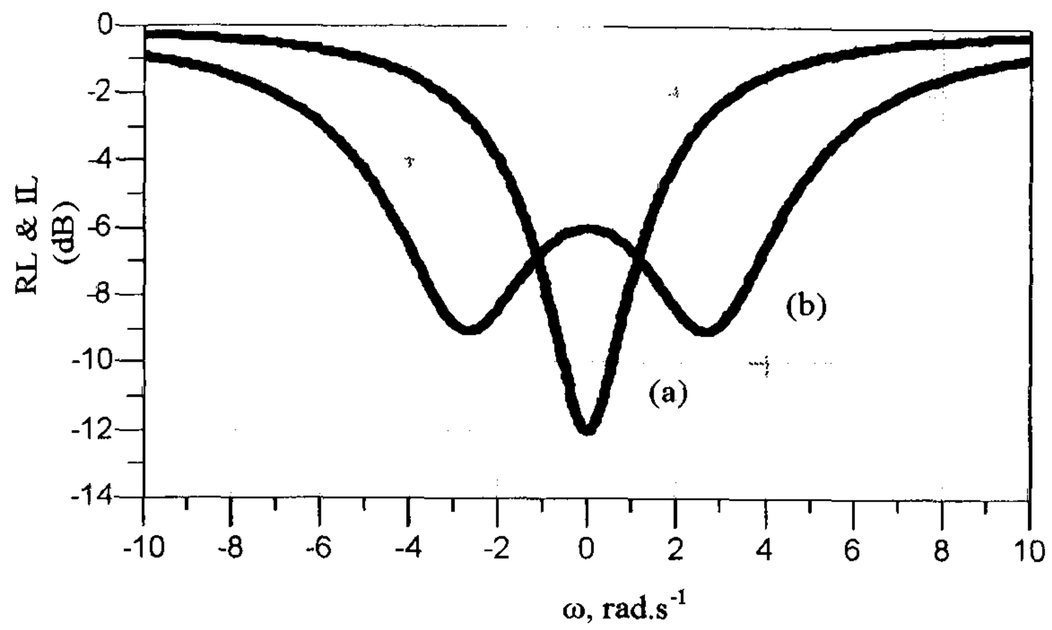

Fig. 5 (a) Optimised single mode and (b) Dual-mode antenna showing wider bandwidth.

Furthermore, using techniques based on filter theory, the circuit shown in figure 4 can be transformed into the one in figure 6, and therefore operated as a dual-band antenna, the theory will be descried in future publication [8]. The circuit transformation results in invariant frequency reactance at each mode, one negative and the other positive. These detune the two resonant modes of the antenna one up and one down in frequency, and hence the input can be matched at two distinct frequencies S_{12A} and S_{12B} as shown in figure 7.

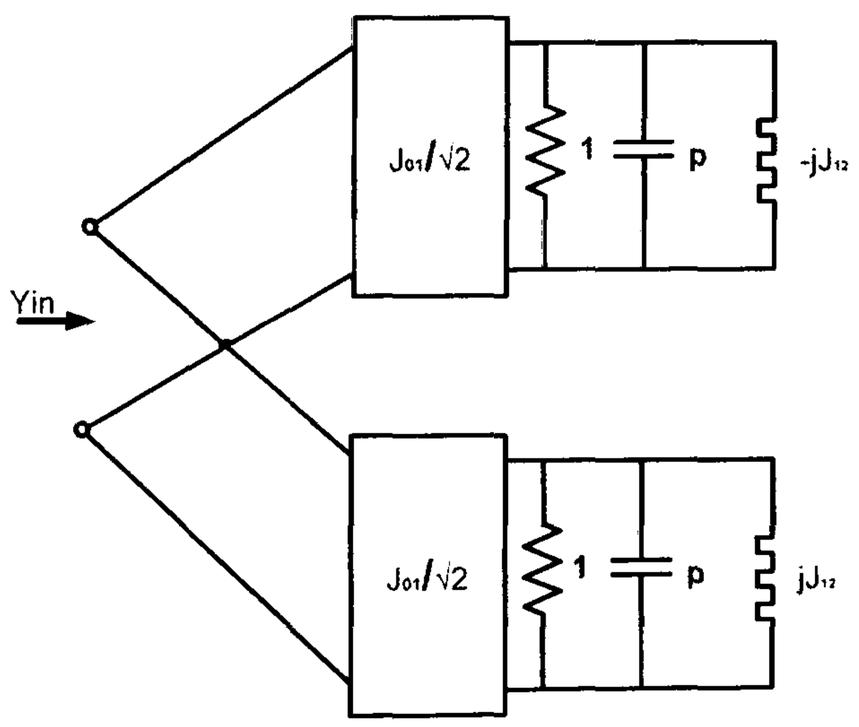

Fig. 6 The equivalent circuit of the Dual-mode antenna after circuit rotation resulting in a dual-band antenna.

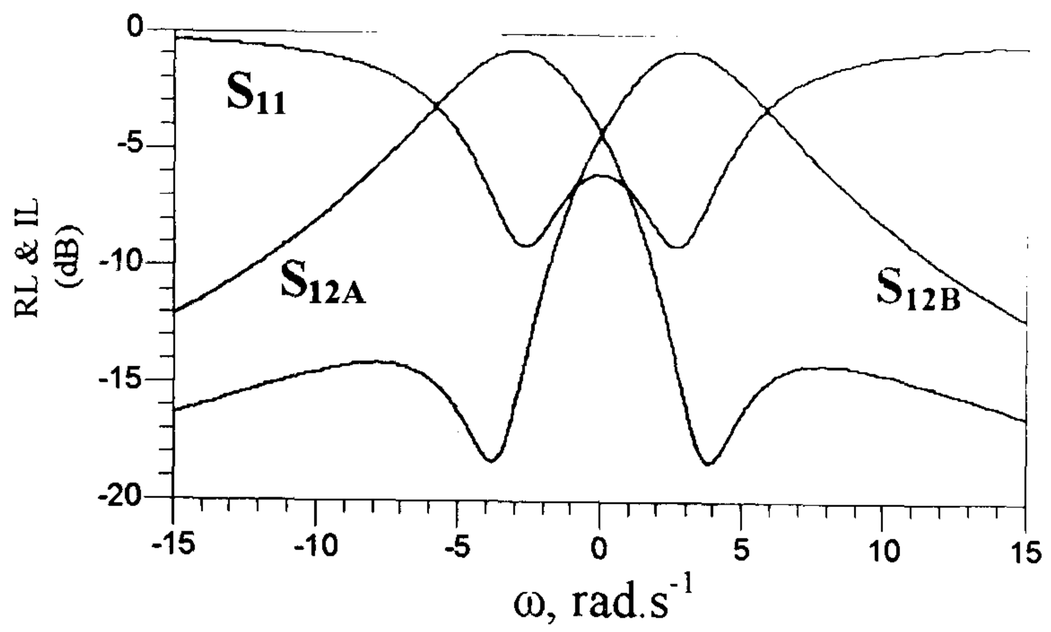

Fig.7 Dual-band antenna equivalent circuit simulation results, showing the polarization into the two modes (A&B) at two different frequencies.

Microstrip patch antennas have relatively narrow bandwidth due to the quick change of the input impedance with respect to frequency and the high quality factor [9]. Derneryd has shown that the antenna can be excited at two different frequencies off resonance, using a two-section impedance transformer as shown in figure 8 and 9 [9]:

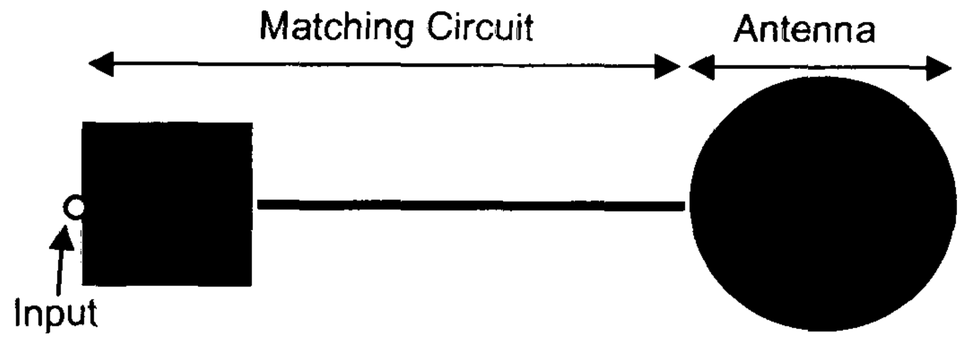

Fig. 8 Circular Microstrip patch antenna with a mtching circuit.

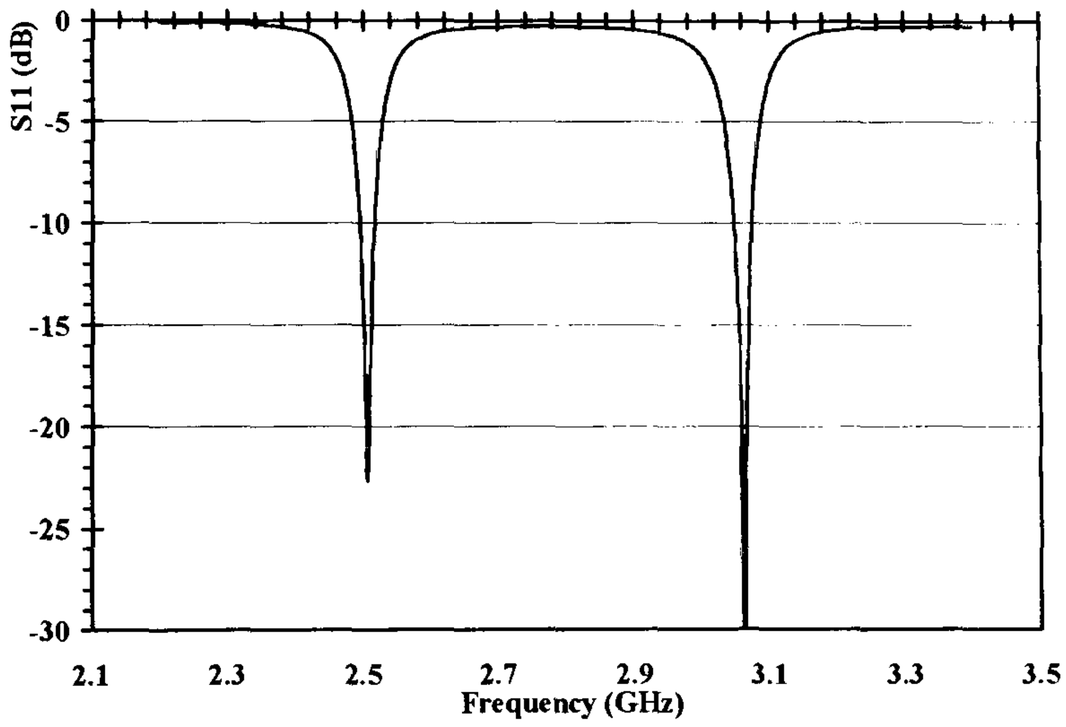

Fig. 9. Circular Microstrip patch antenna response matched at two frequencies using matching network.

The dimensions of the matching network can be computed, however, it essentially consists of an open circuited stub (capacitive) and a transmission line (inductive), together allowing the antenna to radiate at frequencies off resonance.

III. MULTI-BAND PATCH ANTENNA TRANSECEIVER

The dual mode property of patch antennas and the dual band matching technique presented earlier can now be both integrated to a single design. If two inputs are connected to two matching circuits and then coupled to both resonant modes of the antenna, which are detuned by frequency invariant reactances, one up and one down in frequency, then by theory, each input can be matched at two distinct frequencies different from those matched at the other port, as shown in figure 10.

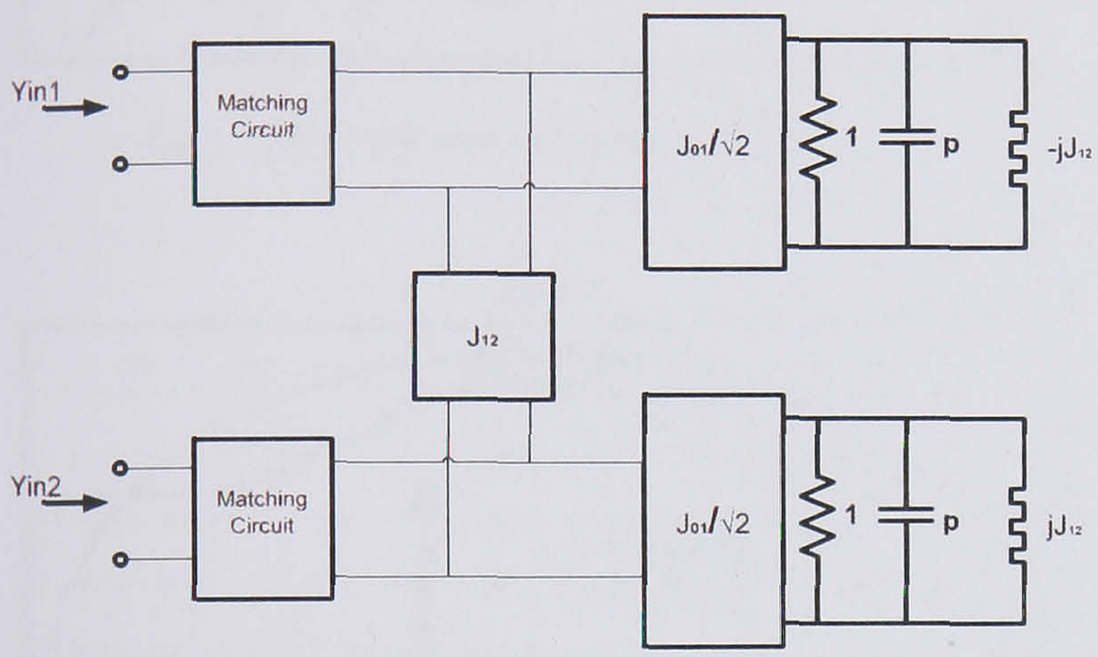

Fig. 10. The equivalent circuit of the multimode patch antenna transceiver.

In principle, if two matching circuits, 90° apart, are employed to feed the antenna and a notch was introduced at one mode and the metal was extended at the orthogonal mode, hence the circuit in figure 10 can be realised in practice as shown in figure 11

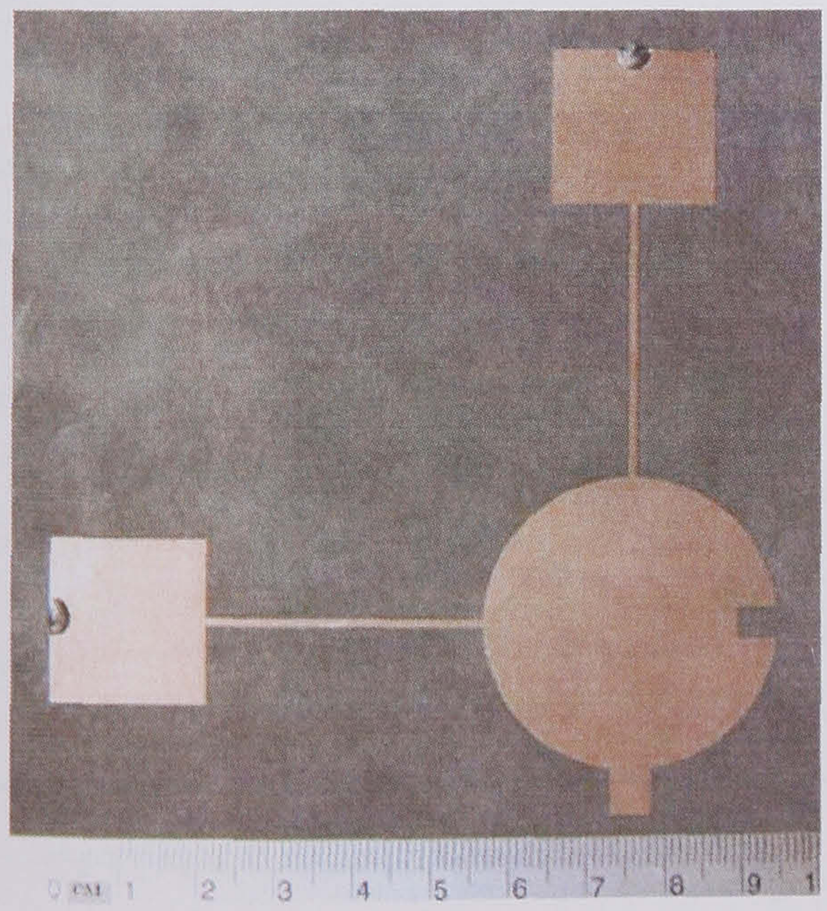

Fig. 11. Multimode patch antenna comprising matching circuits.

The radius of the antenna can be found using equation (1) [2]:

$$f_r = \frac{1.841.c}{2\pi a(\varepsilon_r)^{1/2}} \quad (1)$$

Where c is the speed of light, a is the radius, fr is the resonant frequency and εr is the permittivity of the substrate. The antenna was designed using duriod 5880, where ε_r is approximately 2.2, the radius of the antenna is 1.897cm and the central resonant frequency is around 2.8GHz. A matching circuit was then designed that allowed the antenna to resonate at frequencies off resonance. Two identical matching circuits consisting of a short circuit stub (21.5x20.5mm) and a transmission line (35.5x1mm) were integrated 90° apart to the antenna, and then a notch was introduced at one mode (5x4mm) and the metal was extended (5.4x6.13mm) on the orthogonal mode. The antenna was fabricated and the results are shown in figure 12.

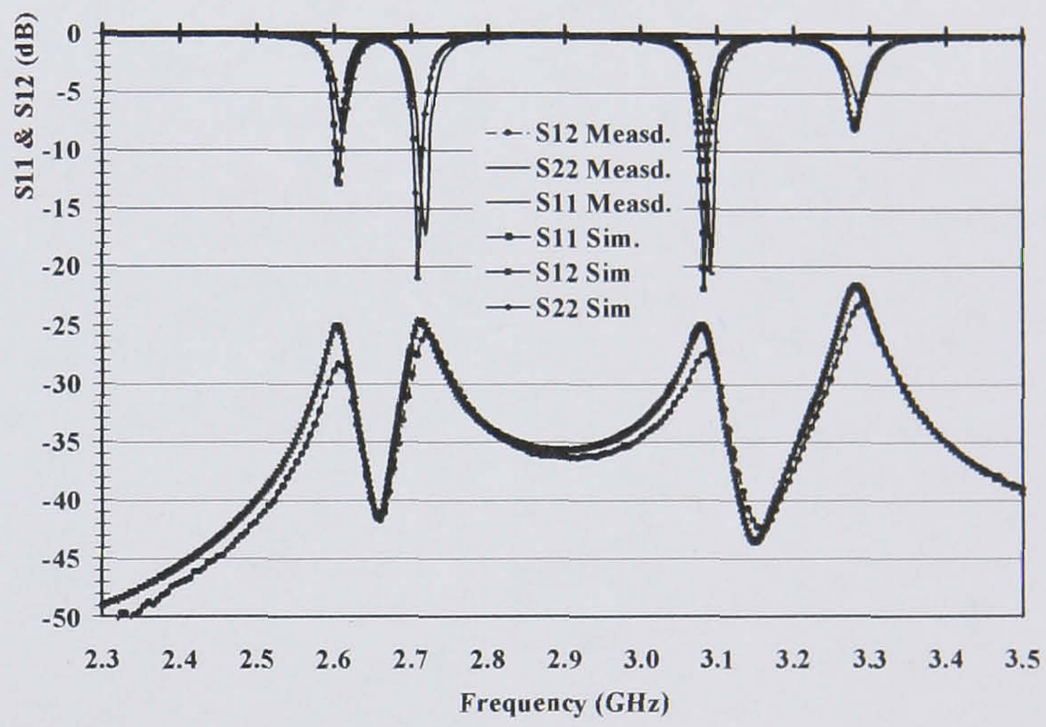

Fig. 12. Simulation and measured results of the multimode antenna.

The simulation and measured results in figure 12 shows that the antenna is now matched at 4 distinct frequencies and fed by two ports. A crucial point here is the isolation between the ports, which is shown to be over 22dB. Hence, a self diplexing multimode antenna transceiver shown in figure 11 is developed. The separation between the resonant modes highly depends on the notch and the extended metal at each mode, the bigger they are the more separation achieved, however, as the resonant frequencies moves away from the central resonance, the matching into the network becomes weaker and therefore parts of the signal starts to be reflected. Figures 13-16 shows the radiation pattern of the antenna at the four frequencies.

Fig. 13. Far E-Field pattern of the antenna at 2.6GHz.

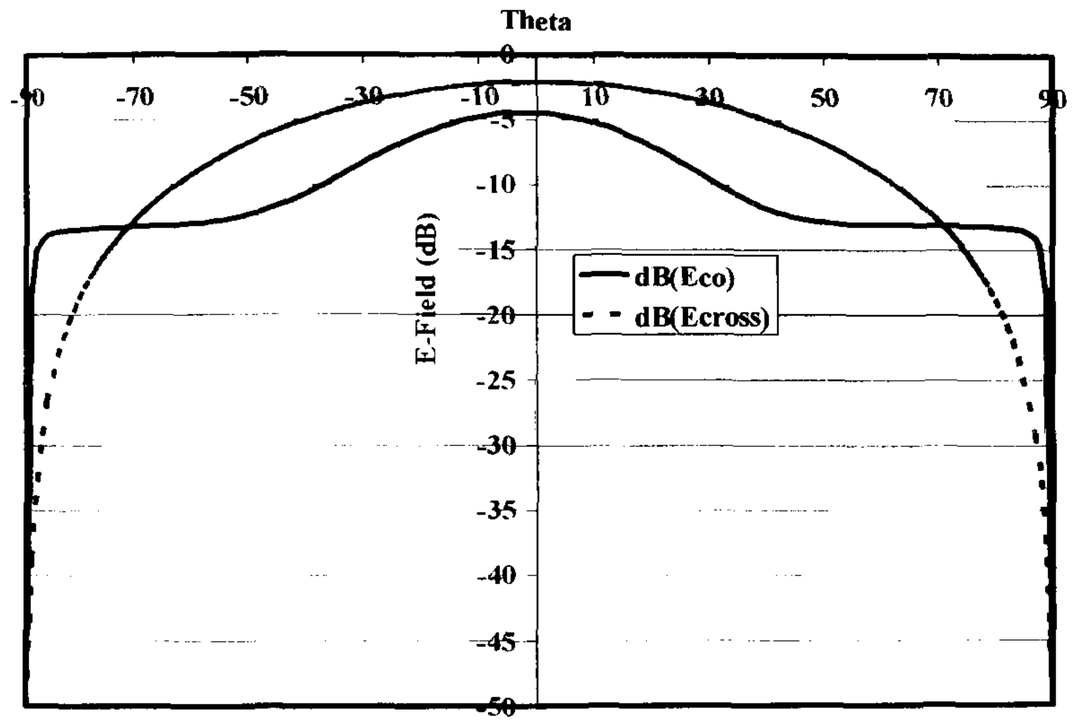

Fig. 14. Far E-Field pattern of the antenna at 2.75GHz.

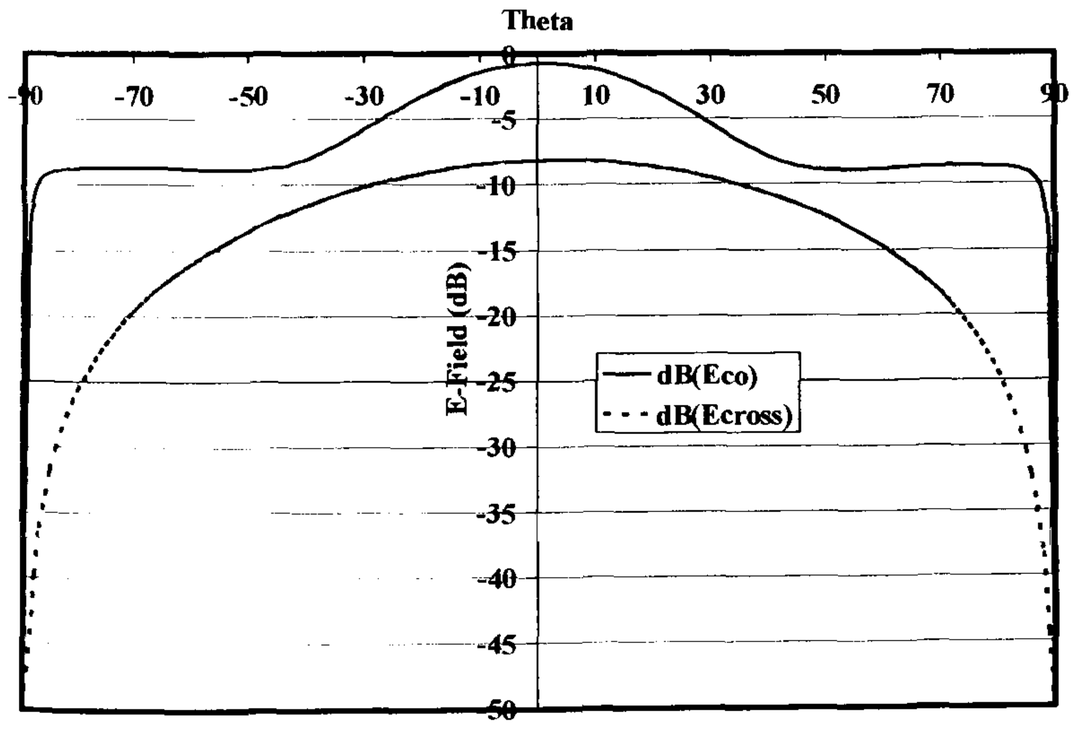

Fig. 15. Far E-Field pattern of the antenna at 3.1GHz.

Fig. 16. Far E-Field pattern of the antenna at 3.27GHz.

IV. CONCLUSIONS

Several wireless applications require separate bands for transmitting and receiving, as well as multi-band transmission. A quad-band circular microstrip patch antenna was presented, exploiting the fact that circular patch antennas can support two orthogonal resonant modes, alongside simple matching techniques to separate the modes has allowed the antenna to be matched at four distinct frequencies. Hence the antenna can operate as a transceiver multimode patch antenna, where the isolation between the ports was found to be over 22dB, without the need for complicated multi-layer design or complicated feeding techniques. This technique can be adopted and further developed for applications such as GPS navigation and GSM communication systems where multi-band operation is required.

REFERENCES

[1] R. Garg, *Microstrip antenna design handbook*: Artech House, 2001.

[2] C. A. Balanis, *Antenna theory: analysis and design*, 2nd ed: Wiley, 1997.

[3] I. Hunter, *Theory and Design of Microwave Filters*. London: IEE, 2001.

[4] H. C. Bell, "The Coupling Matrix in Low-Pass Prototype Filters," in *Microwave Magazine, IEEE*, vol. 8, 2007, pp. 70-76.

[5] K. Chang, *Microwave Ring Circuits and Antennas*: Wiley, 1996.

[6] I. Hunter, "Broad-band matching of antennas using dual-mode radiators," presented at 33rd European Microwave Conference, 2003.

[7] A. I. Abunjaileh, I. C. Hunter, and A. H. Kemp, "Application of dual-mode filter techniques to the broadband matching of microstrip patch antennas," *Microwaves, Antennas & Propagation, IET*, vol. 1, pp. 273, 2007.

[8] A. I. Abunjaileh, I. C. Hunter, and A. H. Kemp, "A Circuit-Theoretic Method of Multi-band Matching for Microstrip Patch Antennas," *Submitted to IEEE Transactions on Microwave Theory and Techniques*, Submitted on May 2007.

[9] A. Derneryd, "Microstrip Disc Antenna Covers Multiple Frequencies," *Microwave Journal*, vol. 21, pp. 77-9, 1978.

A Circuit-theoretic Approach to the Design of Quadruple-Mode Broadband Microstrip Patch Antennas

Alaa I. Abunjaileh, *Student Member IEEE*, Ian C. Hunter, *Fellow IEEE* and Andrew H. Kemp

Abstract— **A novel method for the design of broadband patch antennas is described. The approach taken is to broadside couple two dual-mode patch antennas, resulting in a quad resonance antenna. The equivalent circuit of the antenna is similar to that of microwave filters, thus filter design techniques maybe employed to synthesize the antenna to obtain maximum return loss bandwidth. This is the first time an increase in the bandwidth is achieved on a relatively thin substrate antenna as a result of coupling four resonant modes using two stacked circular microstrip patches. Electromagnetic simulation and measured results demonstrate bandwidth improvement of over 4 times that of a single mode design.**

Index Terms— **Microstrip Antennas, Microstrip Filters, Multifrequency Antenna, Microwave Filters, Resonators.**

I. Introduction

Circular microstrip patch antennas are widely used in wireless applications for their well known advantages of ease of construction, strong mechanical structure, low profile and low cost. However, the major problem of this type of antenna is their inherent narrow bandwidth [1]. Multilayer microstrip antennas were proposed in the seventies [2-4], where two or three layer stacked microstrip patches provided a considerably wider bandwidth, due to the multi-resonator effect [1, 5, 7, 8]. Since then more research has been carried out, reporting various methods of stacked resonators [5, 6]. Structures such as circular, square and triangular microstrip patch antennas can support two orthogonal resonant modes, or two polarizations [9]. In previous papers by the authors [10, 11] it was shown that it is possible to design a dual-polarized patch antenna as if it was a dual-mode filter, which significantly improves the bandwidth. In this paper, a new stacked two layer antenna is presented, from theory which has been extended to the design of a quadruple-mode antenna (this is described in section II). Electromagnetic simulations and measured results presented in section III show over 4 times bandwidth enhancement of the single mode antenna.

II. Theory and Design Analysis

In the previous dual mode design [10] the input feeds into one mode which is then coupled to the orthogonal mode via a discontinuity (notch) in the structure. This discontinuity is located at an angle of 135° from the feed line.[9, 11, 12]. The theory related to this design can be clearly illustrated in terms of the equivalent circuit shown in figure 1. Here the admittance inverters J_{01} and J_{12} are networks commonly used in filter design, with transfer matrix T given by (1).

$$[T]=\begin{bmatrix} 0 & jJ_{01} \\ j/J_{01} & 0 \end{bmatrix} \quad (1)$$

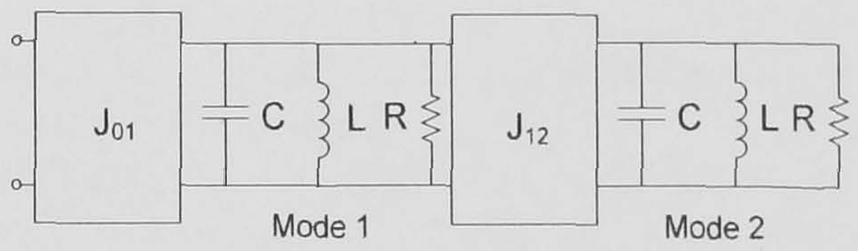

Fig.1. Dual-mode antenna equivalent circuit.

The equivalent circuit resistors represent the radiation resistance of each mode, the capacitors and inductors represent the resonant modes of the antenna. The admittance inverters J_{01} and J_{12} represent the input matching to the antenna and the coupling between the two modes respectively. By correct choice of J_{01} and J_{12} the input return loss bandwidth can be maximized. The theory of the coupling matrix in filter prototypes is further explained in [12, 13].

A. Quadruple-mode Antenna Basic Theory

The dual-mode design approach can be extended by stacking two dual-mode antennas, as shown in figure 2. Here, the arrows represent the 2 orthogonal resonant modes on each layer (1 and 2 on the bottom layer and 3 and 4 on the top layer). The input feeds into mode 1 which is coupled to mode 2 via a discontinuity. Couplings may then exist between all four modes, and therefore, all those couplings must be analyzed.

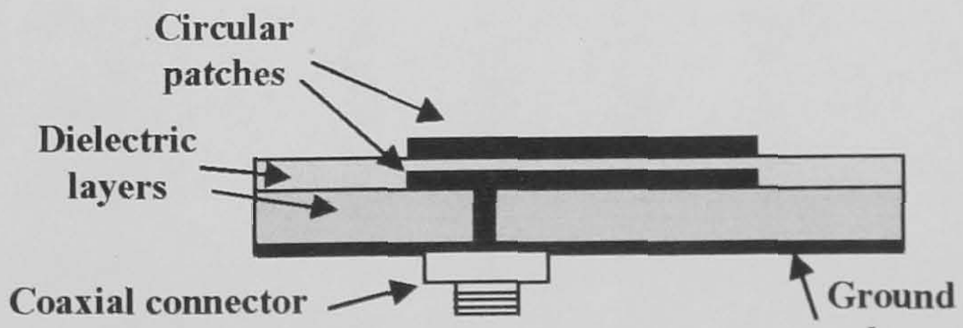

Fig. 2a Quad-mode patch antenna physical design (side view).

Manuscript received June 16th, 2007.

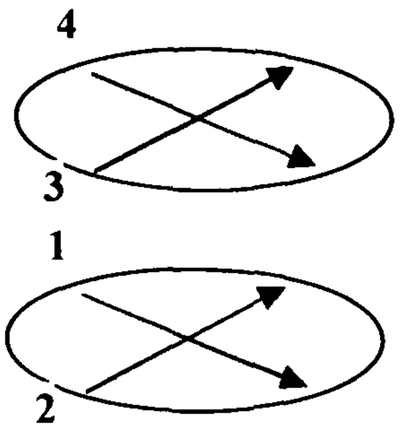

Fig. 2b The four resonant modes in the quadruple mode patch antenna.

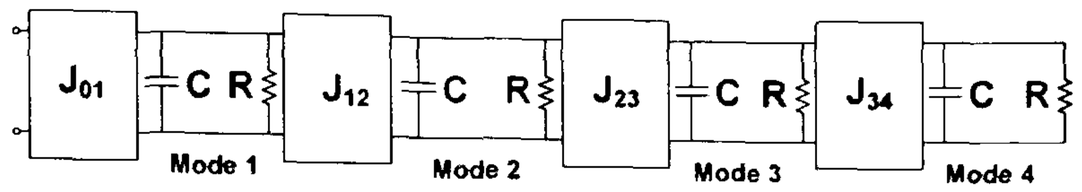

Fig. 5. Forth order lowpass ladder network (N=4 and R = C = 1).

The correct coupling values J_{01}-J_{34} can be determined by designing the network to have a quasi-equiripple return loss characteristics using techniques described in [12, 14]. The return loss function for lowpass equiripple prototype resonator of order "r" is shown in (3) [14].

$$S_{11}(p)=\frac{p^4+p^3(4-J_{01}^2)+p^2(6-3J_{01}^2+J_{12}^2+J_{23}^2+J_{34}^2)+p(4-3J_{01}^2+2J_{12}^2+2J_{23}^2+2J_{34}^2-J_{01}^2J_{34}^2-J_{01}^2J_{23}^2)+(1-J_{01}^2+J_{12}^2+J_{23}^2+J_{34}^2+J_{12}^2J_{34}^2-J_{01}^2J_{34}^2-J_{01}^2J_{23}^2)}{p^4+p^3(4+J_{01}^2)+p^2(6+3J_{01}^2+J_{12}^2+J_{23}^2+J_{34}^2)+p(4+3J_{01}^2+2J_{12}^2+2J_{23}^2+2J_{34}^2-J_{01}^2J_{34}^2-J_{01}^2J_{23}^2)+(1+J_{01}^2+J_{12}^2+J_{23}^2+J_{34}^2+J_{12}^2J_{34}^2+J_{01}^2J_{34}^2+J_{01}^2J_{23}^2)} \quad (2)$$

The generalized equivalent circuit of the antenna is shown in figure 3, denormalized to lowpass prototype form.

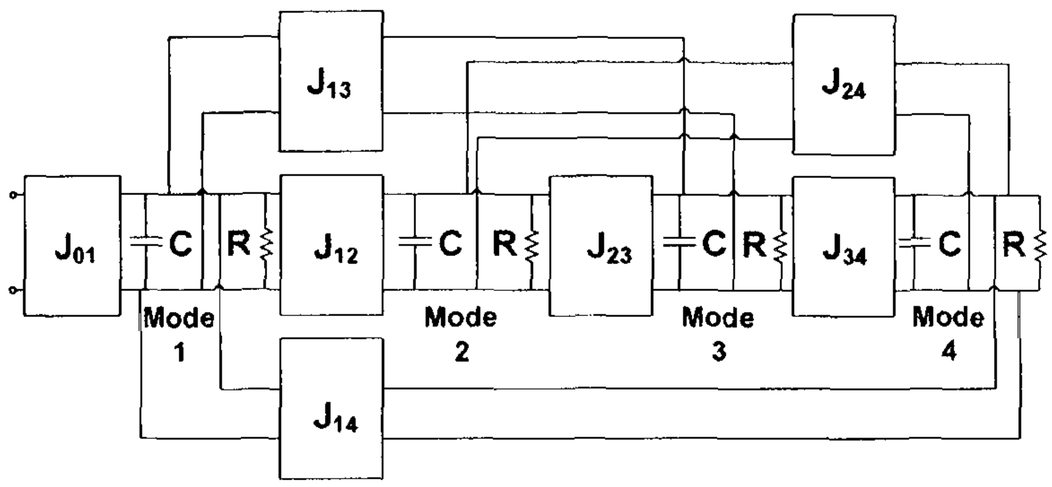

Fig. 3. Quad-mode circular microstrip patch antenna lowpass prototype considering all the possible electromagnetic couplings between the 4 modes in the physical model.

In reality, electromagnetic couplings between the patches should only occur between modes 1-4 and 2-3. The couplings between modes 1-3 and 2-4 can be assumed zero at this stage. Considering these assumptions, the circuit in figure 3 reduces to the one in figure 4;

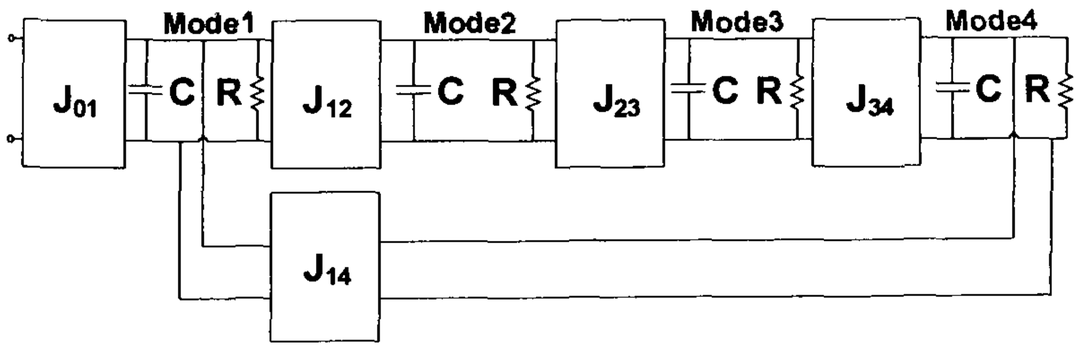

Fig. 4. Quad-mode circular microstrip patch antenna lowpass prototype.

In section B, it is shown how the prototype networks in figures 3 and 4 above can be derived analytically, reaching an equivalent circuit for the antenna with the correct coupling values.

B Mathematical Transformations

Figure 5 shows a fourth order lowpass ladder network, where all the capacitances and resistances are normalized to unity. The expression for the reflection coefficient $S_{11}(p)$ of this network can be derived using circuit analysis techniques in [12], this is shown in equation (2).

$$S_{11(p)}=\prod_{r=1}^{n}\frac{p-j\omega_r}{p-j\omega_r+2/Q} \quad \text{where } Q=\omega CR \quad (3)$$

For the quadruple-mode antenna being considered here, "n" is equal to 4, Q is equal to 1 (assuming R=C=1) and using optimization techniques, the ω_r value for r = 1→n can be found to achieve an equiripple response. Therefore, with a 6 dB return loss ripple level (which is typical for handset antennas), the expression of the reflection coefficient $S_{11}(p)$ is given by:

$$S_{11}(p)=\frac{p^4+46.4425p^2+201.3561}{p^4+8p^3+70.4425p^2+217.77p+403.1261} \quad (4)$$

(with $\omega_1=\pm 2.2\ s^{-1}$ and $\omega_2=\pm 6.25\ s^{-1}$)

By equating the coefficients of equations (2) and (4), the coupling values (J_{01}-J_{34}) can be obtained, these are:

$$J_{01}=2,\ J_{12}=5.296,\ J_{23}=3.898 \text{ and } J_{34}=2.976 \quad (5)$$

The network in figure 5 is simulated using these values and the response is shown in figure 6. The couplings values in (5) shows a 6 dB bandwidth increase compared to a single mode design of 5.7 times.

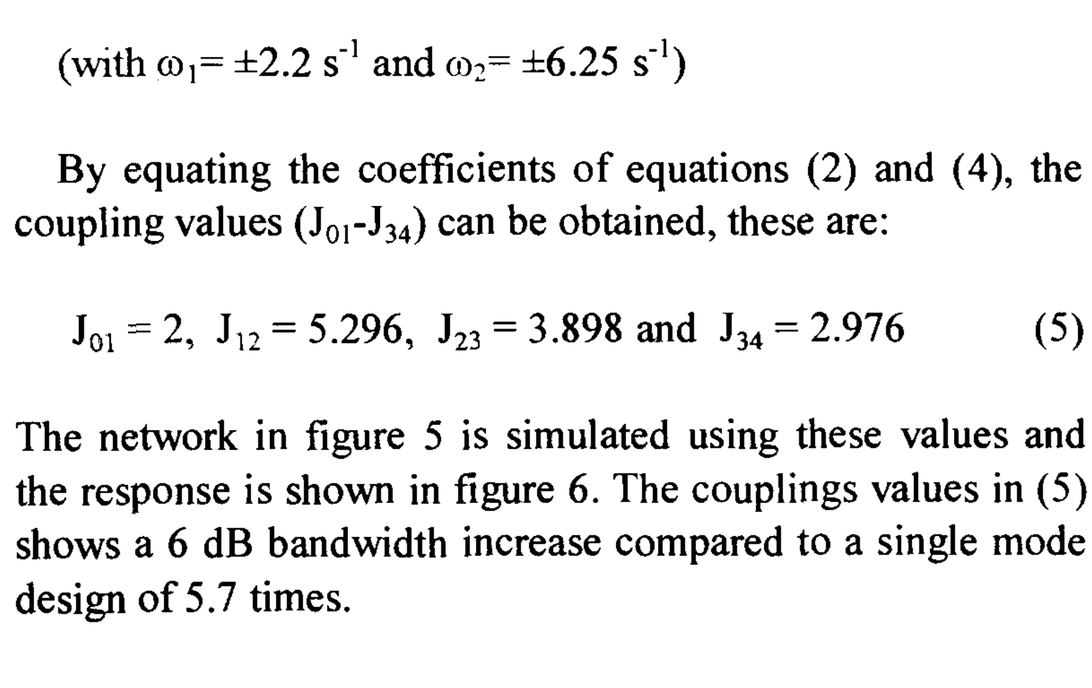

Fig. 6. Simulation results of the equivalent lowpass circuit prototype of (a) single mode antenna and (b) quad-mode antenna.

However, the actual equivalent circuit of the practical antenna includes non-adjacent couplings between modes, as shown in figure 3.
The admittance matrix of the lowpass prototype in figure 5 is:

$$[y]=\begin{bmatrix} 0 & jJ_{01} & 0 & 0 & 0 \\ jJ_{01} & 1+p & jJ_{12} & 0 & 0 \\ 0 & jJ_{12} & 1+p & jJ_{23} & 0 \\ 0 & 0 & jJ_{23} & 1+p & jJ_{34} \\ 0 & 0 & 0 & jJ_{34} & 1+p \end{bmatrix} \quad (6)$$

Or,

$$[y]=\begin{bmatrix} 0 & 0 & 0 & 0 & 0 \\ 0 & 1+p & 0 & 0 & 0 \\ 0 & 0 & 1+p & 0 & 0 \\ 0 & 0 & 0 & 1+p & 0 \\ 0 & 0 & 0 & 0 & 1+p \end{bmatrix}+\begin{bmatrix} 0 & jJ_{01} & 0 & 0 & 0 \\ jJ_{01} & 0 & jJ_{12} & 0 & 0 \\ 0 & jJ_{12} & 0 & jJ_{23} & 0 \\ 0 & 0 & jJ_{23} & 0 & jJ_{34} \\ 0 & 0 & 0 & jJ_{34} & 0 \end{bmatrix} \quad (7)$$

Where the second part of (7) is known as the coupling matrix j[J] [12, 13].

This coupling matrix may be pre and post multiplied by rotational matrices without altering the input reflection coefficient response, provided that these matrices do not operate on the first row and column. This process is known as matrix rotation [12]. If 2-4 and 2-3 rotations are applied to the coupling matrix [J], the result is shown in equations (8)-(11);

$$[J_{2x4}]\rightarrow[\mathrm{T}_{24}]^{-1}\begin{bmatrix} 0 & J_{01} & 0 & 0 & 0 \\ J_{01} & 0 & J_{12} & 0 & 0 \\ 0 & J_{12} & 0 & J_{23} & 0 \\ 0 & 0 & J_{23} & 0 & J_{34} \\ 0 & 0 & 0 & J_{34} & 0 \end{bmatrix}[\mathrm{T}_{24}] \quad (8)$$

$$[J]\rightarrow[\mathrm{T}_{23}]^{-1}[J_{2x4}][\mathrm{T}_{23}] \quad (9)$$

where

$$[\mathrm{T}_{24}]=\begin{bmatrix} 0 & 0 & 0 & 0 & 0 \\ 0 & 0 & 0 & 0 & 0 \\ 0 & 0 & C_{2x4} & 0 & S_{2x4} \\ 0 & 0 & 0 & 0 & 0 \\ 0 & 0 & -S_{2x4} & 0 & C_{2x4} \end{bmatrix} \text{ and } [\mathrm{T}_{23}]=\begin{bmatrix} 0 & 0 & 0 & 0 & 0 \\ 0 & 0 & 0 & 0 & 0 \\ 0 & 0 & C_{2x3} & S_{2x3} & 0 \\ 0 & 0 & -S_{2x3} & C_{2x3} & 0 \\ 0 & 0 & 0 & 0 & 0 \end{bmatrix}$$

and the final result is;

$$[J]\rightarrow\begin{bmatrix} 0 & J_{01} & 0 & 0 & 0 \\ J_{01} & 0 & C_{2x3}.C_{2x4}J_{12} & S_{2x3}.C_{2x4}J_{12} & S_{2x4}J_{12} \\ 0 & C_{2x3}.C_{2x4}J_{12} & -2S_{2x3}.C_{2x3}(C_{2x4}J_{23}-S_{2x4}J_{34}) & -S_{2x3}^2.(C_{2x4}J_{23}-S_{2x4}J_{34})+C_{2x3}^2.(C_{2x4}J_{23}-S_{2x4}J_{34}) & -S_{2x3}.(S_{2x4}J_{23}+C_{2x4}J_{34}) \\ 0 & S_{2x3}.C_{2x4}J_{12} & -S_{2x3}^2.(C_{2x4}J_{23}-S_{2x4}J_{34})+C_{2x3}^2.(C_{2x4}J_{23}-S_{2x4}J_{34}) & 2S_{2x3}.C_{2x3}.(C_{2x4}J_{23}-S_{2x4}J_{34}) & C_{2x3}.(S_{2x4}J_{23}-C_{2x4}J_{34}) \\ 0 & S_{2x4}J_{12} & -S_{2x3}.(S_{2x4}J_{23}+C_{2x4}J_{34}) & C_{2x3}.(S_{2x4}J_{23}-C_{2x4}J_{34}) & 0 \end{bmatrix} \quad (10)$$

Where
$$C_{2x4}=\cos(\theta_{2x4}) \text{ and } S_{2x4}=\sin(\theta_{2x4})$$
$$C_{2x3}=\cos(\theta_{2x3}) \text{ and } S_{2x3}=\sin(\theta_{2x3}) \quad (11)$$

This result takes into account all the possible electromagnetic couplings in the physical structure in figure 2. The coupling between modes 1-3, 1-4, 2-3 and 2-4 are now nonzero, this matrix describes the circuit in figure 3.

It can be assumed that the coupling between modes 2-3 and 1-4 are equal, as are the cross couplings between modes 2-4 and 1-3. Hence, θ_{23} and θ_{24} can be found by equating the values for the coupling between modes 2-3 and 1-4, and coupling between modes 1-3 and 2-4 in equation (10). This will force the cross couplings J_{13} and J_{24} to zero and equalize the adjacent couplings J_{14} and J_{23} to reach a circuit similar to the one in figure 4, thus:

$$jS_{2x3}.C_{2x4}J_{12}=-jS_{2x3}.(S_{2x4}J_{23}+C_{2x4}J_{34}) \quad (12)$$

$$jS_{2x4}J_{12}=-jS_{2x3}^2.(C_{2x4}J_{23}-S_{2x4}J_{34})+jC_{2x3}^2.(C_{2x4}J_{23}-S_{2x4}J_{34}) \quad (13)$$

The values of θ_{2x3} and θ_{2x4} that satisfy equations (12)-(13) are:

$$\theta_{2x3}=\pi \text{ and } \theta_{2x4}=0.44029 \quad (14)$$

These values alongside the coupling values found in equation (5) were used to evaluate [J] in equation (10) and the result is shown in equation (15) and depicted in figure 7.

$$[J]\rightarrow\begin{bmatrix} 0 & 2 & 0 & 0 & 0 \\ 2 & 0 & -4.793 & 0 & 2.26 \\ 0 & -4.793 & 0 & 2.26 & 0 \\ 0 & 0 & 2.26 & 0 & -4.354 \\ 0 & 2.26 & 0 & -4.354 & 0 \end{bmatrix} \quad (15)$$

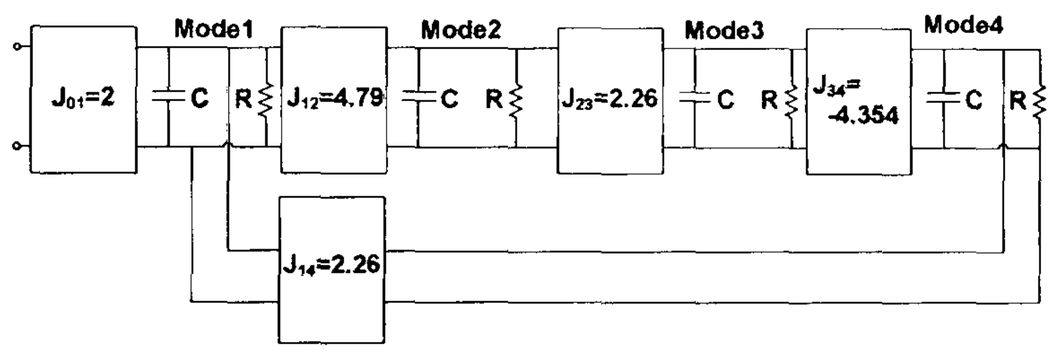

Fig. 7. Quad-mode circular microstrip patch antenna lowpass prototype

Here it can be clearly seen that there will definitely be equal couplings between modes 1-4 and 2-3. The other couplings between modes 1-3 are 2-4 are zero as expected.

I. Electromagnetic Simulations and Measured Results

The resonant frequency of a circular microstrip patch antenna in the dominant TM_{110} mode is given by [15-17]:

$$f_r = \frac{c \cdot \chi'_{mn}}{2\pi a(\varepsilon_r)^{1/2}} \qquad (16)$$

Where f_r is the resonant frequency, χ'_{mn} are the zeros of the Bessel function of order "n", and equal to 1.8412 for the dominant TM_{110} mode and "a" is the radius of the circular patch. The radius of circular microstrip patch antenna fabricated on Duriod 5880, ε_r =2.2, thickness is 787 mm and operating at 2GHz is approximately 30 mm. In designing a quadruple-mode antenna, the most logical procedure is to start with the bottom patch and obtain the correct coupling between the first two modes. For instance if the circuit in figure 7 is simulated with couplings J_{12}, J_{23}, J_{34} and J_{14} are all reduced to zero, this would leave us with the bottom patch only, and hence, the simulated return loss at the centre frequency is -4.4 dB. This result enables us to locate the position of the feed point across the radius of the patch [1], at 17 mm from the center point.

The second step is to introduce the coupling between the first two modes on the bottom patch, i.e. J_{12}. If the circuit in figure 7 is simulated with all couplings reduced to zero apart from J_{01} and J_{12}, the result indicates the return loss bandwidth of modes 1-2 only. The coupling level between them is found to be approximately 3 dB. A notch 6.17x5 mm placed at 135° from the feed line is introduced at the bottom patch, and with the aid of computer simulations, it can be designed to achieve a coupling of 3 dB between modes 1-2 in the same manner as [10].

At this stage, the bottom patch is now designed. The top patch may now be introduced and the dimensions of the second notch may be evaluated. Three tuning parameters were found useful to achieve the overall maximum 6 dB return loss bandwidth, these are the thickness of the substrate between the two patches which controls the coupling strength between the two layers, a notch at one mode and a metal extension on the other mode controlling the couplings J_{23} and J_{14} respectively. By tuning the circuit using computer simulation, a 5.55x5 mm notch is placed at 135° from the feed line on the upper patch and a metal extension of 3.87x5 mm placed at 225° from the feed line on the top patch, where the top substrate thickness is 0.381 mm

A quadruple-mode antenna (figures 8-9) has been designed, with total thickness 1.168 mm. Simulated and measured results in figures 10 shows a bandwidth increase of over 4.2 times compared to a single mode.

The far field radiation pattern plot is shown in figure 11. This is similar to single mode patch antenna.

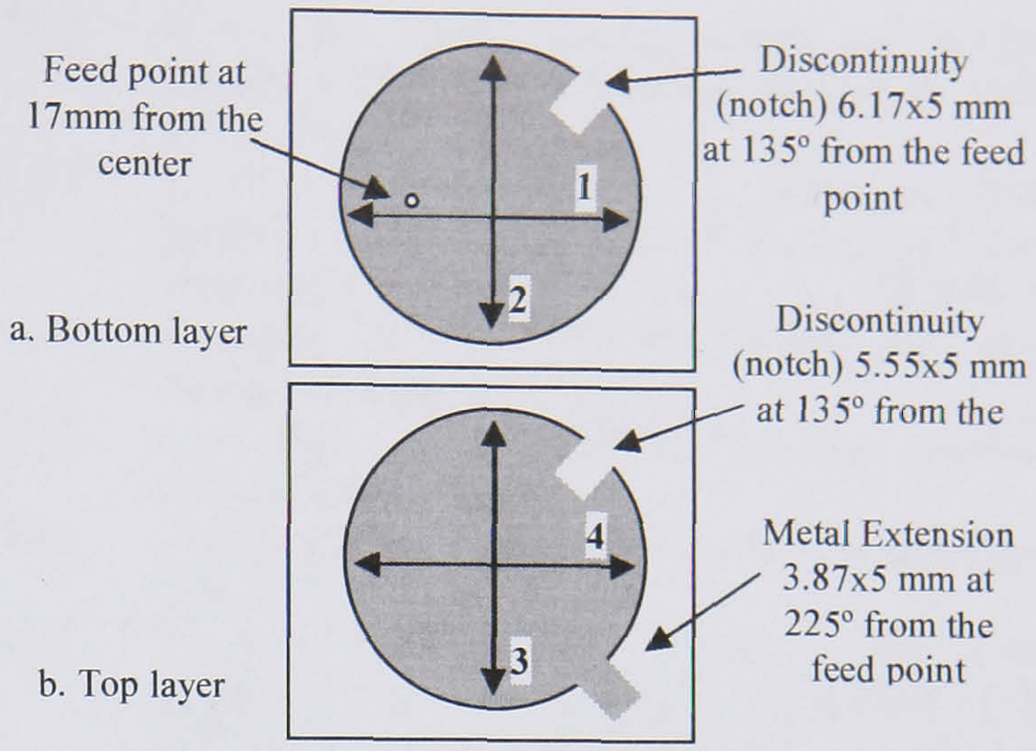

Fig. 8 The physical dimensions of the antenna.

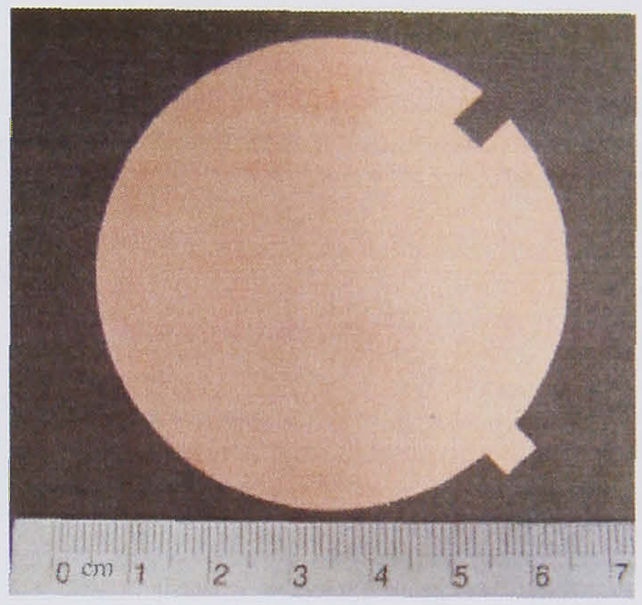

Fig. 9. Quade-mode patch antenna prototype (Top view).

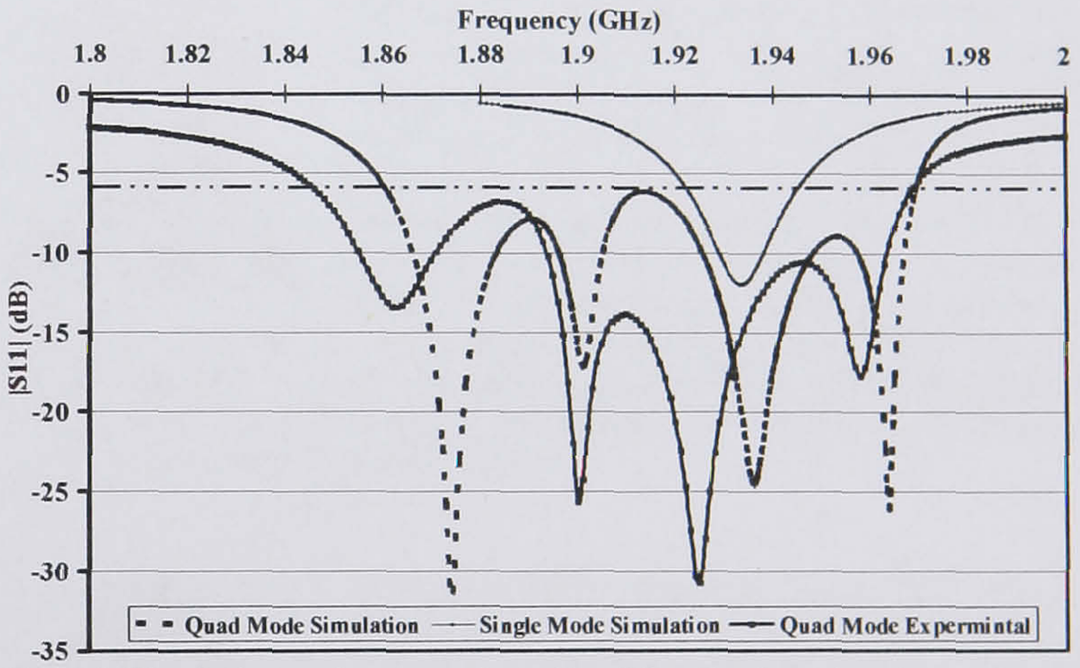

Fig. 10. Simulation and measured results of the Quad-mode antenna design showing 4.2 times wider 6 dB return loss bandwidth compared to single mode.

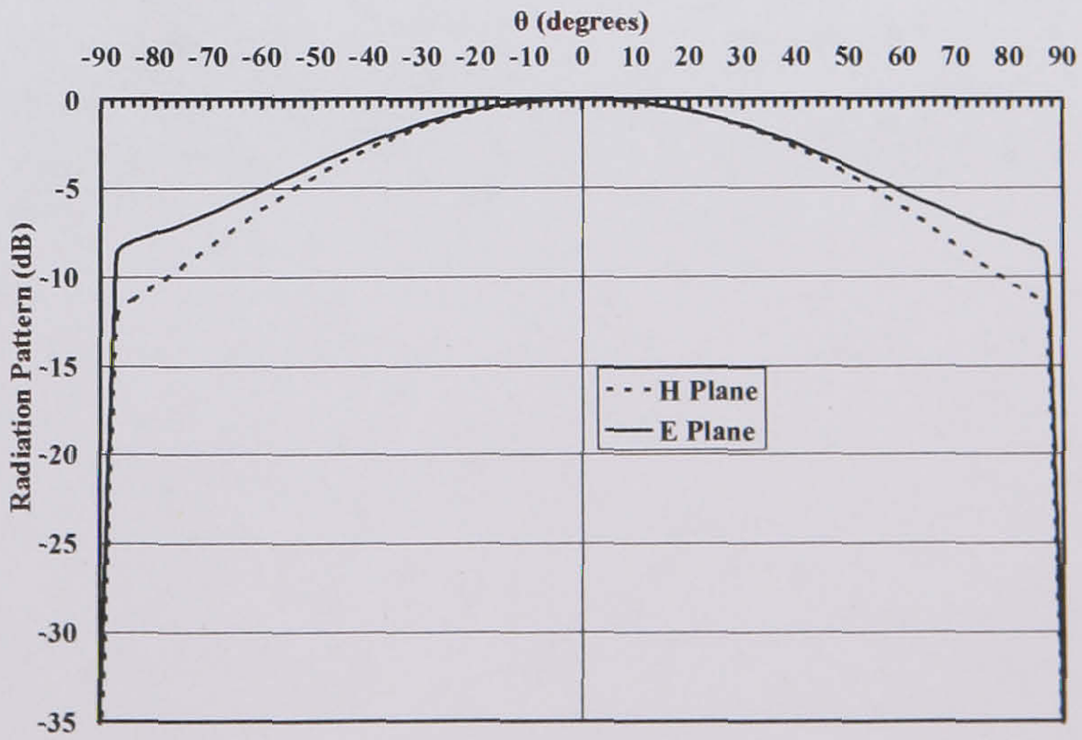

Fig. 11. Far field radiation pattern of the antenna.

II. Conclusion

Microstrip patch antennas enjoy many advantages and qualities; however, one major issue is the inherent narrow bandwidth. This paper presents a new approach for the synthesis of dual layer, quadruple-mode circular microstrip patch antenna. Using matrix rotation techniques normally employed in filter design, the equivalent circuit and coupling values were found. These were then applied to the antenna synthesis, resulting in increasing the return loss bandwidth by 4.2 times compared to a single mode design. Circuit and electromagnetic simulations show excellent results, which agree well with the measured results. This is the first time that such an approach of designing antennas as multi-mode filters has been demonstrated.

Acknowledgment

The authors wish to acknowledge Dr. Andy Guyette of Naval Research Lab, Washington DC, for his helpful comments.

References

[1] R. Garg, *Microstrip Antenna Design Handbook* Artech House, 2001.

[2] G. Sanford, "Multiple Resonance Radio Frequency Microstrip Antenna Structure," vol. 4070676, U. S. Patent, Ed. USA: Ball Corporation, Muncie, Ind., 1978.

[3] S. A. Long and M. D. Walton, "A Dual-Frequency Stacked Circular-Disc Antenna," *IEEE Transactions on Antennas And Propagation*, vol. AP-27, , pp. 270-273, 1979.

[4] P. S. Hall et al, *Wide Bandwidth Microstrip Antennas for Circuit Integration*, vol. 15: Electronic Letters, 1979.

[5] G. Kumar and K. P. Ray, *Broadband Microstrip Antennas*: Artech House London, 2003.

[6] S. Maci and G. B. Gentili, "Dual-frequency patch antennas," *Antennas and Propagation Magazine, IEEE*, vol. 39, pp. 13-20, 1997.

[7] K. Lee and W. Chen, *Advances in Microstrip and Printed Antennas*: John Whiley & Sons, Inc, 1997.

[8] D. M. Pozar and D. Schaubert, *Microstrip Antennas*. New Jersey: John Wiley & Sons, Inc, 1995.

[9] K. Chang, *Microwave Ring Circuits and Antennas*: Wiley, 1996.

[10] A. I. Abunjaileh, I. C. Hunter, and A. H. Kemp, "Application of dual-mode filter techniques to the broadband matching of microstrip patch antennas," *Microwaves, Antennas & Propagation, IET*, vol. 1, pp. 273, 2007.

[11] I. Hunter, "Broad-band matching of antennas using dual-mode radiators," presented at 33rd European Microwave Conference, 2003.

[12] I. Hunter, *Theory and Design of Microwave Filters*. London: IEE, 2001.

[13] H. C. Bell, "The Coupling Matrix in Low-Pass Prototype Filters," in *Microwave Magazine, IEEE*, vol. 8, 2007, pp. 70-76.

[14] J. D. Rhodes, "Microwave Reflection Filter Including A Ladder Network Of Resonators Having Progressively Smaller Q Values," vol. 5781084, U. S. Patent, Ed. USA: Filtronic Comtek PLC, West Yorkshire England, 1998, pp. 12.

[15] I. J. Bahl and P. Bhartia, *Microstrip antennas*: Artech House 1980.

[16] C. A. Balanis, *Antenna theory : analysis and design*, 2nd ed: Wiley, 1997.

[17] N. Kumprasert and W. Kiranon, "Simple and accurate formula for the resonant frequency of the circular microstrip disk antenna," *Antennas and Propagation, IEEE Transactions*, vol. 43, pp. 1331, 1995.

Alaa I. Abunjaileh was born in Amman, Jordan. He received BEng(Hons,1st) degree at the age of 19 in 2004 in electronic and communications engineering from the University of Leeds, UK, where is now a PhD student, and was also appointed as a research and teaching assistant. During his undergraduate studies he spent almost a year in industry as an Electronic and Communications Engineer within firms in the UK at Siddal and Hilton and overseas at SITA International. He has also worked as a research assistant in joint projects between the University of Leeds, Rio Tinto, DTI UK, TDK & Wansfell Design Ltd.

Ian C. Hunter graduated from Leeds University, with BSc Hons 1st Class, 1978 and PhD, 1981. His early employment was at Aercom and KW Engineering, California, and Filtronic, UK, developing broadband microwave filters for EW. applications. From 1995-2001 he was at Filtronic Comtek, working on advanced filters for cellular radio. He is a Professor at the University of Leeds, School of Electronic and Electrical Engineering, teaching Circuit Theory, Electromagnetism and Microwave Engineering. His research includes linear and non-linear microwave filters. He is the author of "Theory and Design of Microwave Filters", 2001. He also investigates applications of microwaves in Biology.

Andrew H. Kemp gained his BSc in Electronics at the University of York, U.K. in 1984 and after a period in industry his PhD in 1991from the University of Hull, U.K . Since 1998 he has been at the University of Leeds where he is now a Senior Lecturer and his research interests include statistical characterization of multipath propagation environments, WSN with localization and investigating Internet quality of service issues. Dr Kemp is a member of the IEE and a fellow of the Higher Education Academy of the UK.

A Circuit-Theoretic Method of Multi-band Matching for Microstrip Patch Antennas

Alaa I. Abunjaileh, *(Student Member IEEE)*, een1aian@leeds.ac.uk, School of Electronic and Electrical Engineering, The University of Leeds, West Yorkshire, LS2 9JT.

Ian C. Hunter, *(Fellow IEEE)*, i.c.hunter@leeds.ac.uk, School of Electronic and Electrical Engineering, The University of Leeds, West Yorkshire, LS2 9JT.

Andrew H. Kemp, a.h.kemp@leeds.ac.uk, School of Electronic and Electrical Engineering, The University of Leeds, West Yorkshire, LS2 9JT.

Abstract—**This paper presents a new method of multi-band matching for circular microstrip patch antennas. The input impedance of a patch antenna can be represented as a second order ladder network of coupled resonators where each resonator is coupled to a load resistor. Analysis based on circuit theory shows that the antenna can be used as a dual-band antenna, exploiting the fact that circular microstrip patch antennas can support two orthogonal resonant modes. This is confirmed with an experimental dual-band circular microstrip patch antenna. The antenna is then further developed providing designs for a self diplexing patch antenna transceiver.**

Index Terms— Microstrip Antennas, Microwave Antennas, Microstrip Filters.

I. INTRODUCTION

Microstrip antennas are widely used in modern microwave systems, supporting the trend towards utilisation of internal antennas in wireless devices. During the last decade, there has been research on frequency agility and multi-band matching for

microstrip antennas, where an increase in length or height of the antenna were expected or use of multilayer design has been adopted [1, 2]. However, space is usually limited, and this may significantly reduce system performance. Small antennas working at low frequencies may have a very restricted bandwidth of operation, sometimes even being required to operate on more than one frequency. In a workshop presented at the IMS2007, it was pointed that the next generation of mobile phones are expected to operate at 9 different bands, and the demand for multiband antennas is likely to continue [3].

Figure 1 shows a circular microstrip patch antenna, fed using a coaxial cable from the ground plane. It is well known that the dominant mode of this antenna is the TM_{110} mode [4, 5], where each of the resonant modes radiate and can each be represented by an equivalent resonant circuit terminated in a resistor [6].

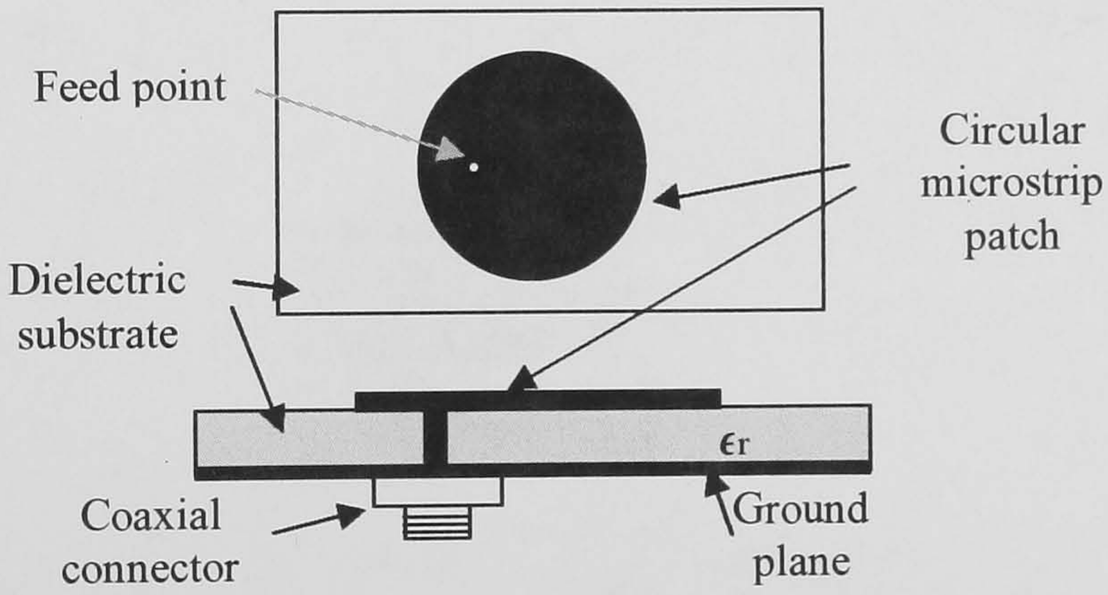

Fig. 1 Circular patch microstrip antenna.

In terms of circuit theory, the equivalent circuit of a single mode antenna is shown in figure 2.

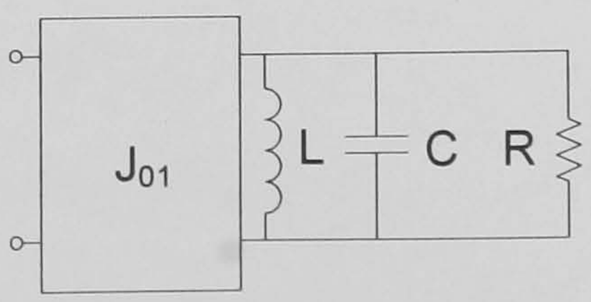

Fig. 2 Single mode antenna equivalent circuit.

It consists of an admittance inverter J_{01}, representing the coupling between the port and the antenna, an inductor and a capacitor representing resonance and a resistor representing power loss due to radiation from the antenna. However, this can be replaced by the low pass prototype network shown in figure 3 for comparison purposes.

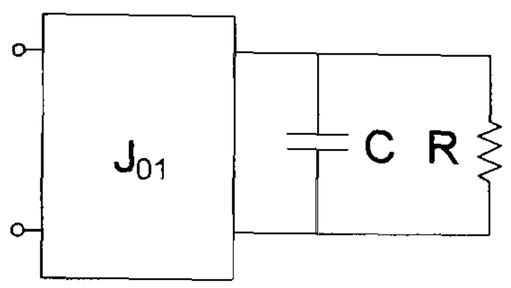

Fig. 3 Single mode antenna lowpass equivalent circuit.

Furthermore, in [6] it was shown that the input couple into one mode which is then coupled to the second mode via a discontinuity in the structure as shown in figure 4.

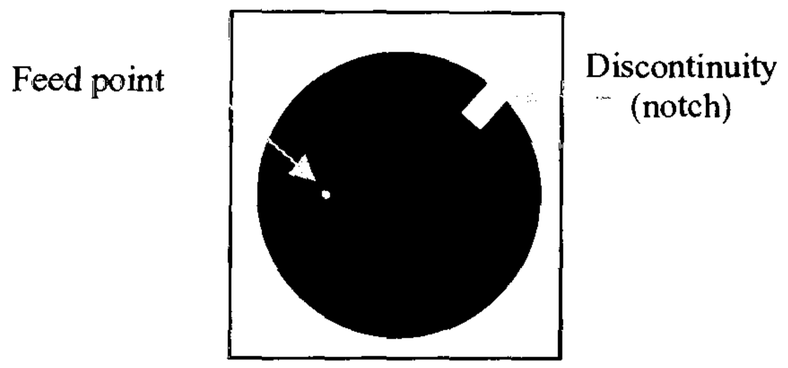

Fig. 4 Dual mode circular microstrip patch antenna.

The equivalent circuit of this structure is a second order ladder network shown in figure 5. Each resonant mode is terminated in a resistor R, representing its own internal losses and radiation, and J_{01} and J_{12} are admittance inverters represent the coupling between the source and the resonant modes. Results have shown that in terms of the return loss bandwidth, the dual mode antenna has approximately 3 times the 6dB-bandwidth as compared to a single mode antenna [6] as shown in figure (6).

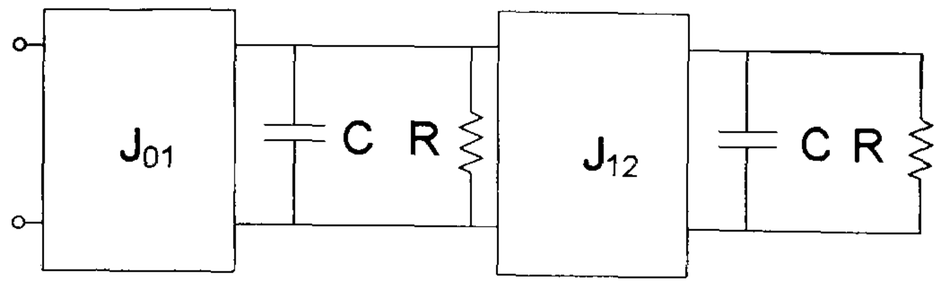

Fig. 5 Equivalent lowpass circuit of dual-mode Antenna (R=C=1).

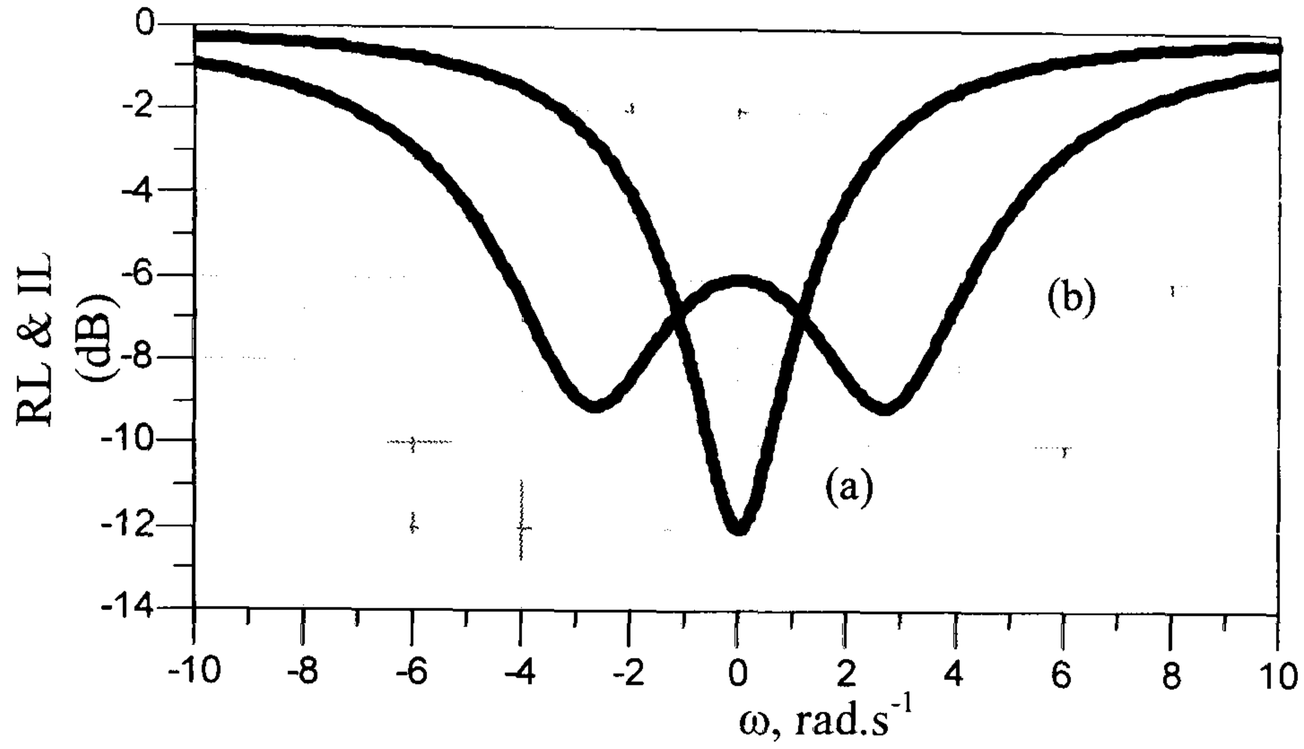

Fig. 6 (a) Optimised single mode and (b) Dual mode antenna equivalent circuit simulated results showing wider bandwidth.

The next section describes a theoretical method of transforming the dual-mode network into a dual-band network. Using techniques commonly used in circuit theory, it is shown how the antenna can be matched at two distinct frequencies, and the design of an experimental antenna will be demonstrated. Section III describes how the dual-band antenna can be further developed into a self diplexing microstrip antenna transceiver. Circuit and electromagnetic simulations agree well with the experimental results.

II. Dual Band Circular Microstrip Patch Antenna

The dual mode antenna in figure 4 can be considered in terms of two distinct transfer functions, these are S_{12A} and S_{12B} each presenting the coupling into the two polarisation modes. The squared total transfer function is given by the sum of the

magnitude squared of S_{12A} and S_{12B}, i.e.;

$$|S_{12Total}(j\omega)|^2 = |S_{12A}(j\omega)|^2 + |S_{12B}(j\omega)|^2 \tag{1}$$

The lowpass equivalent circuit of the dual mode antenna is shown in figure 7 [6]:

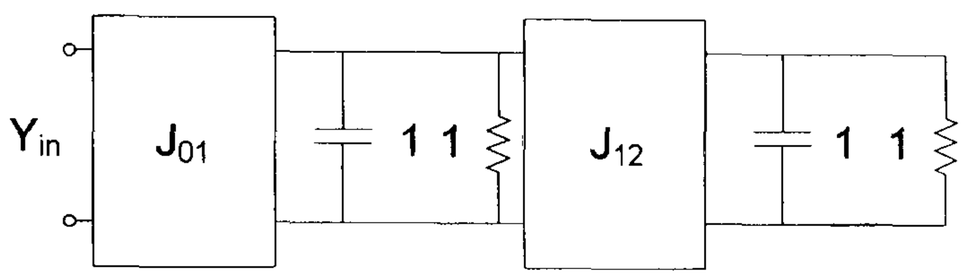

Fig.7. Dual-mode antenna low pass prototype.

Where $J_{01} = \sqrt{\frac{14}{3}}$ and $J_{12} = \sqrt{13}$.

It is interesting to note that there are different network realisations for this network, each with a different transfer function into the two polarisations. The resistor and capacitor values were set to unity in previous studies to enable direct comparison with the single-mode case, and the admittance matrix of the lowpass prototype is shown in equation (2).

$$[Y] = \begin{bmatrix} 0 & jJ_{01} & 0 \\ jJ_{01} & 1+p & jJ_{12} \\ 0 & jJ_{12} & 1+p \end{bmatrix} \tag{2}$$

it can also be re-written as;

$$[Y] = \begin{bmatrix} 0 & 0 & 0 \\ 0 & 1+p & 0 \\ 0 & 0 & 1+p \end{bmatrix} + \begin{bmatrix} 0 & jJ_{01} & 0 \\ jJ_{01} & 0 & jJ_{12} \\ 0 & jJ_{12} & 0 \end{bmatrix} \tag{3}$$

The second part of equation (3) is known as the coupling matrix j[J] [7, 8].

This coupling matrix may be pre and post multiplied by rotational matrices

without altering the input reflection coefficient of the network [8]. Thus if a 2-3 rotation of angle θ is performed as shown in equation (4) [8]:

$$[J]\rightarrow\begin{bmatrix}1 & 0 & 0\\ 0 & C & S\\ 0 & -S & C\end{bmatrix}\begin{bmatrix}0 & \mathrm{jJ}_{01} & 0\\ \mathrm{jJ}_{01} & 0 & \mathrm{jJ}_{12}\\ 0 & \mathrm{jJ}_{12} & 0\end{bmatrix}\begin{bmatrix}1 & 0 & 0\\ 0 & C & -S\\ 0 & S & C\end{bmatrix} \tag{4}$$

Where $C=\cos(\theta), S=\sin(\theta)$; thus $[J]$ becomes;

$$[J]=\begin{bmatrix}0 & \mathrm{jJ}_{01}C & -\mathrm{jJ}_{01}S\\ \mathrm{jJ}_{01}C & 2\mathrm{jJ}_{01}SC & \mathrm{jJ}_{12}(C^2-S^2)\\ -\mathrm{jJ}_{01}S & \mathrm{jJ}_{12}(C^2-S^2) & -2\mathrm{jJ}_{01}SC\end{bmatrix} \tag{5}$$

And hence $[Y]$ becomes:

$$[Y]=\begin{bmatrix}0 & \mathrm{jJ}_{01}C & -\mathrm{jJ}_{01}S\\ \mathrm{jJ}_{01}C & 1+2\mathrm{jJ}_{01}SC+p & \mathrm{jJ}_{12}(C^2-S^2)\\ -\mathrm{jJ}_{01}S & \mathrm{jJ}_{12}(C^2-S^2) & 1-2\mathrm{jJ}_{01}SC+p\end{bmatrix} \tag{6}$$

As expected, the capacitor values are not affected by this transformation, however, the coupling to each mode is different. The equivalent circuit representing the matrix in equation (6) is shown in figure 8.

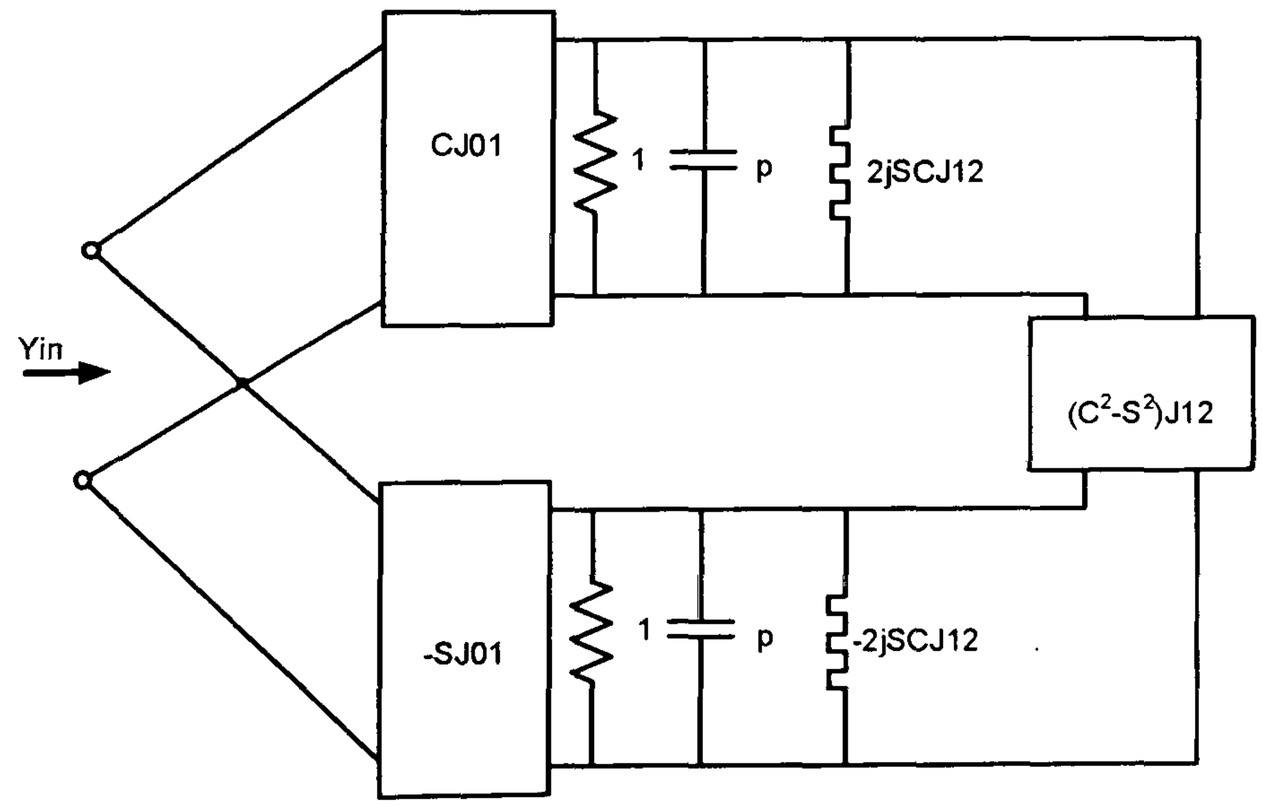

Fig. 8 The equivalent circuit of the dual-mode antenna after performing 2-3 matrix rotation.

Here we see that the input is now coupled to both resonant modes individually, which are detuned by frequency invariant reactances, one up and one down in frequency. However, the modes are still coupled to each other. The correct choice of the rotation angle θ can help to eliminate the coupling between the modes, i.e.:

$$C^2 - S^2 = 0 \tag{7}$$

The solution to equation (7) is

$$\theta = -45^\circ \text{ giving } C = \tfrac{1}{\sqrt{2}} \ \& \ S = \tfrac{-1}{\sqrt{2}} \tag{8}$$

and therefore equation (6) become

$$[Y] = \begin{bmatrix} 0 & \frac{jJ_{01}}{\sqrt{2}} & \frac{jJ_{01}}{\sqrt{2}} \\ \frac{jJ_{01}}{\sqrt{2}} & 1 - jJ_{01} + p & 0 \\ \frac{jJ_{01}S}{\sqrt{2}} & 0 & 1 + jJ_{01} + p \end{bmatrix} \tag{9}$$

Hence, the circuit reduces to the one shown in figure 9. The coupling into each mode is equal and is detuned by equal reactances up and down in frequencies (these are the transfer functions S_{12A} & S_{12B} of the dual mode antenna [9]). The simulation results of this circuit is shown in figure 10. Here, it is clear that the antenna now behaves like a multimode transmitter/receiver, with lower frequencies radiating in polarisation B and higher frequencies in polarisation A as shown in figure 10.

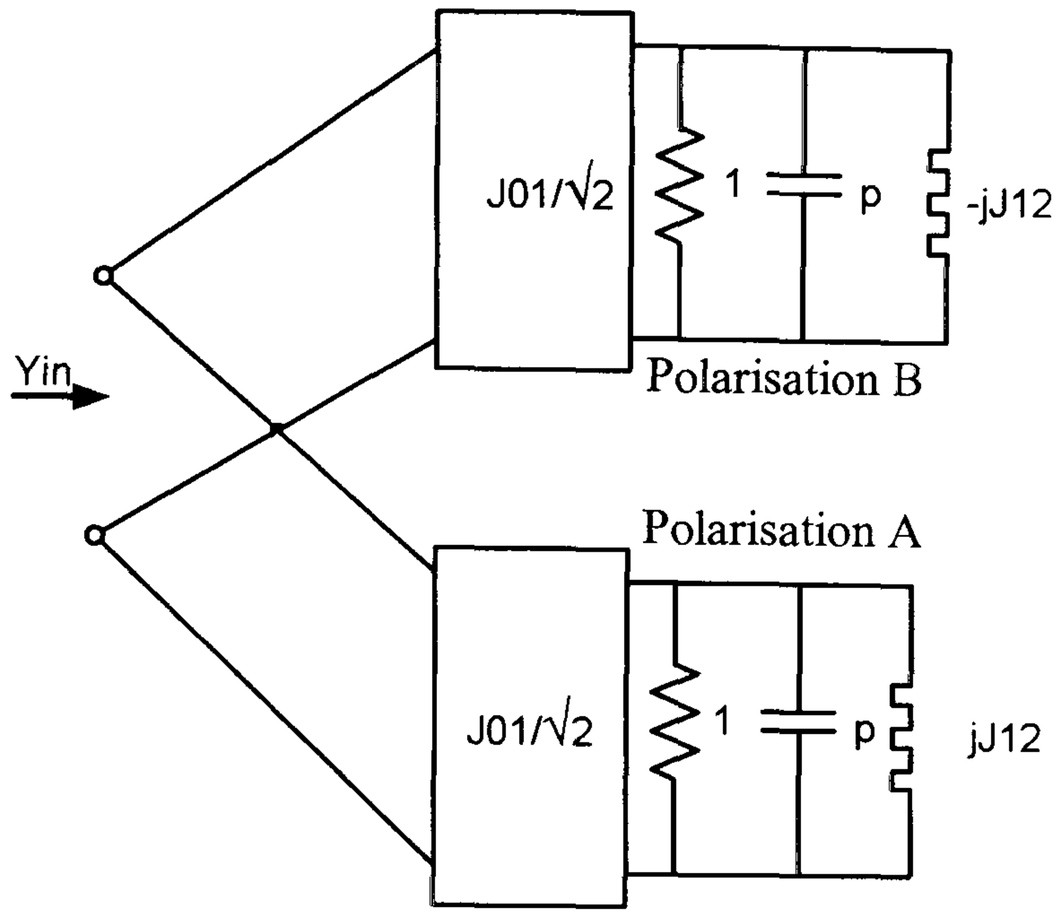

Fig. 9 The equivalent circuit of the Dual-band antenna showing how the coupling between the modes can be eliminated.

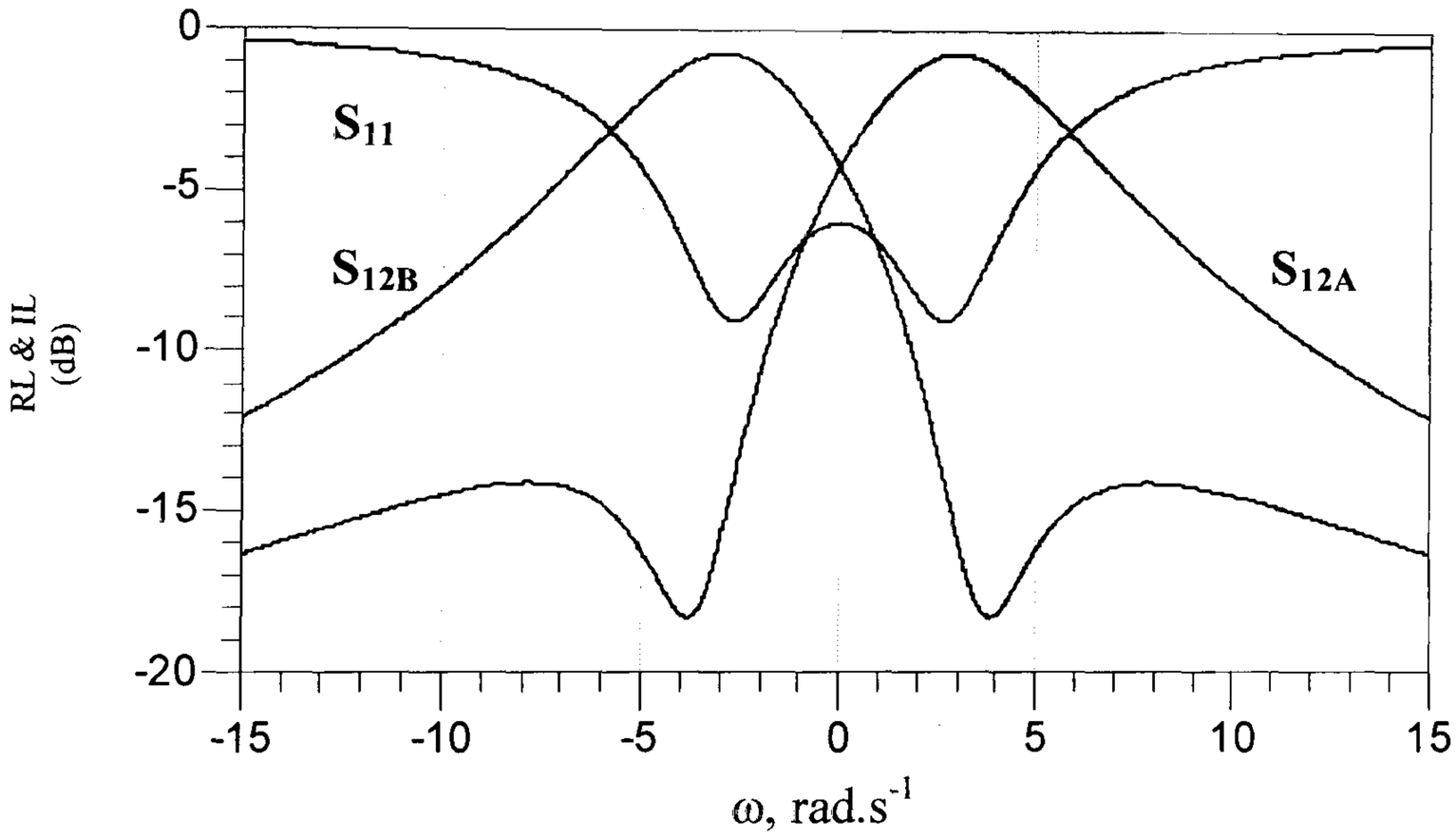

Fig.10 Dual-band antenna equivalent circuit simulation results, showing the polarization into the two modes (A&B) at two different frequencies.

Simulations and Measured Results

In order to demonstrate the theoretical results derived earlier, the experimental prototype antenna designed in [6] can be used again here. Consider the antenna in figure 11.

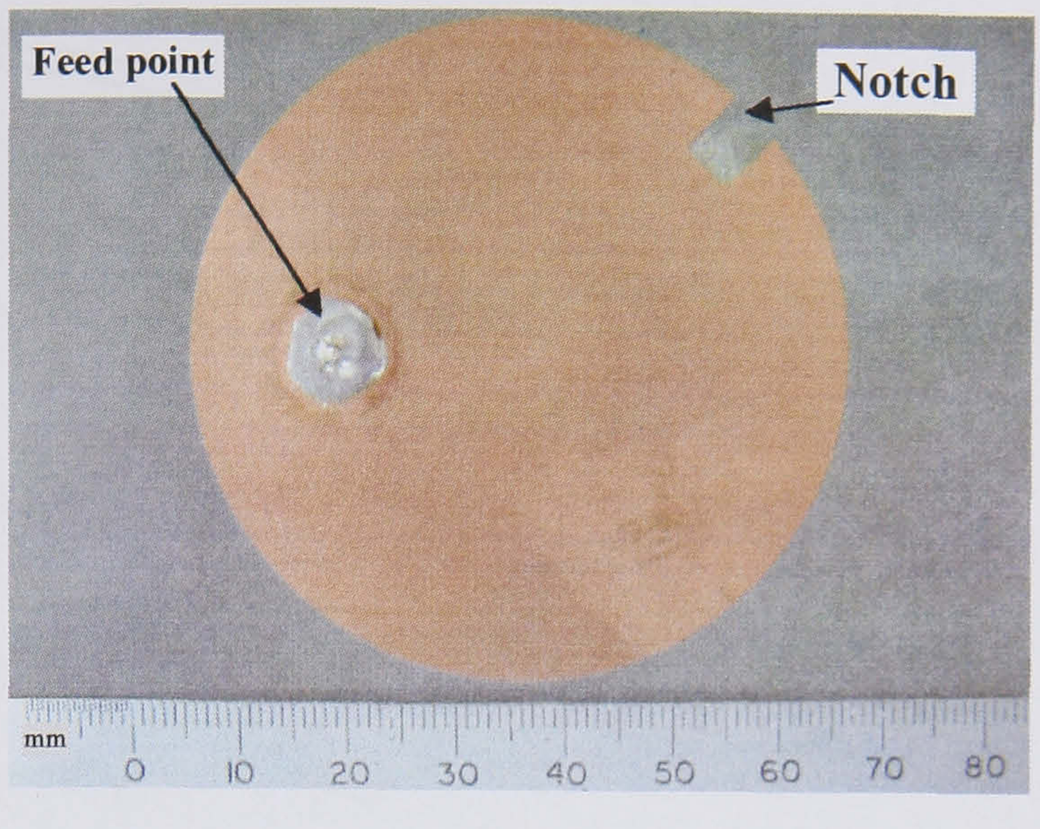

Fig.11 Dual-mode circular patch antenna designed at 2 GHz.

The antenna is built on Duroid 5880 (ϵ_r=2.2, thickness = 0.787mm). The disc radius is 3cm. For the antenna to operate at two distinct frequencies, the two modes need to be split one up and the other down from the centre frequency and maintain the same insertion loss response. A coupling notch which perturbs the fields on the patch disturbing the symmetry has been used to couple the two orthogonal modes in [6] and achieve a wider bandwidth. The antenna shown in figure 11 can radiate at each of the two polarisations individually by physically rotating the antenna through 90º, or facing it with two antennas, one vertically polarised and another horizontally polarised. The result of this is shown in figure 12.

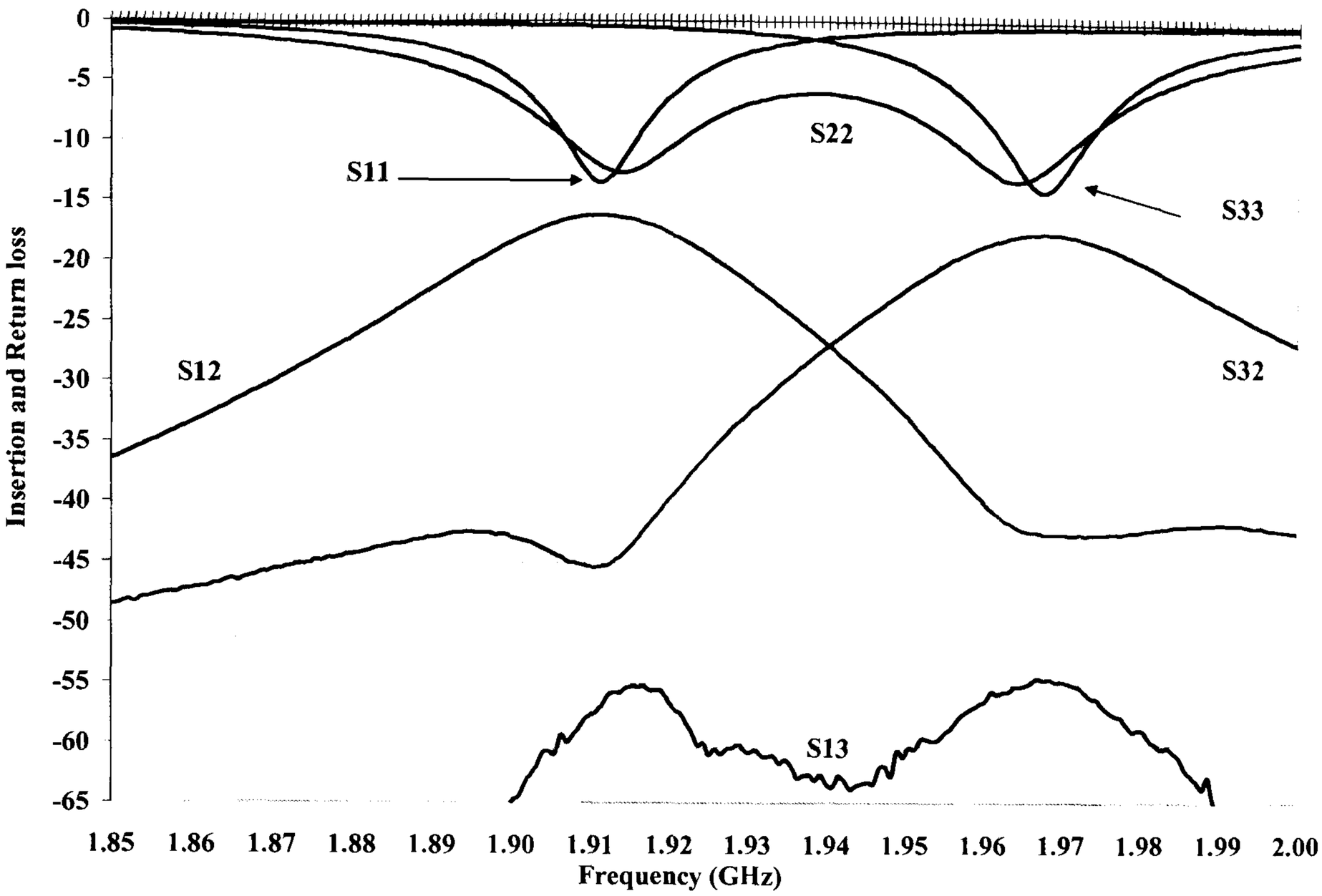

Fig.12 Measured results of the dual band circular patch antenna experimental setup, where:

- Port 2 is the dual-band antenna.
- Port 1 is the vertically polarised single mode antenna.
- Port 3 is the horizontally polarised single mode antenna.

As expected, the return loss response does not change. However, the insertion loss response is similar to the one anticipated in the circuit analysis in figure 10. From a different prospective, the notch makes the antenna looks electrically smaller at one mode and therefore increase its resonant frequency. Conversely if the metal area is extended on the orthogonal mode, the antenna looks electrically longer on that mode, and therefore decrease its resonant frequency. In principle if the notch in is further extended in and an extra metallization is extended out on the orthogonal mode, the two resonant modes will move further apart. Another dual-band antenna that radiates at 1.82GHz and 1.96GHz was designed. The fabricated antenna, simulated and practical results are shown in figure 13 and 14.

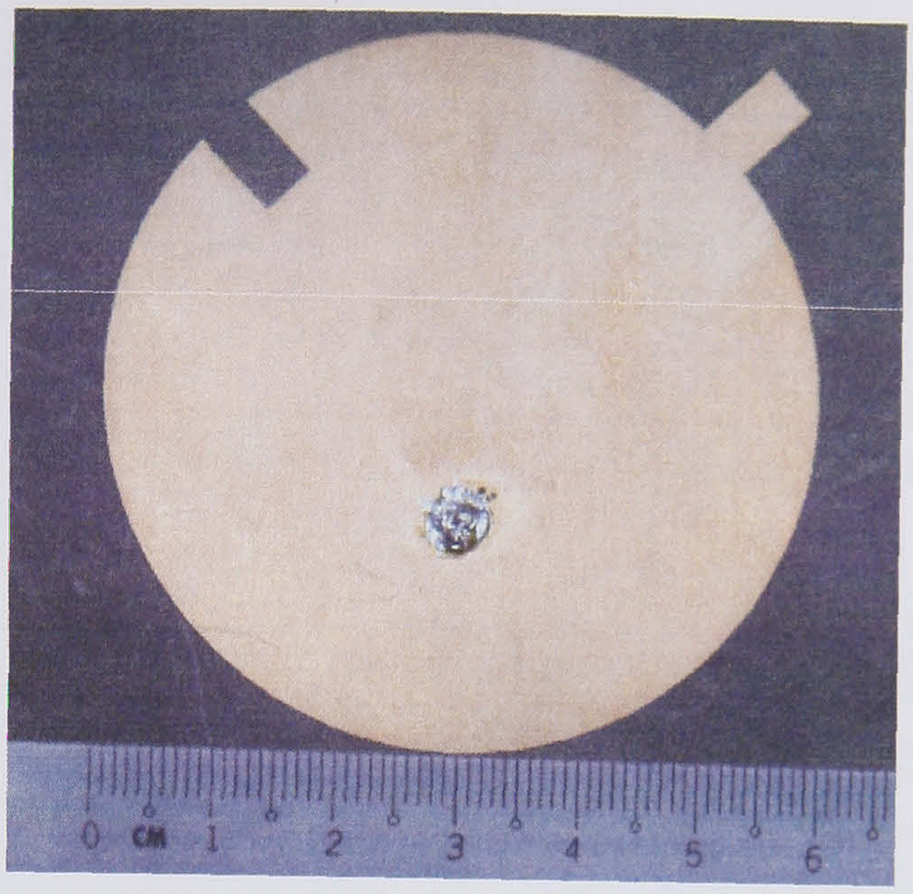

Fig.13 Dual-band circular patch antenna designed at 1.82GHz and 1.96GHz.

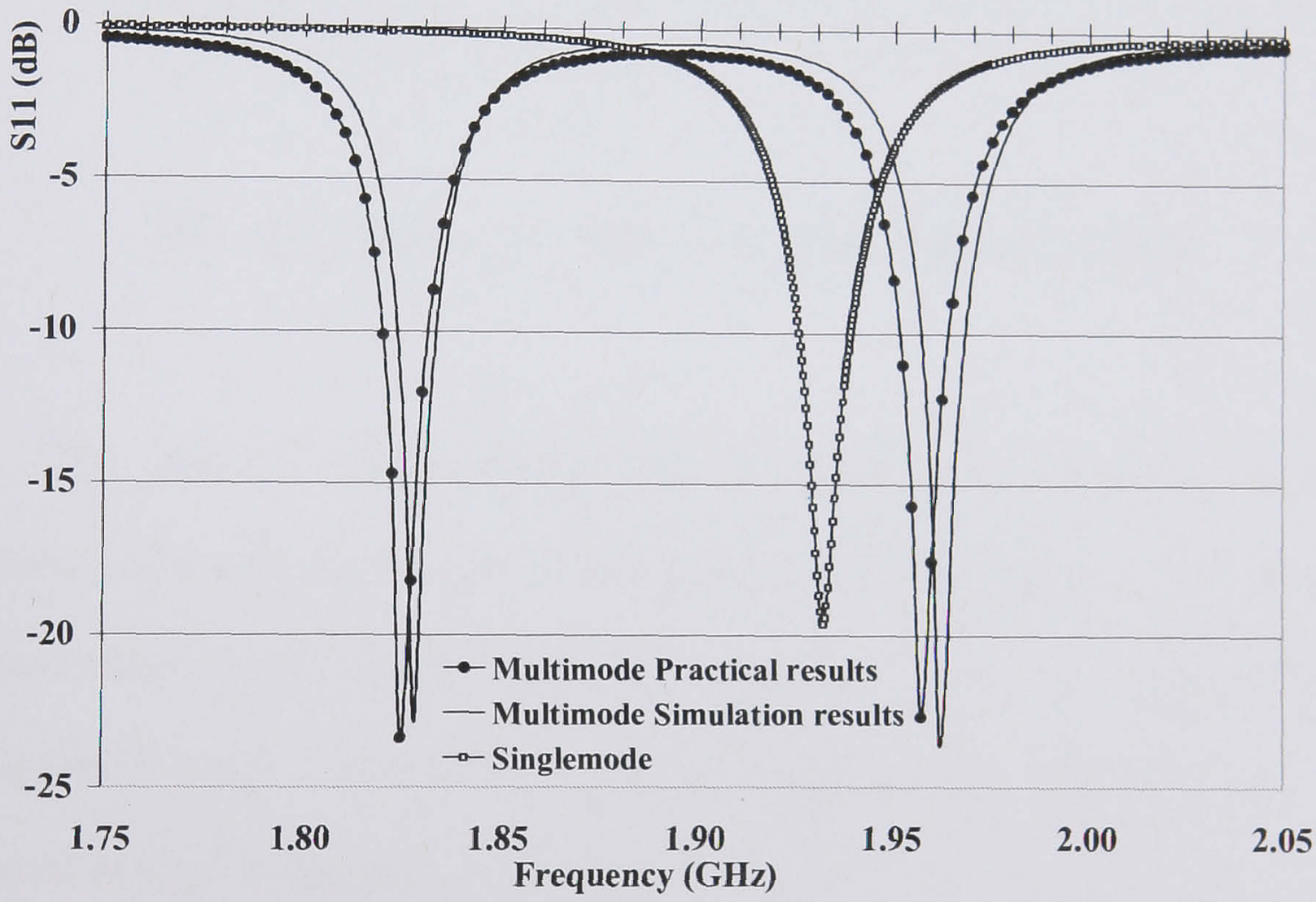

Fig.14 EM simulations and measured results of the dual band circular patch compared to an optimised single mode.

This result show that the antenna can be used at 2 distinct frequencies, and therefore can be utilised as a dual band antenna for communication systems. Figure 15 shows the far field pattern of the antenna, which is similar at both frequencies.

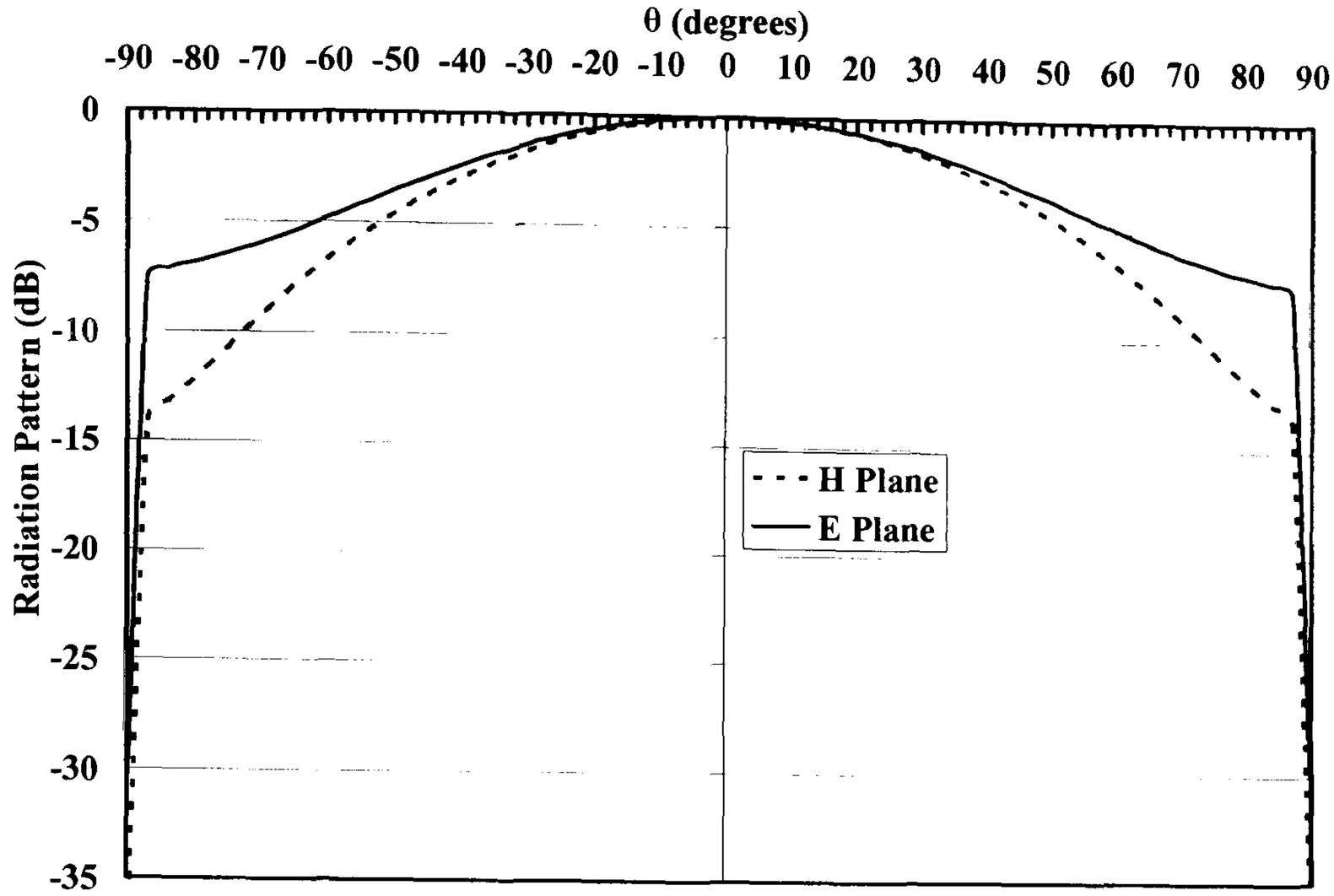

Fig.15 Far field radiation pattern of the antenna in figure 13.

III. SELF DIPLXING PATCH ANTENNA TRANSCEIVER

The Antenna characteristics can be represented using the scattering parameters. For instance, a single mode antenna can be considered as a 2 port device. One port represents the interface with the transmitter/receiver, and the other port with free space [5, 8-12]. The antenna presented in section II is considered as a 3-port device (as shown in figure 9).

This section explains how the antenna in section II can be further developed into an antenna transceiver, utilising 4-ports, 2 of which represent the interface with free space at two distinct polarisations and 2 act as transmitter/receiver.

For two port devices, the S-parameters only involve the insertion and return loss of the antenna, i.e. S_{11} and S_{12}. However, the dual-mode antenna discussed in this section comprises four-port network. Hence, other crucial parameters becomes evident, i.e. S_{21}, S_{14} & S_{23} this is the isolation (or the coupling) between the two input (or output) ports as shown in figure 16 [12].

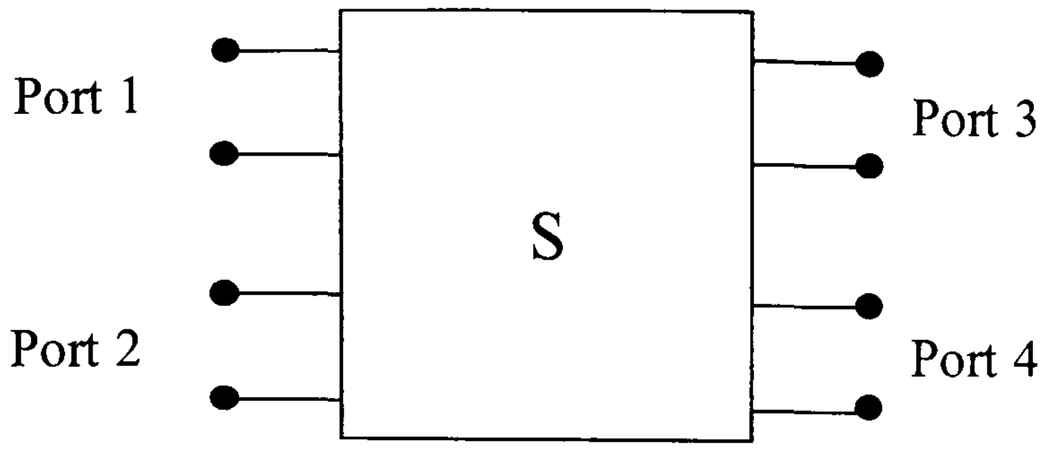

Fig. 16. S-parameters representation of dual mode antenna transceiver

In this network, S_{21} corresponds to the part of the signal to be transmitted at port 1 that is coupled into port 2, and known as "isolation parameter". S_{14} and S_{23} corresponds to the part of the signal to be transmitted at port 1 that is coupled into port 4 or to be transmitted at port 2 that is coupled into port 3. These are known as 'cross polarisation' [12]. Taking these issues into consideration brings attention to the fact that diplexing between the ports is essential.

As explained earlier, microstrip antennas can support two orthogonal resonant modes, therefore, two ports can be coupled into each mode individually and hence the equivalent circuit in figure 9 changes to the one shown in figure 17, where Jx represent the isolation between the ports.

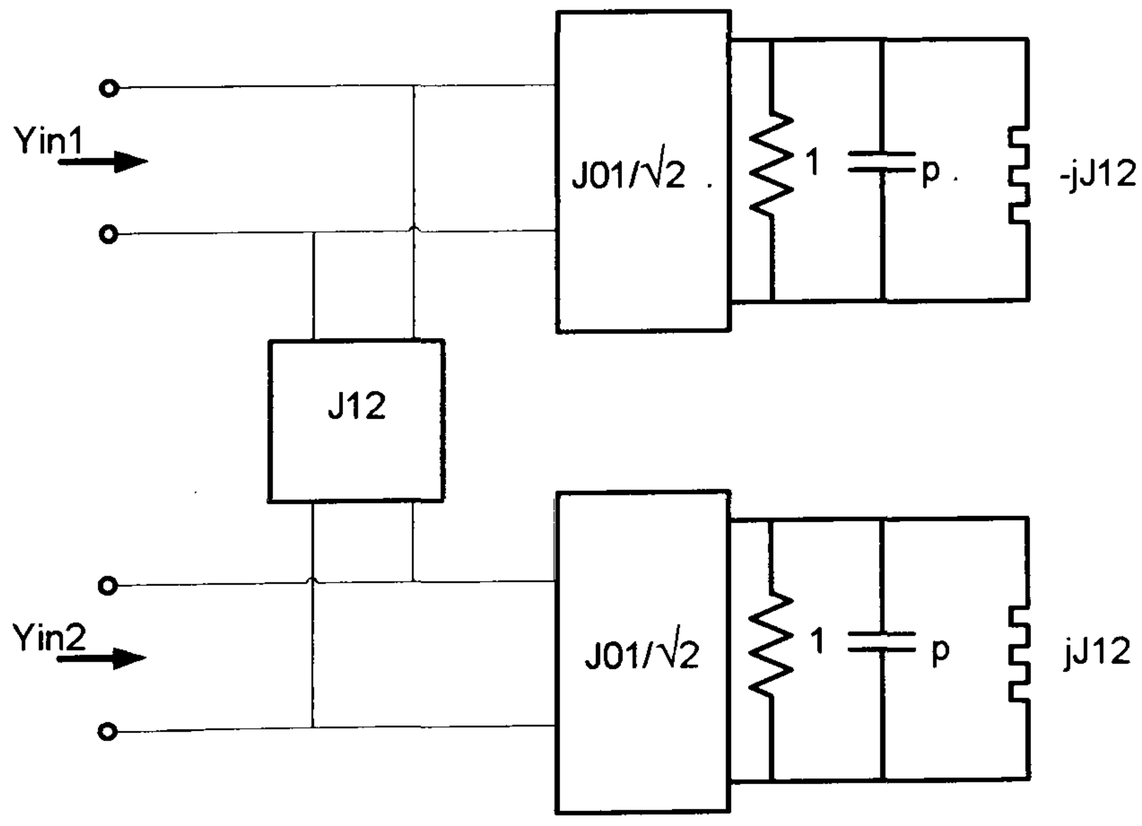

Fig. 17. The equivalent circuit of the self diplexing patch antenna transceiver..

Here, we see the antenna now behaves like a multimode transceiver. There are 2 inputs now coupled to each resonant mode respectively. These modes are detuned by

frequency invariant reactances, one up and one down in frequency, with lower frequencies radiating in polarisation B and higher frequencies in polarisation A. The circuit above can be applied to the antenna design, and therefore the new design is depicted in figure 18.

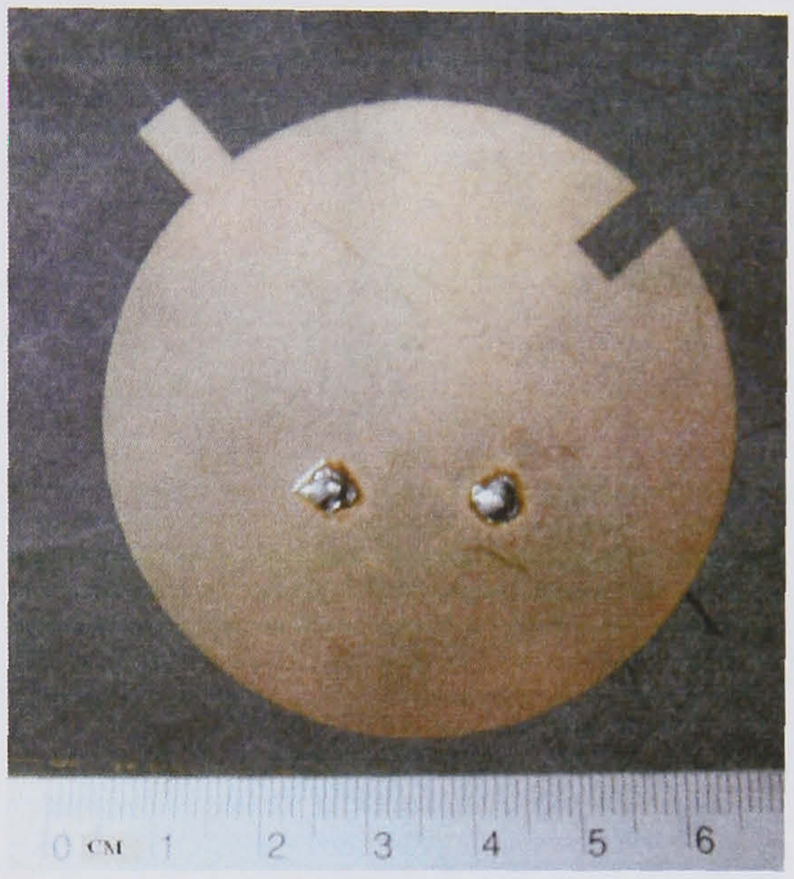

Fig. 18. Dual-band antenna transceiver designed at 1.84GHz and 1.97GHz.

The electromagnetic simulations and measured results are shown in figure 19.

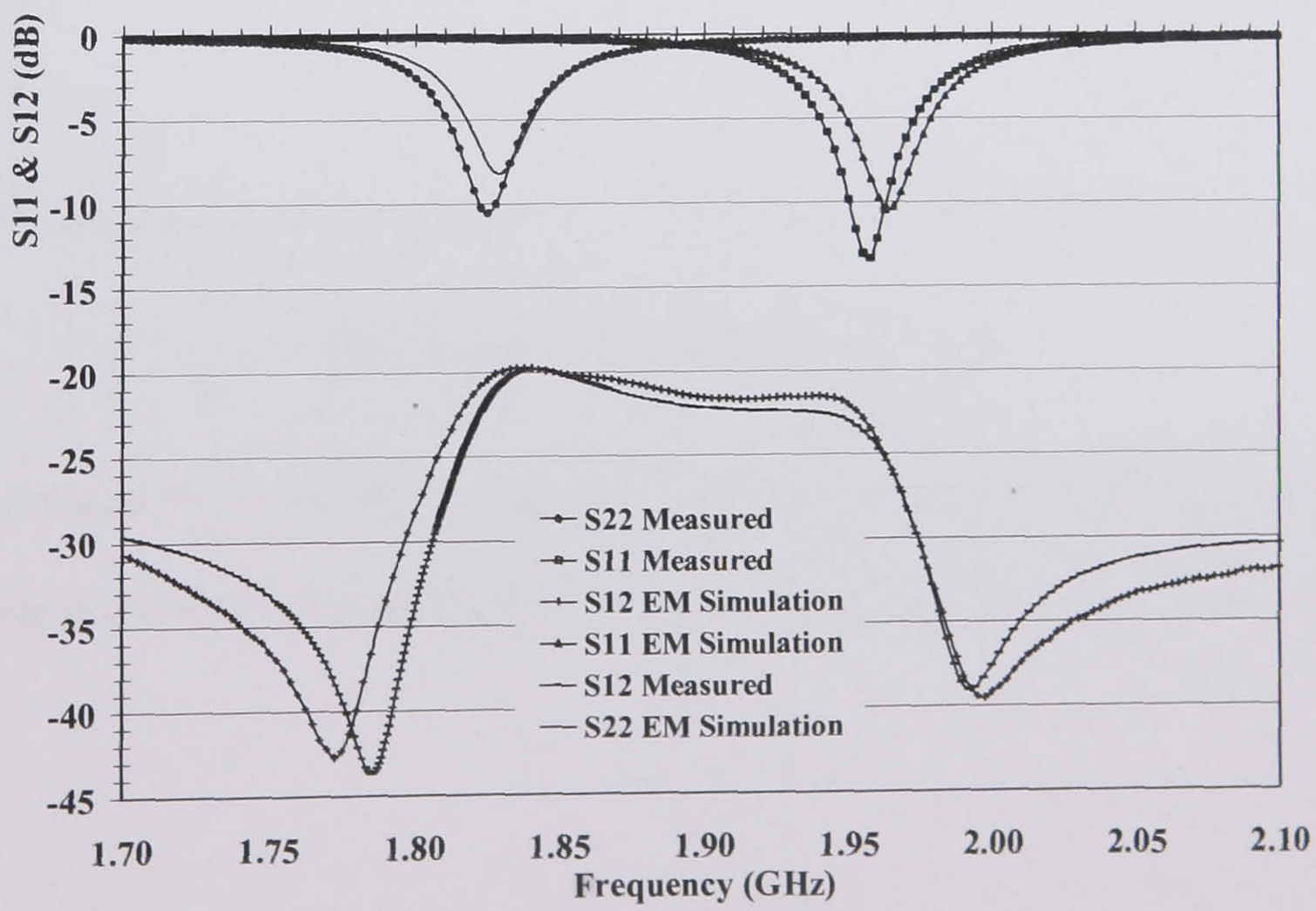

Fig. 19 Electromagnetic simulations and experimental results of the dual-band antenna transceiver.

As shown in figure 19, each port transmits/receives at a different frequency. The isolation between the two ports is over 20dB (this is represented by J_{12} in figure 17), which is satisfactory for diplexing the transmitted/received signals. This design can be used in a dual band transceiver with 20dB isolation between the ports, but fairly narrow bandwidth.

Figure 20 shows the E-field pattern frequency, which is very similar at the two frequencies.

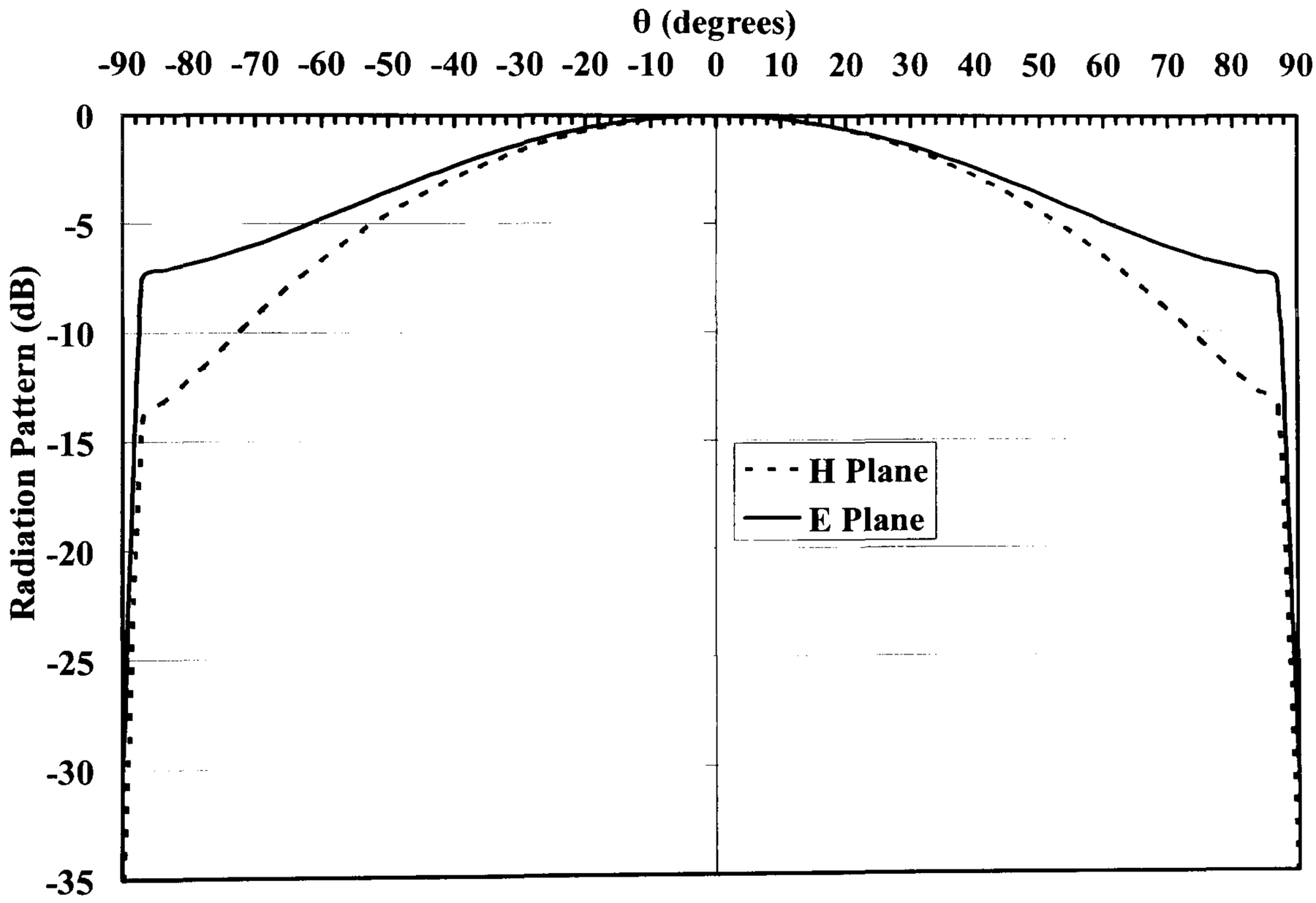

Fig. 20. Far field pattern of the antenna.

This technique was further developed into a quad band microstrip antenna by integrating an external matching network. This was presented at the EuMC in [13].

IV. Conclusion

The motivation behind this work is to improve the performance of microstrip patch antennas. A simple theoretical design method for maximising the return loss bandwidth of a circular microstrip patch antenna was presented in earlier work [6]. By theoretical study, the antenna was represented as a filter network, and in this paper it was shown that the use of matrix rotations enable different transfer functions into the two radiation polarizations to be obtained. Accordingly, the input is then coupled to each of the resonant modes individually, which are detuned up and down in frequency. Hence, the antenna may operate as a multimode transmitter/receiver, where the two bands radiating in the two orthogonal polarizations. The theory has been demonstrated by introducing a notch at one mode, and extending the metallization on the orthogonal mode to separate the 2 bands further apart. The theoretical derivation presented has practically shown that the antenna can efficiently operate at two bands, with isolation between the ports exceeding 20dB.

V. References

[1] S. U. Xiang-Fei Peng (Sch. of Commun. & Inf. Eng., China); Shun-Shi Zhong; Sai-Qing Xu; Qiang Wu, "Compact dual-band GPS microstrip antenna," *Microwave and Optical Technology Letters*, vol. 44, pp. 58-61, 2005.

[2] D. Sanchez-Hernandez and I. D. Robertson, "Analysis and design of a dual-band circularly polarized microstrip patch antenna," *IEEE Transactions on Antennas and Propagation*, vol. 43, pp. 201-205, 1995.

[3] S. M. El-Ghazaly, "Reconfigurable Antennas for Universal Wireless Receivers," in *Reconfigurable and Smart Antennas Workshop, IEEE International Microwave Symposium*. Hawaii, 2007.

[4] C. A. Balanis, *Antenna theory : analysis and design*, 2nd ed: Wiley, 1997.

[5] R. Garg, *Microstrip Antenna Design Handbook* Artech House, 2001.

[6] A. I. Abunjaileh, I. C. Hunter, and A. H. Kemp, "Application of dual-mode filter techniques to the broadband matching of microstrip patch antennas," *Microwaves, Antennas & Propagation, IET*, vol. 1, pp. 273, 2007.

[7] H. C. Bell, "The Coupling Matrix in Low-Pass Prototype Filters," in *Microwave Magazine, IEEE*, vol. 8, 2007, pp. 70-76.

[8] I. Hunter, *Theory and Design of Microwave Filters*. London: IEE, 2001.

[9] I. Hunter, "Broad-band matching of antennas using dual-mode radiators," presented at 33rd European Microwave Conference, 2003.

[10] K. Chang, *Microwave Ring Circuits and Antennas*: Wiley, 1996.

[11] N. Kumprasert and W. Kiranon, "Simple and accurate formula for the resonant frequency of the circular microstrip disk antenna," *Antennas and Propagation, IEEE Transactions*, vol. 43, pp. 1331, 1995.

[12] D. Pozar, D. Schaubert, and P. Hall, "Review of Techniques for Dual and Circularly Polarised Microstrip Antennas," *Microstrip Antennas The Analysis and Design of Microstrip Antennas and Arrays*, pp. 107-116, 1995.

[13] A. I. Abunjaileh, I. C. Hunter, and A. H. Kemp, "Multi-band Matching Technique for Microstrip Patch Antenna Transceivers," presented at The 37th European Microwave Conference (EuMC), Munich, Oct. 2007.